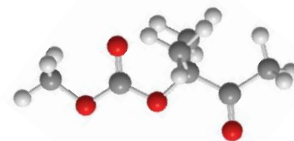
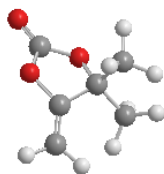




UNIVERSITY OF LIEGE

FACULTY OF SCIENCE

Cascade approaches towards functional CO₂-sourced cyclic carbonates and polycarbonates



A dissertation presented by

Charlene Gabriela NGASSAM TOUNZOUA

In fulfilment of the requirements for the degree of

Doctor of Philosophy in science

Supervisor. Dr Christophe Detrembleur, FNRS Research Director

Center for Education and Research on Macromolecules (CERM)

Academic year **2021/2022**

This thesis was funded by the Fonds National de la Recherche Scientifique (F.R.S.-FNRS) via a FRIA grant call 2017 - B1 and call 2019 - B2

Public defense on the 1st of July 2022

Members of the Jury

Prof. Dr. Jean Christophe Monbaliu University of Liege (President)
Dr. Bruno Grignard University of Liege (Secretary)
Dr. Christophe Detrembleur University of Liege (Supervisor)
Prof. Dr. Carmela Aprile University of Namur
Dr. Olivier Coulembier University of Mons
Dr. Thomas Schaub BASF, Germany

Summary

Polycarbonates (PCs) belong to some of the world-leading polymers that are widely used in aircraft or automotive applications (windows, etc.), in safety equipment (helmets, bullet proof glass, etc.),... However, their industrial production requires the use of toxic compounds such as phosgene, high temperatures, and is not compatible with the introduction of some functional groups along the polymer backbone. Making plastics more sustainable by valorising CO₂ as a cheap, inexhaustible and renewable feedstock imposes itself as a strategic driver for developing low carbon footprint materials. In 2017, our research group reported a new process for the preparation of a novel family of regioregular PCs (i.e. poly(*oxo*-carbonate)s) by the facile organocatalysed polyaddition of CO₂-sourced bis(α -alkylidene cyclic carbonate)s (bis α CCs) with diols under ambient conditions. These bis α CCs were prepared by the organocatalysed carboxylative coupling of CO₂ to bis(propargylic alcohol)s.

The goal of my PhD thesis work was to investigate the fundamentals to permit the synthesis of these new PCs in a one-pot process, wherein bis α CCs are produced *in-situ* and directly involved in polymerisation. Firstly, we designed various organic salts that were tested as catalysts for the carboxylative coupling of CO₂ with propargylic alcohols. We investigated the influence of the structure of the organocatalyst (mainly the type and structure of the cation and anion) on the catalytic performances. Optimum activity resulted from the best compromise between ion-pair separation controlled by steric effects and the basicity of the anion. Organic salts with too basic anions increased the rate of the reaction but at the expense of the selectivity. Then we optimised the activity of the organic catalyst by incorporating a metal cocatalyst (CuI or AgI) that allowed to synthesise the bis α CCs with a high selectivity (> 95%) under mild conditions (25-40 °C, 15 bar). Eventually, we implemented the one-pot cascade approach to prepare *oxo*-alkylcarbonate scaffolds and poly(*oxo*-carbonate)s from CO₂, propargylic alcohols, and mono-alcohols under moderate operating conditions (PCO₂ = 1-15 bar, T = 40-80 °C). By varying the nature of the bis(propargylic alcohol) and the diol, various poly(*oxo*-carbonates) were successfully prepared. Lastly, we prepared new alkyne-1-n-diols and studied their reactivity for the carboxylative coupling with CO₂. By carefully choosing the reaction conditions and the diols, we prepared diverse keto-cyclic carbonates, elusive tetrasubstituted carbonate scaffolds and poly(*oxo*-carbonate) oligomers. This thesis includes operando FT-IR/ATR and DFT computational studies that allowed to understand and explain the mechanism of the reactions investigated. In conclusion, this work contributes to the quest to develop simple catalytic systems for the transformation of CO₂ into useful compounds (cyclic carbonates and poly(*oxo*-carbonate)s).

Résumé

Les polycarbonates (PCs) représentent une classe de polymères importante, utilisés notamment dans le domaine de l'aviation ou de l'automobile (fenêtres), pour la fabrication d'équipements de protections individuelles (casques, vitres pare-balles, etc), ... Cependant, leur production industrielle nécessite l'utilisation de composés toxiques tels que le phosgène, et de hautes températures. De plus, le procédé n'est pas compatible avec l'introduction de groupements fonctionnels variés le long de la chaîne polymère. De ce fait, rendre la synthèse de plastiques plus durable en valorisant le CO₂, un gaz abondant et bon marché, comme matière première d'origine renouvelable s'impose comme une stratégie réaliste pour le développement de matériaux à faible empreinte carbone. En 2017, notre groupe de recherche a développé un procédé pour la préparation d'une nouvelle famille de polycarbonates (des poly(*oxo*-carbonate)s) qui consiste en la polyaddition d'un bis(carbonate cyclique d' α -alkylidène)s (bis α CCs) CO₂-sourcé avec des diols, en présence d'un organocatalyseur à température ambiante. Ces bis α CCs ont été préparés par le couplage catalysé du CO₂ avec un bis(alcool propargylique).

L'objectif de ma thèse était de rechercher comment nous pouvons préparer ces nouveaux PCs par un procédé de type "one-pot" dans lequel le bis α CC est produit *in-situ* et directement impliqué dans la polymérisation. Premièrement, nous avons préparé divers sels organiques qui ont été testés comme catalyseurs pour le couplage du CO₂ avec des alcools propargyliques. Nous avons étudié l'influence de la structure de l'organocatalyseur (principalement le type et la structure du cation et de l'anion) sur les performances catalytiques. Une activité optimale résulte d'un bon compromis entre la séparation des paires d'ions, qui est contrôlée par des effets stériques et la basicité de l'anion. Les sels organiques avec des anions trop basiques accélèrent la vitesse de réaction mais au détriment de la sélectivité. Ensuite, nous avons optimisé l'activité du catalyseur organique en incorporant un co-catalyseur métallique (CuI ou AgI) qui a permis de synthétiser les bis α CCs avec une très bonne sélectivité (> 95%) dans des conditions douces (25-40 °C, 15 bar). Ensuite, nous avons mis en œuvre la synthèse en cascade en "one-pot" d'*oxo*-alkylcarbonates et de poly(*oxo*-carbonate)s à partir de CO₂, d'alcools propargyliques et d'alcools aliphatiques ou aromatiques dans des conditions modérées (PCO₂ = 1-15 bar, T = 40-80 °C). En faisant varier la nature du bis(alcool propargylique) et du diol, différents poly(*oxo*-carbonate)s ont été préparés avec succès. Enfin, nous avons synthétisé de nouveaux alcyne-1-n-diols et étudié leur réactivité pour le couplage carboxylatif avec le CO₂. En choisissant soigneusement les conditions expérimentales et les alcools, nous avons préparé divers céto-carbonates cycliques, des carbonates d'éthylène tétra-substitués ainsi que des oligomères de poly(*oxo*-carbonate)s. Cette thèse inclut des études par spectroscopie FT-IR/ATR et des calculs computationnels de type DFT, lesquels nous ont permis de comprendre et proposer des mécanismes réactionnels. En conclusion, ce travail contribue au développement de systèmes catalytiques simples et efficaces permettant la transformation du CO₂ en composés utiles (carbonates cycliques et poly(*oxo*-carbonate)s).

Acknowledgements

This journey, which began a little over 4 years ago has been filled with hurdles. It would not have been a success without the help and guidance of many people, to whom I wish to express my profound gratitude.

Je tiens à remercier mon promoteur, Dr Christophe Detrembleur, pour avoir encadré ma thèse, pour les discussions, les nombreuses corrections, les désaccords car tout cela m'a permis de développer à la fois mes compétences scientifiques et de forger mon caractère. Merci pour les mécanismes dessinés à la main et scanné pour m'aider à terminer rapidement mes révisions.

J'aimerais remercier la Prof. Christine Jérôme pour m'avoir donné la possibilité de faire un mémoire dans son laboratoire le CERM, ce qui m'a permis de déboucher sur cette thèse de doctorat.

Je tiens à remercier le Prof. Jean Christophe Monbaliu d'avoir accepté de présider ma défense de thèse, et d'avoir fait partie de mon comité de thèse durant ces années. Merci de m'avoir proposé quelques idées pour avancer dans mon travail et de m'avoir prêté de l'équipement de micro fluidique, ce qui m'a permis de découvrir une nouvelle façon de faire de la chimie.

I would like to thank the members of the jury, Prof. Dr Carmela Aprile, Dr Thomas Schaub, Dr Olivier Coulembier for accepting to evaluate my manuscript.

Je ne saurais trouver les mots pour te montrer toute mon appréciation Bruno alias "Mr Grignard". Tu as rendu chaque jour de cette thèse un peu plus facile à vivre. Je pouvais débarquer dans ton bureau à n'importe quel moment pour poser une/des questions et tu étais toujours prêt à y répondre. Merci pour tous les conseils, merci pour toutes les histoires, merci de m'avoir écouté me plaindre de tout et de rien. À mes moments les plus bas quand je songeais à tout abandonner, tu me disais, regardes, encore une année de manips et tu as finis ta thèse. Merci merci merci, mille fois merci.

J'aimerais remercier l'équipe de Bordeaux, le Prof. Thierry Tassaing et le Dr Raphael Mereau, pour la réalisation des calculs DFT, qui ont été essentiels à la compréhension de mes expériences. Nous avons d'ailleurs publié 2 articles ensembles.

I would also like to thank the Prof. Arjan Kleij of the ICIQ group, Tarragona, and his team for the fruitful collaboration which resulted in a beautiful article.

Durant ma thèse, j'ai également pu compter sur l'aide de nombreux d'autres seniors tels que Antoine, Philippe et des post-doctorants, notamment Jean-Mi, Farid, Raph et Abdel.

La vie au laboratoire serait bien difficile sans l'aide quotidienne de nos chère(s) techniciens Greg, Valérie, Martine et Charlotte. Merci Greg et Martine pour toutes les analyses RMN et GPC en urgence. Greg lorsque

tu étais malade ou en congé on le ressentait très bien. Martine, je te remercie pour ta discrétion car cela m'a permis de me confier lorsque j'en avais besoin. Je suis très reconnaissante envers Valerie qui, durant ma grossesse, a continué à réaliser des expériences pour moi et bien après d'ailleurs. Merci pour toute l'attention et la gentillesse en mon égard.

Je tiens à remercier Sophie, notre secrétaire mais bien plus encore. Tu es à l'écoute de tous. Tu nous aides à trouver des solutions à nos problèmes au laboratoire mais pas seulement. Ta joie de vivre et ton amour pour la fête est quelque chose que je trouve rafraichissant.

The life of a PhD student is not the easiest, and only another fellow PhD can possibly understand the hassle.

Pierre, cette thèse aurait été bien triste sans toi à mes côtés. Quel plaisir de pouvoir débarquer dans ton bureau et te raconter toutes mes inquiétudes. Ton oreille attentive et ta discrétion ont été une source de réconfort. Derrière ton caractère froid d'ardennais se cache quelqu'un d'attentionné et tu me l'as démontré à plusieurs reprises.

Phil, getting to know you was probably one of the best things that happened to me in 2018. You are absolutely fun to be around, you light up my mood even on the gloomiest days. I can't wait to make you some nice food to eat.

Antoine, dit mon petit Antoine, merci pour tout l'aide que tu m'as apporté notamment lors de la mise en place du spectro infrarouge et pour son utilisation. Travailler à tes côtés fut un réel plaisir et d'autant plus rassurant car nos manip ne fonctionnaient pas. Merci pour les discussions tant de la chimie mais aussi de la vie. Merci d'avoir élargi ma culture musicale.

Merci Romain de m'avoir accompagné lors de mes expériences de microfluidiques. C'était cool de travailler avec toi et de discuter de divers sujets.

Anna, tu es une magnifique personne, ne l'oublie jamais. Tu as rendu mon année 2021 un peu moins triste. Discuter avec toi de mes multiples problèmes m'a apporté du réconfort. Merci à toi Jeremie pour les chouettes moments et les apéros organisés chez toi. Merci Florent pour ton optimisme qui m'a aidé à aller de l'avant même quand je n'obtenais pas les résultats désirés. Je ne vous oublie pas Fabiana, François, Lionel, Luca, Malihéh, Marco, Maxime, Maxime, Oscar, Sofia, Thomas, thank you for the cool memories be it in the office or at the multiple dinners we have had the occasion to spend together.

There is a saying which goes "friends are the family we chose"

J'aimerais remercier ma meilleure amie Diane. Tu me permets de relativiser à tout moment. De prendre les choses telles qu'elles sont, de ne pas désespérer, de ne pas être en colère. Tu m'écoutes, tu me rassures, tu me réconfortes, tout en me disant la vérité.

Nathalie and Livie, my boarding school sisters, although there are thousands of kilometers separating us, I have never felt less loved or lack of support from you. Your reassuring phone and video calls were all I needed to get me through some gloomy days. Your absolute confidence in my capabilities gave me the boost I needed throughout all my studies.

Kesnelle, Adeline, Gaëtan, Yasmina, Frederique. You have made me forget my troubles times and again, by simply allowing me to rant, taking me out for a walk/dinner. Thank you for all the words of encouragements. I am grateful to have you in my life.

We all know in life, your family can either lift you or crush you. Mine has been the literal rock on which I stood throughout all these years.

J'aimerais remercier toute la grande famille Nana pour m'avoir soutenu dans mon projet d'aller poursuivre des études supérieures en Belgique et d'avoir contribué financièrement, physiquement et moralement. Je suis particulièrement reconnaissante envers tata Mireille et tonton Robert, car sans vous ma vie aurait été bien misérable en Belgique. Je ne t'oublie pas Francine ma sœur à qui je confie mes joies et mes peines. Ensemble, vous avez veillé et contribué à mon bien être.

J'aimerais remercier mon compagnon de toujours et papa de notre fille, Robin Deprez. Merci pour ton soutien. Ce titre de Docteur, tu le mérites presque autant que moi. Tu as su gérer toutes mes humeurs qui dépendaient bien évidemment de comment avançaient mes manips et comment s'était déroulées mes réunions. À travers ton amour pour moi, j'ai eu accès à une deuxième grande famille.

Merci à la grande famille Deprez de m'avoir accueilli et adopté. Vous m'avez apporté la chaleur qui me manquait dans ce pays à la météo imprévisible.

Enfin, j'aimerais remercier mes mamans, oui j'en ai deux, Maman Marthe et Maman Rose. L'une m'a mis au monde et les deux m'ont élevée. Vous m'avez laissé m'épanouir et développer mon caractère. Vous n'avez jamais essayé de me briser. Vous avez sacrifié tout ce que vous aviez pour que j'aie une bonne éducation. Vous avez toujours cru en moi et ceci m'a permis d'avancer à des moments les plus sombres de ma vie.

I dedicate this work to

My brother, Ngassam Nana Yvon Morrin

my baby, Deprez Naha Rose Stephanie

gone too soon leaving a big void in my heart

and

to my baby Annaya Cécile Ngassop Deprez

List of abbreviations

Abbreviation	Name	Abbreviation	Name
General			
2D	Two-dimensional	MOF	Metal organic framework
3D	Three-dimensional	M_n	Number average molar mass
Cat	Catalyst	M_p	Molar mass at the peak
cocat	Cocatalyst	M_w	Weight average molar mass
CC	Cyclic carbonates	ϕ	Diameter
CDC	carbodicarbene	P	Pressure
COV	Covalent organic framework	ROP	Ring-opening polymerisation
α CC	Exovinylene cyclic carbonates	RT	Room temperature
DFT	Density functional theory	SGP	Step-growth polymerisation
\mathcal{D}	Dispersity	SI	Supporting info
h	Hour	T	Temperature
IL	Ionic liquids	T_g	Glass transition temperature
LB	Lewis bases	T_m	Melting temperature
MIR	Medium infrared	TON	Turn-over number
Characterisation techniques			
ATR	Attenuated Total Reflectance	HSQC	Heteronuclear single quantum coherence spectroscopy
COSY	Correlation spectroscopy	IR	Infrared spectroscopy
DSC	differential scanning calorimetry	MS	Mass spectrometry
FTIR	Fourier transform infrared spectroscopy	NMR	Nucleus magnetic resonance

Abbreviation	Name	Abbreviation	Name
Chemicals and polymers			
ACN	Acetonitrile	LDA	Lithium diisopropylamide
BMIm	Butyl methyl imidazolium	Lev	Levulinate
nBu	Linear butyl	MIm	Methyl imidazolium
CNT	Carbon nanotubes	MTBD	7-Methyl-1,5,7-triazabicyclo[4,4,0]dec-5-ene
Cy	Cyclohexyl	NHC	<i>N</i> -heterocyclic carbene
DBU	1,3-Diaza-bicyclo-undec-7-ene	NHO	<i>N</i> -heterocyclic olefine
DIPEA	<i>N,N</i> -diisopropylethylamine	OAc	Acetate
DMAc	<i>N,N</i> -dimethylacetamide	OPh	Phenolate
DMAcC	4,4-Dimethyl-5-methylene-1,3-dioxolan-2-one	PC	Polycarbonate
DMPA	2,2-Dimethoxy-2-phenylacetophenone	Ph	Phenyl
DMF	Dimethylformamide	PHU	Polyhydroxyurethane
DMSO	Dimethyl sulfoxide	PU	Polyurethane
Et	Ethyl	PS	Polystyrene
EMIM	Ethylmethyl imidazolium	TBD	1,5,7-Triazabicyclo[4,4,0]dec-5-ene
Er-NHC	Expanded ring <i>N</i> -heterocyclic Carbene	TFE	Trifluoroethylene
Im	Imidazolium	THF	Tetrahydrofuran
Lact	Lactate	VAc	Vinyl acetate

Table of Contents

CHAPTER 0.....	1
General introduction and aims of the thesis	2
CHAPTER 1. Literature review.....	5
1. Introduction	7
2. Synthesis of exovinylene cyclic carbonates	9
2.1. Homogenous single activation catalysts	11
2.2. Dual activation by Ag- and Cu- based catalysts.....	17
3. Exovinylene cyclic carbonates in organic synthesis.....	20
3.1. Aminolysis.....	21
3.2. Alcoholysis	25
3.3. Hydrolysis.....	29
3.4. Carbonylation of ethanolamines	30
3.5. Addition of S-nucleophiles.....	31
3.6. Heck coupling	32
4. Exovinylene cyclic carbonates in macromolecular engineering.....	33
4.1. Polyurethanes.....	36
4.2. Polycarbonates	39
4.3. Sulphur-containing polymers	42
4.4. Vinyl-type copolymers.....	43
5. Conclusions and outlook.....	44
6. Supplementary information.....	48
CHAPTER 2.....	50
1. Introduction	52
2. Results.....	53
2.1. Catalyst synthesis.	53

2.2. Screening of the catalyst's activity.	55
2.3. Kinetic studies by in situ Raman Spectroscopy	62
2.4. Influence of reaction conditions.....	65
2.5. Screening of other propargylic alcohols.....	66
3. Conclusions	68
4. Experimental section	69
4.1. Material	69
4.2. Characterisation	69
4.3. Experimental procedures	70
5. Supplementary information.....	75
CHAPTER 3.....	83
1. Introduction	85
2. Results.....	87
2.1. Preliminary experiments.....	87
2.2. Screening of metal salts cocatalysts and solvent	88
2.3. Kinetic studies by infrared spectroscopy	89
2.4. Mechanism of the reaction.....	95
3. Conclusions	97
4. Experimental section	98
4.1. Materials.....	98
4.2. Analytical methods	98
4.3. Experimental procedures	98
5. Supplementary Information	100
CHAPTER 4.....	104
1. Introduction	106
2. Results.....	107

2.1. Synthesis of <i>oxo</i> -alkylcarbonates	107
2.2. Synthesis of poly(<i>oxo</i> -carbonate)s	112
3. Conclusions	121
4. Experimental section	122
4.1. Materials.....	122
4.2. Analytical methods	122
4.3. Experimental procedures	123
5. Supplementary informations	126
CHAPTER 5.....	137
1. Introduction	139
2. Results.....	140
2.1. Coupling of CO ₂ with alkyne-1,2-diols	140
2.2. Coupling of CO ₂ with alkyne-1,3-diols	144
2.3. Mechanistic investigation of the formation of the keto-carbonate and tetrasubstituted ethylene carbonate	149
2.4. Coupling of CO ₂ with alkyne-1,4-diols	156
2.5. Coupling of CO ₂ with alkyne-1,5- and 1,6- diols	160
2.6. Coupling of CO ₂ with internal alkyne-1- <i>n</i> -diol	165
3. Conclusions	166
4. Experimental section	167
4.1. Materials.....	167
4.2. Analytical methods	167
4.3. Experimental procedures	168
5. Supplementary information.....	174
CHAPTER 6.....	199
CHAPTER 7. Perspectives	204

1. Introduction	205
2. Results.....	207
2.1. Determining the optimum parameters for the synthesis of α CC in flow.....	207
3. Experimental section	210
3.1. Reagents.....	210
3.2. Apparatus.....	210
3.3. Experimental procedures.....	211
Bibliography	212

CHAPTER 0

General introduction and aims of the thesis

General introduction and aims of the thesis

Polycarbonates (PCs) belong to some of the world-leading polymers that are industrially produced by polycondensation. They are widely used in aircraft or automotive applications (windows, etc.), in safety equipment (helmets, bullet proof glass, etc.), data storage (DVD), coatings, etc. However, their industrial production requires the use of toxic compounds such as phosgene, high temperatures, and is not compatible with the introduction of some functional groups along the polymer backbone.

Making plastics more sustainable by valorising CO₂ as a cheap, inexhaustible and renewable feedstock imposes itself as a strategic driver for developing low carbon footprints materials. When this PhD thesis started, two main routes were used to prepare PCs from CO₂: (i) the (co)polymerisation of CO₂-based building blocks or (ii) the direct copolymerisation of CO₂ with appropriate comonomers. In the first approach, molecules which can polymerise such as (cyclic) carbonates are transformed into PCs by the catalysed ring-opening polymerisation (ROP) of cyclic carbonates^[1-4] or the polycondensation of (a)cyclic carbonates with diols^[5,6] Although diverse PCs are prepared by polycondensation by varying the diol structure, harsh reaction conditions are employed, and the released alcohols have to be removed to push the process to completion.^[5] In contrast, the ROP process yields well-defined PCs under milder conditions. Although the ROP of 6-membered cyclic carbonates is facile, that of the more stable 5-membered cyclic carbonates (5CCs) (i.e. the most common synthon prepared by coupling CO₂ to epoxides)^[7,8] is challenging. Catalysts developments have allowed the synthesis of PCs from 5CCs but examples were scarce when this thesis work started.^[9,10] The second strategy for PCs consisted in the direct catalysed copolymerisation of CO₂ with epoxides or oxetanes.^[11-15] However, the variety of functional groups made available on the PCs backbone was very limited. The synthesis of PCs from CO₂ and diols was also shown feasible, although harsh reaction conditions were used and only low molar mass polymers were produced.^[16,17] 5CCs prepared by the CO₂/epoxide coupling reaction were certainly the most interesting and easily accessible CO₂-sourced monomers for PCs, however, their low reactivity prevented the PCs preparation by polyaddition of bis-5CCs to diols under mild conditions.

In 2017, our research group reported a new process for the preparation of a novel family of regioregular PCs (i.e. poly(*oxo*-carbonate)s) by the facile organocatalysed polyaddition of CO₂-sourced bis(α -alkylidene cyclic carbonate)s (bis α CCs) with diols under ambient conditions.^[18] These bis α CCs were prepared by the organocatalysed carboxylative coupling of CO₂ to bis(propargylic alcohol)s. The presence of the exocyclic olefinic groups in bis α CCs enhanced the reactivity of the 5-membered cyclic carbonates against various nucleophiles (such as alcohols) and selectively formed one regioisomer. The thermodynamic driving force for this regioselective ring-opening relies on the formation of an enol species that rapidly rearranges into a more stable β -keto tautomer.^[19] By varying the structure of the bis α CCs and the diols,

a large variety of poly(*oxo*-carbonate)s was in principle accessible, opening new perspectives of applications for CO₂-based PCs.

The goal of my PhD thesis was to investigate the fundamentals to permit the synthesis of these new PCs in a one-pot process, wherein bis α CCs are produced *in-situ* and directly involved in polymerisation. I will thus study how the terpolymerisation of CO₂, the bis(propargylic alcohol) and the diol can be achieved. The main objectives are to first understand and optimise each step of the process separately, before merging the optimised systems to achieve the preparation of PCs in a one-pot process. The project will therefore focus on (i) the identification of highly active organocatalysts for the efficient and selective synthesis of bis α CCs by carboxylative coupling of CO₂ to bis(propargylic alcohol)s, (ii) the identification of the optimal conditions for the polyaddition of bis α CCs and diols, and (iii) the terpolymerisation of CO₂ with diols and bis(propargylic alcohol)s using the appropriate operating conditions identified in the previous steps. This project is highly challenging as step-growth polymerisations are highly dependent on the perfect stoichiometry of the reactive groups and very high monomer conversions must be attained to obtain high molar mass polymers. Any side reactions will result in a deviation from the perfect stoichiometry and hence cause the termination of the domino terpolymerisation.

This thesis is divided into five main chapters with specific objectives that are illustrated in **Scheme 1** and discussed below.

In chapter one, we summarise the recent advances made in the synthesis of exovinylene cyclic carbonates (α CCs) by coupling CO₂ to propargylic alcohols, with a particular focus on the catalysts needed for their preparation. We also discuss the unique reactivity of these CO₂-based heterocycles for synthesising diverse organic building blocks and (functional) polymers. Lastly, we address the challenges and the future perspectives in the field.

In chapter two, we explore the design of an efficient catalytic system based on ionic liquids or organic salts for the selective synthesis of exovinylene cyclic carbonates (α CCs). We show how by carefully choosing the cation (ammonium) and anion (carboxylates, alcoholates) component of the organic salt, we can tune both the activity and the selectivity of the catalyst. The best catalytic system is then evaluated for the synthesis of various α CCs.

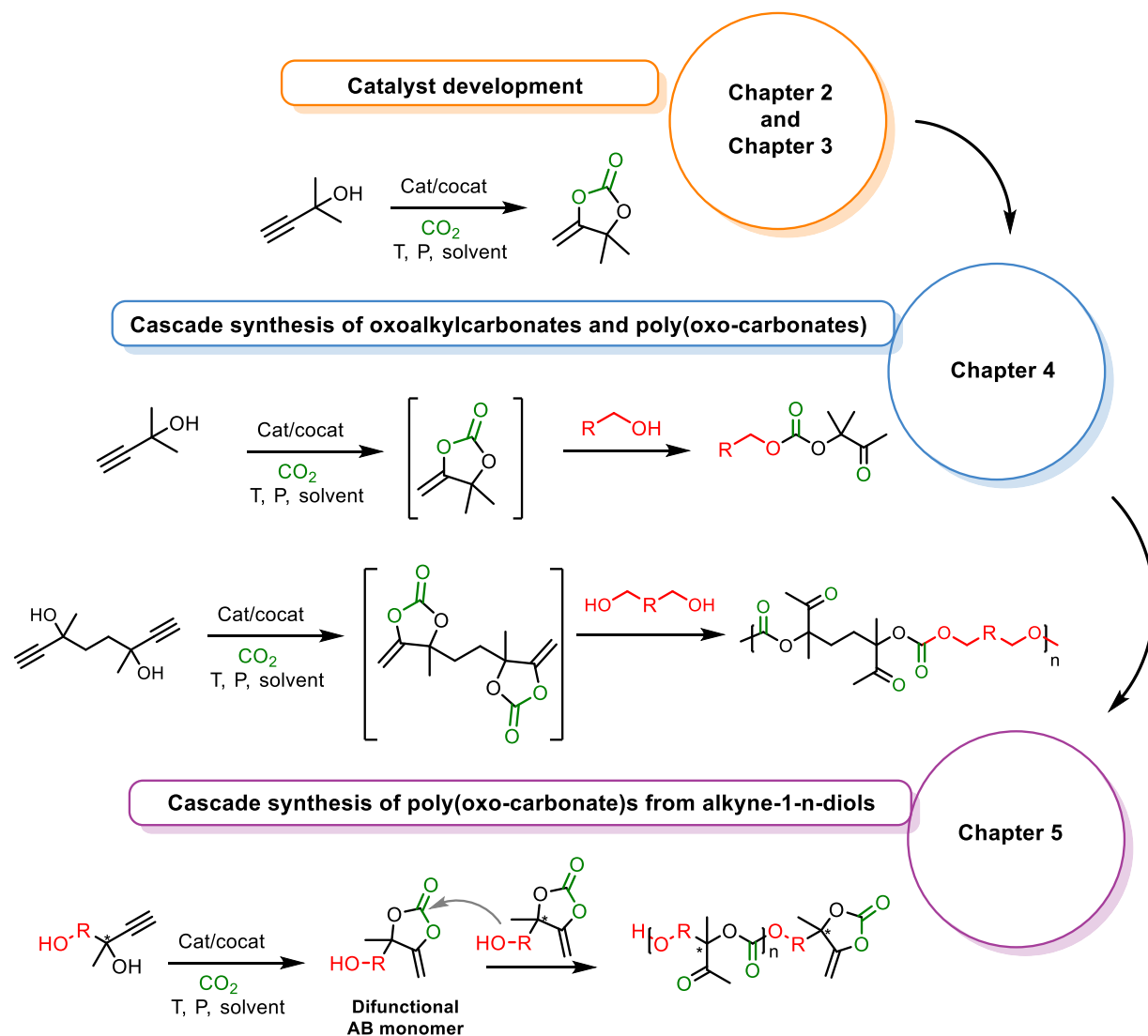
In chapter three, we further optimise the catalytic system identified in chapter 2 by incorporating a metal cocatalyst (AgX or CuX) that can activate the triple bond and is expected to allow the preparation of exovinylene cyclic carbonate monomers under milder conditions. Kinetic studies by FT-IR spectroscopy and a detail mechanistic study by DFT are conducted for the model reactions.

In chapter four, we investigate the cascade synthesis of simple linear *oxo*-alkylcarbonates by reaction of a propargylic alcohol, CO₂ and a monoalcohol with the goal to identify the optimal reaction conditions for high yield and selectivity, a prerequisite prior to evaluating the process for the polymerisation. We then utilise these reaction conditions for the terpolymerisation of

bispropargylic alcohols, CO₂ and diols. The influence of reaction parameters such as temperature, pressure and solvent are evaluated, and various diols are tested for the terpolymerisation to extend the substrate scope.

In order to avoid some stoichiometry issues encountered in chapter 4, we then explore in chapter five the synthesis of new alkyne-1-n-diols and their utilisation for producing poly(oxo-carbonate)s by copolymerisation with CO₂. It is hypothesised that the *in-situ* carboxylation of the alkyne-1-n-diols will provide an exovinylene cyclic carbonate bearing an alcohol function, thus an AB monomer, that is expected to homopolymerise. Various alkyne-1-n-diols are prepared and tested for the reaction. Kinetics studies supported by DFT computation enabled to explain the formation of some unexpected products.

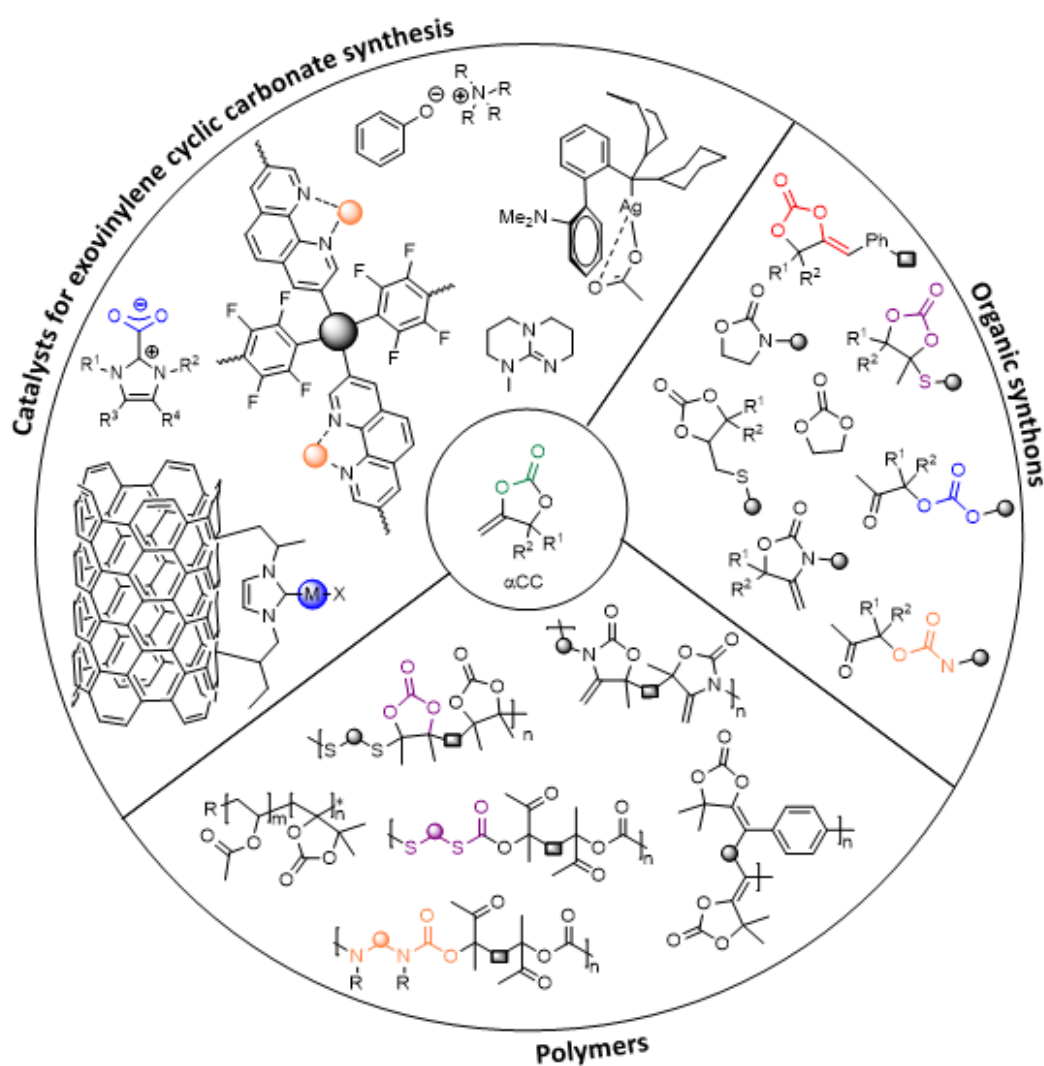
This thesis ends with a general conclusion and some perspectives. We discuss the limitations encountered with the terpolymerisation approach and we propose a potential avenue.



Scheme 1. Summary of the objectives of the different chapters.

CHAPTER 1. Literature review

Exovinylene cyclic carbonates: From synthesis to utilization in modern chemistry and polymer sciences



Chapter 1

This chapter is published as a review article in;

Charlene Ngassam Tounzoua, Bruno Grignard and Christophe Detrembleur. *Angewandte Chemie, International Edition* <https://doi.org/10.1002/anie.202116066>

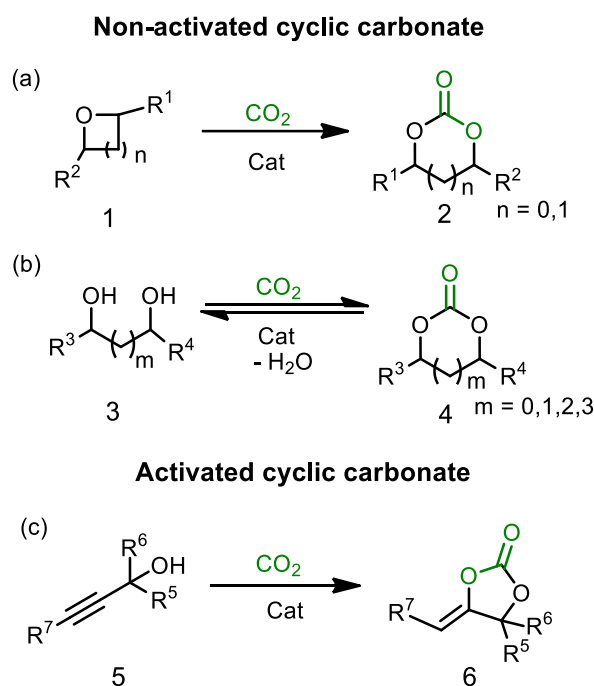
Table of contents

1. Introduction	7
2. Synthesis of exovinylene cyclic carbonates	9
2.1. Homogenous single activation catalysts	11
2.2. Dual activation by Ag- and Cu- based catalysts	17
3. Exovinylene cyclic carbonates in organic synthesis	20
3.1. Aminolysis	21
3.2. Alcoholysis	25
3.3. Hydrolysis	29
3.4. Carbonylation of ethanolamines	30
3.5. Addition of S-nucleophiles	31
3.6. Heck coupling	32
4. Exovinylene cyclic carbonates in macromolecular engineering	33
4.1. Polyurethanes	36
4.2. Polycarbonates	39
4.3. Sulphur-containing polymers	42
4.4. Vinyl-type copolymers	43
5. Conclusions and outlook	44
6. Supplementary information	48

1. Introduction

On the path to sustainability and circularity, the upgrading of CO₂ into value-added organic scaffolds and polymers has become a vibrant field of research. The development of new catalytic systems and efficient CO₂ activation modes have enabled to overcome the kinetic and thermodynamic stability of this highest oxidised state of carbon. A variety of products are now accessible, ranging from commodities (methanol, formic acid, urea) to more sophisticated ones (organic carbonates, polyurethanes, polycarbonates). Amongst the multitude of CO₂-sourced organic molecules, cyclic carbonates have emerged as important building blocks for fine chemistry (e.g. to construct carbamates, key intermediates for the pharmaceutical and agro industries), polymer design (e.g. polyols used to formulate polyurethane foams), or as solvents and electrolytes for batteries.^[20]

Three main routes are implemented to prepare cyclic carbonates by the direct reaction of CO₂ with a substrate (**Scheme 1**).



Scheme 1. Synthesis of cyclic organic carbonates (a) from oxiranes or oxetanes (b) diols or (c) propargylic alcohols.

The first and most widely developed method consists in coupling CO₂ to oxiranes in the presence of appropriate metal- or organo-catalysts.^[21–25] The 100% atom economy [3+2] fixation of CO₂ onto epoxides affords selectively and quantitatively 5-membered cyclic carbonates even under mild and solvent-free conditions.^[7] Six-membered cyclic carbonates are also accessible from oxetanes.^[26–29] The great availability of oxiranes from petro- or bio-based origin thus gives access to a large library of cyclic carbonates with diverse structures and functionalities.^[30]

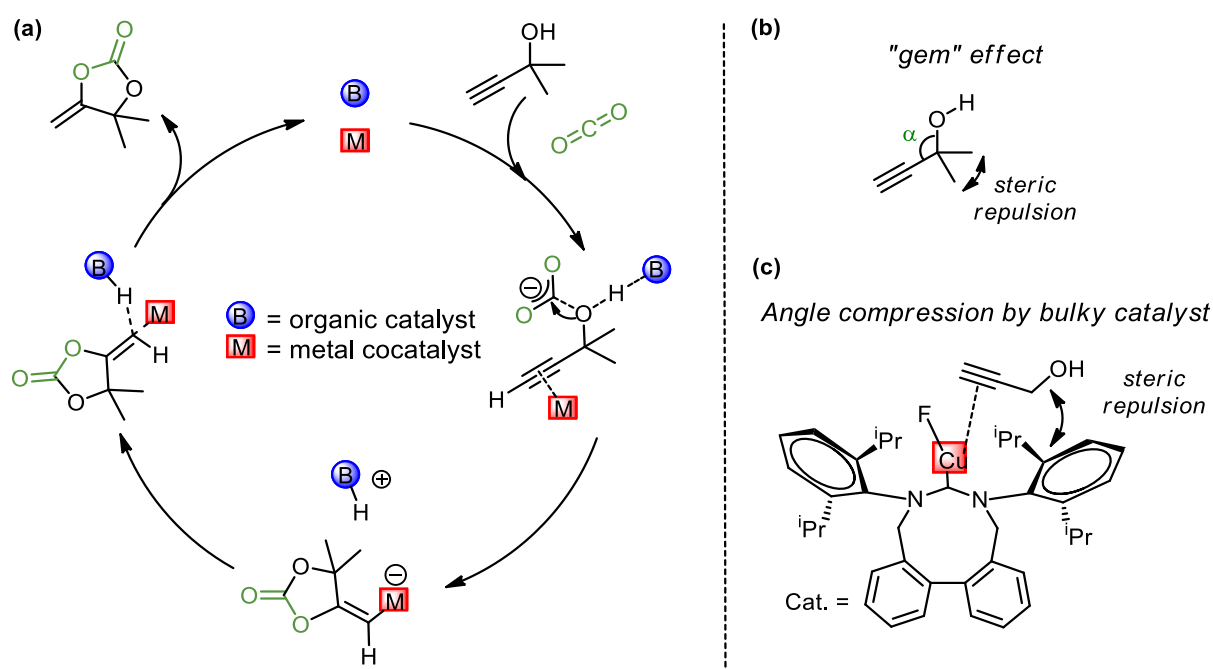
Chapter 1

The second approach involves the challenging condensation of CO₂ with polyols, which gives access to 5- and 6-membered cyclic carbonates but also to larger 7- or 8-membered cyclic carbonates which are not achievable with the former.^[31–36] Although potentially the most interesting in terms of valorisation of natural polyols (e.g. glycerol, sorbitol), this reaction remains less explored. Indeed, the reaction is thermodynamically limited by the release of water, whose removal is mandatory to prepare the cyclic carbonates in quantitative yields. Some strategies have been developed to partly overcome this problem, notably by activating the alcohol using metal-based catalysts in combination to dehydrating agents,^[36,37] or by using bases (tertiary amine or superbases)^[38] in combination with alkylating agents (e.g. alkyl halides, sulfonyl halides).^[32,35] Nonetheless, these processes require harsh conditions and release considerable wastes, rendering them not sustainable.

The third route provides α -exovinylene cyclic carbonates (α CCs) by the carboxylative coupling of CO₂ with propargylic alcohols. These synthons are promising and appealing, even from an industrial perspective, as they offer multiple opportunities in organic and polymer chemistry for the design of advanced CO₂-derived products. The presence of an exocyclic olefin renders these heterocycles highly reactive towards S-, N- and O-nucleophiles via the regioselective ring-opening of the cyclic carbonate, but also towards radicals or aryl halides via the addition onto the olefin. This makes them unique and central building blocks to design linear or cyclic carbamates and carbonates, and important polymer families (e.g. polyurethanes, polycarbonates, polyvinyls or sulfur-containing polymers). This chapter discusses the general concepts for the synthesis of this emerging class of cyclic carbonates and their exploitation in organic synthesis and polymer sciences.

2. Synthesis of exovinylene cyclic carbonates

The mechanism of formation of α CCs by the catalysed carboxylative coupling of CO_2 to propargylic alcohols is illustrated in **Scheme 2**. It involves first the formation of a carbonate salt intermediate via the reaction between a propargylic alcohol, CO_2 and a base; the base activating the alcohol for the carbonation. Then, the carbonate ion undergoes a conformational rotation, followed by a ring-closure step via an intramolecular nucleophilic addition onto the triple bond. The resulting exocyclic alkenyl anion generates the cyclic carbonate upon protonation and completes the catalytic cycle.^[39,40] Alternatively, a dual activation mechanism makes use of a metal-based cocatalyst that coordinates to the triple bond and facilitates the cyclisation of the carbonate ion, yielding an alkenyl metal intermediate, which gives the α CC upon proto-demetalation.^[41]

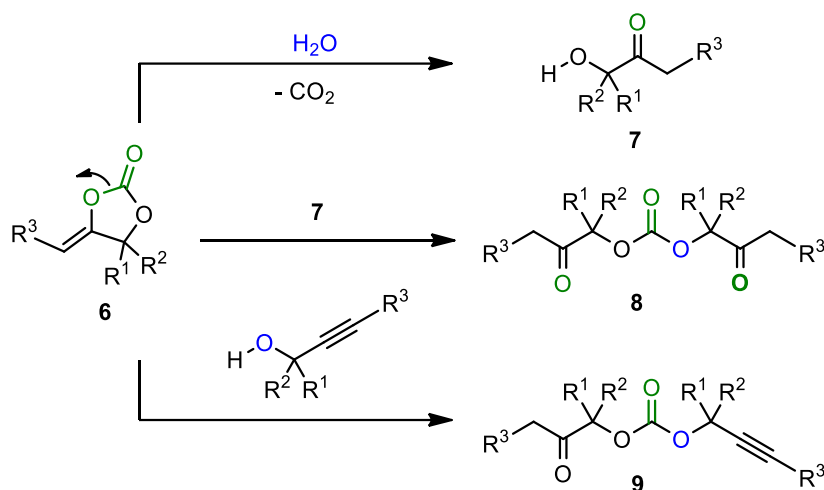


Scheme 2. (a) General mechanism for the formation of α CC by carboxylative cyclisation of propargylic alcohol shown for a dual activation mechanism, (b) illustrations of the steric repulsions induced by the "gem" or (c) catalyst-driven "angle compression" effects.

The carboxylative coupling was long restricted to tertiary propargylic alcohols, the driving force of the carboxylation being the presence of the two *gem* substituents onto the substrate that creates a compression angle via the Thorpe Ingold effect, hence facilitating the carbonate ring closure.^[42] With secondary and primary propargylic alcohols, this effect is absent, rendering their cyclisation more challenging. To surpass these hurdles, recent catalytic findings by Schaub et al. utilise dual catalysts made of a metal salt and a sterically congested ligand which provokes an angle torsion of the substrate similar to the "gem-effect" and allows

for the efficient carboxylative cyclisation of secondary and primary propargylic alcohols^[43] (**Scheme 2 (c)**).

The choice of the catalyst and the reaction conditions are also crucial to prevent side reactions commonly associated to this transformation, i.e. the hydrolysis of α CC by residual water into the hydroxy ketone **7**, the alcoholysis of α CC either by the in situ formed hydroxyketone or by the unreacted propargylic alcohol yielding the corresponding acyclic carbonates **8** or **9** (**Scheme 3**).



Scheme 3. Secondary reactions of the carboxylation of propargylic alcohols by CO_2 .

In the next section, we first benchmark the performances of a selection of the most relevant homogeneous catalysts, using customised spider charts highlighting their strengths and weaknesses, without needing extensive discussions. While these illustrations give an “instant” comparison of the activities of state-of-the-art catalysts, it is important to underline that most of the works are conducted under different operating conditions which complexifies this benchmarking. Furthermore, parameters that can be highlighted as weaknesses (long reaction time, high temperature, low yields...) might result from non-optimised conditions. Therefore, we believe that these charts will constitute an elegant approach to provide guidelines to the readers to identify the most relevant parameters to turn the less efficient catalysts into more competitive systems. The data are also presented in tables (see SI) for the readers who are more adept to the traditional methods.

For ease of comparison and to identify the main trends, we have selected works dealing with the formation of a model α CC that is largely reported in the scientific literature, 4,4-dimethyl-5-methylene-1,3-dioxolan-2-one (DMACC) prepared by coupling CO_2 to 2-methyl-3-butyn-2-ol.

2.1. Homogenous single activation catalysts

Organic bases

Phosphines and nitrogen bases such as amines, amidines and guanidines were evaluated for the transformation of CO₂ into αCCs (**Figure 1**).

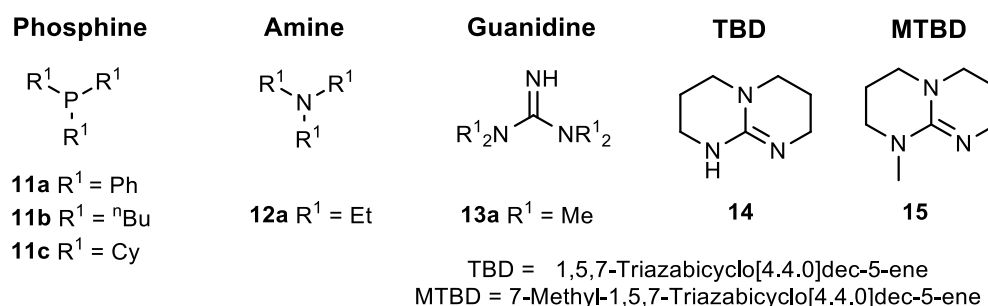


Figure 1. Selected examples of organic bases used as catalysts for the carboxylative coupling of CO₂ with propargylic alcohols.

Phosphines provided DMACC with yields of 8-99% within 8-15 h using 50-100 bar of CO₂ at 100-140 °C and a catalyst loading of 5-9 mol%.^[44-46] In his seminal work, Dixneuf highlighted a significantly higher activity of P(C₄H₉)₃ compared to triphenyl- or tricyclohexyl-phosphine.^[45]

The weak base NEt₃ was inefficient in catalysing the formation of DMACC in organic medium or under neat conditions (T = 30-80 °C, PCO₂ = 5-10 bar, catalyst loading = 0.25-1 eq, t = 5-10 h).^[47] Superbases such as TBD or MTBD were shown by Ca et al. to promote the total conversion of the propargylic alcohol at 10 mol%, 100 °C for 24 h with 50 bar of CO₂, however the reaction was non-selective, with a DMACC yield of only 21 to 25%. Both bases favored the side alcoholysis of DMACC by the propargylic alcohol or the hydroxyketone.^[48] The selectivity of MTBD for DMACC was significantly improved by reducing the catalyst loading to 1 mol% and the temperature to 60 °C at a PCO₂ = 30 bar or by working under diluted conditions in acetonitrile for a shorter time at 80 °C, 30 bar and a catalyst loading of 5 mol%.^[49]

The respective performance of selected organocatalysts are benchmarked in **Figure 2**. On the basis of the data reported under conditions specific to each catalyst, tributylphosphine emerged as one of the most efficient base, affording DMACC selectively with a yield close to 100% in a reasonable time frame. Nevertheless, moderate to high pressure and temperature were required. With nitrogen bases, the basicity of the catalyst is a crucial factor. Low pKa amine displayed no catalytic activity while stronger (super)bases such as TBD and MTBD catalysed the reaction, however with a moderate selectivity for DMACC. Therefore, the ideal organic base should display a sufficient basicity to activate the OH moiety of the propargylic alcohol and facilitate the fixation of CO₂. However, the basicity should remain low enough to avoid competitive side alcoholysis of the DMACC with the unreacted precursors or hydroxylated side-products (cf. **Scheme 3**).

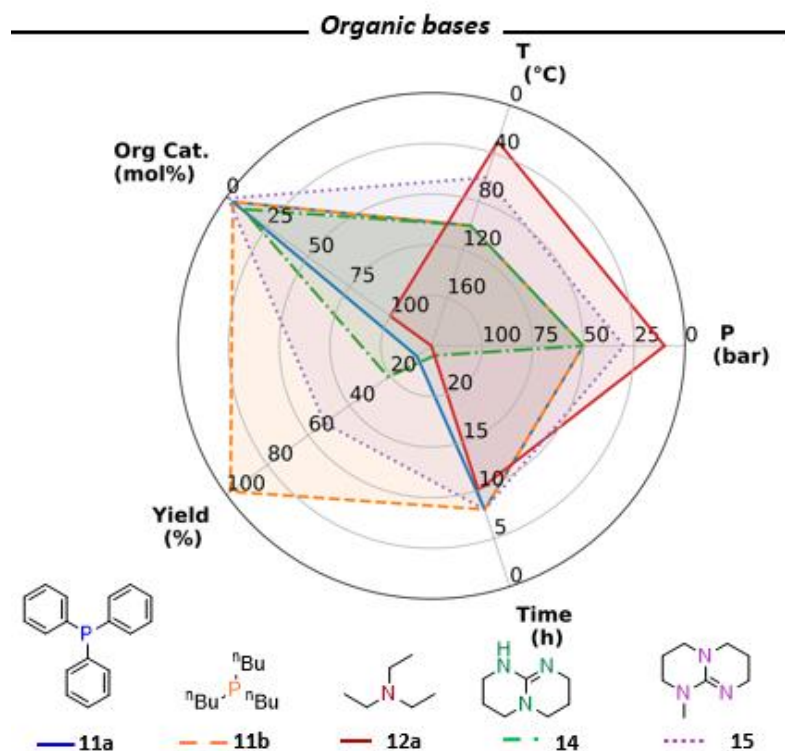


Figure 2. Comparison of the activity of some selected bases for the synthesis of DMACC. Data used for plotting presented in **Table S1**.

Lewis base-CO₂ adducts

Owing to the high electrophilicity of the carbon atom in CO₂, Lewis bases (LB) of nitrogen containing heterocycles can react with CO₂ to form zwitterionic adducts. The diversity of the LB-CO₂ adducts and the easy structural modulation of their flanking groups make them efficient catalysts in organic synthesis, including for CO₂ conversion. The most common LB-CO₂ adducts are based on the (unsaturated) *N*-heterocyclic carbene template (NHC-CO₂) (**Figure 3**). NHC-CO₂ adducts catalysed the fixation of CO₂ onto propargylic alcohols at 60-80 °C and 45-60 bar. DMACC was obtained with an excellent yield of 99% in 15 h, especially with the catalyst **16c** at a loading of 5 mol%.^[50] Besides, other Lewis bases-CO₂ adducts have been designed. The carbodicarbene-CO₂ (CDC-CO₂, catalyst **17d**) appeared less efficient than NHC-CO₂ adducts and afforded DMACC in 94% yield within 12 h at a loading of 5 mol% and 20 bar of CO₂ at 80 °C.^[51] The most efficient catalytic systems were *N*-heterocyclic olefin-CO₂ (NHO-CO₂)^[52], alkoxide functionalised imidazolium betaines-CO₂ (AFIB-CO₂)^[53] or tetrahydropyrimidin-2-ylidene-CO₂ derived from 5-diazabicyclo[4.3.0]non-5-ene (DBN-CO₂).^[54] All the Lewis base-CO₂ adducts especially **18d**, **19d** and **20a** operated under smoother conditions compared to NHC-CO₂ (20 bar of CO₂, T = 60 °C, catalyst loading of 5 mol% except AFIB-CO₂ (2 mol%)) and provided DMACC with excellent yields of 91-96% in 1 to 5 h. **Figure 4** benchmarks the activity of the various LB-CO₂ adducts which evolves in the order CDC-CO₂ < NHC-CO₂ < NHO-CO₂ ~ AFIB-CO₂ ~ DBN-CO₂.

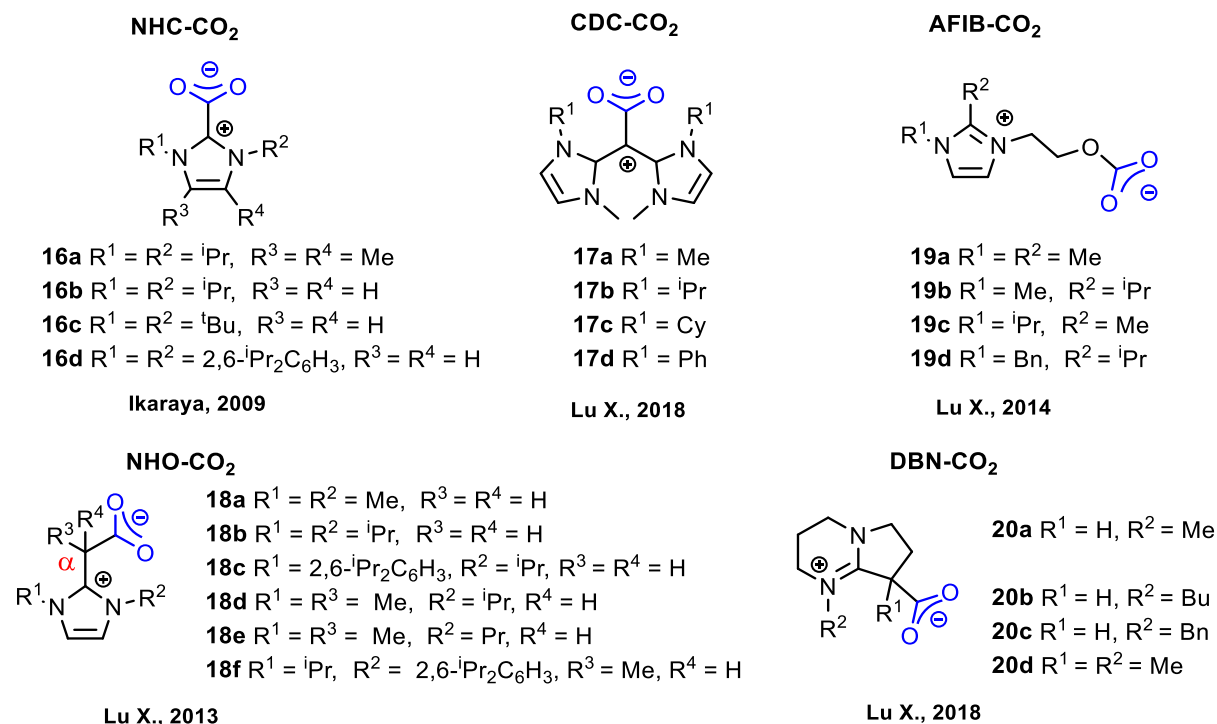


Figure 3. Selected examples of LB-CO₂ diadducts used for the carboxylative coupling of CO₂ to propargylic alcohols.

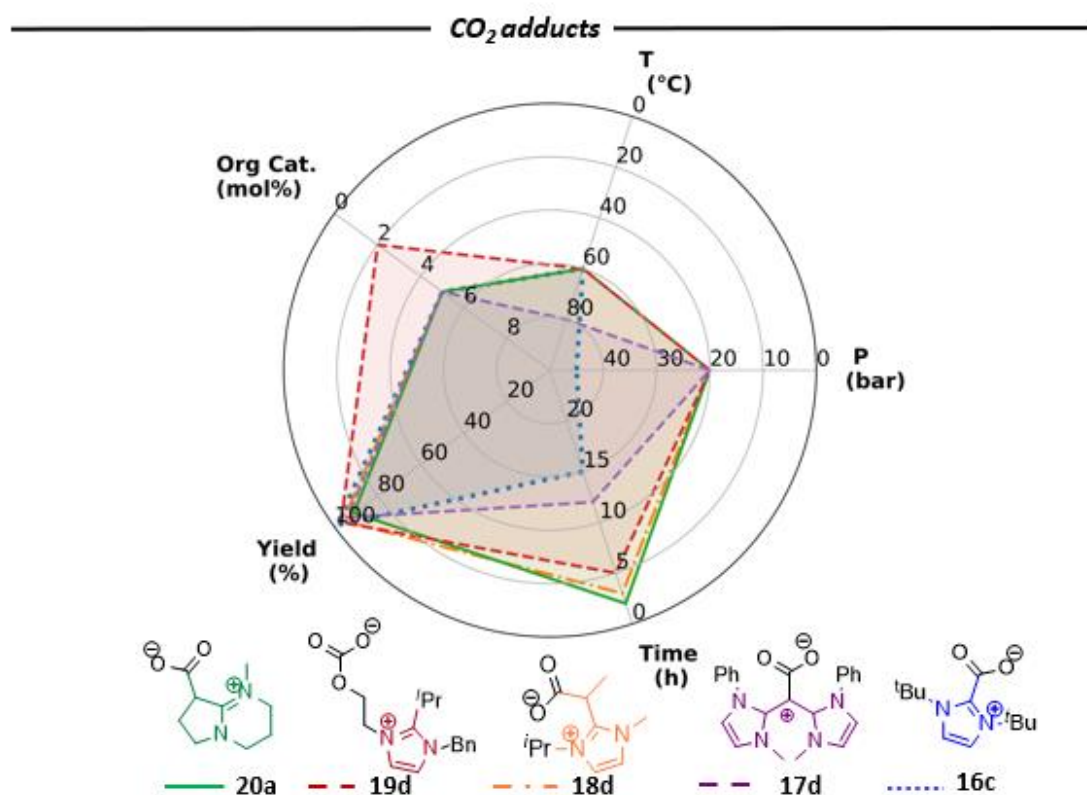


Figure 4. Comparison of the activity of some selected Lewis-base adducts for the synthesis of DMACC. Data used for plotting presented in Table S2.

Some authors rationalised the higher activity observed for NHOs in comparison to NHCs by the increased nucleophilicity of the α -carbon in NHOs arising from the aromatisation of the *N*-heterocyclic ring in *N,N*-disubstituted 2-methylene imidazolines. In addition, they proposed that the longer $C_{\text{carboxylate}}-C_{\text{NHO}}$ bond in comparison to $C_{\text{carboxylate}}-C_{\text{NHC}}$ as well as the presence of electron donating (bulky) substituents onto their α carbon, rendered NHO-CO₂ adducts less stable and hence more prone to liberate free carbene.^[55] Ikariya et al. also demonstrated the existence of a cut-off temperature for NHC-CO₂ adducts at 60 °C and 45 bar, above and beyond which the yield of the α CC decreased.^[50] This observation was further confirmed by Tommassi, who obtained lower α CC yields when working at a higher temperature of 100 °C and 60 bar.^[56] Reducing the catalyst content influenced the selectivity of the reaction, with the side-formation of acyclic carbonates. The high reactivity of DBN-CO₂ adducts is probably due to the high basicity of free DBN. It has to be noted that phosphorus ylides-CO₂ (P-Ylides-CO₂) were also tested, however they are not included in this comparative description because they have not been tested for the preparation of DMACC.^[57] However, their catalytic activities do not differ from those of NHC-CO₂ that were tested under identical conditions using a similar substrate.

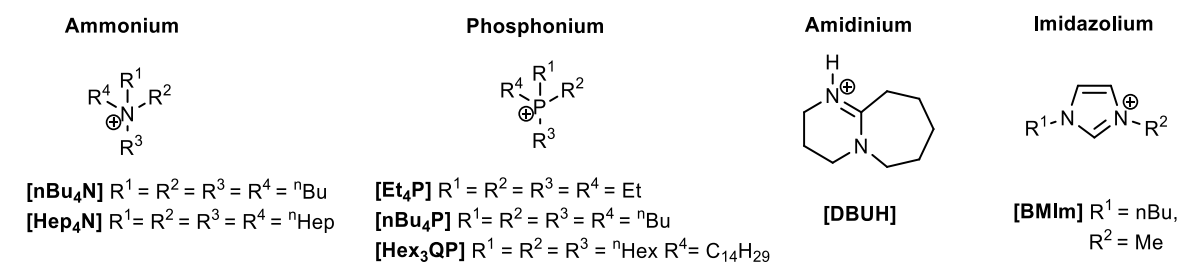
Ionic liquids

Due to their intrinsic properties such as non-volatility, recyclability, tunability and thermal stability, ionic liquids (IL) have gained popularity for CO₂ transformation. Indeed, their catalytic activity is easily modulated by the nature of the cation/anion pair, that influences the salt dissociation and hence the basicity of the anion. Moreover, ILs show a propensity to solubilise significant amount of CO₂. Various ILs made of phosphonium^[58], imidazolium^[41], ammonium^[59] or amidinium^[60] cations, and carboxylate, alcoholate/phenolate, halide, azide, thio-/iso-cyanate, cyanide, azole, imidazolide anions or featuring multiple active sites^[61] have been reported in the literature to catalyse the carboxylative coupling of CO₂ with propargylic alcohols (**Figure 5**).

To benchmark the activity of ILs, we have selected those that are used in catalytic amount (5 mol%) only. The reason being that at high loading, the IL may influence the reactions by acting as a solvent potentially influencing the overall reaction mechanism, e.g. by (de)stabilising some transition states/reactive intermediates. Acetate-type ILs are chosen as representative organocatalysts to evaluate the influence of the cation on their performance. This is justified by the rather large scope of acetate/cation pairs that were tested under strictly identical experimental conditions (T = 80 °C, P_{CO₂} = 50 bar, t = 6 h), which facilitates the benchmarking of the ILs activity.

As illustrated in **Figure 6**, the DMACC yield increased with the cation structure in the order [N-butyl-Imidazolium] < [DBUH] < [nBu₄P⁺] < [nBu₄N⁺]. [nBu₄N⁺][Ac⁻] was identified as the only ILs that afforded DMACC in a quantitative and selective way, while the other systems were poorly active (yield of DMACC < 20%) or even inactive.^[59]

Cations



Anions

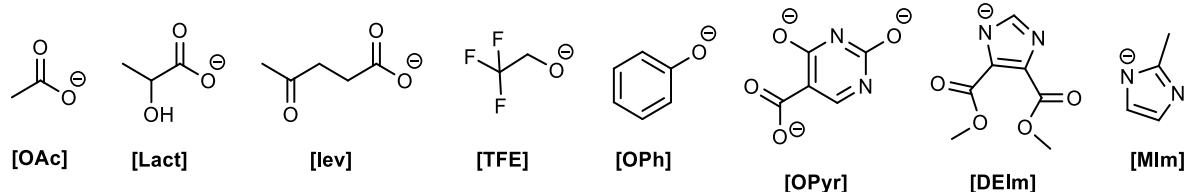


Figure 5. Selected examples of the most used cations and anions for the design of ionic liquid catalysts.

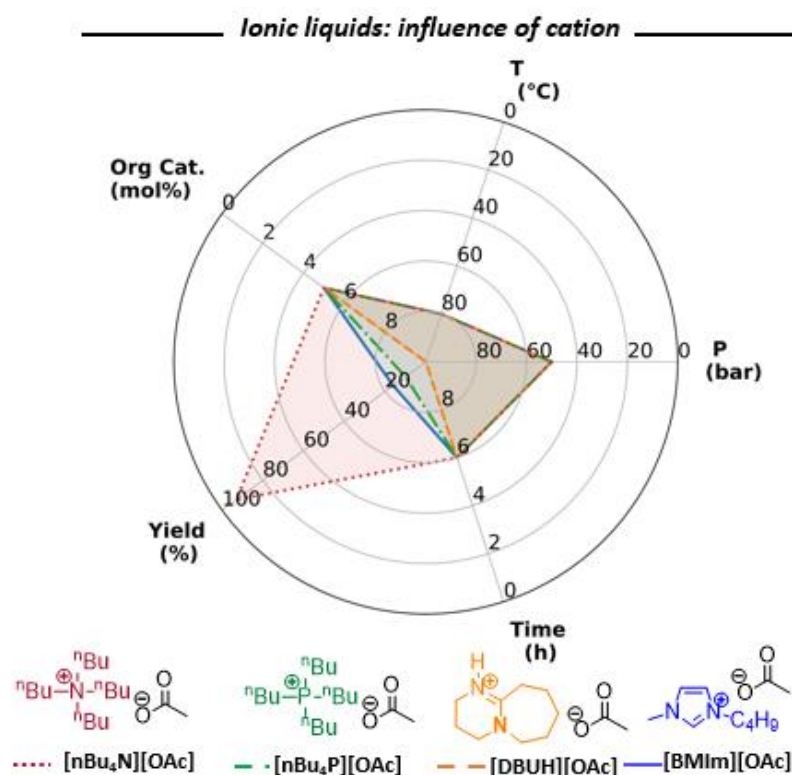


Figure 6. Comparison of the activity of some selected ionic liquid catalysts for the synthesis of DMACC: influence of the nature of the cation. Data used for plotting presented in **Table S3**.

The influence of the alkyl substituent of quaternary ammoniums also revealed an optimum chain length in C₄ above and beyond which the conversion in propargylic alcohol declined. This is the result of a complex interplay between ion pair dissociation and steric hindrance. Note that this trend is only valid for acetate-type ILs with ammonium cations, as comparable studies for other types of ILs differing by the structure of both the cation and the anion are

not reported. Therefore, any generalisation of this trend to other IL families might give inadequate guidelines to tailor the next generation of more active organocatalysts.

The basicity of the anion is a key parameter in determining the reaction rate. Generally, the higher the basicity, the faster the reaction rate. This is reflected in **Figure 7** wherein the very low basicity of fluoride gave the lowest DMACC yield (~10%). Switching to anions with stronger basicity such as cyanide ($pK_a = 7$), phenolate ($pK_a = 9.95$) or imidazolide ($pK_a = 9.2$) significantly accelerated the reaction and enabled quantitative conversion, unfortunately, at the detriment of the selectivity in DMACC which decreased to 87-93%.

Anions of intermediate basicity such as azide ($pK_a = 4.6$) or carboxylates ($pK_a = 4.6-4.9$) provided ILs of moderate activity, nonetheless, they were highly selective for DMACC. The above observations are in line with Chen's postulate, which proposed an optimum pK_a value of the anion of ~ 7.6 , above which the selectivity in the α CC significantly declined, and beyond which the reaction rate slowed down.^[62] The pK_a value of the anions thus provides a guide to design ILs for the selective conversion of CO_2 into α CC.

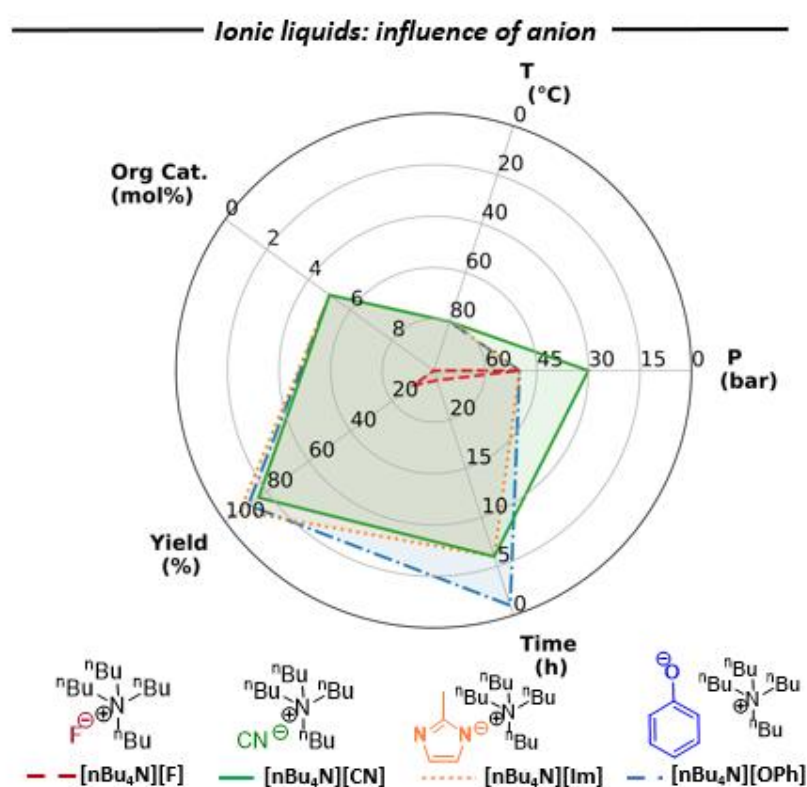


Figure 7. Comparison of the activity of some selected ionic liquid catalysts for the synthesis of DMACC: influence of the nature of the anion. Data used for plotting presented in **Table S4**.

Furthermore, the catalytic activity also depends on the catalyst dissociation in the reaction medium. Determining relationships between the catalyst performance and its dissociation requires ion pair dissociation constants and/or ions partial charges of ILs, which unfortunately are not available in the literature. Thus, only general considerations are given to guide the reader in designing more competitive IL catalysts. According to Watanabe, the "ionicity" of

ILs reflects the strength of coulombic interactions upon ion pairing.^[63] This is correlated to the Lewis acidity of the cation and the basicity of the anion, both of which are dependent on their ionic structure. The ionicity and consequently the dissociation ability of ILs is favoured by selecting weak basic anions and acid organic cations. Beside the steric hindrance, longer alkyl chain lengths usually found in the organic cations impact van der Waals interactions. These may create segregation of the ILs into polar and non-polar domains, affecting not only the partial charges of the ions but also their solvation.^[64] Last but nonetheless, the reactant, i.e. the propargylic alcohol, may also act as a polar solvent for the catalyst. Its OH moiety creates a solvation shell around the anion via H-bonding interactions, producing solvent-separated ion pairs.^[64]

2.2. Dual activation by Ag- and Cu- based catalysts

A large variety of transition metal salts derived from ruthenium^[65], cobalt^[66], palladium^[67], zinc^[47] have been tested for the envisioned reaction, however, the silver and copper ones are the most preferred cocatalysts in the literature, justifying the focus for further reviewing. Nonetheless, one can refer to Vessaly's review^[68] for details on the other metal-based dual systems. CuX, AgX or Ag₂Y (with X = I⁻, Br⁻, Cl⁻, SO₄⁻, NO₃⁻, OAc... and Y = CO₃²⁻, WO₄²⁻, O²⁻) are typical salts used in combination with basic additives (ILs, PPh₃, nitrogen bases) to drive the formation of DMACC under neat conditions or optionally in a solvent such as ACN, DMF or THF. Three main catalytic scenarios have been identified:

- low activity dual catalysts relying on a low content of Ag or Cu salts (2 mol%) with (large) excess of IL (50 to 200 mol%) that simultaneously acted as a base, a solvent and CO₂ absorbent. Such type of catalyst provided DMACC with yields > 91-97% in 2.5-8 h at 25 to 120 °C and 1 to 10 bar of CO₂.^[41,69,70]
- moderate activity catalysts based on a high loading of metal salt (10 mol%) and basic ILs (20 mol%) that delivered DMACC with 91-93% yield in 5-24 h at 30 °C and 1 bar CO₂.^[62]
- highly active catalysts consisting in a (very) low loading of Cu or Ag salts (1-5 mol%) and some base additives (1-5 mol %) that produced DMACC with 89-100% yield in 1-12 h at 25-60 °C and 1-15 bar of CO₂.^[71-73]

The literature survey highlights some key features and trends that may guide the design of more active systems. Whatever the organic catalyst, the activity of dual catalysts made of Cu(I) or Ag(I) halide salts is influenced by the counter anion and evolves in the order I⁻ > Br⁻ > Cl⁻ ^[41,71,74,75] in line with the easier dissociation ability of iodide vs bromide or chloride salts. In addition, Han et al. illustrated that introducing oxo-moiety^[75] within the microstructure of carboxylate-type ILs or using acetone as solvent further improved the dissociation of CuI, due to the coordination ability of the carbonyl group with Cu⁺. One also notes the crucial role of WO₄²⁻ anion, which provides a unique interaction with CO₂ that is beneficial for the CO₂ insertion and carbonate formation.^[73] Using acetate type or PPh₃ as organic catalysts,

Verpoort^[41] and He^[76] showed that cocatalytic activity of the silver metal salts evolved in the order $\text{AgI} > \text{Ag}_2\text{CO}_3 > \text{AgOAc}$.

Finally, **Figure 8** underlines the role of the base cocatalyst on the formation of DMACC using AgOAc, which is one of the most frequently used Ag salts. ILs of weak basicity [PHex₃Q][Im] required large amounts, and drove the reaction slowly to completion, while operating under ambient conditions (rt and CO₂ pressure of 1 bar). The ammonium salt [nHept₄N][Br] appeared as a good compromise in terms of activity under mild conditions. However, as this salt displays no basicity, we believe that an exchange between the acetate and bromine anions occurred in the reaction medium yielding AgBr and [nHept₄N][OAc]^[72] which were the catalytic species.

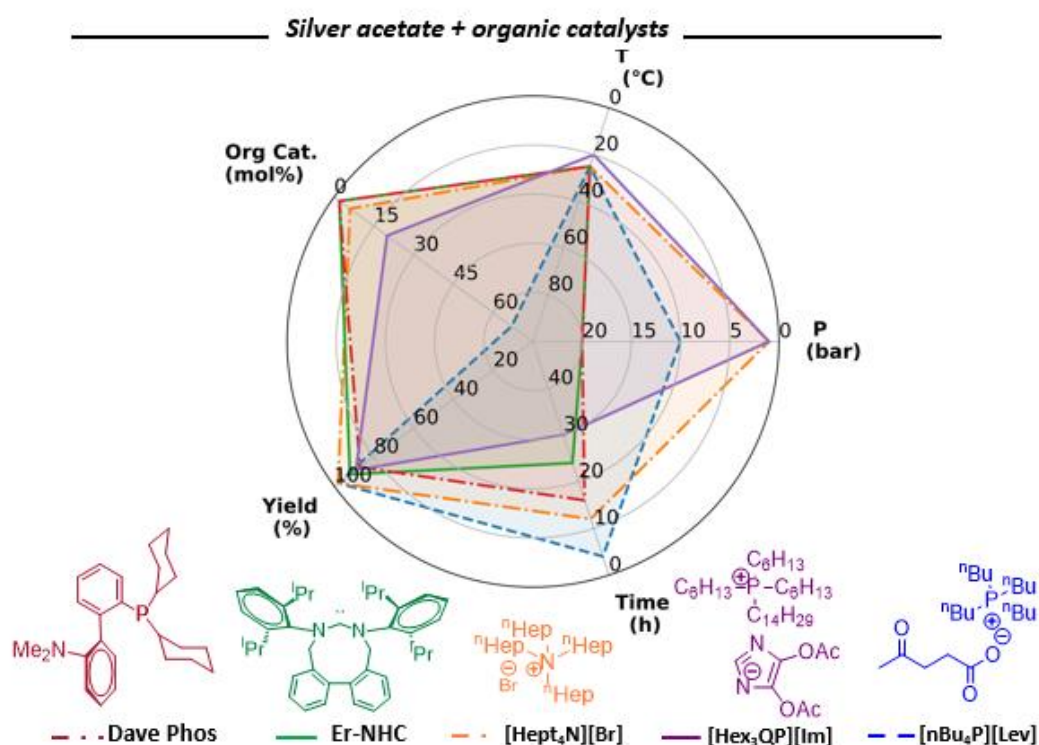


Figure 8. Comparison of the activity of some selected dual catalysts for the synthesis of DMACC. Dave Phos and Er-NHC catalysts used in combination with ACN. Data used for plotting presented in **Table S5**.

In our opinion, the systems based on phosphine (Dave Phos)^[77] or expanded-ring NHC^[43], despite not being the most performant, are remarkable catalytic options. They are active for the transformation of the challenging primary, secondary and internal propargylic alcohols and present a high tolerance towards various functional groups (e.g. acetate, acrylate, carbonates). One of their weaknesses, is their sensitivity to moisture, which limits their recyclability (50% loss of activity after the first reuse). In a recent study, Schaub et al. proposed a recyclable catalytic system, based on the use of lipophilic Ag-based catalysts and a biphasic organic reactive medium (acetonitrile/cyclohexane). The catalyst was recovered by

liquid-liquid extraction in the cyclohexane phase, while the cyclic carbonates remained in the acetonitrile phase (average yields of 86 – 90%).^[78]

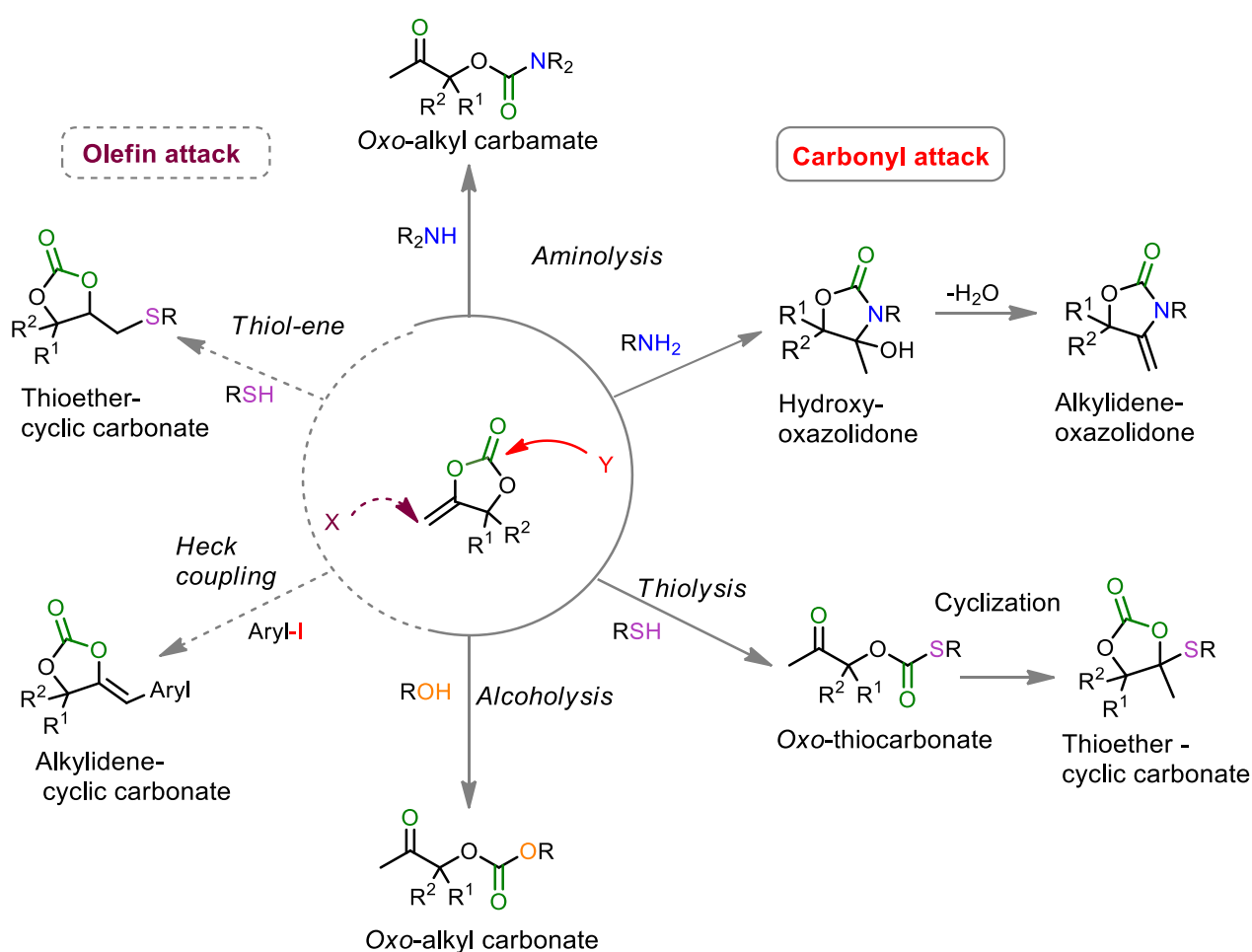
Heterogenous/hybrid dual activation catalysts

As a result of the limited recyclability of homogenous catalysts, most of the systems are costly, limiting their industrial interest. This limitation could be overcome by using heterogenous catalysts wherein a base or an active metal is anchored onto an inert support or dual hybrid systems combining an immobilised metal (salt) and a free base additive. They have the advantage of being easily separated and recovered from products, in most cases by simple filtration. The preparation of heterogenous catalysts relies on the development of efficient inert supports. A variety of supports exist, which includes polymers^[79–81], carbon materials^{[82][83]} and metal/covalent organic frameworks (MOF/COV^[84,85]). The supports can be either non-porous, in which case the catalytic reaction takes place at the surface, or porous, wherein the reaction takes place within the pores. The porous supports have the advantage of a larger surface area available for catalysis. Furthermore, they can either be directly grafted with an organic base or a ligand which coordinates to the metal center or decorated with metallic nanoparticles or simply with a precipitated metal salt and used in combination with a free base.

Various systems have been reported in the literature and are discussed in the review published in *angewandte*. However, in the scope of this thesis, we have decided to not review these systems as the thesis work focuses mainly on homogenous catalysis.

3. Exovinylene cyclic carbonates in organic synthesis

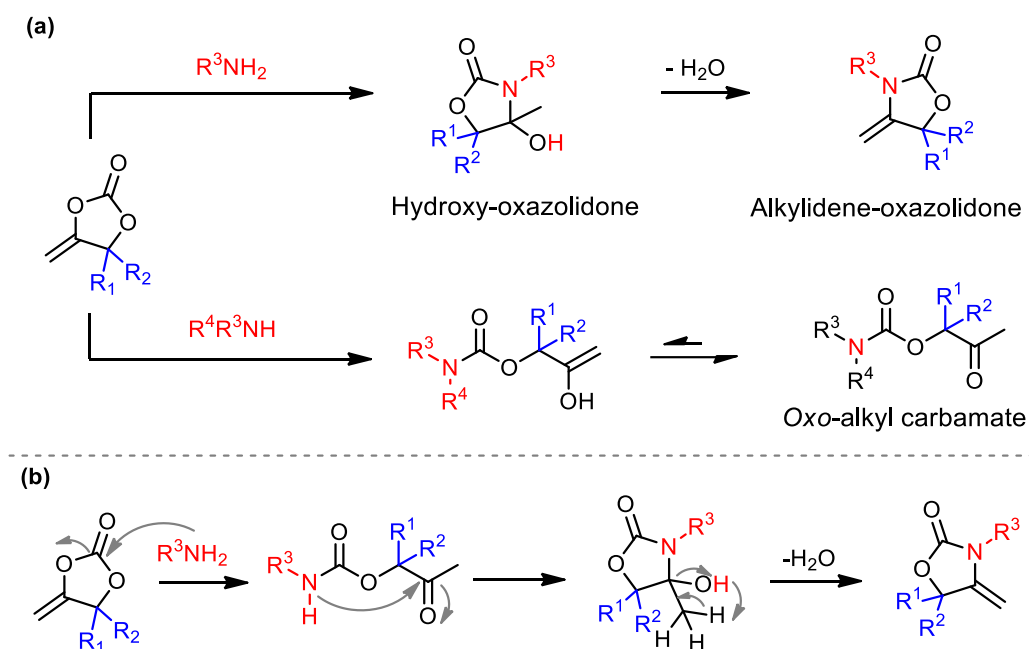
α CCs present two distinct reactive sites, i.e., the carbonate and the olefin groups, which can undergo selective reactions. **Scheme 4** summarises the main reactions of α CCs and the families of products that have been obtained. The presence of the exovinylene moiety in α CCs associated to the strain release enables the facile and regioselective ring-opening of the cyclic carbonate by nucleophiles (amines, alcohols, thiols). The driving force of this reaction lies in the formation of an enol upon ring-opening, that tautomerises spontaneously into the corresponding ketone. The olefin group can also be involved in a multitude of reactions, such as thiol-ene or Heck coupling reactions, although only a few of them have been explored to date.



Scheme 4. Examples of α CCs transformations.

3.1. Aminolysis

The reaction of α CCs with secondary amines yields carbamates, which are important intermediates in the agrochemical and pharmaceutical^[86] industry. This reaction offers an attractive alternative to the conventional routes for carbamates that involve the use of toxic phosgene,^[87] carbamoyl chlorides or isocyanates^[88,89]. Depending on whether a primary or secondary amine is involved in the reaction with α CCs, a cyclic or linear carbamate is obtained, respectively (**Scheme 5**). The addition of an amine on α CCs yields an *oxo*-alkyl carbamate due to the enol-keto tautomerism.^[76] However, in the case of primary amines, an intramolecular cyclisation spontaneously occurs by the nucleophilic addition of the NH of the carbamate moiety to the ketone group, yielding a hydroxy-oxazolidone (a cyclic carbamate). Depending on the reaction conditions and the structure of the hydroxy-oxazolidone, this molecule may dehydrate into an alkylidene oxazolidone.^[90]



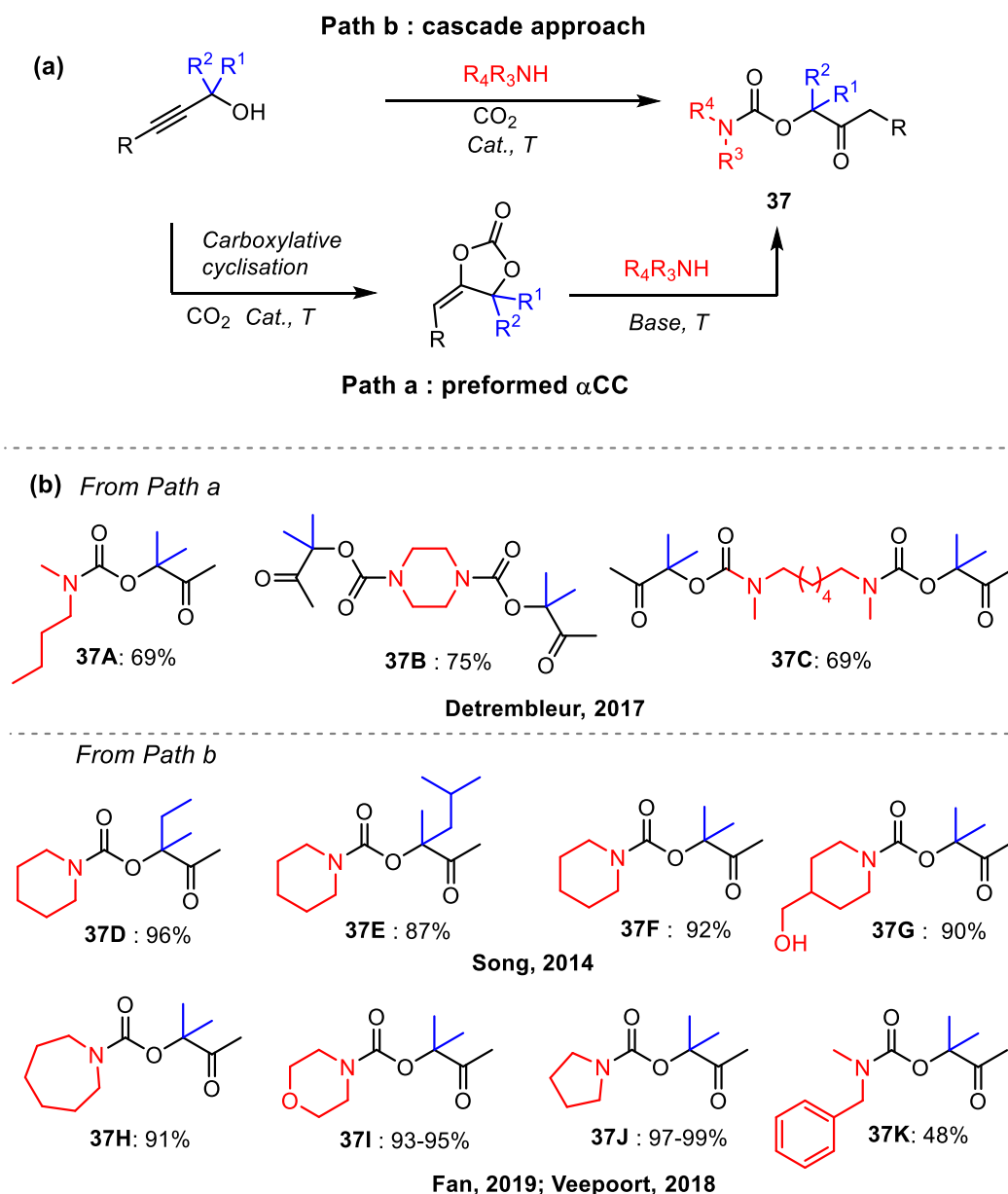
Scheme 5. Reaction of primary or secondary amines with α CCs.

Two main strategies exist to transform α CCs into carbamates. The first one consists in reacting the amine with the preformed α CCs (path a); it does not require any catalyst to proceed at room temperature, although the addition of a base catalyst fastens the reaction.

The second (path b) involves the three-component cascade reaction between a propargylic alcohol, CO_2 and the amine. In this case, α CC is formed *in-situ* and directly reacts with the amine. A catalyst is required for the first step of the reaction, i.e. the formation of the α CC intermediate. Hence, most of the catalysts used for this reaction are those which have been found to catalyse the formation of α CCs. In general, the reactivity of the amines is strongly dependent on their stereo-electronic properties.^[91]

With secondary amines

Detrembleur et al. demonstrated that 4,4-dimethyl-5-methylene-1,3-dioxolan-2-one (DMACC) provided the *oxo*-carbamate in good yields by reacting with *N*-methylbutylamine,^[18] or the symmetric bis-*oxo*-carbamate in the presence of di-secondary amines, i.e. piperazine or *N,N*-dimethyl-1,6-hexanediamine, at rt (products **37A-C**) (Scheme 6).^[92]



Scheme 6. Routes to *oxo*-alkylcarbamates from exovinylene cyclic carbonates and secondary amines: (a) general strategies and (b) selected substrate scope.

The one-pot three components reaction is the most investigated for producing *oxo*-carbamates. Various catalytic systems were tested such as $[\text{RuCl}_2(\text{Norbornadiene})]_n$ ^[93], $[\text{Cu}(\text{MeCN})_4]\text{PF}_6$ ^[94], $\text{Ag}_2\text{CO}_3/\text{PPh}_3$ ^[76] or $(p\text{-MeOC}_6\text{H}_4)_3\text{P}$ ^[95] and $\text{AgCl}/\text{Et}_4\text{NCl}$ ^[96]. Ru and Cu catalysts required harsher conditions (40-50 bar, 70-100 °C) to obtain high yields in

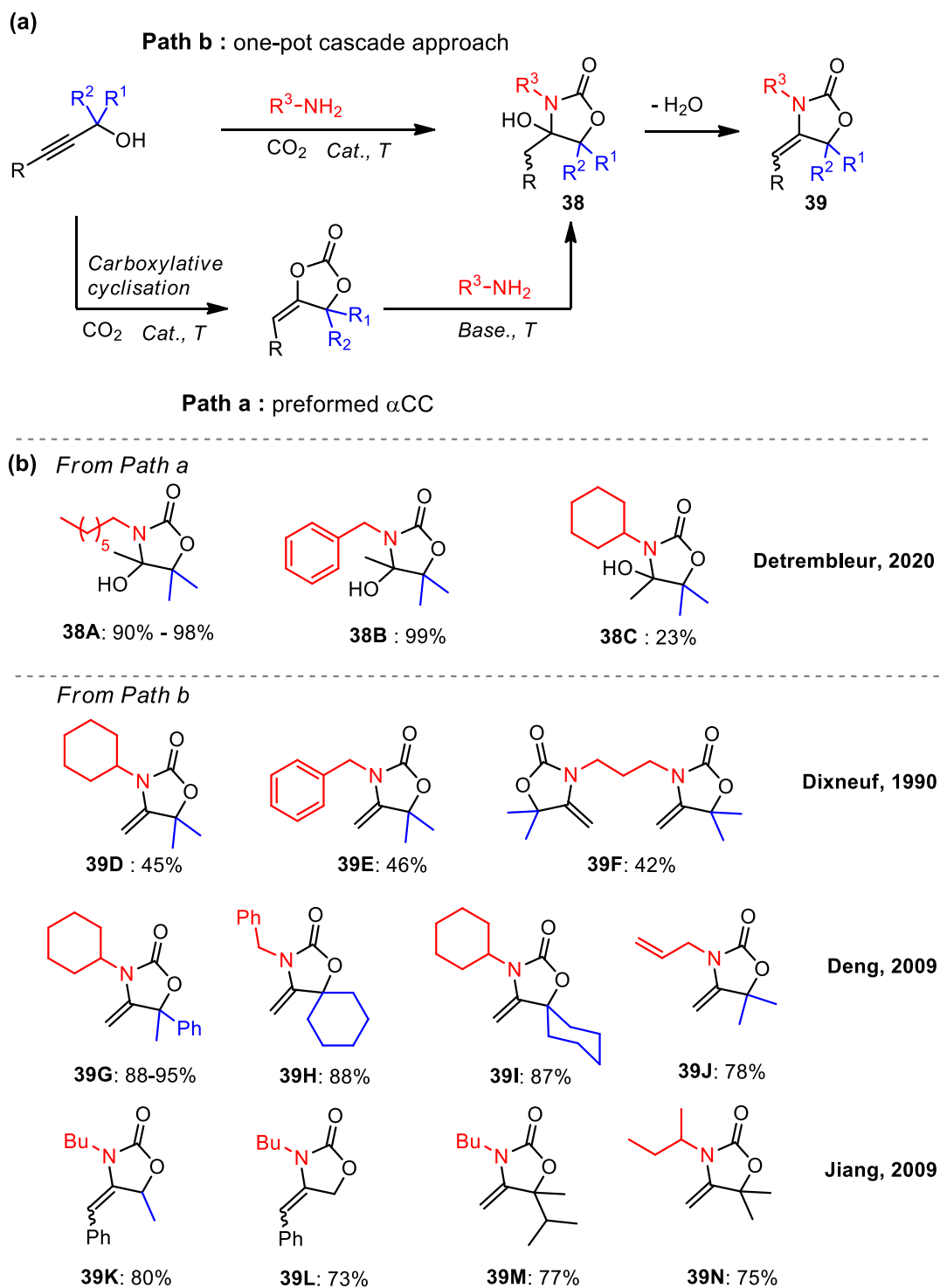
carbamates, in comparison to Ag-based ones which are the most efficient under mild conditions (1 bar, 30-60 °C). High yields (up to 98%) in carbamates were generally achieved with 3° propargylic alcohols (**37D-G**), whilst lower yields (40-57%) were obtained with 2° and 1° propargylic alcohols under identical conditions. Zhang et al. prepared carbamates by using silver/copper-based catalysts immobilised to carbon nanotubes (CNT-NHC-Ag/Cu) and showed an influence of the amine substituent on the yield, with a slight decrease in yield in the order pyrrolidine (99%) > diethylamine > di-n-propylamine (96%) > di-n-butylamine (92%).^[97] In 2019, Fan et al. reported an enzyme catalysed synthesis of a large scope of carbamates (**37H-K**) from α CCs by using laccase immobilised onto phosphosilicate nanoparticles at 15 bar. This immobilised enzyme was active for 30 days, and was reused 10 times without a significant loss in activity.^[98]

With primary amines

Detrembleur et al. demonstrated that the aminolysis of α CC (DMACC) into hydroxy-oxazolidone was complete in few hours at rt without any catalyst with 1-heptylamine, benzyl amine or cyclohexylamine (**Scheme 7**) (**38 A-C**).^[18,91] The addition of DBU as catalyst accelerated the reaction process.^[91] The corresponding hydroxy-oxazolidone could also be quantitatively dehydrated into α -alkylidene-oxazolidone by refluxing in glacial acetic acid.^[91]

When the three-components approach was considered, a catalyst and a higher temperature were required to generate *in-situ* the α CCs, that consequently reacted with the amine. Under these conditions, the alkylidene-oxazolidone was obtained as the main product, the hydroxy-oxazolidone was never isolated. Dixneuf^[90], Hua R^[99], Deng^[100] proposed metal-free systems based on phosphines, pyridines and [DMIIm][BF₄], respectively. At a temperature of 110-140 °C, and pressure of 25-50 bar, the authors converted 3° propargylic alcohols in poor to good yields (38-89%) (**Scheme 7**) (**39D, E**). The lowest activity was noted with phosphines. Dixneuf et al. prepared a bis-alkylidene oxazolidone (**39F**) in 42% yield by reacting DMACC with 1,3-diaminopropane.^[90] Deng et al. prepared α -alkylidene-oxazolidones (**39 G-I**) with high yields (78-95%) by using a dual system based on CuCl₂/[BMIIm][BF₄], although the ionic liquid was used as solvent for the reaction. However, they remained limited to the transformation of 3° propargylic alcohols only.^[101]

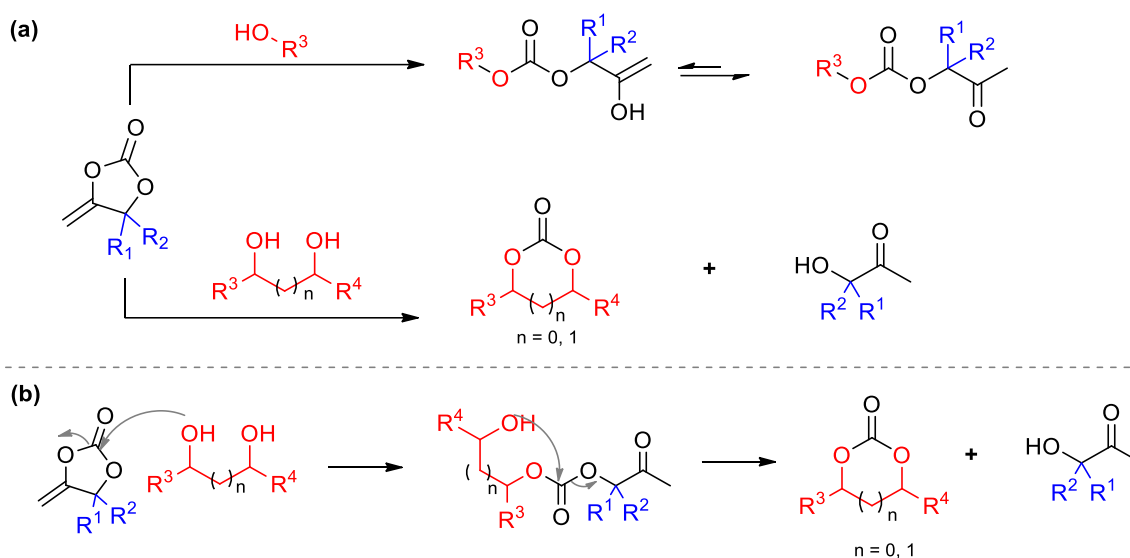
Jiang et al. showed that CuI^[102] and AgOAc^[103] could be used as sole catalyst to convert internal 3°, 2° and 1° propargylic alcohols into the corresponding alkylidene-oxazolidones (**39 K-N**) in moderate to high yields (70-96%) at a pressure of 80 bar. The carboxylative cyclisation of propargylic alcohols does not usually proceed in the absence of an organic catalyst, thus the reactivity of the sole metal catalysts could be rationalised by the presence of large amounts of the amines which played the role of reagent and catalyst. Xu et al. synthesised alkylidene oxazolidones with yields of up to 88% without the use of any catalyst, under supercritical conditions (140 bar, 120 °C) with an excess of amine and 48 h of reaction.^[104]



Scheme 7. Synthesis of hydroxy-oxazolidones and α -alkylidene-oxazolidones: (a) general strategies and (b) selected substrate scope.

3.2. Alcoholysis

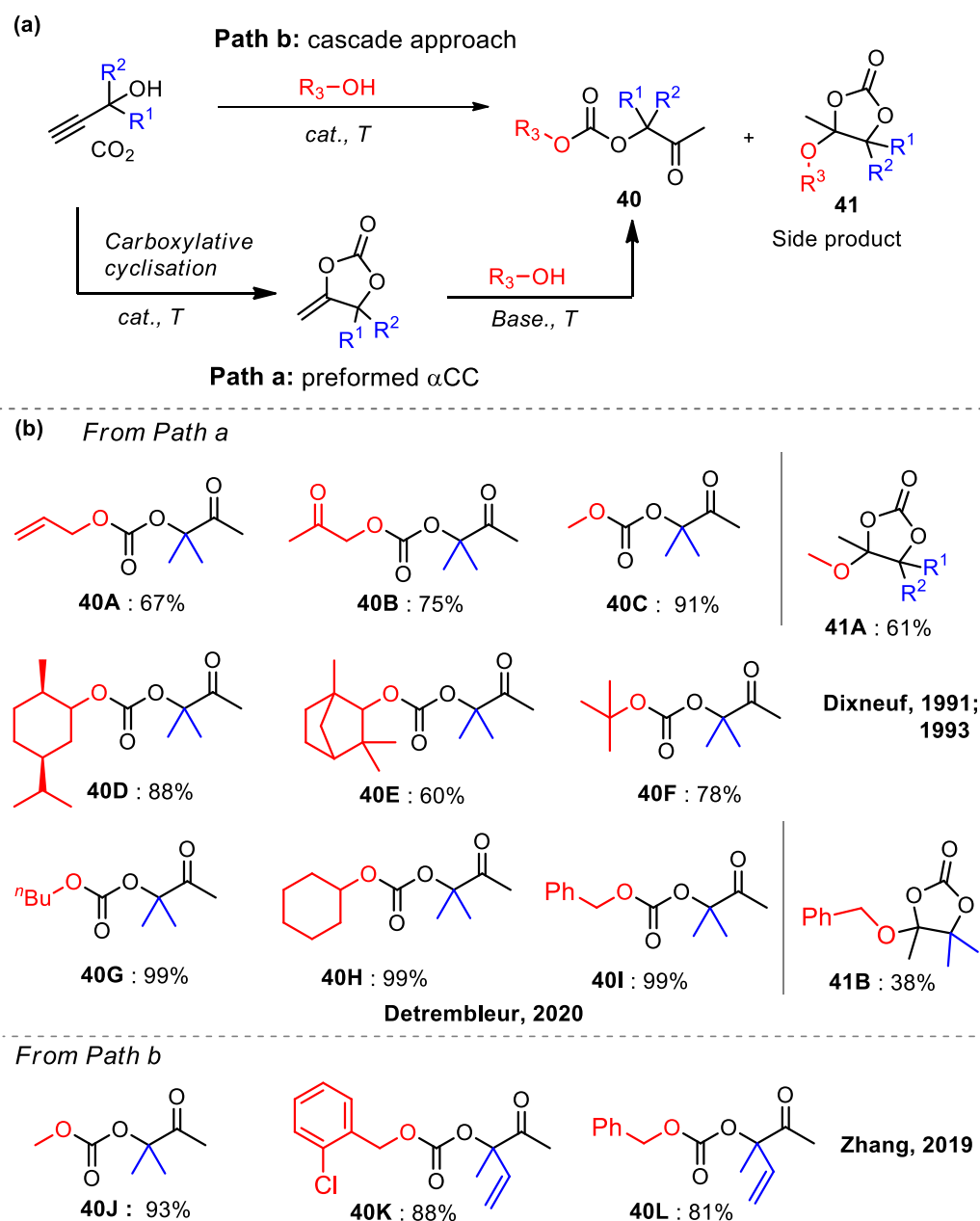
The ring-opening of α CCs by alcohols appears as a phosgene-free approach to produce carbonates of high structural diversity. In the case of mono-alcohols, linear *oxo*-alkyl carbonates are produced (**Scheme 8a**). With di- or polyols, an intramolecular attack of the second OH group on the carbonate function results in a cyclisation, yielding a five- or six-membered cyclic carbonate and a α -hydroxy ketone as secondary product (**Scheme 8b**). Similarly to the reactions with amines, α CCs can be prepared separately and then reacted with mono- or diols or be generated *in-situ* from propargylic alcohol and CO₂ in the presence of mono- or diols.



Scheme 8. (a) Reaction of mono-alcohols or di-/polyols with α CCs and (b) mechanism of formation of cyclic carbonates by reaction of polyols with α CCs.

With mono alcohols

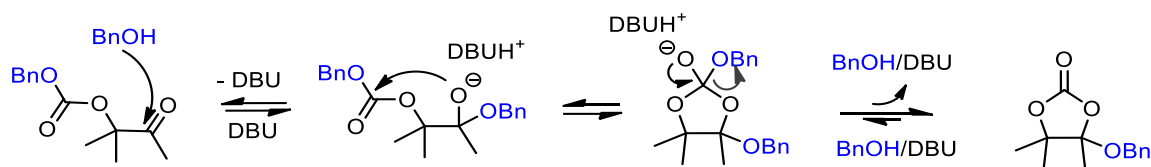
Seminal works by Dixneuf et al. showed that *oxo*-alkylcarbonates were obtained in moderate to high yields (67-90%) by reacting α CCs (DMACC) with various primary or secondary alcohols under relatively mild conditions (0-40 °C, 4-20 h) provided that triethylamine (70 mol% vs α CC) was used to catalyse the reaction.^[105] The process was compatible with alcohols bearing an olefin or a ketone group (**Scheme 9, 40A,B**). Tertiary alcohols failed to react even at a higher temperature (60 °C), however the use of KCN instead of NEt₃ made the reaction possible at 20 °C with yields of 60-70%. Importantly, when methanol was used, the *oxo*-alkyl carbonate was not isolated at 20 °C, the elusive tetrasubstituted ethylene carbonate (**41A**) was obtained instead with both NEt₃ or KCN. No mechanism was proposed for the formation of this tetrasubstituted ethylene carbonate. Decreasing the reaction temperature to 0 °C provided the *oxo*-alkylcarbonate **40C** in high yield. In a subsequent study, Dixneuf et al. showed that *oxo*-alkylcarbonates could be obtained in good yields from tertiary and/or bulky alcohols using 2-hydroxypyridine (10 mol%) as catalyst at 60 °C (**40D-F**).^[106]



Scheme 9. Reaction of α CCs with monoalcohols: (a) general strategies and (b) selected substrate scope.

Recently, Detrembleur et al. showed that a low amount of DBU (5 mol% vs α CC) was sufficient to catalyze the addition of 1-butanol^[18], benzyl alcohol or cyclohexanol^[107] on DMACC with the selective and quantitative formation of the corresponding oxo-alkylcarbonates. Due to steric hindrance, the reaction with cyclohexanol was slower. By carrying out the reactions at 80 °C, 1-butanol and benzyl alcohol provided quantitatively the corresponding oxo-alkylcarbonate (**40 G, I**) in 15 min, while few hours were required for cyclohexanol **40H**. Importantly, the authors also observed the formation of a tetrasubstituted ethylene carbonate with benzyl alcohol (**41B**) when working at 80 °C (38 mol% after 48 h).

Mechanistic investigations evidenced that the reaction proceeded through a nucleophilic attack of the alcohol on the ketone group of the formed *oxo*-alkylcarbonate, inducing cyclisation as illustrated on **Scheme 10**. The DBU catalyst influenced the intermediate stability by forming a strong hydrogen-bonded complex with benzyl alcohol and π -type interactions (e.g., cation- π , π - π , and π -induced dipole interactions), thus facilitating the reaction.

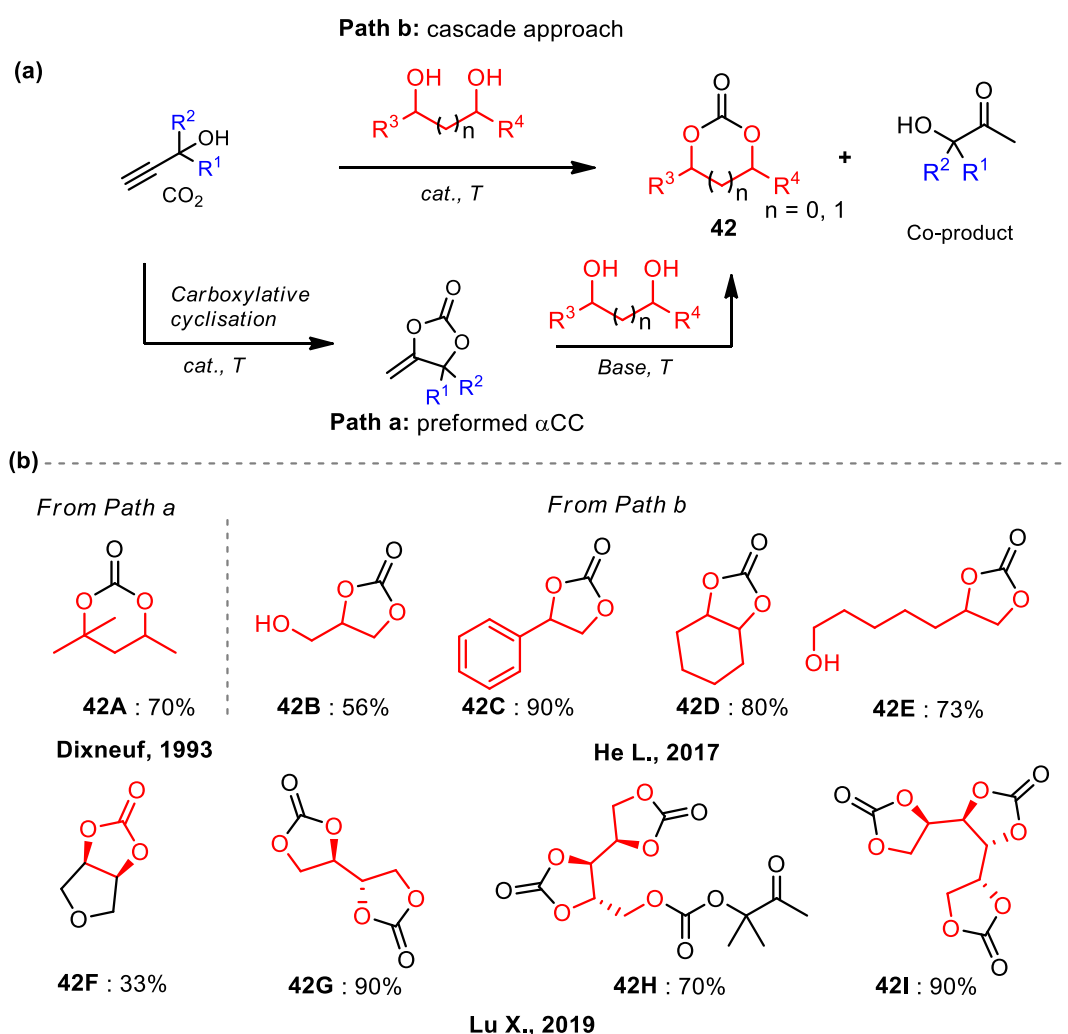


Scheme 10. Mechanism of DBU-catalysed formation of tetrasubstituted ethylene carbonate from 40H.^[107]

Various *oxo*-alkylcarbonates were also prepared by the three-component reaction of CO₂, propargylic alcohol and monoalcohols (**Scheme 9, 40G-I**). Song et al. showed that Zn-based catalysts (ZnCl₂/DBU, 20/50 mol%) catalysed the synthesis of *oxo*-alkylcarbonates in high yield provided that a 50% excess of the monoalcohol was used at 80 °C and 10 bar.^[108] Under similar conditions, He et al. reported high yield (98%) in *oxo*-alkylcarbonates at lower catalyst loading (5-10 mol%) using Ag₂CO₃/PPh₃.^[109] By using AgCl/[BMIM][OAc], Han et al. synthesised *oxo*-alkylcarbonates under mild conditions (1 bar, 30 °C), however a high amount of the ionic liquid (100 mol%) was utilised.^[110] The most efficient systems using a low catalyst loading (5 mol%) and a moderate temperature (60-80 °C) were those proposed by Zhang et al.^[111] (Ag sulfadiazine/[NBu₄][Br] that afforded high yields in *oxo*-alkyl carbonates (**40J-L**).

With di- or polyols

The reaction of di- or polyols with α CCs was proposed as an alternative route for the synthesis of saturated 5- or 6-membered cyclic carbonates from diols. Dixneuf et al. reported the formation of 6-membered cyclic carbonates (**Scheme 11**) (**42A**) by reacting α CC with a 1,3-diol at 100 °C with KCN as catalyst.^[106] Song et al. prepared various 5CCs (**42B-E**) in good to high yields by the cascade reaction of propargylic alcohol, CO₂ and vicinal diols, catalysed by Ag₂CO₃/phosphines^[112], ZnCl₂/DBU^[108] or Agsulfadiazine/Et₄NBr^[113] at 80 °C and 1-10 bar. This strategy was also exploited by Lu et al. to prepare mono-, di- or tri-cyclic carbonates (**42F-I**) from biomass-derived polyols (e.g. glycerol, erythritol, xylitol) using a tandem catalyst composed of NHO-CO₂/MTBD (5 mol%).^[114]

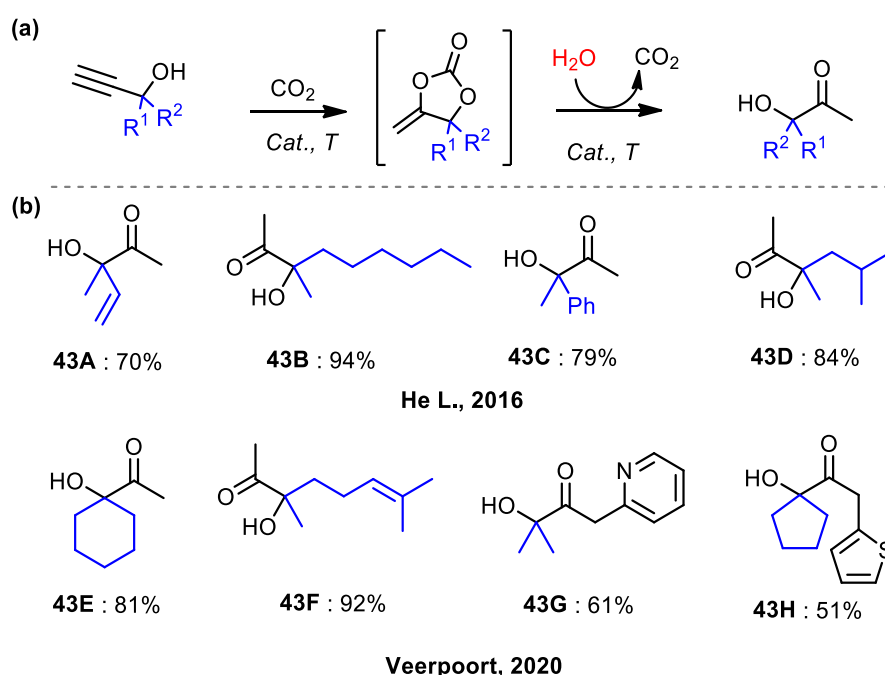


Scheme 11. Reaction of α CCs with di- or polyols: (a) general strategies and (b) selected substrate scope with yields.

3.3. Hydrolysis

α -hydroxy ketones are a class of biological active fragments in natural or pharmaceutical products and important building blocks in fine organic chemistry.^[115] They are usually obtained by the Hg-catalysed hydration of propargylic alcohols which produces unwanted co-products.^[116,117] The hydrolysis of α CC represents an attractive route to produce α -hydroxy ketones, with CO₂ as the only by-product of the reaction. All the published works reported the *in-situ* hydrolysis of α CCs by reacting propargylic alcohols with CO₂ in the presence of water and a catalyst (**Scheme 12**).

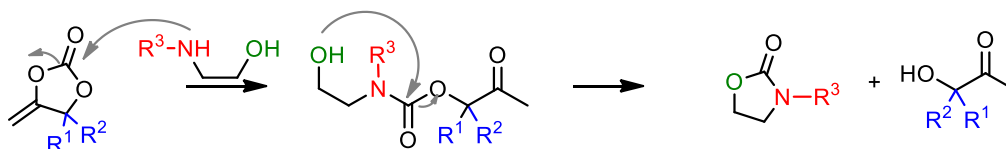
The catalytic systems consists of either of an ionic liquid catalyst such as [Bu₄P][Im]/CO₂,^[118] dual systems such as AgOAc/DBU,^[119] ZnCl₂/DBU^[108] and AgOAc/EMIM,^[120] or a ternary system composed of Cu₂O/PPh₂Cy/DBU.^[121] In general, the catalysts operated under moderate conditions (1-20 bar, 60-90 °C) and afforded a large scope of α -hydroxy ketones from both terminal (**43A-F**) and internal (**43 G, H**) propargylic alcohols in moderate to high yields. Nonetheless, for all the systems, large amounts of the organic cocatalyst were used (50-300 mol%). There is thus still a need to develop more efficient catalysts for the synthesis of α -hydroxy ketones by the *in-situ* synthesis and hydration of α CCs.



Scheme 12. Formation of α -hydroxy ketones by hydrolysis of *in-situ* generated α CCs: (a) general scheme and (b) selected substrate scope.

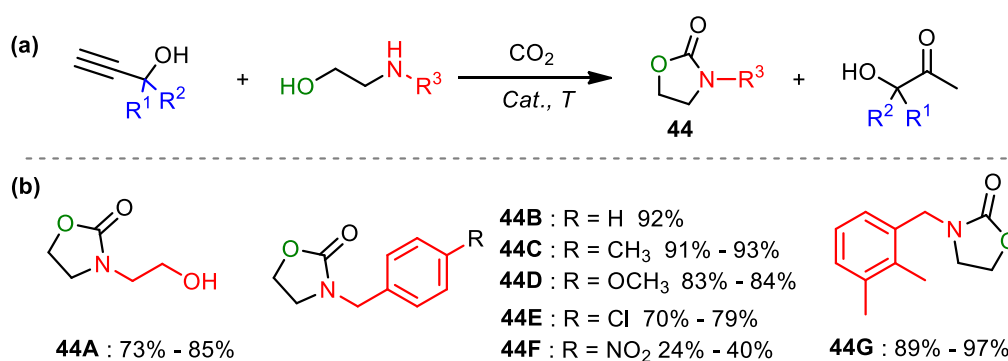
3.4. Carbonylation of ethanolamines

The reaction of α CC with ethanolamines is an attractive route for synthesizing (*N*-substituted) oxazolidinones, with the release of α -hydroxyketone as co-product. As illustrated in **Scheme 13**, the reaction proceeds by the formation of a linear carbamate, which then undergoes an intramolecular cyclisation by the nucleophilic attack of the alcohol onto the C=O of the carbamate.



Scheme 13. Mechanism of the reaction of ethanolamines with α CC.

This reaction was illustrated by He et al. who screened various phosphine ligands and silver salts for the three-component reaction of CO₂, propargylic alcohols and 2-aminoethanol. They found that Ag₂CO₃ / 4,5-bis(diphenylphosphino)-9,9-dimethylxanthene (Xantphos) was the most efficient catalyst to yield oxazolidinones with good to high yields (60 °C, 10 bar, 18 h) (**Scheme 14**).^[122] In a following study, they evaluated the performance of various copper-based salts combined to phosphine ligands and organic bases, and found that the CuI/1,10-phen/tBuOK (5/5/10 mol%) was the most active catalyst at 5 bar and 80 °C. Various *N*-substituted ethanolamines were converted into the corresponding 2-oxazolidinones (**44A-G**) in moderate to good yields (24-97 %).^[123]



Song, 2016; He L., 2018

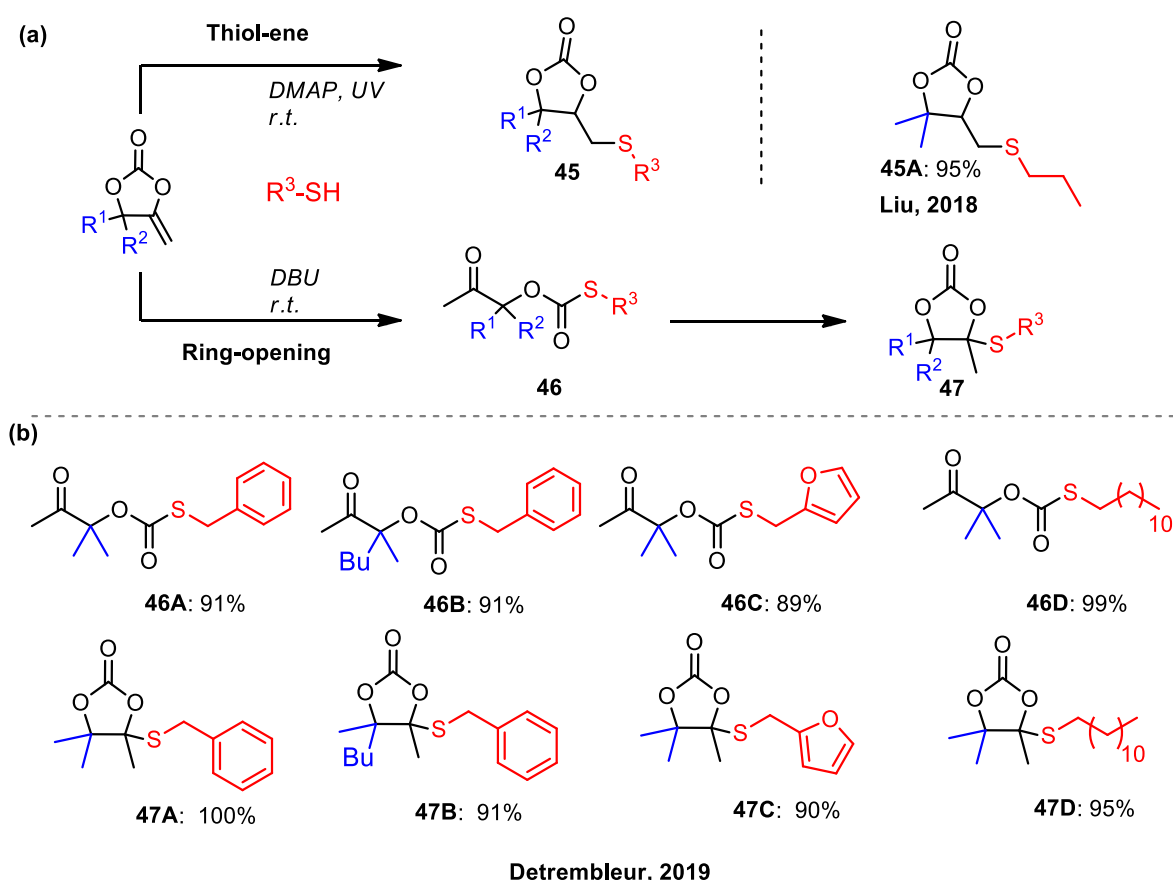
Scheme 14. Reaction of ethanolamines with α CC: (a) general scheme and (b) selected substrate scope.

Recently, Verpoort et al. reported the synthesis of oxazolidinones under similar conditions to He (60°C, 1 bar) in good to excellent yields using BMImOAc as organic catalyst and either CuBr^[124] or AgNO₃^[125] as cocatalyst.

3.5. Addition of S-nucleophiles

Organosulfur compounds play a key role in the biochemistry of most living organisms and are widely present in synthetic drugs and bioactive natural products.^[126–128] Unlike amines and alcohols, thiols can react both on the carbonate or alkene group, depending on the operating conditions. As illustrated in **Scheme 15**, tri- or tetrasubstituted 5-membered cyclic carbonates bearing a thioether function (**45,47**) or *oxo*-thiocarbonates (**46**) are accessible in high yield depending on the type of reaction involved. Liu et al. showed the first thiol-ene reaction of α CCs with the formation of trisubstituted ethylene carbonates at high yield (95%) (**45A**), using 2,2-dimethoxy-2-phenylacetophenone (DMPA) as a free radical generator under UV light irradiation at rt.^[129]

By analogy to the addition of alcohols to α CCs, Detrembleur et al. investigated the ring-opening of α CCs by thiols, catalysed by DBU. The authors showed that thiols ring-opened α CCs extremely rapidly (< 1 minute) with the formation of the corresponding *oxo*-thiocarbonates (kinetic product) with high yields (90–99%) at rt with only 1 mol% DBU (**46A–D**).^[130] Importantly, the authors showed that when the reaction was not rapidly quenched (by the addition of acetic acid to deactivate DBU), the thiocarbonates were almost quantitatively converted into the elusive tetrasubstituted ethylene carbonates (thermodynamic product) with a high selectivity (95–100%; **47A–D**), following a domino reaction mechanism.

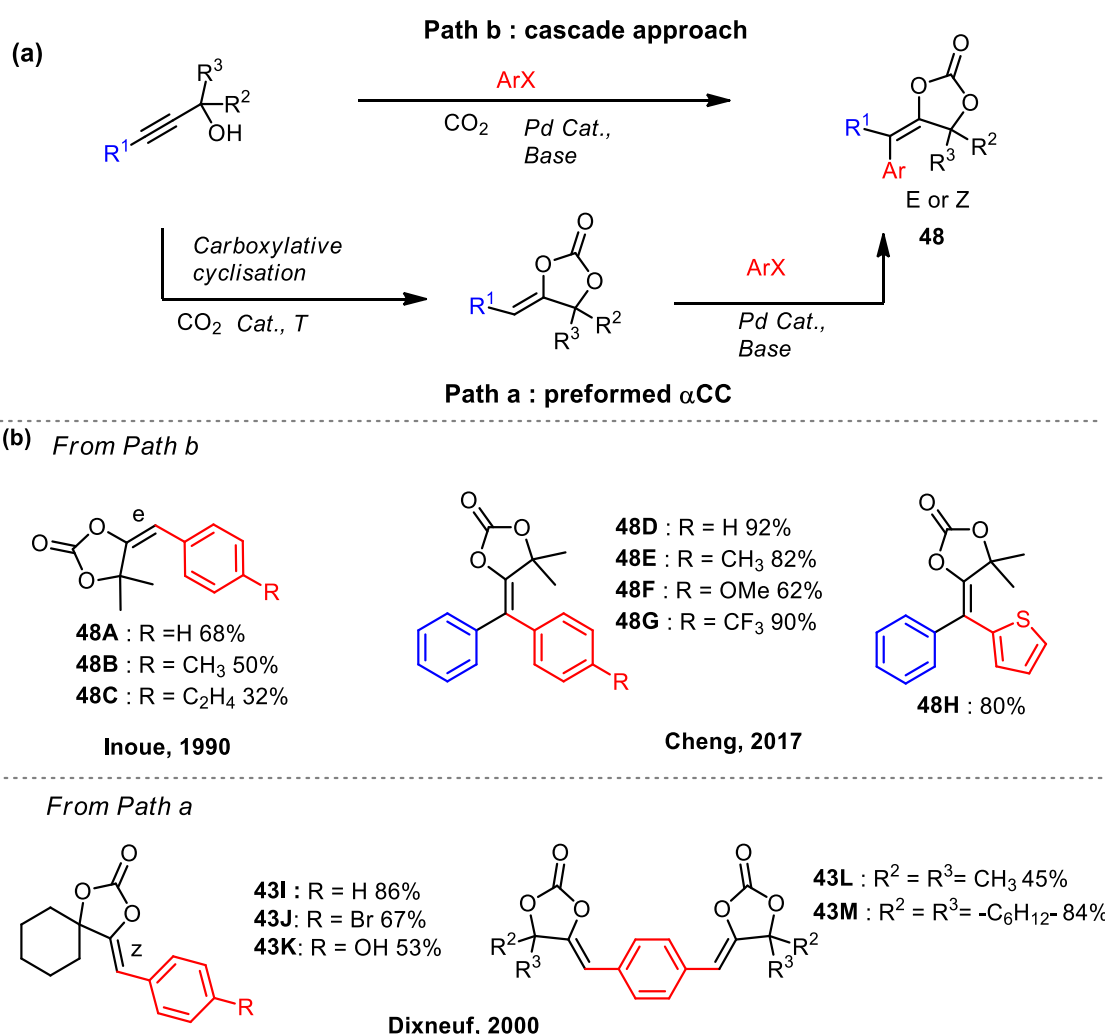


Scheme 15. Reaction of α CCs with thiols: (a) general scheme (b) selected substrate scope.

3.6. Heck coupling

Trisubstituted E alkylidene cyclic carbonates (**Scheme 16**) (**48A-C**) were prepared by Inoue et al. by the Heck-type coupling reaction between α CCs generated *in-situ* (by coupling CO₂ to 3° propargylic alcohols with terminal alkynes) and aryl- or alkenyl halides in the presence of a palladium catalyst (Pd(PPh₃)₄, 2 mol%) and an excess of a base (NaH).^[131] The substrate scope was significantly enlarged two decades later by Cheng et al. who reported the formation of tetra-substituted Z/E α CCs from 3° propargylic alcohols with internal alkynes (**Scheme 16**) (**48D-H**) in low to high yields (6-95%) using Pd(dba)₂ and LiO^tBu as catalytic system.^[67]

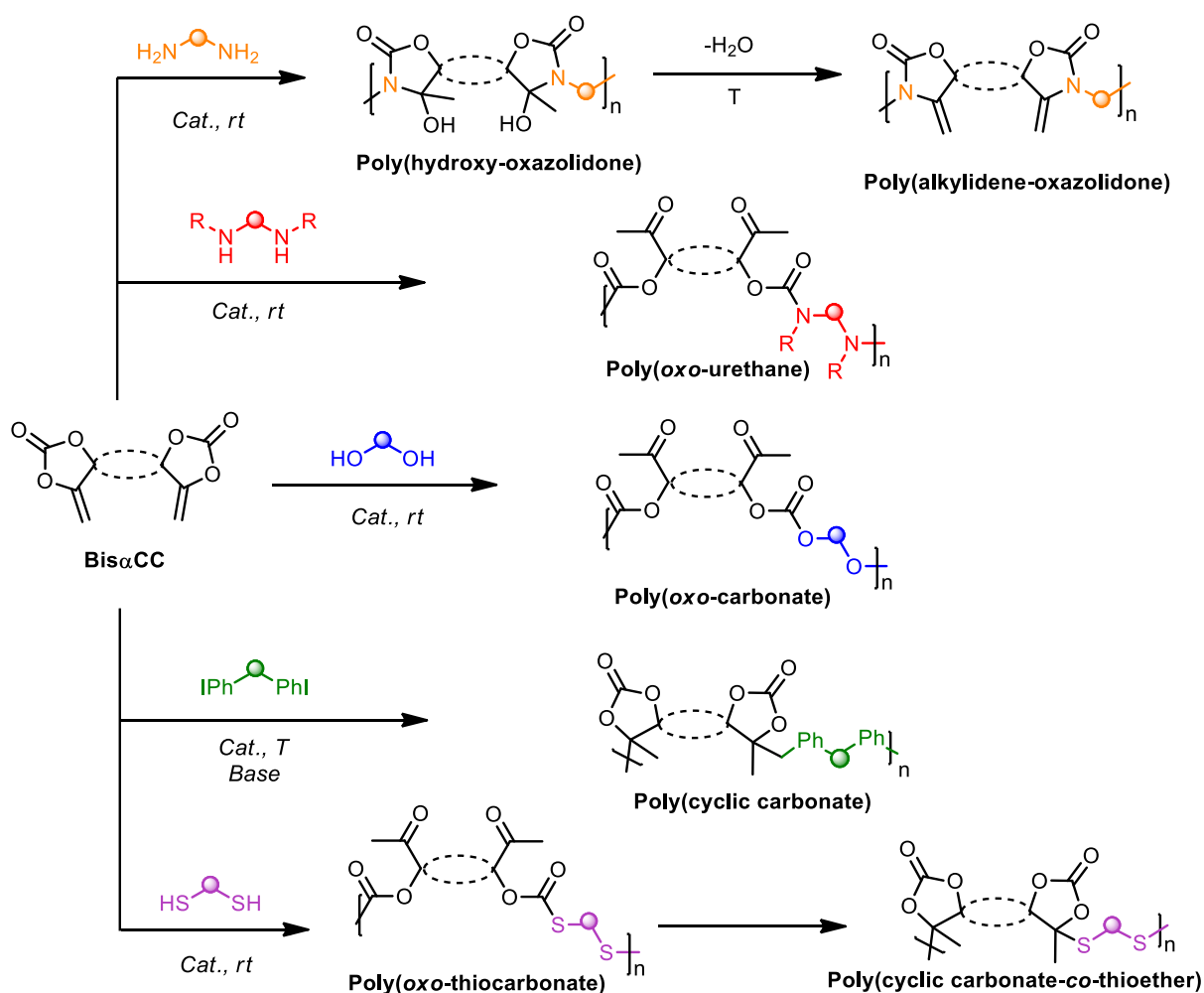
The stereoselective synthesis of Z-trisubstituted α CCs (**48I-K**) and of Z-bis α CCs (**48L, M**) was reported by Dixneuf et al. in moderate to good yields (40-87%) by reacting preformed α CCs and aryl iodide compounds in the presence of PdOAc, PPh₃, CF₃COOAg. Only aryl iodides were suitable for the reaction in contrast to the classical aryl bromide Heck substrate.^[132]



Scheme 16. Synthesis of tri- or tetra-substituted alkylidene cyclic carbonates by Heck-type coupling reaction: (a) general strategies and (b) selection of substrate scope.

4. Exovinylene cyclic carbonates in macromolecular engineering

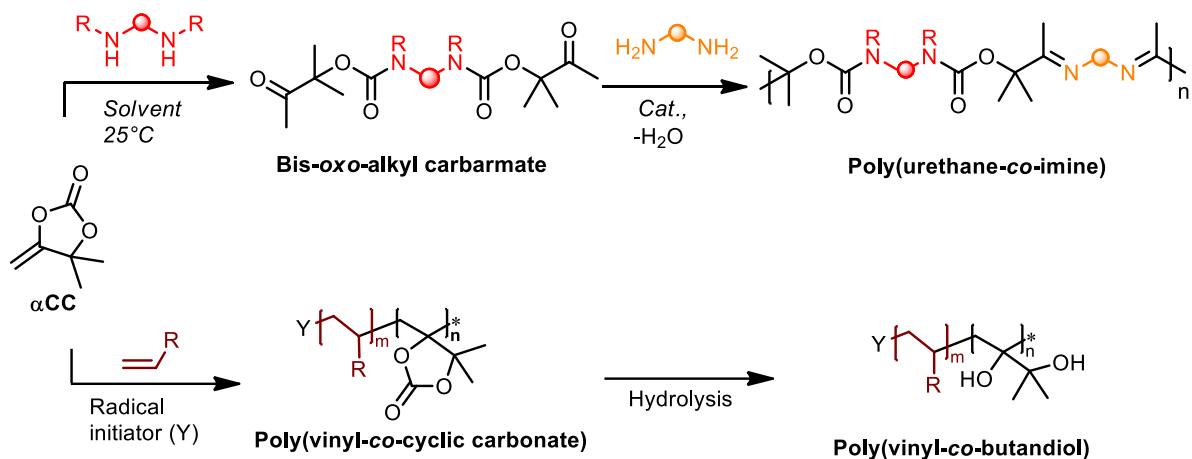
The enhanced reactivity of exovinylene cyclic carbonates for various nucleophiles vs the saturated versions, as well as their reactivity towards carbon- or sulfur-centered radicals, have recently inspired polymer chemists to exploit this chemistry to prepare diverse functional polymers. As illustrated in **Scheme 17**, bis(α -alkylidene cyclic carbonate)s (bis α CCs) were involved in step-growth polymerisations (SGP) with difunctional nucleophiles (diols, diamines or dithiols) to yield novel classes of polycarbonates, polyurethanes or sulfur containing polymers, with diiodoaryl compounds to provide new poly(cyclic carbonate)s by Heck coupling, and with dithiols to afford other types of sulfur containing poly(cyclic carbonate)s under thiol-ene reaction conditions.



Scheme 17. General structures of the polymers prepared from bis(α -alkylidene cyclic carbonate)s (bis α CCs).

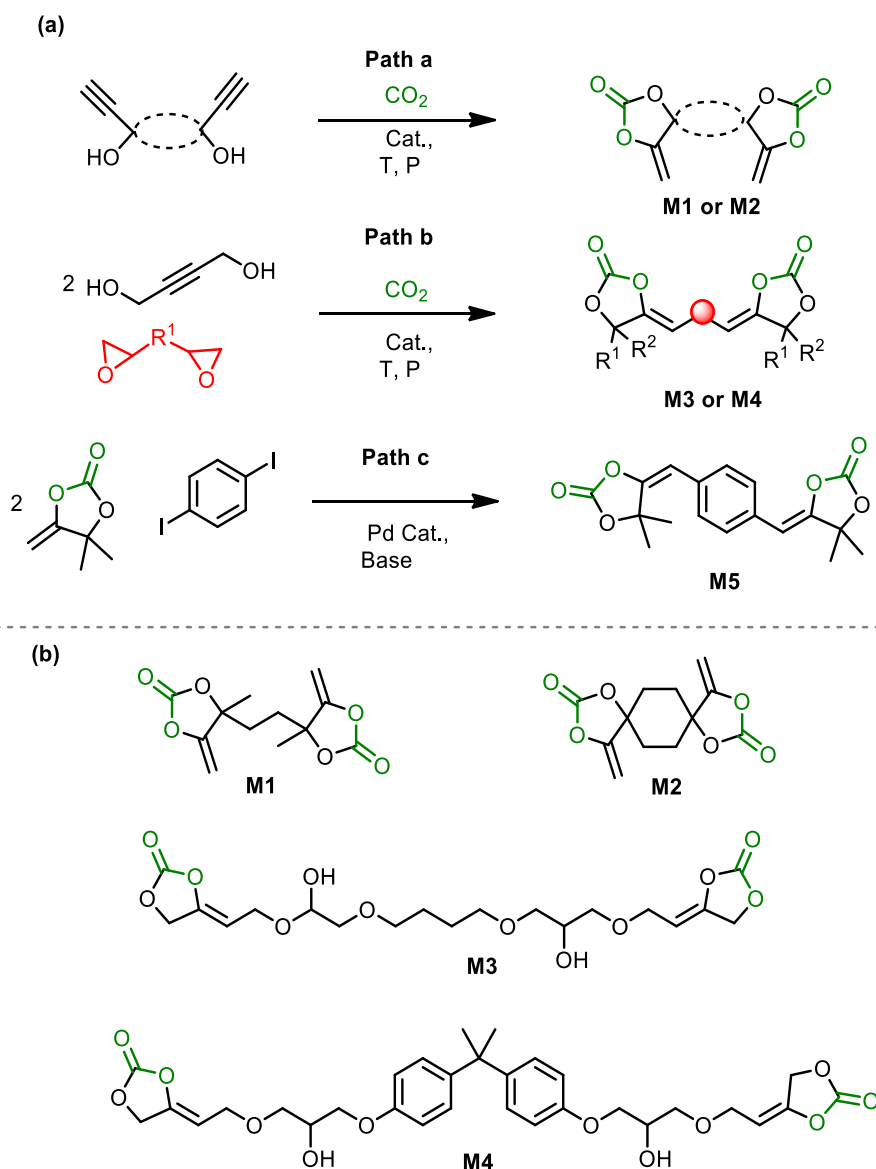
Chapter 1

The (controlled) radical (co)polymerisation of α CCs enlarged the scope of functional poly(vinyl monomer)s by introducing cyclic carbonates along the polymer skeleton. Diketones were also produced by reaction of α CCs with di-secondary amines, that were then involved in a polycondensation reaction with di-primary amines to furnish degradable polyurethanes (Scheme 18).



Scheme 18. General structures of the polymers prepared from α -alkylidene cyclic carbonates (α CCs).

Bis α CCs used in SGP were prepared by two main methods. The first consists in the carboxylative cyclisation of bispropargylic alcohols with CO_2 , affording bis α CCs with either an external (**M1**, **M2**) or an internal olefin (**M3**, **M4**) (**Scheme 19**, paths a and b). The bispropargylic alcohols were synthesised by the reaction of diketones with ethynylmagnesium bromide,^[18] or from butynediol (an industrial waste) and bisepoxides.^[133] The second approach involves the Heck coupling of α CCs with diodobenzene, initially reported by Dixneuf et al.,^[132] which generates bis α CCs with internal olefins (**M5**).



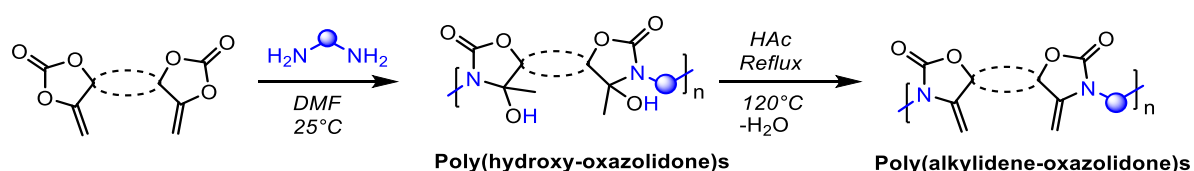
Scheme 19. Synthetic strategies for bis(α -alkylidene cyclic carbonate)s and some examples.

4.1. Polyurethanes

Polyurethanes (PU) are important polymers produced at about 18MT/year. They are found in diverse products (e.g. coatings^[134], adhesives,^[135] foams,^[136,137] elastomers), in various sectors (construction, transportation, personal protection equipment's, textile, biomedical, etc.).^[138–140] PUs are industrially obtained by the polyaddition of diols to diisocyanates.^[141] However, isocyanates are toxic compounds, produced from the even more toxic phosgene gas.^[142] REACH regulations now tend to restrict the use of isocyanates, urging researchers to develop alternative isocyanate-free routes to produce PUs. Several strategies were developed and have been the topic of recent reviews, e.g. the transurethanisation of dialkylcarbamates, the ring-opening polymerisation of cyclic carbamates,^[143,144] or the polyaddition of bicyclic carbonates with diamines.^[114–120] In this context, the reactivity of bis α CCs towards amines provides new opportunities for the design of non-isocyanate polyurethanes under mild operating conditions as it will be exemplified below.^[18]

Poly(hydroxy-oxazolidone)s

In 2017, Detrembleur et al. reported the first polyaddition of bis α CCs to primary diamines with the formation of poly(hydroxy-oxazolidone)s under catalyst-free conditions at rt (**Scheme 20**).^[18] Although the process functioned under catalyst-free conditions, the addition of DBU accelerated the polymerisations. The monomer **M5** with internal olefins was found more reactive than the one with external ones (**M1**), and yielded polymers with ketone groups within the polymer backbone compared to pendant ketones with **M1** (**Table 2**).^[18] Later on, Schaub et al. prepared poly(oxo-urethane)s from **M3** or **M4** and *N,N'*-dimethyl-1,2-ethanediamine at rt (**Table 1**).^[133]



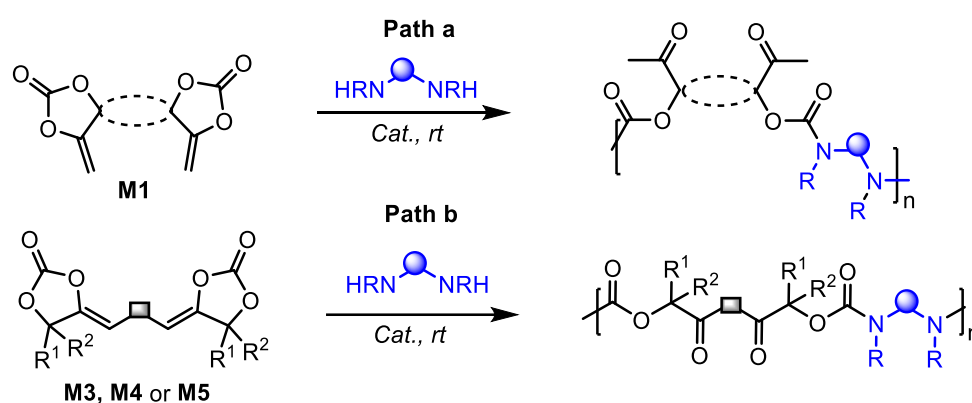
Scheme 20. Synthesis of poly(hydroxy-oxazolidone)s.^[69]

Table 1. Synthesis of poly(hydroxy-oxazolidone)s. Selected examples.^[69]

Diamine	Bis α CC	Poly(hydroxy-oxazolidone)s M_n (g/mol)	Poly(alkylidene-oxazolidone)s M_n (g/mol)	T_g (°C)
	M1	79200	36700	89
	M1	7200	4300	130
	M1	15900	4600	nd

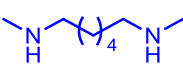
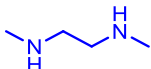
Poly(oxo-urethane)s

The selective formation of regioregular poly(oxo-urethane)s was demonstrated by Detrembleur et al. by reacting bis α CCs with a secondary diamine (*N,N'*-dimethyl-1,6-hexanediamine) at rt (**Scheme 21**). Although the process functioned under catalyst-free conditions, the addition of DBU accelerated the polymerisations. The monomer **M5** with internal olefins was found more reactive than the one with external ones (**M1**), and yielded polymers with ketone groups within the polymer backbone compared to pendant ketones with **M1** (**Table 2**).^[18] Later on, Schaub et al. prepared poly(oxo-urethane)s from **M3** or **M4** and *N,N'*-dimethyl-1,2-ethanediamine at rt.^[133]



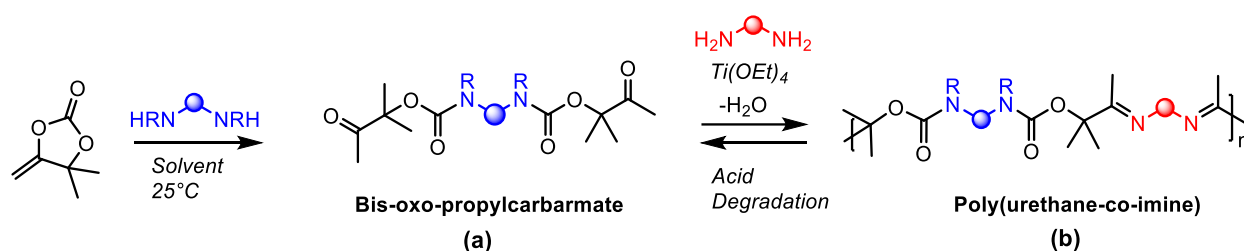
Scheme 21. Synthesis of poly(oxo-urethane)s.

Table 2. Synthesis of poly(oxo-urethane)s. Selected examples.

Diamine	Bis α CC	Path	M_n (g/mol)	Ref
	M1	a	3000-13500	[18]
	M5	b	11000-21500	[18]
	M3	b	3800	[133]
	M4	b	5200	[133]

Poly(urethane-co-imine)

Degradable PUs were prepared by Detrembleur et al. by inserting pH sensitive imine bonds within the polymer backbone. The polymers were obtained by the sequential aminolysis of DMACC with a secondary diamine (piperazine or *N,N*-dimethyl-hexanediamine), that yielded the corresponding bis-oxo-alkylcarbamate at rt, followed by their polycondensation with a primary diamine (e.g. 1,8-octanediamine, *m*-xylylenediamine) in the presence of $Ti(OEt)_4$ as dehydrating agent at 60 °C (**Scheme 22, Table 3**). Preliminary degradation tests showed that the polymers were completely degraded into the bis(oxo-carbamate) in 1 h when immersed in an acidic water solution (pH of 1).^[92]



Scheme 22. Synthesis of degradable polyurethanes.^[92]

Table 3. Synthesis of degradable polyurethanes. Selected examples.^[92]

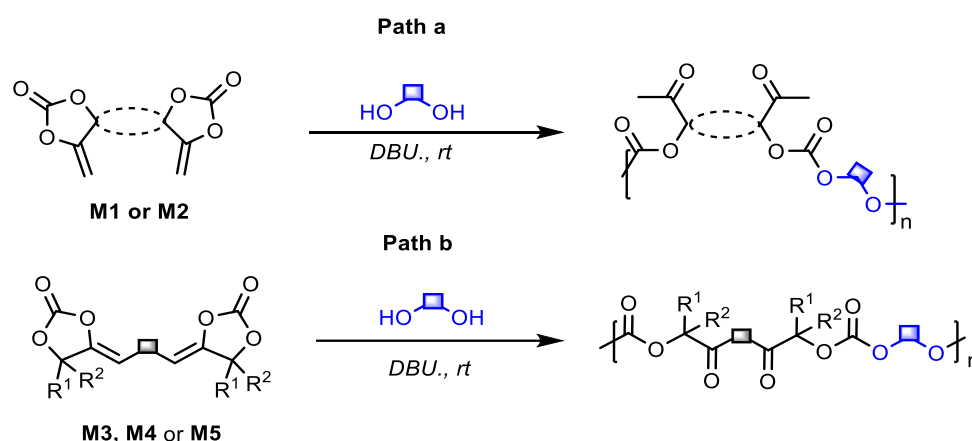
2° amine	1° amine	(b) M _n (g/mol)
		8300
		3000
		7600
		4900

4.2. Polycarbonates

Polycarbonates (PCs) are commodity polymers produced at about 5.1 MT/year and used in a variety of domains such as electronics, construction and automotive industry. Traditionally, PCs were obtained by the polycondensation of bisphenol A with phosgene or derivatives. The need to develop phosgene free-routes, coupled with the desire to valorise CO₂, has led to the development of new processes such as the polycondensation of CO₂-based dialkyl/arylcarbonates with diols^[155], the ROP of CO₂-based cyclic carbonates^[1,2,10,156–161] and the ROCOP of epoxides with CO₂^[12,162–171] which have been the subject of recent excellent reviews. The latter two processes provides aliphatic PCs which are applied in the biomedical sectors,^[172] as building block (e.g. Cardyon[®]) for the synthesis of polyurethane foams,^[173,174] and as solid electrolytes for batteries.^[175] More recently, the utilisation of bis α CCs has opened the door to the synthesis of new functional PCs as will be discussed shortly.

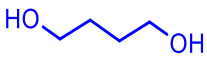
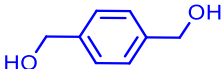
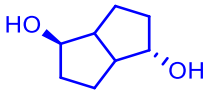
Poly(oxo-carbonate)s

In 2017, Detrembleur et al. prepared regioregular poly(oxo-carbonate)s by the polyaddition of monomers **M1** or **M5** with 1,4-butanediol in the presence of DBU (5 mol%) as catalyst at rt (**Scheme 23**).^[18] In contrast to the polymerisation with diamines, no reaction was noted without DBU. This process was later on extended to multiple diols derived from biomass (e.g. isosorbide) and lignin (e.g. 1,4-benzenedimethanol). Depending on the monomers used, some semi-crystalline PCs with a T_m ranging from 60 to 343 °C were prepared.^[107] Extension to poly(ethylene glycol) diols enabled to design polymers used as solid electrolytes for battery applications.^[176] In 2020, Schaub et al. designed poly(oxo-carbonate)s from monomers **M3** or **M4** and 1,4-butanediol (**Table 4**).^[133]



Scheme 23. Synthesis of poly(oxo-carbonate)s, general strategies.

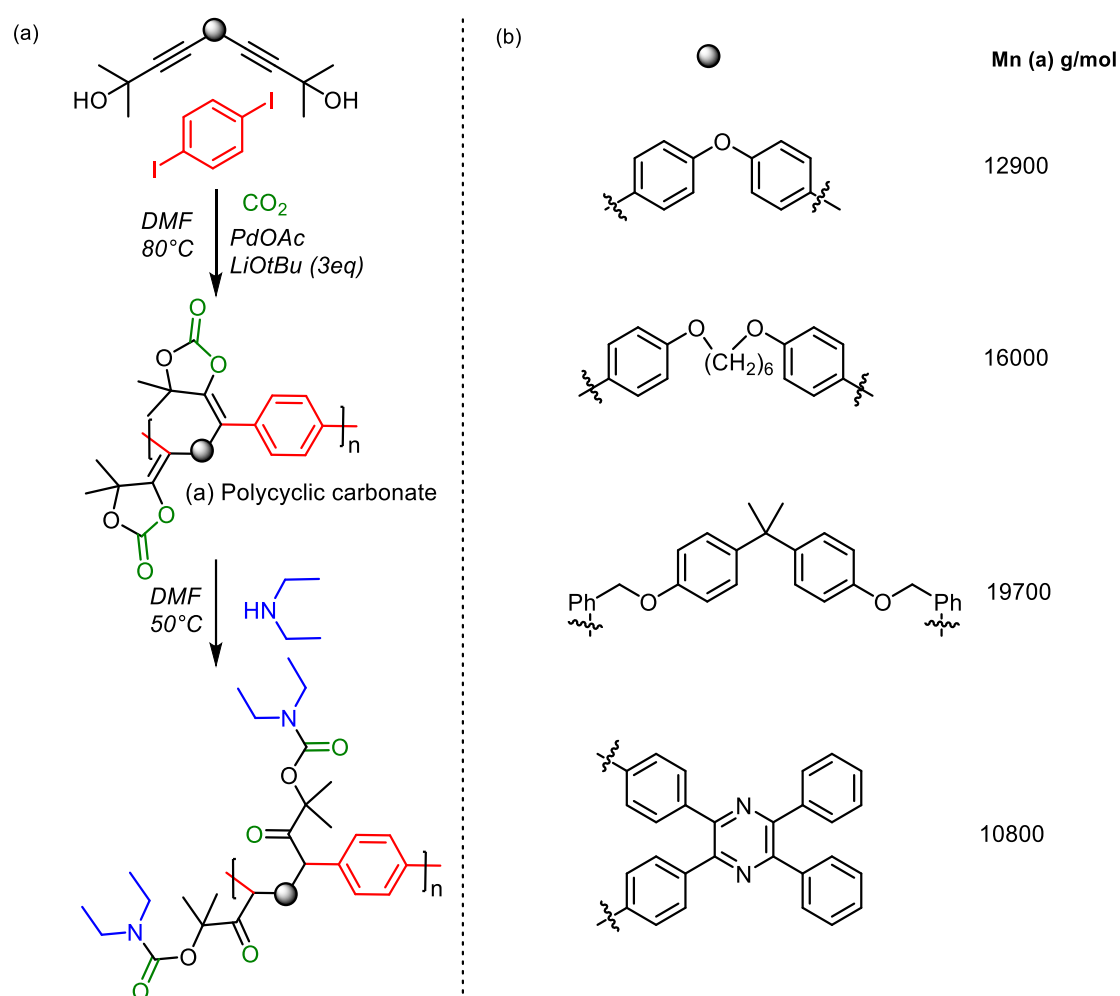
Table 4. Synthesis of poly(oxo-carbonate)s. Selected substrate scope.

Alcohol	Bis α CC	Path	M _n (g/mol)	T _g /T _m (°C)	Ref
	M1	a	13400	41/60	[107]
	M3	b	17000	ng	[18]
	M4	b	1900	ng	[133]
	M5	b	2100	ng	[133]
	M1	a	6000	71/84	[107]
	M2	a	ng	___/343	
	M1	a	4500	88/___	[107]
	M2	a	6800	153/174	

*ng = not given

Poly(alkylidene cyclic carbonate)s

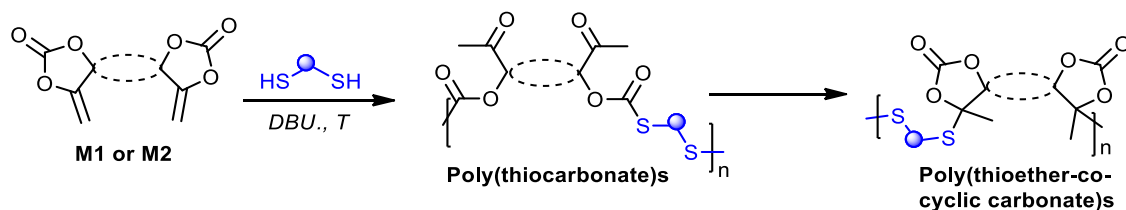
In 2019, Tang et al. developed a one-pot three components process for the synthesis of a rather large scope of poly(alkylidene cyclic carbonate)s from bis(propargylic alcohol)s, CO₂ and dihalides. The bis α CCs formed *in-situ* reacted with the dihalide by Heck coupling, using a catalytic system based on PdOAc and LiO^tBu at 80 °C (**Scheme 24**). The alkylidene cyclic carbonate linkages within the backbone were easily ring-opened by a secondary amine under catalyst-free conditions, enabling the facile post polymerisation modification. To demonstrate the diversity of their protocol, the authors also designed AB type monomers (i.e. molecules bearing both a propargylic alcohol and an iodo-aryl complementary reactive groups) which they successfully polymerised. By using different combinations of di-, tri- and tetra-functional monomers, the authors accessed hyperbranched polymers.^[177]



Scheme 24. Preparation of poly(alkylidene cyclic carbonate)s: (a) general reaction and (b) selected examples.^[177]

4.3. Sulphur-containing polymers

When the DBU-catalysed polyaddition of bis α CC to diols was extended to thiols, unprecedented poly(thioether-co-cyclic carbonate)s were produced instead of the expected poly(monothiocarbonate). By analogy to the reaction of α CC with thiols (see section 3.5.), it was expected that the thiocarbonate linkages were initially formed, however they were progressively converted into the cyclic carbonate ones during the polymerisation process (**Scheme 25**). When DBU (1 mol%) was used in combination to a fluorinated alcohol (1,3-bis(2-hydroxyhexafluoroisopropyl) benzene; 3 mol%), this linkage transformation was slowed down and polymers with 80 mol% thiocarbonate linkages were obtained. By varying the fluorinated alcohol content, the ratio of thiocarbonate/cyclic carbonate linkages was modulated, which strongly influenced the thermal properties of the polymers. Indeed, for similar molar masses, polymers with 100 % cyclic carbonates linkages presented a Tg of 126 °C compared to 61 °C when it contained 19 mol%.^[130] (**Table 5**) The concept was extended to the DBU-catalysed terpolymerisation of bis α CCs (**M1**) with a mixture of dithiol and diol (PEGdiol) to produce a polymer containing both oxo-carbonate and cyclic carbonate linkages.^[178]



Scheme 25. Synthesis of poly(monothiocarbonate)s and poly(cyclic carbonate-co-thioether)s.

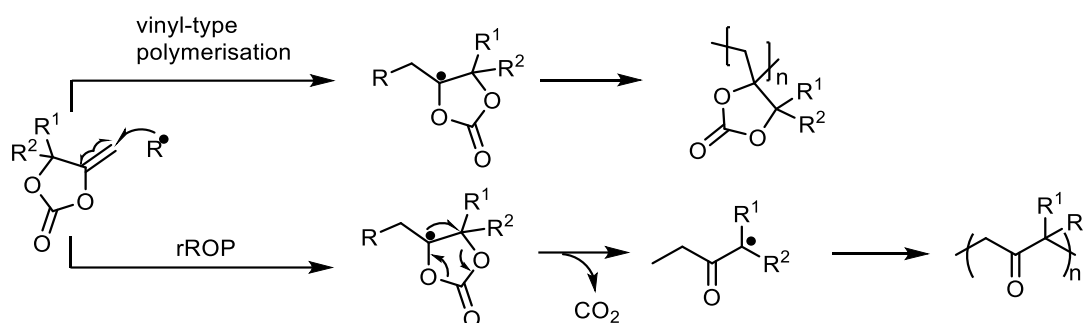
Table 5. Selected substrate scope.^[130]

Dithiol	Bis α CC	M_n (g/mol)	Ratio (b/a)	Tg (°C)
	M1	54000	99/1	47
	M1	9200	18/82	9
	M2	15700	99/1	76
	M1	22000	99/1	126
	M1	21300	19/81	61
	M2	20800	84/16	115

(a) Thiocarbonate linkage and (b) thioether linkage

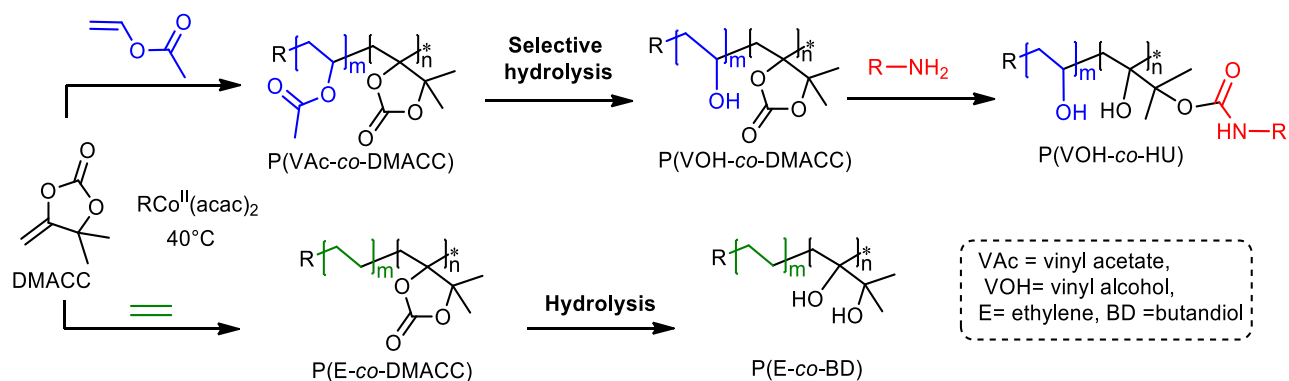
4.4. Vinyl-type copolymers

The pendant olefin of α CCs can be exploited to produce polymers by radical polymerisation. Although α CCs substituted by methyl (DMACC) or phenyl groups could not be homopolymerised at 60 °C,^[179] Endo et al. successfully achieved their homopolymerisation at a higher temperature (120 °C). Under these conditions, their radical ring-opening polymerisation (rROP) followed by decarboxylation could however not be avoided and competed with the vinyl-type polymerisation mechanism, yielding a polymer containing both cyclic carbonates and ketone functions (**Scheme 26**).



Scheme 26. Competing reaction mechanisms for the polymerisation of DMACC by a radical pathway at 120 °C.

More recently, Detrembleur et al. demonstrated the copolymerisation of DMACC with vinyl acetate (VAc)^[180] or ethylene (E)^[181] by cobalt-mediated radical polymerisation (CMRP)^[182] at 40 °C. This low polymerisation temperature enabled to cancel the rROP pathway (**Scheme 27**). Various copolymers of precise composition and controlled molar masses were thus made available. The selective methanolysis of VAc units of P(VAc-co-DMACC) furnished a poly(vinyl alcohol) (PVOH) bearing cyclic carbonates that was further functionalised by aminolysis into PVOH bearing urethane pendants. Under stronger hydrolysis conditions, both VAc and DMACC units of the copolymer were hydrolysed, leading to poly(vinyl alcohol) bearing vicinal diols.^[180] Similar procedures applied to P(E-co-DMACC) yielded polyethylene bearing vicinal diols in the main chain.^[181]



Scheme 27. Cobalt-mediated radical polymerisation of DMACC with VAc or E, and further derivatization of the copolymers.

5. Conclusions and outlook

Herein, we have reviewed the advances made in the synthesis of α -alkylidene cyclic carbonates (α CCs) from CO₂, their multiple transformation options into structurally divergent organic scaffolds and their brilliant potential for the construction of a broad diversity of novel polymers. The emerging success of α CCs in contemporary sciences highly depends on the catalytic breakthroughs needed to prepare them from CO₂ and propargylic alcohols. The state-of-the-art testifies that a large diversity of highly efficient and selective catalysts have been developed to promote this transformation. The lack of standardised protocols to access α CCs makes however the benchmarking of the catalysts' performances difficult. In this context, we have utilised customised spider-charts to highlight the strengths and weaknesses of selected relevant homogeneous systems and propose further guidelines to improve their efficiency.

Single component catalysts including organic bases, task specific ionic liquids or Lewis base-CO₂ adducts generally display moderate to good activity under demanding operative conditions. To surpass these hurdles, high loading or even excess of catalyst are proposed as a mean to promote the transformation at milder temperature and/or under low CO₂ pressure. This feature is typically exemplified with ILs that are not only easy to recycle but also offer the benefit of solubilising high contents of CO₂ which favours the overall CO₂ fixation. Binary catalysts using Ag(I) or Cu(I) salts in synergy with organic bases are by far more competitive and enable the production of α CCs under milder conditions, even at room temperature and/or atmospheric CO₂. Ways to activate CO₂ (e.g. by privileging WO₄²⁻ ions), to enhance salt dissociation (e.g. by utilising ketone solvents) or the CO₂ solubility/concentration within the reaction mixture (e.g. by using fluorocompounds) have been identified as some valuable options to further facilitate the reaction.

When the preparation of α CCs from tertiary propargylic alcohols is envisioned, one recommends the use of dual catalytic systems made of an Ag(I)X or Cu(I)X salt in combination with an organic base (superbase or basic ILs combining ammonium, phosphonium or imidazolium cations, and carboxylate or phenolate anions). These catalysts operate under mild conditions (PCO₂ < 5-20 bar, T = 25-40 °C, t < 24 h) and generally provide the cyclic carbonates with high yields and excellent selectivity.

Nonetheless, most of the homogeneous catalysts are mainly efficient for the carboxylative coupling of CO₂ to tertiary propargylic alcohols. Recent findings utilise a smart catalyst made of a silver salt complexed by sterically congested phosphines or expanded-ring NHC mimicking the "gem" effect encountered with tertiary alcohols to allow the transformation of challenging secondary and primary propargylic alcohols. When the large scale carboxylation of secondary or primary acetylenic alcohols by CO₂ is considered, Ag(OAc)/Dave phos systems^[77] or Er-NHC complexes^[43] of Cu(I) used in synergy with CsF are currently the best options. They operate under mild conditions (r.t., PCO₂ < 15-20 bar, t < 24h) and provide the

corresponding product in moderate to good yields with excellent selectivity. Furthermore, the Dave Phos catalyst was rendered recyclable by modifying the phosphine ligand with hydrophobic alkyl chains. It was easily recovered by liquid-liquid extraction and reused for a few cycles, which is a significant step towards the design of cost-effective catalytic processes.^[78]

Additional issues remain unsolved, such as the evaluation of the catalyst toxicity and the sustainable supply of propargylic alcohol substrates from biobased or waste feedstocks. Currently, various propargylic alcohols are accessible at the multi-thousand ton scale, e.g. by BASF, the world's largest producer of propargylic alcohols by alkynylation of ketones or aldehydes.^[183] This company also valorises industrial wastes by producing 1,4-butyne-3-diol from CaC_2 and formaldehyde.^[77] Therefore, the sourcing of these propargylic alcohols does not seem to be a limitation of the technology. Nonetheless, further reducing their carbon footprint requires the utilisation of renewable acetylene and ketones. Promising solutions are emerging to produce green acetylene, such as by electrochemical reduction of CO_2 and water.^[184] Although very attractive, the process needs to be optimised to increase yields and selectivity, moreover, renewable electricity is required to decrease the carbon footprint. Ketones and aldehydes can be easily obtained by oxidation of alcohols,^[185–188] which are abundant in nature.

α CCs display two reactive sites that are easily discriminated to drive selective transformations, rendering them unique building blocks for organic synthesis and polymer design. The ring-strain release and the keto-enol equilibrium are the main driving forces that facilitate their regioselective ring-opening, even at room temperature, by *N*-, *O*- or *S*-nucleophiles. With amines, α CCs are converted into (a)cyclic carbamates (oxazolidones and *oxo*-carbamates) under catalyst-free conditions or optionally by adding an organobase catalyst. With alcohols or thiols, the base is mandatory to produce acyclic (thio)carbonates or tetrasubstituted ethylene carbonates with a (thio)ether moiety. Importantly, these scaffolds are also accessible by the catalytic cascade multicomponent reactions enabling the generation of α CCs *in-situ* prior to their further transformation. The scope of ring-opening reactions is further complemented by using α CCs as carbonylation agent of vicinal or 1,3-diols and ethanolamines, furnishing 5- or 6-membered cyclic carbonates and oxazolidones or as reactive intermediate in acetylenic hydration to deliver α -hydroxyketones. Besides, the exovinylene moiety was also exploited for thiol-ene “click” reaction or Heck coupling, further extending the product scope.

Although the applications of these organic compounds are not yet investigated, due to their similarity to already existing conventional products (carbamates, carbonates, hydroxyketone), we expect similar applications. For example, oxazolidones could serve as building blocks for drug design. Furthermore, α CCs are efficient carbonylation agents, offering alternatives to toxic phosgene and derivatives, or to low reactivity dialkyl- or diaryl-carbonates.

The extension of this α CC chemistry to polymer synthesis is in its infancy, however a diversity of functional polymers (polyurethanes, polycarbonates, polyvinyls and sulfur-containing polymers) is now easily accessible under mild operating conditions. First, the reactivity of the exovinylene moiety towards radicals is exploited for producing polymers bearing cyclic carbonates by (controlled) radical polymerisation. Hydrolysis or aminolysis of the cyclic carbonate groups has given access to multiple modification possibilities, enlarging the scope of functional polymers. For instance, polyethylene bearing polar 1,2-diol groups are now accessible by copolymerising α CCs with ethylene followed by the cyclic carbonate hydrolysis, opening new perspectives in the preparation of polar polyolefins. Second, the facile regio-selective ring-opening of α CCs by various nucleophiles has been utilised to furnish various regio-regular polymers by step-growth copolymerisation of bis(α -alkylidene cyclic carbonate)s (bis α CCs) with nucleophilic comonomers (i.e. diamines, diols or dithiols). Remarkably, from a given bis α CC, 5 different polymer microstructures were prepared by selecting the nucleophilic comonomer, and from a given bis α CC/nucleophile pair, the type of polymer linkages can be modulated on demand by the choice of the catalyst.

As most of the polymers accessible from (bis)exovinylene cyclic carbonates are produced by conventional polymerisation methods virtually compatible with existing industrial equipment's, their cost will mainly depend on the production cost of the monomers and on the ability to recycle the catalyst easily and efficiently. Much effort has thus to be devoted to utilise cost-effective propargylic alcohols and to develop efficient routes to recycle the catalysts. We have to emphasise that most of the polymerisations involving (bis)exovinylene cyclic carbonates are performed under mild operating conditions (25°C, ambient atmosphere), which is beneficial to decrease the carbon footprint of the process in comparison to the conventional procedures that involve high temperatures and vacuum, e.g. for the preparation of polycarbonates by polycondensation.

Currently, the sourcing of the bispropargylic alcohols remains the main bottleneck to access a wide range of bis α CCs monomers at reasonable cost and large volume for the scaling up of the technology. Recent contributions by BASF have shown that cheap bulk chemical 1,4-butanediol can be used to produce bis α CCs, which should contribute to accelerate the developments in the field.^[77] Many questions remain unanswered, for example how to design polymers of high molar masses, what are the properties of these materials, how to enlarge the range of bis α CCs from biosourced or waste chemical products, etc. These answers are essential to define the scope of applications, e.g. for foams, adhesives, biomaterials, packaging.... Some poly(carbonate)s prepared by this α CC chemistry have already been evaluated as solid electrolytes for lithium-ion batteries working at room temperature with excellent cycling performance^[176,178] or for luminescent materials^[177] and isocyanate-free polyurethanes that are degradable on-demand by using pH as a trigger^[86] or that present a high thermal stability^[91] were also developed.

Chapter 1

It is important to note that little data are currently available to fairly compare the properties of the polymers prepared from α CCs to those obtained by the conventional techniques. They are also structurally different, e.g. α CCs-based polycarbonates contain pendant or in-chain ketone groups, poly(oxazolidone)s contain hydroxyl moieties - functionalities that are difficult to obtain in a direct way by the conventional techniques. The properties of the new polymers are thus expected to be different, however this needs to be investigated.

In conclusion, this review has highlighted the extremely rich α CC chemistry that is expected to be impactful in the fields of organic and polymer chemistries as a multitude of important chemical groups can be easily added mostly by 100% atom economy reactions under mild operating conditions. This chemistry is no more a curiosity and new products are expected in the next future in view of the recent patents of Henkel and BASF.^[189–193]

6. Supplementary information

Catalysts for α CCs synthesis

Homogenous single activation catalysts

Table S 1. Catalytic performances of selected organic bases for the carboxylative coupling of CO₂ with 2-methyl-3-butyn-2-ol in neat conditions (results plotted in **Figure 1**).

Catalyst	Loading (mol%)	Temp (°C)	P (bar)	Conv (%)	Yield DMACC (%)	Duration (h)	Ref
PPh ₃	8	140	50	100	78	20	[45]
PBu ₃	5	100	100	100	99	15	[194]
NEt ₃	100	30	10	0	0	10	[47]
TBD	10	100	50	91	21	24	[48]
MTBD	1	60	30	100	52	8	[49]

Table S 2. Catalytic performances of selected Lewis base-CO₂ adducts for the carboxylative coupling of CO₂ with 2-methyl-3-butyn-2-ol in neat conditions (results plotted in **Figure 2**).

Catalyst	Loading (mol%)	Temp (°C)	P (bar)	Conv (%)	Yield DMACC (%)	Duration (h)	Ref
NHC-CO ₂	5	60	45	100	99	15	[50]
NHO-CO ₂	5	60	20	100	96	3	[55]
DBN-CO ₂	5	60	20	100	91	2	[54]
CDC-CO ₂	5	80	20	100	94	12	[51]
AFIB-CO ₂	2	60	20	100	97	5	[53]

Table S 3. Catalytic performances of selected Ionic Liquids for the carboxylative coupling of CO₂ with 2-methyl-3-butyn-2-ol in neat conditions – Influence of the cations (results plotted in **Figure 3**).

Catalyst	Loading (mol%)	Temp (°C)	P (bar)	Conv (%)	Yield DMACC (%)	Duration (h)	Ref
[nBu ₄ N][OAc]	5	80	50	100	93	6	[59]
[nBu ₄ P][OAc]	5	80	50	100	10	6	[59]
[DBUH][OAc]	5	80	50	100	0	6	[59]
[BMIm][OAc]	5	80	50	100	16	6	[59]

Table S 4. Catalytic performances of selected Ionic Liquids for the carboxylative coupling of CO₂ with 2-methyl-3-butyn-2-ol in neat conditions – Influence of the anions (results plotted in **Figure 4**).

Catalyst	Loading (mol%)	Temp (°C)	P (bar)	Conv (%)	Yield DMACC (%)	Duration (h)	Ref
[nBu ₄ N][OPh]	5	80	50	100	89	1	[59]
[nBu ₄ N][Im]	5	80	50	100	93	6	[59]
[nBu ₄ N][CN]	5	80	30	100	84	6	[40]
[nBu ₄ N][F]	5	100	50	100	10	24	

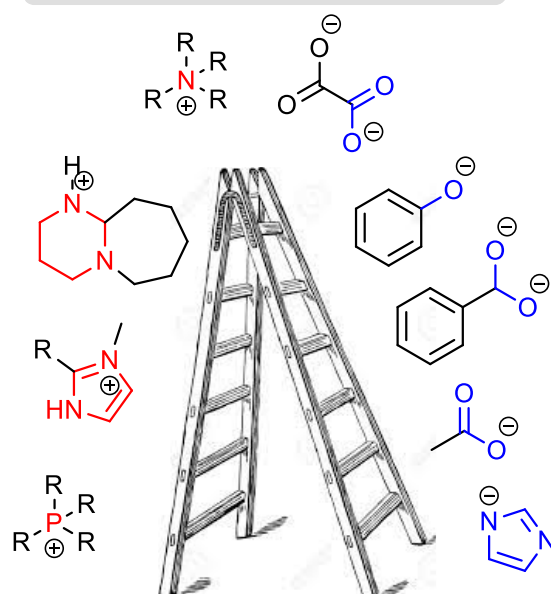
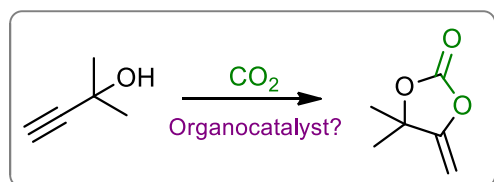
Table S 5. Catalytic performances of dual catalytic systems for the carboxylative coupling of CO₂ with 2-methyl-3-butyn-2-ol in neat conditions – Influence of the metal salt (results plotted in **Figure 5**).

Org.catalyst/ AgOAc	Loading (mol%)	Temp (°C)	P (bar)	Conv (%)	Yield DMACC (%)	Duration (h)	Ref
[nBu ₄ P][Lev]	(67/2)	25	10	100	98	4	[75]
[nHept ₄ N][Br]	(6/1)	25	1	100	98	12	[72]
*Er-NHC	(2/2)	25	20	100	92	24	[43]
*Dave Phos	(2/2)	25	20	100	87	16	[77]
[Hex ₃ QP][Im]	(10/1)	20	1	100	89	30	[62]

*in acetonitrile

CHAPTER 2

**Boosting the performance of organic salts
for the fast and selective synthesis of α -
alkylidene cyclic carbonates from carbon
dioxide and propargylic alcohols**



Chapter 2

The results presented in this chapter are published in

Bruno Grignard, Charlène NgassamTounzoua, Sandro Gennen, Bernard Gilbert, Raphaël Méreau, Christine Jérôme, Thierry Tassaing, Christophe Detrembleur, CHEMCATCHEM, 2018, 10, 2584-2592. <http://dx.doi.org/10.1002/cctc.20180006>

The DFT computational studies were conducted by Dr Raphael Méreau of the university of Bordeaux.

Table of contents

1. Introduction	52
2. Results.....	53
2.1. Catalyst synthesis.	53
2.2. Screening of the catalyst's activity.	55
2.3. Kinetic studies by in situ Raman Spectroscopy	62
2.4. Influence of reaction conditions.....	65
2.5. Screening of other propargylic alcohols.....	66
3. Conclusions	68
4. Experimental section	69
4.1. Material	69
4.2. Characterisation	69
4.3. Experimental procedures	70
5. Supplementary information.....	75

1. Introduction

The carboxylative cyclisation of alkynols with CO₂ requires a catalyst to proceed, and for that purpose, various metal-free systems derived from (organic) bases such as phosphines,^[45,194] guanidine,^[48] K₂CO₃, N-heterocyclic carbenes (NHC)^[50,195,196] and olefins (NHO),^[55] or ionic liquids^[60] have been developed. However, most of these catalysts were efficient at temperatures comprised between 60-100 °C and pressures of 25-100 bar. Moreover, long reaction times and/or high catalyst loading were required to attain high propargylic alcohol conversion. Liu et al. developed novel phosphonium-based organocatalysts by introducing the concept of multiple-site activation of CO₂ via the use of anions derived from carboxylic acid and/or hydroxyl multifunctional pyridines. With a loading of 10 mol%, these catalysts showed good activity at 1 bar and 30 °C, with yields between 33-91% after 20 h.^[61] The rare examples of the organocatalysed coupling reactions promoted at low CO₂ pressure (1 bar) were performed with a large excess of the catalyst compared to the reactant.^[118]

In 2016, Wang et al. reported series of novel reusable ionic liquids (ILs) derived from 1,8-Diazabicyclo[5.4.0]undec-7-ene (DBU) that were able to promote the synthesis of αCCs at 60 °C and 25 bar.^[60] Sadly, at an ILs loading of 200 mol% with respect to the propargylic alcohols, the coupling reaction remained slow as attested by yields of 68-89% after 24 h. This moderate activity might be related to the low basicity of ILs. Indeed, Wang et al. correlated the catalytic activity of phosphonium-based ILs with the basicity of their counter-anion. Anions such as imidazolides with a pK_a value close to 7.4 represented the best compromise in terms of reaction yield and selectivity.^[62]

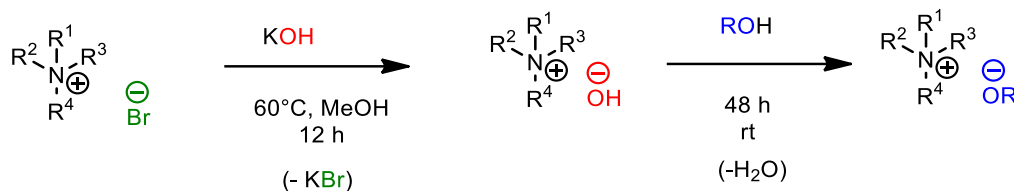
Although huge progresses have been made in the field of organocatalysis, the rational correlation between their structure and their influence on the reaction rate and selectivity is rarely addressed, and the presence of side products not deeply investigated.

In this chapter, various organic salts were prepared and evaluated for the CO₂/alkynols coupling reaction. The objective was to identify the important structural parameters that dictate the performances of the catalyst in terms of both the rate and the selectivity of the reaction, while maintaining the catalyst loading low (5 mol%). Tetrabutylammonium acetate was chosen as a reference catalyst of moderate activity.^[40] By tuning the structure of both the cation (ammonium, phosphonium, imidazolium or guanidinium) and anion ((di-)carboxylates, phenolates, boronate, imidazolidide), the basicity of the catalyst was modulated, which strongly impacted the catalytic activity.

2. Results

2.1. Catalyst synthesis.

The ammonium and phosphonium based catalysts were synthesised by a two-step process according to adapted procedures from the literature (**Scheme 1**).



Scheme 1. General strategy for the synthesis of organic catalysts. R₁ = R₂ = R₃ = R₄ = -CH₃, -C₄H₉, -C₈H₁₇. Nitrogen can be replaced by phosphorus.

The first step consisted in exchanging the halide anion of the quaternary ammonium/phosphonium salts by an OH⁻ anion by reaction with potassium hydroxide. Then, the quaternary ammonium/phosphonium hydroxide salt/IL was neutralised by addition of carboxylic acids of various structures, phenol derivatives, phenyl boronic acid or imidazole.^[197,198] All synthetic procedures and characterisations are detailed in the experimental section and SI-1. **Figure 1** summarises the library of organocatalysts prepared: they are based on ammonium and phosphonium salts with carboxylates, phenolates, boronate or imidazolate counter-anions.

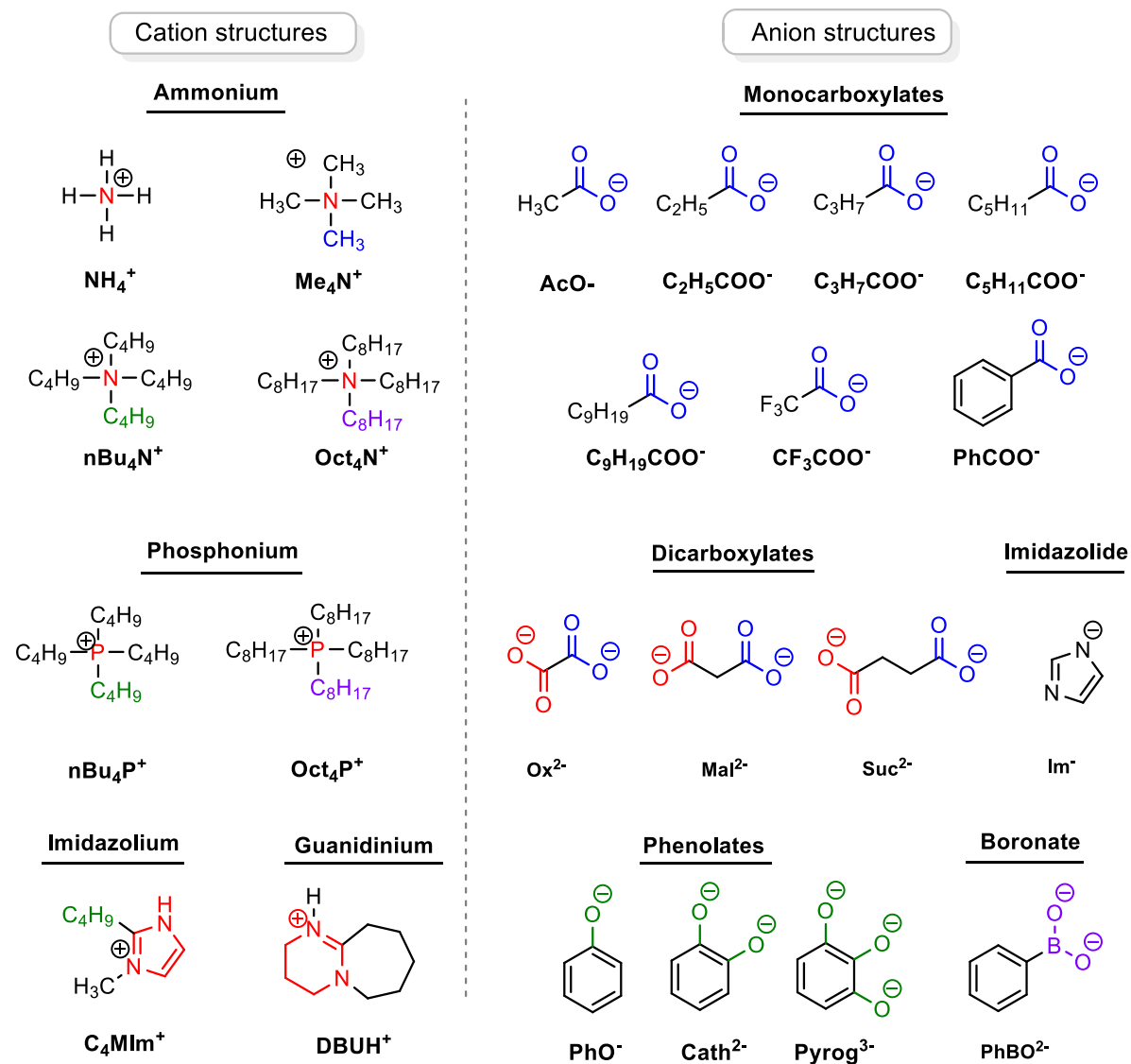
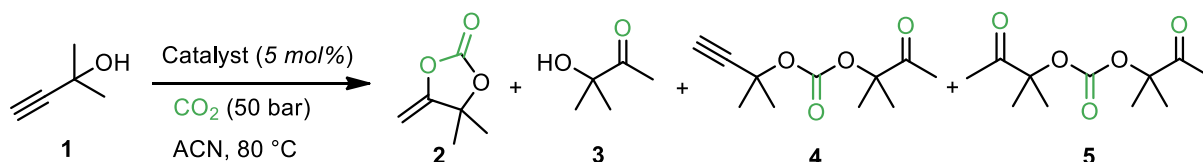


Figure 1. Structures of cations and anions used to design ionic liquid catalysts for the coupling of CO_2 and propargylic alcohols.

2.2. Screening of the catalyst's activity.

The basicity of the catalyst has been shown crucial for the selective coupling of propargylic alcohols with CO₂.^[49,62] In this study, we focused first on organocatalysts based on carboxylate anions; whose basicity can be tuned by varying the structure of their alkyl substituent. Their activity and selectivity towards the formation of αCCs was screened using a model reaction, the cyclisation of 2-methyl-3-butyn-2-ol and CO₂ under solvent-free conditions at 50 bar, 80 °C for 6 h using 5 mol% of catalyst (**Scheme 2**).



Scheme 2. Coupling of CO₂ with propargylic alcohol. Products **3**, **4** and **5** represent the main by-products.

Tetrabutylammonium acetate ([nBu₄N][OAc]) was first tested as the reference catalyst. **Figure S 2** illustrates the ¹H NMR spectra of [nBu₄N][OAc], 2-methyl-3-butyn-2-ol and the crude reaction mixture obtained after 6 h. Formation of αCC, 4,4-dimethyl-5-methylene-1,3-dioxolan-2-one (**Scheme 2**, product **2**) was attested by the appearance of peaks at 4.33 ppm and 4.77 ppm typical of the exocyclic olefinic group of the αCC, and one singlet at 1.61 ppm assigned to the two methyl groups. Meanwhile, complete consumption of 2-methyl-3-butyn-2-ol was highlighted by the absence of any residual peaks of the reactant at 1.55, 2.16 and 2.44 ppm. However, the ¹H NMR spectrum of the crude sample also highlights the presence of two acyclic carbonates by-products. Product **4**, formed by the regio-selective ring-opening of αCC with 2-methyl-3-butyn-2-ol, shows typical resonances of methyl groups at 1.52, 1.72, 2.24 ppm, and one singlet at 2.54 ppm corresponding to the alkyne proton. By-product **5** produced by the addition of α-hydroxyketone **3** (formed by hydrolysis of αCC) onto αCC is also observed by the presence of its characteristic methyl group peaks at 1.53 and 2.18 ppm. Then, the conversion of 2-methyl-3-butyn-2-ol and the selectivity towards the formation of the (a)cyclic carbonates were determined by comparing the relative intensities of the integrations of characteristic peaks of each sample (see **SI-2** for details). [nBu₄N][OAc] afforded a quantitative conversion of 2-methyl-3-butyn-2-ol with the formation of αCC (product **2**) with a selectivity of 93%.

The catalytic performance of all organocatalysts was then tested for the same model reaction. The conversion and the selectivity towards the formation of product **2** were benchmarked with that obtained with [nBu₄N][OAc]. The influence of the structural parameters of the organocatalysts on their activity and selectivity is discussed in detail below.

Influence of the alkyl substituent of the ammonium

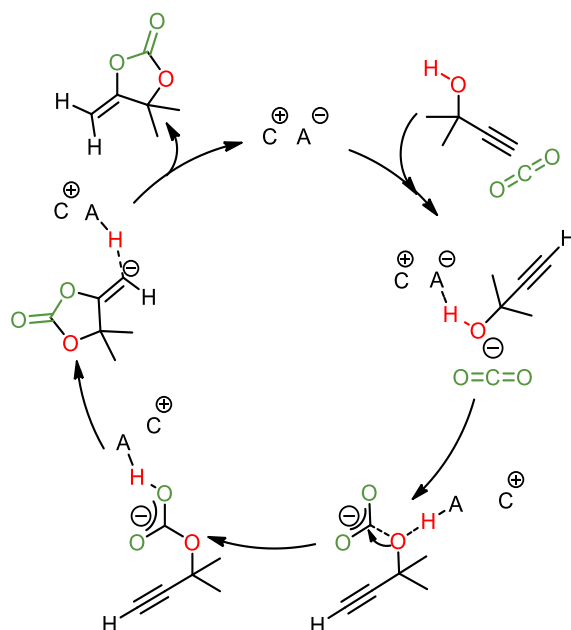
The influence of the nature of the alkyl chain of the ammonium cation and of its length on its catalytic performance was first evaluated for various ammonium bearing AcO^- anion. As illustrated in **Table 1**, (entries 1-4) the evolution of the 2-methyl-3-butyn-2-ol conversion was found strongly dependent on the alkyl chain length of the cation, e.g., 0% with hydrogen, < 6% with methyl or octyl, and 100% with n-butyl. Interestingly, the same evolution pervades for the same ammoniums bearing oxalate counter-anion as attested by a maximum conversion of 100% with a nBu_4N^+ cation (**Table 4**, entries 2-4).

Table 1. Influence of the substituent of the ammonium cation on the activity of the organocatalysts for the coupling of CO_2 to 2-methyl-3-butyn-2-ol.

Entry	Cation	Anion	pKa ^a	Conv. (%)	Selectivity (%)		
					2	4	5
1	NH_4^+	AcO^-	4.78	0	-	-	-
2	Me_4N^+	AcO^-	4.78	<6	93	n.d.	n.d.
3	nBu_4N^+	AcO^-	4.78	100	93	2	5
4	Oct_4N^+	AcO^-	4.78	<4	n.d.	n.d.	n.d.
5	K^+	AcO^-	4.78	0	-	-	-
6 ^b	K^+	AcO^-	4.78	13	92	-	8
7 ^c	K^+	AcO^-	4.78	88	87	5	7

Conditions: $T = 80\text{ }^\circ\text{C}$, $P = 50\text{ bar}$, $t = 6\text{ h}$, 0.03 mol of propargylic alcohol, 5 mol% of catalyst, volume of the cell = 20 ml. ^a pKa values in water of the conjugate acid. ^b reaction in the presence of 18-crown-6, $([\text{K}][\text{OAc}])/[\text{18-crown-6}] = 1$, for 6h. ^c reaction in the presence of 18-crown-6, $([\text{K}][\text{OAc}])/[\text{18-crown-6}] = 1$, for 24h

This trend was explained by the cation-anion interactions impacting the ion pair separation and consequently the catalyst activity. Electrostatic interactions between the acetate anion and NH_4^+ or cations with short alkyl substituents in C_1 are expected to be strong, which disfavours the ion pair separation and lowers the catalytic activity of the acetate. Indeed, the well accepted mechanism^[40] involves the deprotonation of the hydroxyl group of the propargylic alcohol by a basic catalyst and the simultaneous nucleophilic attack of the alkoxide anion onto CO_2 . This first step results in the formation of a cation-carbonate ionic pair and an acid. Then, the ring closure and formation of the α -methylene cyclic carbonate occur via an intramolecular nucleophilic addition of the carbonate anion onto the $\text{C}\equiv\text{C}$ bond with the simultaneous protonation of the alkenyl anion by the acid (**Scheme 3**).



Scheme 3. Proposed general mechanism for the organocatalytic carboxylative coupling of CO₂ with propargylic alcohols with ammonium salts (C⁺A⁻).

From the optimised minimum energy structures of both catalysts calculated by the M06-2X functional using the 6-311G(d,p) basis set^[199] (**Figure 2**), the presence of two supplementary hydrogen bonds for [NH₄][OAc] shortens the distance between the two ions of the ions pair from 4.22 Å for [nBu₄N][OAc] to 2.82 Å for [NH₄][OAc]. This additional interaction observed with [NH₄][OAc] strongly hampers the catalytic activity of the acetate anion due to the energy needed to “break” this ion pair.

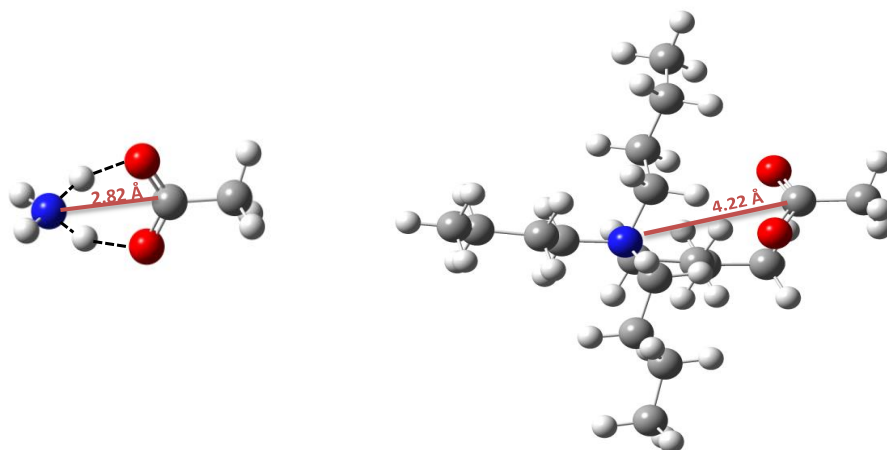


Figure 2. Optimised geometries (M06-2X/6-311G(d,p)) of the structures of [NH₄][OAc] (a) and [nBu₄N][OAc] (b).

In contrast, while substituents in C₈ should favour the ion pair separation, their bulkiness brings steric hindrance that is detrimental for the CO₂/2-methyl-3-butyn-2-ol coupling reaction. The butyl group appears to offer the best compromise in terms of ion pair separation and steric hindrance with a quantitative conversion in 6 h. Note that the poor 2-methyl-3-butyn-2-ol conversion (< 6%) obtained with NH₄⁺, Me₄N⁺ or Oct₄N⁺ prevents us from drawing any reliable conclusion regarding the influence of the alkyl chain length of the ammonium cation on the selectivity towards the formation of product **2**.

The crucial influence of the ion-pair separation on the catalyst activity was further confirmed experimentally by carrying out the coupling reaction in the presence of potassium acetate ([K][OAc]) as catalyst. This acetate salt displayed no catalytic activity (**Table 1**, entry 5) under the experimental conditions that are optimal for [nBu₄N][OAc] (**Table 1**, entry 3). Importantly, the addition of 18-crown-6 ([K][OAc]/[18-crown-6] = 1) activated this ammonium salt for the coupling reaction. Indeed, 13 and 90% of the propargylic alcohol were converted after 6 and 24 h, respectively, with a high selectivity (~ 87%) in αCC (product **2**) (**Table 1**, entries 6-7). The crown ether complexed the potassium cation, favoring the ion-pair separation and therefore the reaction.

Influence of the nature of the cation

The nature of the cation on the activity of AcO⁻-based organocatalysts was then evaluated, and the results are presented in **Table 2** below.

Table 2. Influence of the cation on the activity of the organocatalysts for the coupling of CO₂ to 2-methyl-3-butyn-2-ol.

Entry	Cation	Anion	pKa ^a	Conv. (%)	Selectivity (%)		
					2	4	5
1	nBu ₄ N ⁺	AcO ⁻	4.78	100	93	2	5
2	nBu ₄ P ⁺	AcO ⁻	4.78	11	92	8	0
3	Oct ₄ P ⁺	AcO ⁻	4.78	0	-	-	-
4	C ₄ MIm ⁺	AcO ⁻	4.78	16	100	-	-
5	DBUH ⁺	AcO ⁻	4.78	84	-	86	14

Conditions: T = 80 °C, P = 50 bar, t = 6 h, 0.03 mol of propargylic alcohol, 5 mol% of catalyst, volume of the cell = 20 ml. ^a pKa values in water of the conjugate acid.

By substituting nBu₄N⁺ for the phosphorous counterpart (nBu₄P⁺), the 2-methyl-3-butyn-2-ol conversion strongly decreased from 100% to only 11% (**Table 2**, entry 2), highlighting the importance of the nature of the cation on the catalytic performances. No catalytic activity was also noted for [Oct₄P][OAc] (**Table 2**, entry 3). By using imidazolium acetate

([C₄MIm][OAc]; **Table 2**, entry 4), a low conversion was also measured (16%) with however the product **2** as the main compound.

The catalytic performance of [nBu₄N][OAc] was then benchmarked with that of 1,8-diazabicyclo[5.4.0]-7-undecenium acetate ([DBUH][OAc], **Table 2**, entry 5)^[60] which was reported as a catalyst for the coupling of propargylic alcohols with CO₂ (although no data about the potential formation of by-products was available).^[60] [nBu₄N][OAc] was found slightly more active than [DBUH][OAc] as evidenced by a 2-methyl-3-butyn-2-ol conversion of 100% vs 84%. However, the major difference between the two organocatalysts arises from the selectivity toward the formation of product **2**. While [nBu₄N][OAc] yielded product **2** with a selectivity of 93%, by-product **4** was identified as the main compound with [DBUH][OAc]. This huge difference in selectivity is assumed to be the result of the acid-base equilibrium of [DBUH][OAc] that releases DBU (a superbases) in the reaction medium. Indeed, DBU (and other organic superbases) were shown to promote the formation of the acyclic carbonate at the expense of the cyclic one.^[48,49] Chen et al. also demonstrated that the increase of pK_a of amines for the catalysed propargylic alcohol/CO₂ reaction was found to increase the reaction rate but was detrimental to the selectivity.^[200] This study highlights the impact of the cation structure of AcO⁻ catalysts on their performances and further confirms that nBu₄N⁺ cation should be privileged for tailoring efficient organocatalysts.

Influence of the R group of the carboxylate

We then investigated the influence of the structure of the carboxylate on the activity of the catalyst based on nBu₄N⁺ cation, the results are presented in **Table 3** below.

Table 3. Influence of the R-group of the carboxylate anion on the activity of the organocatalyst for the coupling of CO₂ to 2-methyl-3-butyn-2-ol.

Entry	Cation	Anion	pK _a ^a	Conv. (%)	Selectivity (%)		
					2	4	5
1	nBu ₄ N ⁺	CH ₃ COO ⁻	4.78	100	93	2	5
2	nBu ₄ N ⁺	C ₂ H ₅ COO ⁻	4.88	100	97	3	-
3	nBu ₄ N ⁺	C ₃ H ₇ COO ⁻	4.87	100	97	-	3
4	nBu ₄ N ⁺	C ₅ H ₁₁ COO ⁻	4.84	100	96	-	4
5	nBu ₄ N ⁺	C ₉ H ₁₉ COO ⁻	4.9	7	100	-	-
6	nBu ₄ N ⁺	PhCOO ⁻	4.19	95	98	2	-
7	nBu ₄ N ⁺	CF ₃ COO ⁻	0.05	<5	n.d.	n.d.	n.d.

Conditions: T = 80 °C, P = 50 bar, t = 6 h, 0.03 mol of propargylic alcohol, 5 mol% of catalyst, volume of the cell = 20 ml. ^a pK_a values in water of the conjugate acid.

Although increasing the length of the R alkyl chain of the carboxylate has only a very limited influence on the pKa value of the corresponding acid, the steric hindrance is expected to increase and might affect the catalytic activity. For R substituents in C₂, C₃ or C₅ (**Table 3**, entries 2-4), the activity of the corresponding catalysts was similar to that of [nBu₄N][OAc] (entry 1) with the quantitative conversion of 2-methyl-3-butyn-2-ol into product **2** with a selectivity above 96%. However, with a C₉ substituent (**Table 3**, entry 5), a very poor conversion was noted (< 10%). This difference in catalytic activity is assumed to be the result of the steric hindrance induced by the C₉ chain. Similarly, to the case of the alkyl substituents of ammonium cations, there is therefore an optimum carboxylate chain length beyond which the conversion starts declining. Replacing acetate by a slightly less basic benzoate (**Table 3**, entry 6) led to a slightly lower 2-methyl-3-butyn-2-ol conversion of 95% with a selectivity in product **2** of 98%. When the even less basic trifluoroacetate anion was used (**Table 3**, entry 7), only traces (< 5%) of 2-methyl-3-butyn-2-ol were converted. This result highlights the crucial role of the basicity of the carboxylate anion on the performances of the organocatalysts.

Influence of the nature of the anion

Tetrabutylammonium type organocatalysts composed of various anions (dicarboxylates, phenolate, catecholate, pyrogallolate, boronate, imidazolide) were then prepared and their activity compared under identical experimental conditions (50 bar, 80 °C, 6 h), **Table 4**.

Oxalate (Ox²⁻) was first tested as the anion (**Table 4**, entries 2-4). To account for the presence of 2 carboxylate groups (and thus 2 nBu₄N⁺) per oxalate, 2.5 mol% of catalyst was used instead of 5 mol% in order to compare the activity of the catalyst with the reference ([nBu₄N][OAc]). 2-methyl-3-butyn-2-ol was fully converted into product **2** with a selectivity superior to 99% by using [(nBu₄N)₂][Ox] (93% for [nBu₄N][OAc] and full conversion), compared to 63% conversion with 100% selectivity for [(Me₄N)₂][Ox]. Substituting the butyl or methyl groups of the ammonium by octyl ones was detrimental for the catalytic activity, only less than 4% of the propargyl alcohol was converted (**Table 4**, entry 4).

We then investigated the influence of the spacer between the two carboxylate groups on the catalyst performances by testing tetrabutylammonium malonate and succinate (**Table 4**, entries 5 and 6). The former afforded full conversion of 2-methyl-3-butyn-2-ol, with a similar selectivity for **2** as with [(nBu₄N)₂][Ox]. Although tetrabutylammonium succinate is also highly selective towards the formation of **2**, the 2-methyl-3-butyn-2-ol conversion only reached 44 % under identical experimental conditions. This observation is at first glance surprising based on the higher basicity of succinate. However, the low solubility of this catalyst in propargylic alcohol might account for this difference of activity. The other catalysts were fully soluble in the reaction medium.

We then tested tetrabutylammonium phenolate ($[\text{nBu}_4\text{N}][\text{OPh}]$) as potential catalyst (pK_a of phenol = 9.8, **Table 4**, entry 7). A full conversion of 2-methyl-3-butyn-2-ol was measured, however with a lower selectivity in **2** of 90% as compared to 100% conversion with $[(\text{nBu}_4\text{N})_2][\text{Ox}]$ (pK_{a2} of oxalate = 4.19) and 100% selectivity in **2**. This result confirms that highly basic catalysts are highly active but at the expense of the selectivity as previously discussed. Under identical experimental conditions, nBu_4N^+ with catecholate (Cath^{2-}), pyrogallolate (Pyrog^{3-}), phenylboronate (PhBO^{2-}) or imidazolid (Im^-) gave comparable results to nBu_4NOPh in terms of conversion and selectivity (**Table 4**, entries 8-11). No catalytic activity was observed when the organic anion was substituted for the hydroxyl or bromide one (**Table 4**, entries 12-13).

Table 4. Influence of the type of anion on the activity of the organocatalysts for the coupling of CO_2 to 2-methyl-3-butyn-2-ol.

Entry	Cation	Anion	pK_a^a	Conv. (%)	Selectivity (%)		
					2	4	5
1	nBu_4N^+	CH_3COO^-	4.78	100	93	2	5
2 ^b	Me_4N^+	Ox^{2-}	1.23, 4.19	63	100	-	-
3 ^b	nBu_4N^+	Ox^{2-}	1.23, 4.19	100	>99	trace	-
4 ^b	Oct_4N^+	Ox^{2-}	1.23, 4.19	< 4	n.d.	n.d.	n.d.
5 ^b	nBu_4N^+	Mal^{2-}	2.83, 5.69	100	>99	trace	-
6 ^{b,d}	nBu_4N^+	Suc^{2-}	4.16, 5.61	44	100	-	-
7	nBu_4N^+	PhO^-	9.89	100	90	3	7
8 ^b	nBu_4N^+	Cath^{2-}	9.3, 13	100	98	2	-
9 ^c	nBu_4N^+	Pyrog^{3-}	n.d.	100	90	10	-
10 ^b	nBu_4N^+	PhBO^{2-}	n.d.	100	93	7	-
11	nBu_4N^+	Im^-	6.95	100	93	7	-
12	nBu_4N^+	OH^-	/	-	-	-	-
13	nBu_4N^+	Br^-	/	-	-	-	-

Conditions: $T = 80^\circ\text{C}$, $P = 50\text{ bar}$, $t = 6\text{ h}$, 0.03 mol of propargylic alcohol, 5 mol% of catalyst, volume of the cell = 20 ml. ^a pK_a values in water of the conjugate acid. ^b using 2.5 mol% of catalyst. ^c using 1.66 mol% of catalyst. ^d Catalyst partially soluble.

2.3. Kinetic studies by in situ Raman Spectroscopy

The catalysts screening enabled us to identify the most efficient catalysts. However, full kinetics studies are required to classify them according to their catalytic activity and selectivity. Therefore, kinetic studies of the organocatalysed coupling of 2-methyl-3-butyn-2-ol with CO₂ were carried out by online Raman spectroscopy under similar experimental conditions (i.e., P = 50 bar, T = 80 °C, catalyst loading of 5 or 2.5 mol% (the latter with oxalate based organocatalysts)). The only difference compared to previous experiments arises from the addition of acetonitrile (acetonitrile/2-methyl-3-butyn-2-ol composition of 50/50 v/v) that served as an internal reference. **Figure 3** shows the Raman spectra of the starting product, 2-methyl-3-butyn-2-ol (product **1**), and the pure α CC (product **2**), recorded by using a red ruby laser of $\lambda = 785$ nm. The Raman spectrum of 2-methyl-3-butyn-2-ol shows two peaks at 2117 cm⁻¹ and 710 cm⁻¹ which are characteristic of the ν stretching and the δ C-H out of plane bending mode of the alkyne group, respectively. The Raman spectrum of product **2** shows a distinctive peak at 649 cm⁻¹, characteristic of the C=O out of plane bending vibration of the cyclic carbonate.

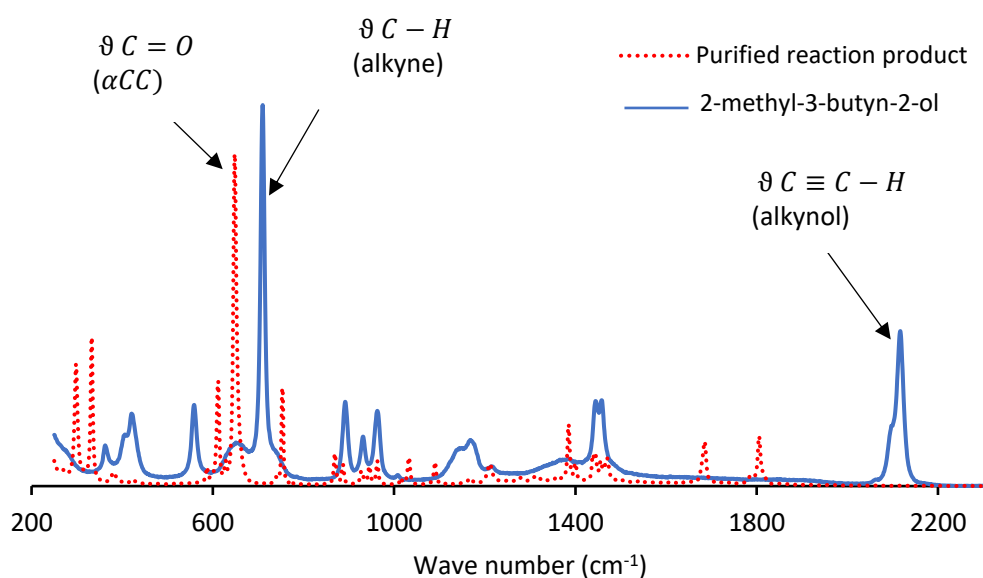


Figure 3. Raman spectra of 2-methyl-3-butyn-1-ol (blue), the crude reaction mixture obtained by [nBu₄N][OAc] promoted coupling of 2-methyl-3-butyn-2-ol with CO₂ (orange), and the purified α CC (green). Spectra recorded with a red ruby laser 785 nm.

The kinetics of the reaction was therefore monitored by following the disappearance of the alkyne peak at 710 cm⁻¹, and the appearance of the peak at 649 cm⁻¹ which is characteristic of the cyclic carbonate as illustrated on a typical 3D superposition of the Raman spectra recorded with time for the reaction catalysed by [nBu₄N][OAc] (**Figure 4 (top)**). The CO₂ peak intensity varied slightly at the early stages of the reaction and then reached a stable value once the propargylic alcohol/acetonitrile liquid phase was saturated by CO₂. The kinetic

profile of each monitored reaction was obtained by plotting the evolution of the relative intensity of the cyclic carbonate peak at 649 cm^{-1} with time.

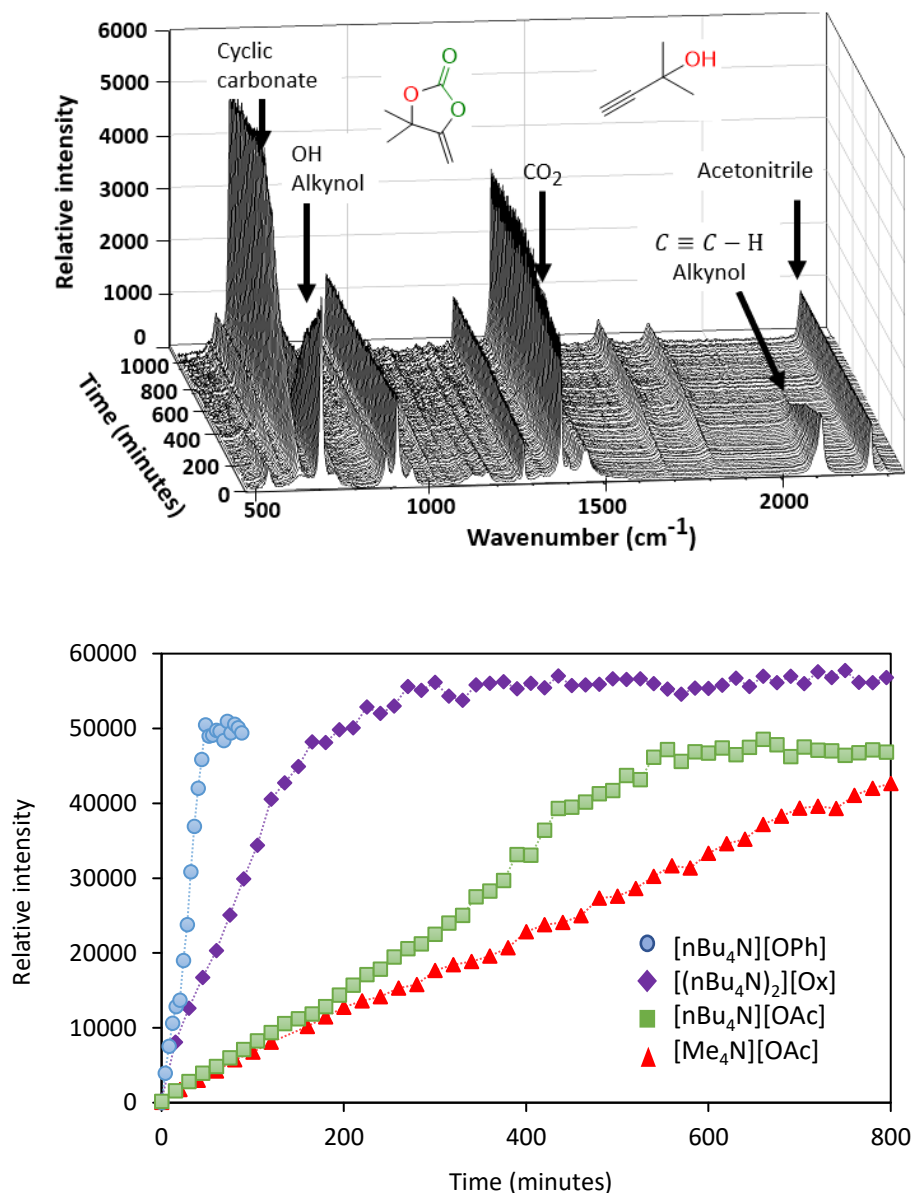


Figure 4. Addition of CO_2 to 2-methyl-3-butyn-2-ol in the presence of various organocatalysts. (top) Evolution of the Raman spectra with time, (bottom) Comparison of the kinetic profiles. Conditions: $T = 80\text{ }^\circ\text{C}$, $\text{PCO}_2 = 50\text{ bar}$, 0.15 mol (15 ml) of propargylic alcohol, 5 mol% of nMe_4OAc , nBu_4OAc and nBu_4OPh and 2.5 mol% for $(\text{nBu}_4\text{N})_2\text{Ox}$, volume of the cell = 80 ml, $v\text{ ACN} = 15\text{ ml}$.

Figure 4 (bottom) shows the kinetic profiles recorded for reactions catalysed by Me₄NOAc, [nBu₄N][OAc], (nBu₄N)₂Ox and nBu₄NOPh. Crucial information on the activity and selectivity of the catalysts was deduced from the slope of the kinetic curves (that is linked to the reaction rate) and from the intensity at which the plateau is reached (that is related to the content in product **2**). These profiles could not be established for (nBu₄N)₂Cath and (nBu₄N)₃Pyrog due to fluorescence of the reaction medium. From **Figure 4**, the organocatalysts were classified regarding their activity in the order Me₄NOAc < [nBu₄N][OAc] < (nBu₄N)₂Ox < nBu₄NOPh. The two latter organocatalysts (nBu₄NOPh and (nBu₄N)₂Ox) were identified as the most active ones as attested by a higher slope and a plateau value that was reached after 50 min and 270 min, corresponding to a 12-fold and ~ 2.5-fold increase of the activity as compared to [nBu₄N][OAc], respectively. Me₄NOAc was significantly less active, and no plateau was reached after 800 min of reaction.

The selectivity of the reaction in product **2** was estimated from the plateau value. With a relative intensity value of ~56000, (nBu₄N)₂Ox was found to be the most selective catalyst with a quantitative formation of the cyclic carbonate **2** as confirmed by ¹H NMR spectroscopy of the reaction medium. All typical signals of product **2** were observed with no side product and the absence of any propargylic alcohol. With respective relative intensity values of ~50000 and ~ 49000, nBu₄NOPh and [nBu₄N][OAc] were slightly less selective than (nBu₄N)₂Ox. By comparing the relative intensity values reached with these catalysts with the one for (nBu₄N)₂Ox, one estimates a selectivity towards product **2** of approximately 90 % that is in agreement with that reported for the catalyst screening experiments carried out under neat conditions (**Table 1**, entry 3 and **Table 4** entry 7).

2.4. Influence of reaction conditions

Influence of the pressure

Our group reported on the phase behaviour of propargylic alcohols/CO₂ biphasic systems and highlighted that the concentration of CO₂ dissolved in the propargylic alcohol phase decreased with a decrease in pressure at a constant temperature.^[201] This effect is reflected on the results we obtained as shown in the **Table 5** (entries 1-6).

Table 5. Influence of the pressure on the coupling reaction between CO₂ and 2-methyl-3-butyn-2-ol.

Entry	Cation	Anion	P (bar)	T (°C)	^b Conv. (%)	^b Selectivity (%)		
						2	4	5
1	nBu ₄ N ⁺	AcO ⁻	5	80	11	100	-	-
2 ^a	nBu ₄ N ⁺	Ox ²⁻	5	80	100	89	5	6
3	nBu ₄ N ⁺	PhO ⁻	5	80	100	35	65	-
4	nBu ₄ N ⁺	AcO ⁻	15	80	20	95	5	-
5 ^a	nBu ₄ N ⁺	Ox ²⁻	15	80	100	94	-	6
6	nBu ₄ N ⁺	PhO ⁻	15	80	100	89	7	4
7	nBu ₄ N ⁺	AcO ⁻	50	80	100	93	-	-
8 ^a	nBu ₄ N ⁺	Ox ²⁻	50	80	100	>99	trace	-
9	nBu ₄ N ⁺	PhO ⁻	50	80	100	90	3	7
10	nBu ₄ N ⁺	AcO ⁻	50	60	16	100	-	-
11 ^a	nBu ₄ N ⁺	Ox ²⁻	50	60	24	100	-	-
12	nBu ₄ N ⁺	PhO ⁻	50	60	63	100	-	-

Conditions: *t* = 6 h, 0.03 mol of propargylic alcohol, 5 mol% of catalyst, volume of the cell = 20 ml. ^a using 2.5 mol% of catalyst. ^b Conversion and selectivity determined by ¹H NMR.

At a constant temperature of 80 °C, reducing the pressure slows down the reaction rate as evidenced for experiments conducted with [nBu₄N][OAc] catalyst for which the conversion which is close to 100% at 50 bar (**Table 5**, entry 7) drops to 20 and 11% at 15 and 5 bar respectively (**Table 5**, entries 4 and 1 respectively). For the other two catalysts, a decrease in the pressure is detrimental for the selectivity towards the formation of the cyclic carbonate, which decreases, especially at extremely low CO₂ pressure. The higher competition between the CO₂ fixation on propargylic alcohol, and the ring-opening of the αCC (product **2**) by unreacted propargylic alcohol could be proposed as a plausible explanation for this trend. Nonetheless, even at 5 bar, the [(nBu₄N)₂][Ox] catalysts remained quite selective as compared to [nBu₄N][OPh] (**Table 5**, entries 2 and 3 respectively).

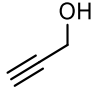
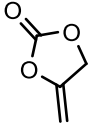
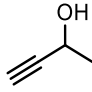
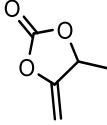
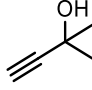
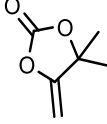
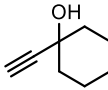
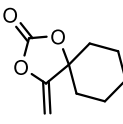
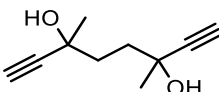
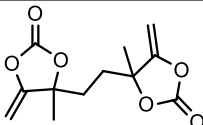
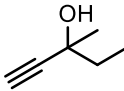
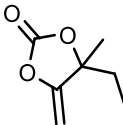
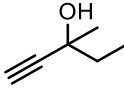
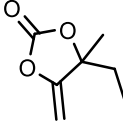
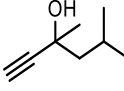
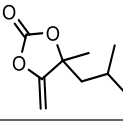
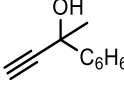
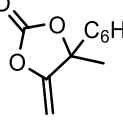
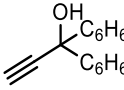
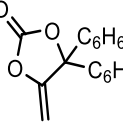
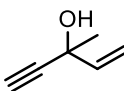
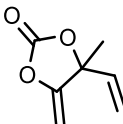
Influence of the temperature

The temperature can impact the reaction in two ways, i.e. by affecting the rate of the reaction, and by changing the solubility of CO₂ in the propargylic alcohol phase. We showed that for a constant pressure, the concentration of CO₂ dissolved in the alcohol phase decreases with the decrease in the temperature.^[201] In **Table 5** are summarised the results obtained for experiments conducted at 60 °C and 50 bar for 6 h using nBu₄NOAc, [(nBu₄N)₂][Ox] and [nBu₄N][OPh]. As expected, lowering the temperature slowed down the reaction as the conversions close to 100% at 80 °C with all catalysts (entries 7-9) decreased to 16, 24 and 63 by using respectively [nBu₄N][OAc], [(nBu₄N)₂][Ox] and [nBu₄N][OPh] (entries 10-12).

2.5. Screening of other propargylic alcohols

In an effort to broaden the scope of α -methylene cyclic carbonates that could be produced by this synthetic approach, the [(nBu₄N)₂][Ox] promoted coupling of CO₂ with various propargylic alcohols precursors was investigated using the optimum experimental conditions, i.e. p = 50 bar, T = 80 °C for 6 h using 2.5 mol% of catalyst (relative to the alcohol). The results obtained are summarised in **Table 6**. No α CC was formed from prop-2-yn-1-ol or but-3-yn-2-ol precursors, whereas 2-methyl-3-butyn-2-ol was fully and selectively converted into product **2** under similar experimental conditions. These results can be explained by the Thorpe-Ingold effect (or “gem effect”) which postulates that the mutual repulsion of gem di-methyl groups favour the cyclisation.^[42] When both methyl groups of 2-methyl-3-butyn-2-ol were replaced by a bulkier cyclohexyl substituent, the conversion was low (12 %) but the reaction was also highly selective (**Table 6**, entry 4). These results show that the steric hindrance induced by bulkier substituents may impede either the addition of CO₂ onto the alcohol, or the cyclisation of the carbonate ion. Interestingly, a polymerisable bis- α CC^[18] was synthesised from a bispropargylic alcohol with a conversion of 35% and a selectivity above 99% (**Table 6**, entry 5). When one of the methyl groups of 2-methyl-3-butyn-2-ol was replaced by an ethyl group, the conversion decreased to 20% but the selectivity remained excellent (100%) (**Table 6**, entry 6). Complete conversion was however reached after 24 h of reaction when using 5 mol% catalyst (**Table 6**, entry 7). Under these conditions, other bulky propargylic alcohols were almost quantitatively converted into the corresponding cyclic carbonates with a high selectivity (60-96%) (**Table 6**, entries 8-11). These experiments clearly highlight that the catalyst is active for the coupling reaction of CO₂ with a broad range of propargylic alcohols.

Table 6. Synthesis of various alkylidene 5-membered cyclic carbonates.

Entry	Reagent	Product	Conversion (%)	Selectivity (%)
1			0	0
2			0	0
3			100	99
4			12	100
5 ^a			35	99
6			20	100
7 ^{a,b}			99	93
8 ^b			99	95
9 ^b			98	95
10 ^b			98	85
11 ^b			100	60

Conditions: T = 80 °C, p = 50 bar, t = 6 h, 0.03 mol of propargylic alcohols, 2.5 mol% of $(nBu_4N)_2Ox$, volume of the cell = 20 ml. ^a experiment for 24 h. ^b 5 mol% of $(nBu_4N)_2Ox$

3. Conclusions

In this work, we tailored various organic salts that were tested as catalysts for the carboxylative coupling of CO₂ with propargylic alcohols. We have investigated the influence of the modulation of the structure of the organocatalyst (mainly the type and structure of the cation and anion) on the catalytic performances. Optimum activity resulted from the best compromise between ion-pair separation controlled by steric effects and the basicity of the anion. Low ion-pair separation might limit the catalytic activity because of stronger electrostatic interactions between the cation and the anion and a lower availability of the anion for the deprotonation of the alcohol. Organic salts with very basic anions increased the rate of the reaction but at the expense of the selectivity. Among the different salts that were tested, tetrabutylammonium oxalate appeared to be the most active catalyst for the 2-methyl-3-butyn-2-ol/CO₂ coupling reaction with quantitative conversion of the starting product into the corresponding α -methylene cyclic carbonate with a remarkable selectivity (> 99%) in less than 6 h of reaction at 50 bar and 80 °C under solvent free conditions. Only 2.5 mol% of catalyst (compared to the propargylic alcohol) were required for this performance. This study clearly opens new avenues for conceiving efficient organocatalysts for CO₂/propargylic alcohol coupling reactions, with potentially less toxicity than the metal-based ones because natural carboxylate anions favour the biodegradability and decrease the toxicity of the corresponding organic salts.^[202]

4. Experimental section

4.1. Material

Tetramethylammonium acetate ([Me₄N][OAc], fluorochem), tetrabutylammonium acetate ([nBu₄N][OAc], Aldrich), tetraoctylammonium bromide (Aldrich), tetrabutylphosphonium chloride, tetramethylammonium chloride, tetrabutylammonium bromide (Sigma-Aldrich), tetrabutylammonium hydroxide, tetraoctylphosphonium bromide, benzoic acid (Sigma-Aldrich), succinic acid (fluka), oxalic acid (Sigma-Aldrich), decanoic acid (Aldrich), acetic acid (VWR), imidazole (Acros), trifluoroacetic acid, propionic acid, butanoic acid, hexanoic acid, phenol (Aldrich), methanol (VWR), potassium hydroxide (Acros), sodium chloride (Acros), phenol (Aldrich), catechol (Aldrich), pyrogallol (Aldrich), phenylboronic acid (Fluorochem), acetonitrile, diethyl ether, ethyl acetate (Acros), acetone (VWR), carbon dioxide (N27, air liquid), 1-butyl-3-imidazolium acetate (abcr), 2-methyl-3-butyn-2-ol (Aldrich), 1-ethynylcyclohexanol (Aldrich), 3-ethyl-1-pentyn-3-ol (Aldrich), 3,5-dimethyl-1-hexyn-3-ol (Aldrich), 3-methyl-1-pentyn-3-ol (Aldrich), 2-phenyl-3-butyn-2-ol (Aldrich), 1,1-diphenyl-2-propyn-1-ol (Aldrich), potassium acetate (Aldrich), 18-crown-6 (Fluorochem), 3-methyl-1-penten-4-yn-3-ol (Aldrich), dimethylformamide (DMF, Acros), deuterated solvents (methanol, chloroform, dimethylsulfoxide, water) (Eurisotop) were used without purification.

4.2. Characterisation

Raman spectroscopy. The experimental setup used for the monitoring of the kinetics by Raman spectroscopy is composed of a mobile powerhead probe, connected to a LabRam 300 Jobin Yvon spectrometer. The laser beam is brought to the mobile probe by an optical fibre (100 µm in diameter), and is focused in the reactor with a lens (12 cm focal length, 4 cm o.d.). The Raman light is collected at 360° by the same lens, driven through an edge filter to remove the laser line, and focused on the entry of the collecting optical fibre, which is connected to the spectrophotometer. A red ruby laser with a wavelength of 785 nm is used. It is important to note that several lines corresponding to the sapphire window may appear on the spectra (418 and 750 cm⁻¹). Nonetheless, by adjusting properly the probe such that the laser beam is focused at approximately 2 mm beyond the sapphire window, this signal is avoided. The Raman spectra obtained during the experiments were subjected to several modifications. The fluorescence induced by the organocatalysts renders the Raman spectra base line not flat. Each spectrum is therefore flattened using either a 3rd or 4th degree polynomial equation. Then, the intensity of the reference peak is normalized to 10000. Acetonitrile peak at 2254 cm⁻¹ was used as reference. The normalization of the acetonitrile peak intensity at 2254 cm⁻¹ is carried out, using 2150 cm⁻¹ as lower bound and 2249 cm⁻¹ as upper bound. All the peak intensities are normalized with respect to that of acetonitrile. The kinetic curve of the CO₂/propargylic alcohol reaction is obtained by plotting the evolution of the intensity of the peak at 649 cm⁻¹ corresponding to the carbonate formation with respect to time. All the data treatment is done using special home-made programs

Nuclear magnetic resonance spectroscopy (NMR). The samples were prepared by dissolving 15-20 mg of product in 0.7 ml of a deuterated solvent. ^1H and ^{13}C NMR spectra were recorded at 298 K with a Bruker advance DRX 400 spectrometer operating at 400.13 MHz, on the Fourier transform mode.

Quantum chemistry calculations - Computational details.

Preliminary calculations of equilibrium structures were performed using a semi-empirical model (AM1-D₃H₄)^[199] to determine the most stable conformations. These semi-empirical calculations were performed using the AMPAC software. The CHAIN algorithm was used for locating intermediates and transition states along the reaction path. The lowest energy structures obtained at the AM1-D₃H₄ level were further investigated using the Density Functional Theory method (DFT) implemented in the Gaussian 09 package.^[203] DFT calculations of geometries, energies, and vibrational frequencies reported in this paper were carried out with the M06-2X functional^[199] using the 6-311G(d,p) basis set. All frequencies of each structure have also been calculated to verify the presence of a single imaginary frequency for transition states and the absence of imaginary frequency for ground states. The intrinsic reaction coordinate (IRC) method has been used to verify that the obtained transition states were effectively connected to the desired minima. For all catalysts, a wide range of possible configurations and interactions have been modelled and the more stable of them are reported in this work. To consider entropic effects, the energies mentioned in this study correspond to the Gibbs free energy (ΔG).

4.3. Experimental procedures

Catalyst synthesis: example of tetrabutylammonium oxalate.

In a 50 ml round bottom flask equipped with a magnetic rod were introduced 4.1006 g (0,0127 mol) of tetrabutylammonium bromide and 10 ml of MeOH. The mixture was stirred, and once the salt had dissolved, a solution of 0.7858 g (0.014 mol) of KOH in 10 ml of MeOH was added dropwise. The flask was heated gradually to 60 °C. After 24 h, the flask was cooled to room temperature and the mixture filtered to isolate the tetrabutylammonium hydroxide ([nBu₄N][OH]) solution from the KBr precipitate. In a second 50 ml flask placed in an ice bath was introduced 0.6302 g (0.007 mol) of oxalic acid dissolved in 2 ml of MeOH. The [nBu₄N][OH] solution was then added dropwise onto the oxalic acid. The mixture was led under stirring at room temperature for 48 h. Afterwards, MeOH was removed in vacuum and the moist salt obtained dried in vacuum at 50 °C for 24 h. A similar procedure was used for the preparation of all the other catalysts at the exception of [DBUH][AC], prepared by neutralizing DBU with acetic acid

All organocatalysts prepared were characterised by ^1H NMR and ^{13}C NMR, the results obtained are given below:

Tetraoctylammonium acetate ([Oct₄N][OAc]): white solid, ¹H NMR (400 MHz, Chloroform-*d*). δ (ppm) = 3.41 – 3.24 (m, 8H), 1.99 (s, 3H), 1.66 (ddd, J = 12.1, 7.8, 4.8 Hz, 8H), 1.34 (dp, J = 32.4, 8.2, 7.7 Hz, 41H), 0.99 – 0.75 (m, 12H). ¹³C NMR (400 MHz, Chloroform-*d*). δ (ppm) = 13.98, 22.21, 22.58, 23.94, 26.49, 29, 29.10, 31.01, 59.40, 176.16.

Tetrabutylphosphonium acetate ([nBu₄P][OAc]): yellow solid, ¹H NMR (400 MHz, Chloroform-*d*). δ (ppm) = 2.39 (m, 8H), 1.96 (s, 3H), 1.51 (m, J = 7.4 Hz, 16H), 1.04 – 0.85 (m, 12H). ¹³C NMR (400 MHz, Chloroform-*d*) δ (ppm) = 13.11, 18.48, 23.72, 23.90, 24.63, 177.14.

Tetrabutylammonium trifluoroacetate ([nBu₄N][CF₃COO]): light yellow solid, δ (ppm) = 3.41 – 3.22 (m, 8H), 1.70 – 1.57 (m, 8H), 1.43 (q, J = 7.3 Hz, 8H), 1.00 (t, J = 7.3 Hz, 12H). ¹³C NMR (400 MHz, Chloroform-*d*) δ (ppm) = 13.78, 19.68, 23.62, 58.90, 160.48, 160.79.

Tetrabutylammonium propanoate ([nBu₄N][C₂H₅COO]): yellow solid, ¹H NMR (400 MHz, Methanol-*d*₄) δ (ppm) = 3.31 – 3.20 (m, 8H), 2.18 (quad, J = 7.6 Hz, 2H), 1.77 – 1.60 (m, 8H), 1.44 (h, J = 7.4 Hz, 8H), 1.11 (t, J = 7.6 Hz, 3H), 1.05 (t, J = 7.4 Hz, 12H). ¹³C NMR (400 MHz, Methanol-*d*₄) δ (ppm) = 9.98, 12.72, 19.68, 23.62, 30.76, 58.90, 182.01.

Tetrabutylammonium butanoate ([nBu₄N][C₃H₇COO]): yellow solid, ¹H NMR (400 MHz, Chloroform-*d*) δ (ppm) = 3.26 – 3.15 (m, 8H), 2.10 – 1.97 (m, 2H), 1.64 – 1.44 (m, 8+2H), 1.34 (h, J = 7.4 Hz, 8H), 0.90 (t, J = 7.4 Hz, 12H), 0.82 (t, J = 7.4 Hz, 3H). ¹³C NMR (400 MHz, Chloroform-*d*) δ (ppm) = 9.98, 13.55, 19.59, 20.24, 23.79, 41.12, 58.56, 178.91.

Tetrabutylammonium hexanoate ([nBu₄N][C₅H₁₁COO]): yellow solid, ¹H NMR (400 MHz, Chloroform-*d*) δ (ppm) = 3.29 – 3.16 (m, 8H), 2.15 – 1.99 (t, 2H), 1.67 – 1.47 (m, 8+2H), 1.37 (h, J = 7.4 Hz, 8H), 1.23 (dq, J = 7.7, 3.6 Hz, 4H), 0.93 (t, J = 7.4 Hz, 12H), 0.86 – 0.73 (t, 3H). ¹³C NMR (400 MHz, Chloroform-*d*) δ (ppm) = 13.56, 14.09, 19.71, 22.73, 23.90, 26.81, 32.18, 39.01, 58.53, 178.91.

Tetrabutylammonium decanoate ([nBu₄N][C₉H₁₉COO]): lemon green solid, ¹H NMR (400 MHz, Chloroform-*d*) δ (ppm) = 3.42 – 3.27 (m, 8H), 2.31 – 2.14 (m, 2H), 1.63 (dt, J = 15.4, 7.9 Hz, 10H), 1.45 (h, J = 7.4 Hz, 8H), 1.36 – 1.16 (m, 8+4H), 1.00 (t, J = 7.3 Hz, 12H), 0.87 (t, J = 6.7 Hz, 3H). ¹³C NMR (400 MHz, Chloroform-*d*) δ (ppm) = 13.68, 14.13, 19.77, 22.68, 24.13, 26.57, 29.35, 29.63, 29.67, 29.87, 32.02, 37.85, 58.74, 178.55.

Tetrabutylammonium benzoate ([nBu₄N][PhCOO]): beige solid, ¹H NMR (400 MHz, Chloroform-*d*) δ (ppm) = 8.34 – 7.78 (m, 2H), 7.28 – 7.24 (m, 3H), 3.36 – 3.15 (m, 8H), 1.66 – 1.48 (m, 8H), 1.37 (h, J = 7.4 Hz, 8H), 0.94 (t, J = 7.3 Hz, 12H). ¹³C NMR (400 MHz, Chloroform-*d*) δ (ppm) = 13.69, 19.68, 23.99, 58.69, 127.02, 128.48, 129.44, 140.90, 171.34.

Tetramethylammonium oxalate ([Me₄N]₂[Ox]): white solid, ¹H NMR (400 MHz, Methanol-*d*₄) δ (ppm) = 3.15 (s, 12H). ¹³C NMR (400 MHz, Methanol-*d*₄) δ (ppm) = 55.85, 169.55.

Tetrabutylammonium oxalate ($[(\text{Bu}_4\text{N})_2][\text{Ox}]$): white solid, ^1H NMR (400 MHz, Chloroform-*d*) δ (ppm) = 3.41 – 3.22 (m, 8H), 1.80 – 1.56 (m, 8H), 1.45 (q, $J = 7.3$ Hz, 8H), 1.00 (t, $J = 7.3$ Hz, 12H). ^{13}C NMR (400 MHz, Chloroform-*d*) δ (ppm) = 13.48, 19.81, 24.41, 58.68, 166.79

Tetraoctylammonium oxalate ($[(\text{Oct}_4\text{N})_2][\text{Ox}]$): white solid, ^1H NMR (400 MHz, Chloroform-*d*) δ (ppm) = 3.40 – 3.19 (m, 8H), 1.65 (ddd, $J = 12.1, 7.9, 4.8$ Hz, 8H), 1.54 – 1.10 (m, 40H), 1.02 – 0.73 (m, 12H). ^{13}C NMR (400 MHz, Chloroform-*d*) δ (ppm) = 14.05, 22.08, 22.53, 26.37, 28.96, 29.13, 31.64, 58.90, 166.16.

Tetrabutylammonium malonate ($[(\text{Bu}_4\text{N})_2][\text{Mal}]$): white solid, ^1H NMR (400 MHz, Chloroform-*d*) δ (ppm) = 3.37 – 3.23 (m, 8H), 3.04 (s, 2H), 1.75 – 1.53 (m, 8H), 1.42 (q, $J = 7.4$ Hz, 8H), 0.98 (t, $J = 7.3$ Hz, 24H). ^{13}C NMR (400 MHz, Chloroform-*d*) δ (ppm): 13.78, 19.43, 23.73, 58.68, 100.04, 173.53.

Tetrabutylammonium succinate ($[(\text{Bu}_4\text{N})_2][\text{Suc}]$): white solid, ^1H NMR (400 MHz, Chloroform-*d*) δ (ppm) = 3.35 – 3.21 (m, 8H), 2.52 (s, 4H), 1.74 – 1.54 (m, 8H), 1.43 (h, $J = 7.4$ Hz, 8H), 1.00 (t, $J = 7.3$ Hz, 12H). ^{13}C NMR (400 MHz, Chloroform-*d*) δ (ppm) = 13.49, 19.71, 23.85, 33.14, 58.78, 177.83.

Tetrabutylammonium phenolate ($[\text{nBu}_4\text{N}][\text{OPh}]$): pale beige solid, ^1H NMR (400 MHz, Chloroform-*d*) δ (ppm) = 7.18 – 7.00 (t, 2H), 6.97 – 6.81 (d, 2H), 6.67-6.59 (t, 1H) 3.26 – 3.05 (m, 8H), 1.69 – 1.44 (m, 8H), 1.38 (h, $J = 7.3$ Hz, 8H), 0.97 (t, $J = 7.3$ Hz, 12H). ^{13}C NMR (400 MHz, Chloroform-*d*) δ (ppm) = 13.78, 19.68, 24.32, 58.90, 116.27, 128.78, 159.07.

Tetrabutylammonium imidazole-1-ide ($[\text{nBu}_4\text{N}][\text{Im}]$): yellow solid, ^1H NMR (400 MHz, Chloroform-*d*) δ (ppm) = 7.66 (s, 1H), 7.04 (d, $J = 1.0$ Hz, 2H), 3.39 – 3.26 (m, 8H), 1.65 (td, $J = 8.0, 4.0$ Hz, 8H), 1.44 (h, $J = 7.3$ Hz, 8H), 1.00 (t, $J = 7.3$ Hz, 12H). ^{13}C NMR (400 MHz, Chloroform-*d*) δ (ppm) = 13.79, 19.53, 23.80, 59.06, 135.06.

Tetrabutylammonium benzene-1,2,-bis(olate) ($[(\text{Bu}_4\text{N})_2][\text{OCath}]$): dark green solid, ^1H NMR (400 MHz, Methanol-*d*₄) δ (ppm) = 7.11 (t, 2H), 6.96 (d, 2H), 6.70 (t, 1H), 3.30 – 3.20 (t, 8H), 1.68 (p, $J = 7.8$ Hz, 8H), 1.44 (h, $J = 7.4$ Hz, 8H), 1.04 (t, $J = 7.4$ Hz, 12H). ^{13}C NMR (400 MHz, Methanol-*d*₄) δ (ppm) = 13.78, 19.68, 24.32, 58.90, 116.27, 128.78, 159.07.

Tetrabutylammonium benzene-1,2,3-tris(olate) ($[(\text{Bu}_4\text{N})_3][\text{Pyrog}]$): dark brown solid, ^1H NMR (400 MHz, Methanol-*d*₄) δ (ppm) = 6.67 (m, 2H) 6.50 (m, 1H), 3.31 – 3.22 (m, 8H), 1.78 – 1.58 (m, 8H), 1.44 (h, $J = 7.4$ Hz, 8H), 1.05 (t, $J = 7.4$ Hz, 12H). ^{13}C NMR (400 MHz, Methanol-*d*₄) δ (ppm) = 12.43, 19.13, 22.98, 57.63, 114.13, 117.67, 149.79, 168.2 .

Tetrabutylammonium phenyl boronate ($[(\text{Bu}_4\text{N})_2][\text{PhBO}]$): pinkish-orange solid, ^1H NMR (400 MHz, Methanol-*d*₄) δ (ppm) = 7.54 – 7.48 (d, 2H), 7.18 – 7.10 (t, 2H), 7.07 - 7.04 (t, 1H), 3.31 – 3.21 (t, $J = 7.9$ Hz, 8H), 1.69 (p, $J = 7.9$ Hz, 8H), 1.45 (hept, $J = 7.8, 7.3$ Hz, 8H), 1.05 (t, $J = 7.3$ Hz, 12H). ^{13}C NMR (400 MHz, Methanol-*d*₄) δ (ppm) = 12.73 , 19.43, 22.98, 58.01, 124.75, 125.81, 132.51.

Organocatalysed carboxylative coupling of neat 2-methyl-3-butyn-2-ol with CO₂.

In a representative experiment, a stainless-steel autoclave with a nominal volume of 12 ml, equipped with a magnetic rod, a manometer and a gas inlet/outlet was charged with 3 mL (30,92 mmol) of 2-methyl-3-butyn-2-ol and 0.4474 g (0.7784 mmol) of $[(\text{Bu}_4\text{N})_2][\text{Ox}]$. The autoclave was equilibrated at 80 °C for 30 min. Then, the reaction was allowed to run during 6 h at constant CO₂ pressure of 50 bar. The crude reaction mixture was analysed by ¹H NMR to determine the conversion, identify the products and determine the selectivity of the reaction. After reaction, 4,4-dimethyl-5-methylene-1,3-dioxolan-2-one was purified by flash chromatography onto silica using CH₂Cl₂ as eluent. The solvent was then removed under vacuum and the dried products further purified by sublimation.

For the kinetics of reaction performed by on-line Raman spectroscopy, similar conditions were used but in this case, and equal volume of acetonitrile (3 ml) with respect to 2-methyl-3-butyn-2-ol was used.

NMR characterisation of products **2**, **3**, **4** and **5**^[48]

4,4-dimethyl-5-methylene-1,3-dioxolan-2-one (Product 2). ¹H NMR (400 MHz, Chloroform-*d*, δ in ppm) = 4.77 (dd, *J* = 4.0, 0.7 Hz, 1H), 4.32 (dd, *J* = 3.9, 0.7 Hz, 1H), 1.62 (s, 6H).

3-hydroxy-3-methylbutan-2-one (Product 3). ¹H NMR (400 MHz, DMSO, δ in ppm), 1.17 (6H, s), 2.15 (3H, s), 5.24 (1H, s)

2-methyl-3-oxobutan-2-yl (2-methylbut-3-yn-2-yl) carbonate (Product 4). ¹H NMR (400 MHz, CDCl₃, δ in ppm), 1.519 (6H, s), 1.72 (6H, s), 2.18 (3H, s), 2.56 (1H, s)

Bis(2-methyl-3-oxobutan-2-yl) carbonate (Product 5). ¹H NMR (400 MHz, CDCl₃, δ in ppm), 1.56 (12H, s), 2.18 (6H, s).

Organocatalysed carboxylative coupling of neat 2-methyl-3-butyn-2-ol with CO₂ using KOAc/18-crown-6 catalysts.

In a representative experiment, a stainless-steel autoclave with a nominal volume of 20 ml, equipped with a magnetic rod, a manometer and a gas inlet/outlet was charged with 5 mL (51.59 mmol) of 2-methyl-3-butyn-2-ol and previously dried overnight at 25 °C, [K][OAc] (2.58 mmol, 0.2531 g) and 18-crown-6 (2.58 mmol, 0.6818 g). The autoclave was equilibrated at 80 °C and allowed to run during 6 h at constant CO₂ pressure of 50 bar. The crude reaction mixture was analysed by ¹H NMR to determine the conversion, identify the products and determine the selectivity of the reaction.

Organocatalysed carboxylative coupling of propargylic alcohol with CO₂: substrate scope

The synthesis of α CCs from 3,5-dimethyl-1-hexyn-3-ol, 3-methyl-1-pentyn-3-ol, 2-phenyl-3-butyn-2-ol, 3-methyl-1-penten-4-yn-3-ol (Aldrich) and 1,1-diphenyl-2-propyn-1-ol, follows a similar protocol to the one described for the synthesis of 4,4-dimethyl-5-methylene-1,3-dioxolan-2-one from 2-methyl-3-butyn-2-ol.

In a representative experiment a stainless-steel autoclave with a nominal volume of 12 ml, equipped with a magnetic rod, a manometer and a gas inlet/outlet was charged with 3,5-dimethyl-1-hexyn-3-ol (5 mL, 34.03 mmol) of 2-methyl-3-butyn-2-ol and 0.4865 g (0.85 mmol) of (nBu₄N)₂Ox. Then, the autoclave was equilibrated at 80 °C and the reaction was allowed to run during 6 h at constant CO₂ pressure of 50 bar. The crude reaction mixture was analysed by ¹H NMR in CDCl₃ to determine the conversion, identify the products and determine the selectivity of the reaction. After reaction, all cyclic carbonates were purified by chromatography onto silica by using a 90/10 petroleum ether (40-60 °C)/ethyl acetate mixture as eluent.

4-ethyl-4-methyl-5-methylene-1,3-dioxolan-2-one (pale yellow oil): ¹H NMR (400 MHz, Chloroform-*d*) δ (in ppm) = 4.83 (d, *J* = 3.9 Hz, 1H), 4.28 (d, *J* = 3.9 Hz, 1H), 1.93 (dq, *J* = 14.7, 7.3 Hz, 1H), 1.78 (dq, *J* = 14.7, 7.4 Hz, 1H), 1.60 (s, 3H), 1.00 (t, *J* = 7.4 Hz, 3H). ¹³C NMR (400 MHz, Chloroform-*d*) δ (in ppm) = 157.58, 151.69, 87.72, 85.71, 33.55, 26.13, 7.49.

4-methyl-5-methylene-4-phenyl-1,3-dioxolan-2-one (Yellow oil): ¹H NMR (400 MHz, Chloroform-*d*) δ (in ppm) = 7.44 (m, 5H), 4.94 (d, *J* = 3.9 Hz, 1H), 4.46 (d, *J* = 3.9 Hz, 1H), 1.97 (s, 3H). ¹³C NMR (400 MHz, Chloroform-*d*) δ (in ppm) = 157.61, 151.30, 139.39, 129.06, 124.84, 88.31, 87.28, 27.66.

4-isobutyl-4-methyl-5-methylene-1,3-dioxolan-2-one (colourless liquid): ¹H NMR (400 MHz, Chloroform-*d*) δ 4.79 (d, *J* = 3.9 Hz, 1H 1H), 4.27 (d, *J* = 3.9 Hz, 1H), 1.79 (m, 1H), 1.67 (m, 1H), 1.57 (s, 6H), 0.96 (t, *J* = 7.4 Hz, 3H). ¹³C NMR (400 MHz, Chloroform-*d*) δ (in ppm) = 158.49, 151.62, 87.47, 85.72, 48.70, 27.18, 24.15.

5-methylene-4,4-diphenyl-1,3-dioxolan-2-one (orange solid, T_m = 64.04°C): ¹H NMR (400 MHz, Chloroform-*d*) δ (in ppm) = 7.40 (m, 10H), 5.18 (d, *J* = 3.9 Hz, 1H), 4.48 (d, *J* = 3.9 Hz, 1H). ¹³C NMR (400 MHz, Chloroform-*d*) δ (in ppm) = 155.52, 150.95, 138.67, 132.23 – 122.96, 91.89.

4-methyl-5-methylene-4-vinyl-1,3-dioxolan-2-one (colourless liquid): ¹H NMR (400 MHz, Chloroform-*d*) δ (in ppm) = 5.96 (dd, *J* = 17.1, 10.7 Hz, 1H), 5.51 (d, *J* = 17.1 Hz, 1H), 5.35 (d, *J* = 10.7 Hz, 1H), 4.90 (d, *J* = 3.9 Hz, 1H), 4.36 (d, *J* = 3.9 Hz, 1H), 1.71 (s, 3H). ¹³C NMR (400 MHz, Chloroform-*d*) δ (in ppm) = 156.29, 151.21, 136.26, 116.78, 87.38, 85.87, 25.74.

5. Supplementary information

SI- 1. NMR characterisation of organocatalysts

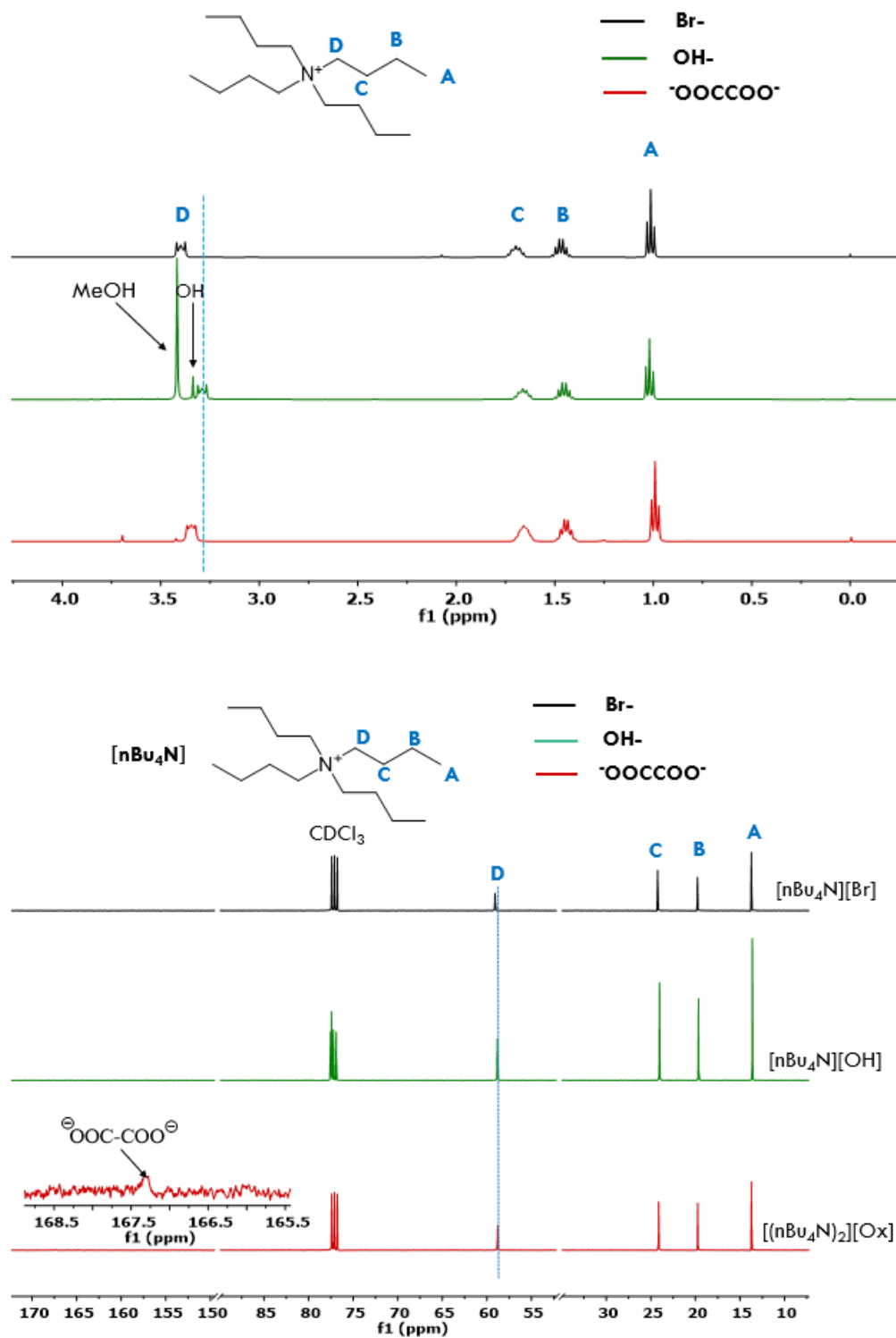


Figure S 1. ^1H & ^{13}C NMR characterisation of [(Bu₄N)₂][Ox] organocatalyst.

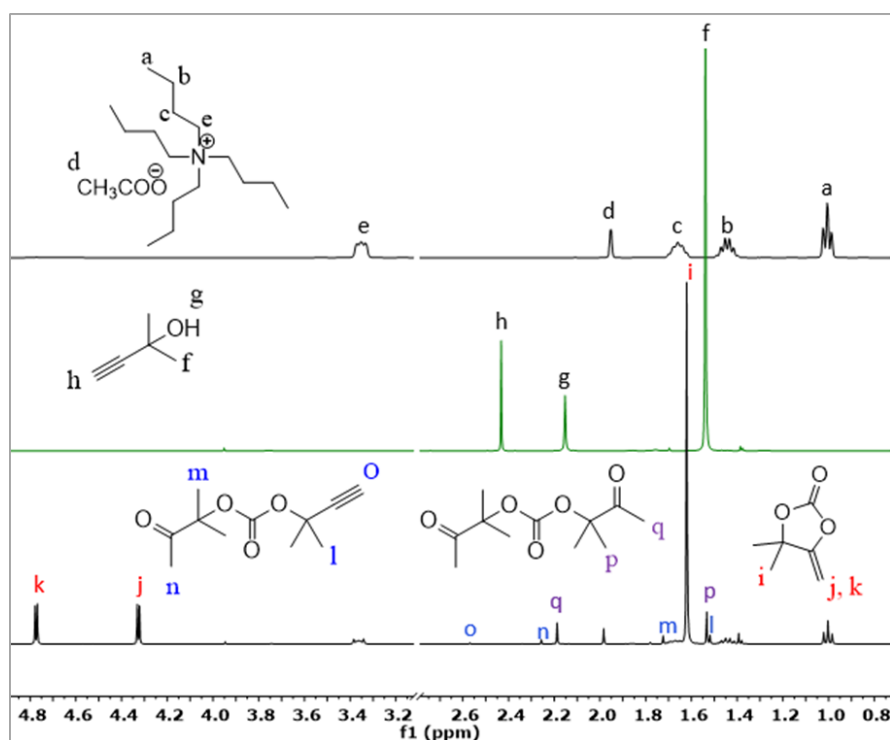
SI- 2. Coupling of 2-methyl-3-butyn-2-ol with CO₂: characterisation of the crude product

Figure S 2. ¹H NMR spectra in CDCl₃ of the catalyst, 2-methyl-3-butyn-2-ol and the crude product obtained after 6 h of reaction of 2-methyl-3-butyn-2-ol, with CO₂ catalysed by [nBu₄N][OAc]. Conditions: 80 °C, 50 bar and 5 mol% of catalyst.

Conversions were estimated according to the formula:

$$X_{alkynol} = 1 - \left(\frac{\int h_{2.44 \text{ ppm}}}{\sum (\int k_{4.77 \text{ ppm}}) + \int \frac{m}{6} (1.72 \text{ ppm}) + \int \frac{q}{6} (2.18 \text{ ppm}) + \int h_{2.44 \text{ ppm}}} \right) \times 100$$

Selectivity toward the formation of product **2**, **4** and **5** were determined by comparing the relative intensities of one proton of the peaks k, m and q, of products **2**, **4** and **5**, according to the formula:

$$\text{Selectivity: } 2 = \frac{\int k_{(4.77 \text{ ppm})}}{\sum (\int k_{(4.77 \text{ ppm})} + \int \frac{m}{6} (1.72 \text{ ppm}) + \int \frac{q}{6} (2.18 \text{ ppm}))} \times 100$$

$$\text{Selectivity: } 4 = \frac{\int m/6_{(1.72 \text{ ppm})}}{\sum (\int k_{(4.77 \text{ ppm})} + \int \frac{m}{6} (1.72 \text{ ppm}) + \int \frac{q}{6} (2.18 \text{ ppm}))} \times 100$$

$$\text{Selectivity: } 5 = \frac{\int q/6_{(2.18 \text{ ppm})}}{\sum (\int k_{(4.77 \text{ ppm})} + \int \frac{m}{6} (1.72 \text{ ppm}) + \int \frac{q}{6} (2.18 \text{ ppm}))} \times 100$$

SI- 3. Supplementary NMR characterisation

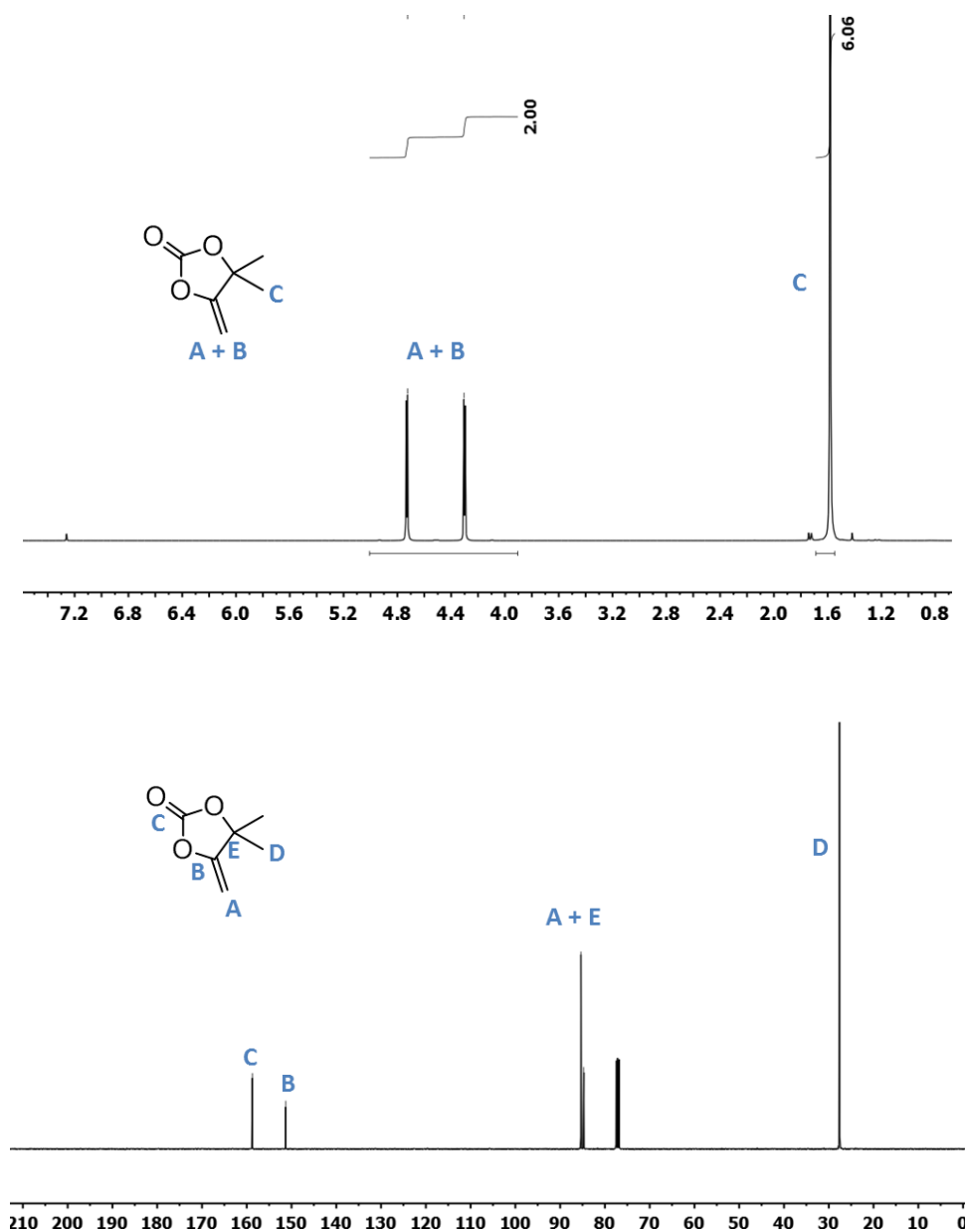


Figure S3. ^1H and ^{13}C NMR characterisations of purified 4,4-dimethyl-5-methylene-1,3-dioxolan-2-one synthesised by $[(\text{nBu}_4\text{N})_2][\text{Ox}]$ promoted coupling of CO_2 with 2-methyl-3-butyn-2-ol (Conditions: 50 bar, 6 h, 80 °C, 5 mol% of catalyst).

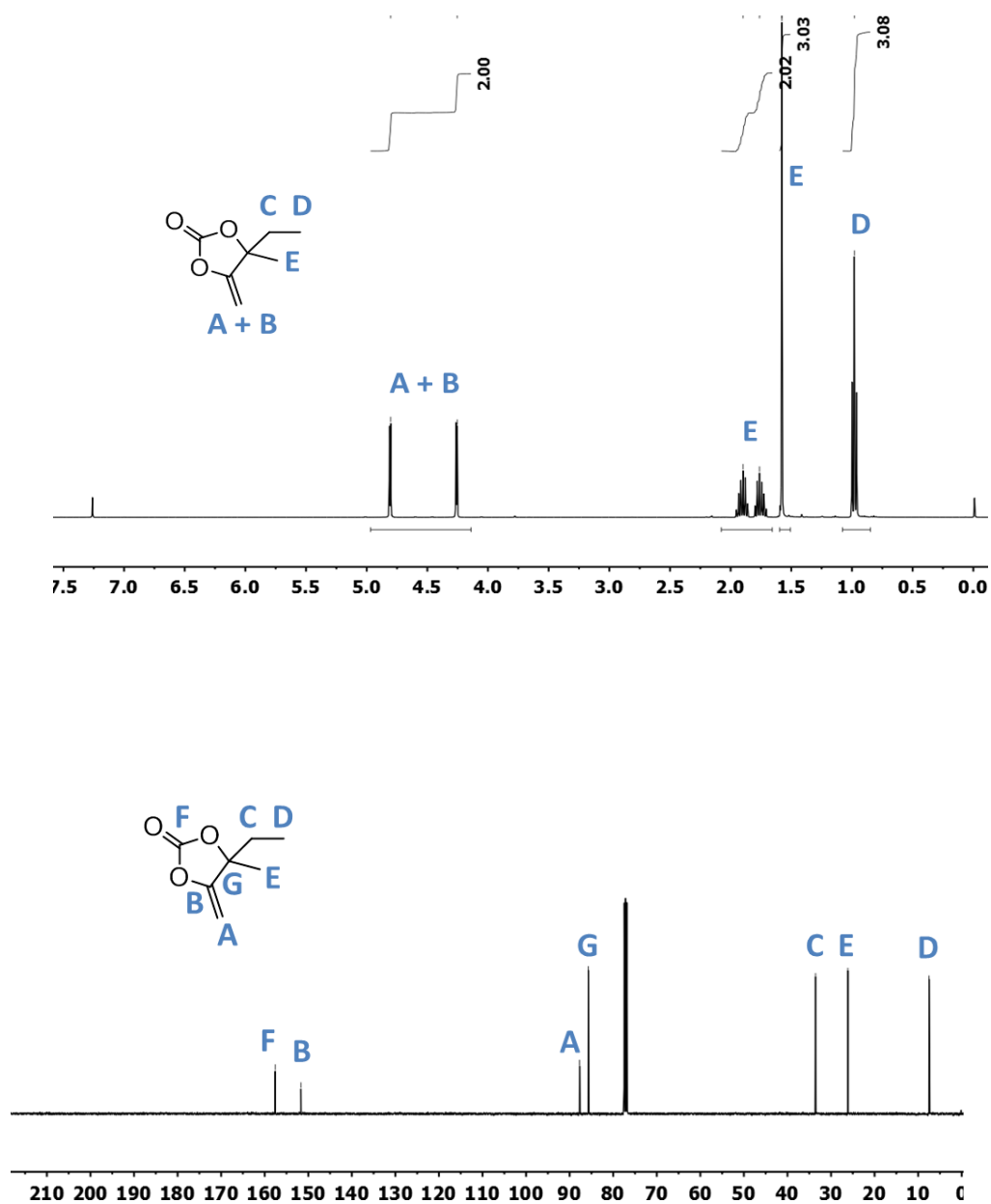


Figure S 4. ^1H and ^{13}C NMR characterisations of purified 4-ethyl-4-methyl-5-methylene-1,3-dioxolan-2-one synthesised by $[(\text{nBu}_4\text{N})_2][\text{Ox}]$ promoted coupling of CO_2 with 2-methyl-3-butyn-2-ol (Conditions: 50 bar, 6 h, 80 °C, 5 mol% of catalyst).

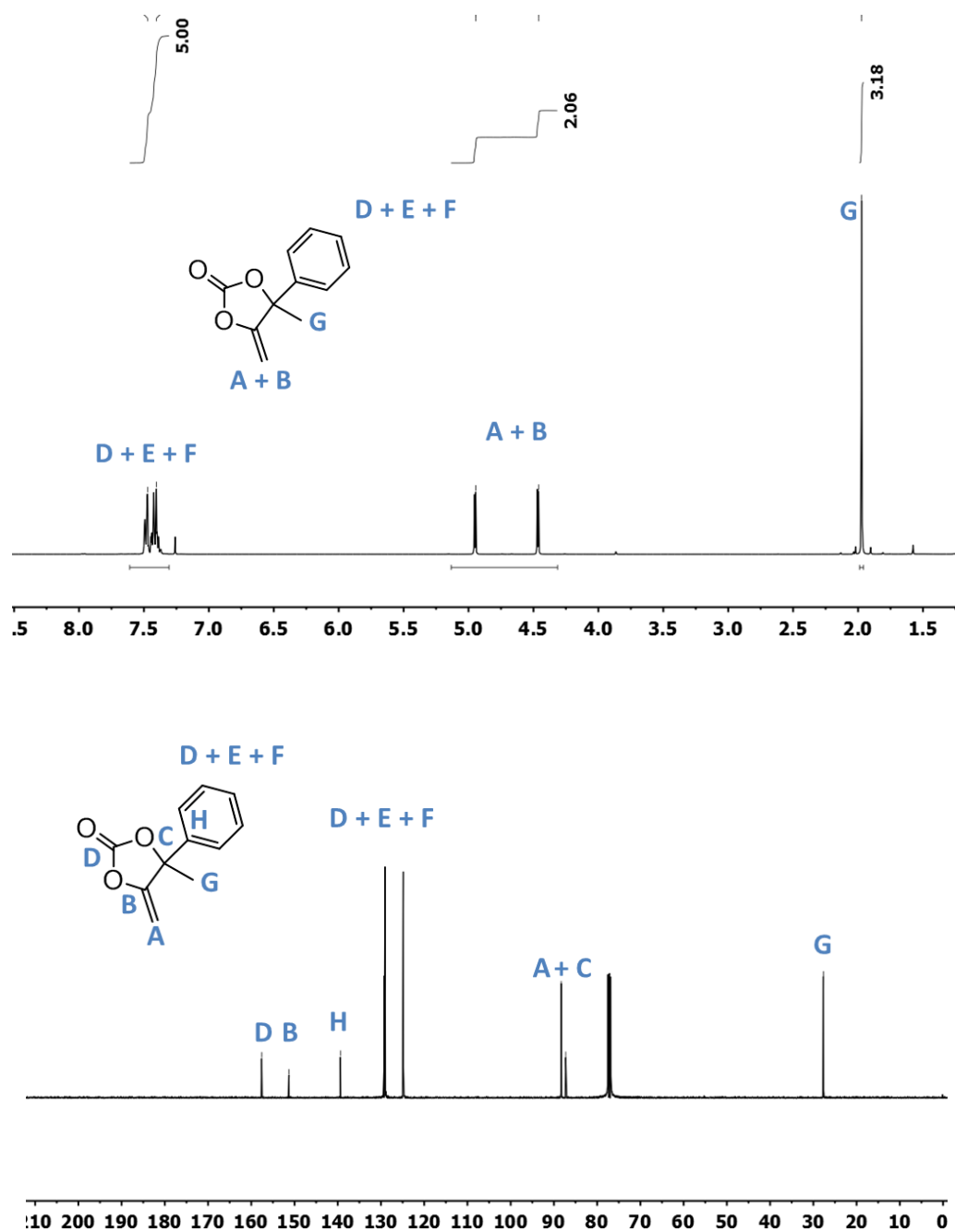


Figure S 5. ¹H and ¹³C NMR characterisations of purified 4-methyl-5-methylene-4-phenyl-1,3-dioxolan-2-one synthesised by [(nBu₄N)₂][Ox] promoted coupling of CO₂ with 2-methyl-3-butyne-2-ol (Conditions: 50 bar, 6 h, 80 °C, 5 mol% of catalyst).

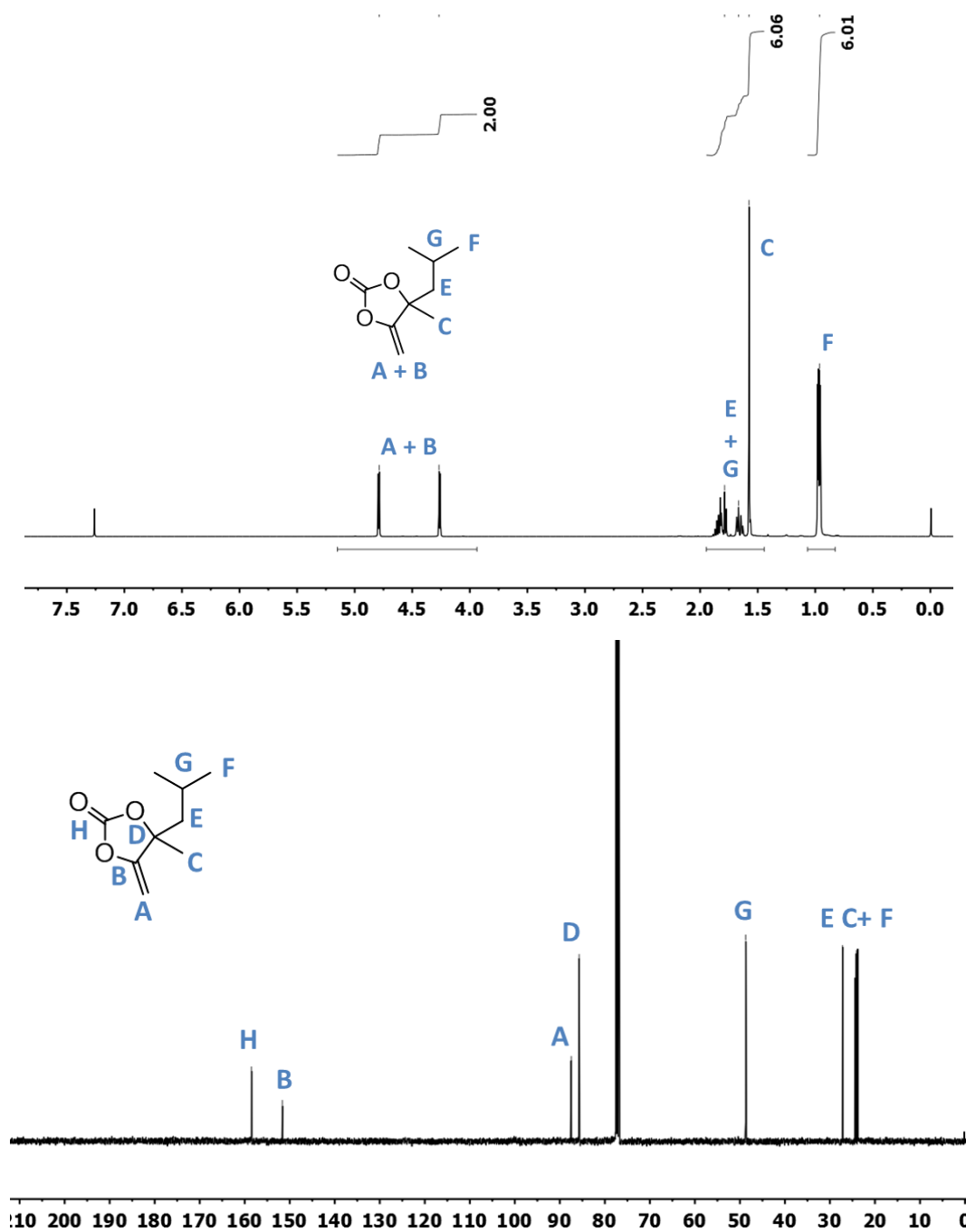


Figure S 6. ^1H and ^{13}C NMR characterisations of purified 4-isobutyl-4-methyl-5-methylene-1,3-dioxolan-2-one synthesised by $[(\text{nBu}_4\text{N})_2][\text{Ox}]$ promoted coupling of CO_2 with 2-methyl-3-butyne-2-ol (Conditions: 50 bar, 6 h, 80 °C, 5 mol% of catalyst).

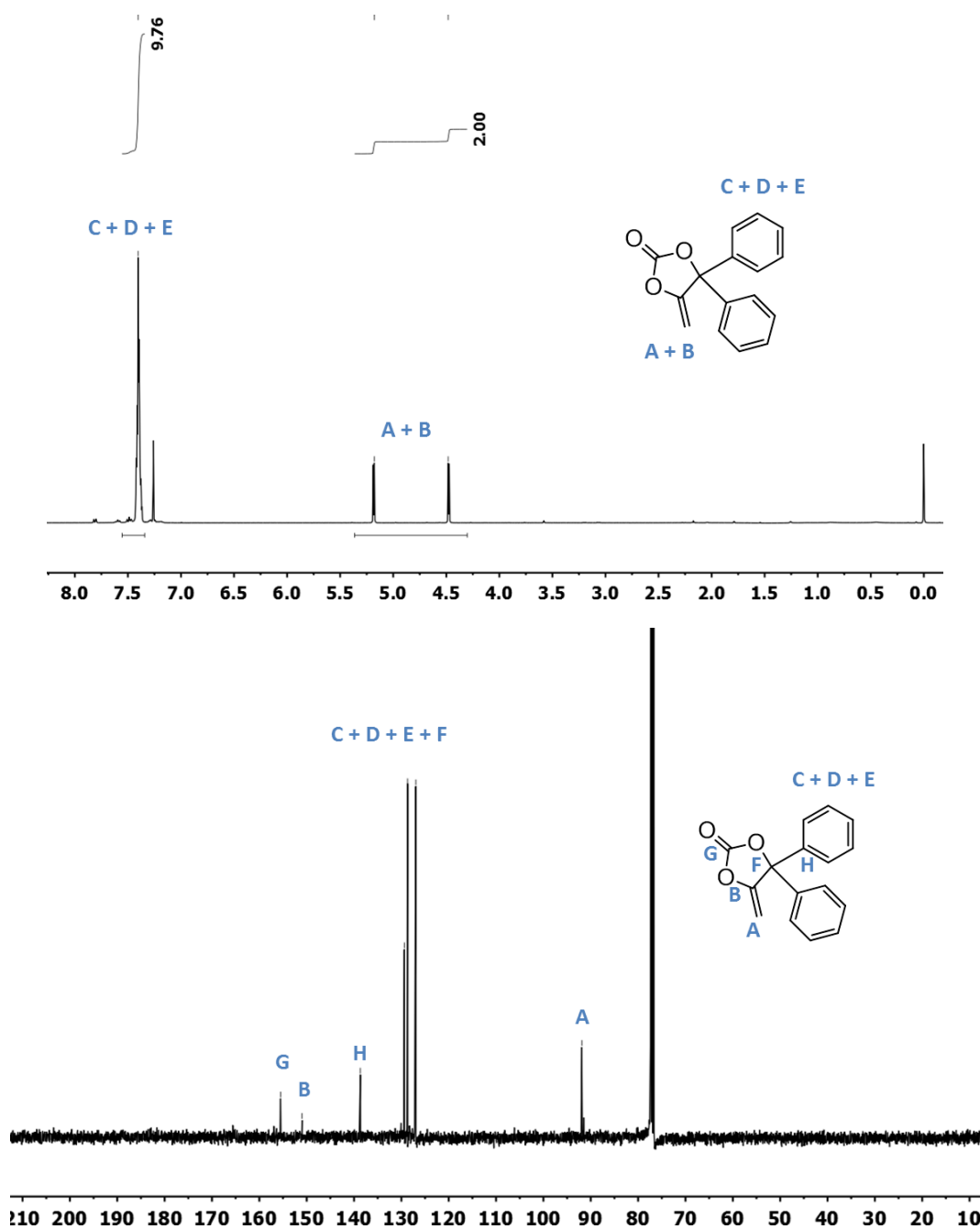


Figure S 7. ^1H and ^{13}C NMR characterisations of purified 5-methylene-4,4-diphenyl-1,3-dioxolan-2-one synthesised by $[(\text{nBu}_4\text{N})_2][\text{Ox}]$ promoted coupling of CO_2 with 2-methyl-3-butyn-2-ol (Conditions: 50 bar, 6 h, 80 $^\circ\text{C}$, 5 mol% of catalyst).

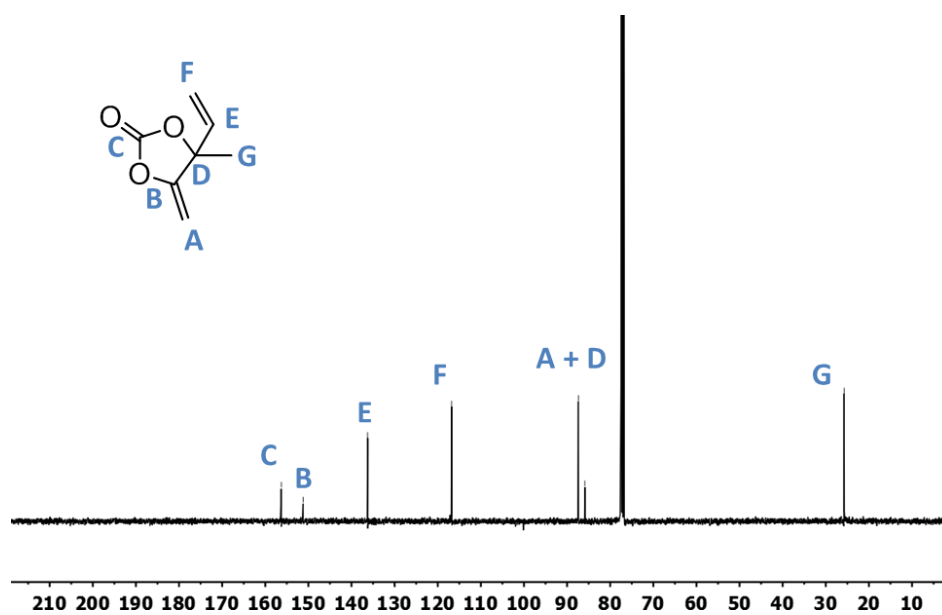
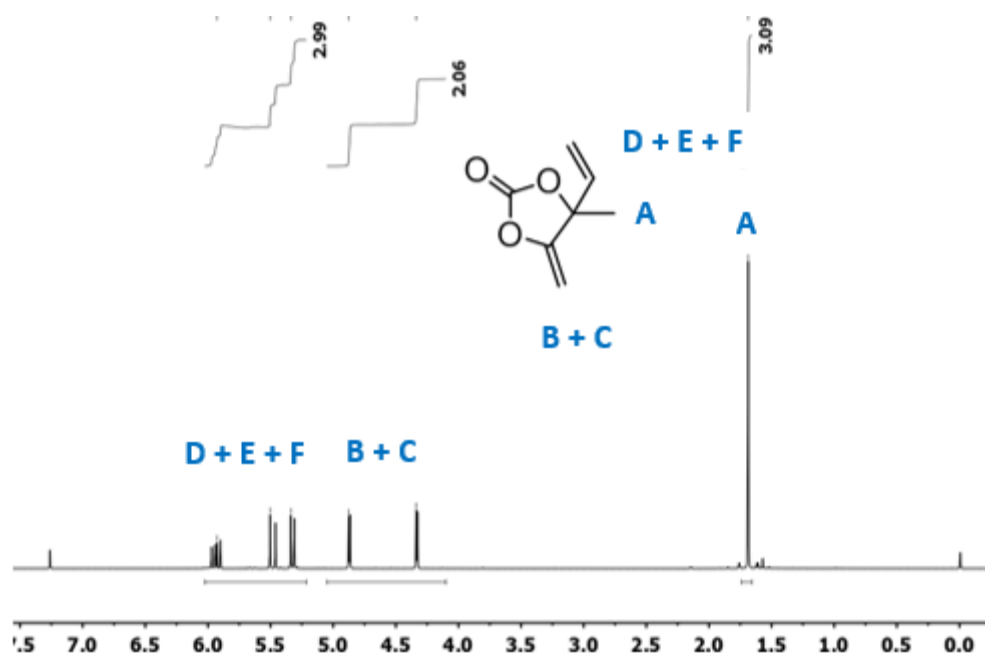
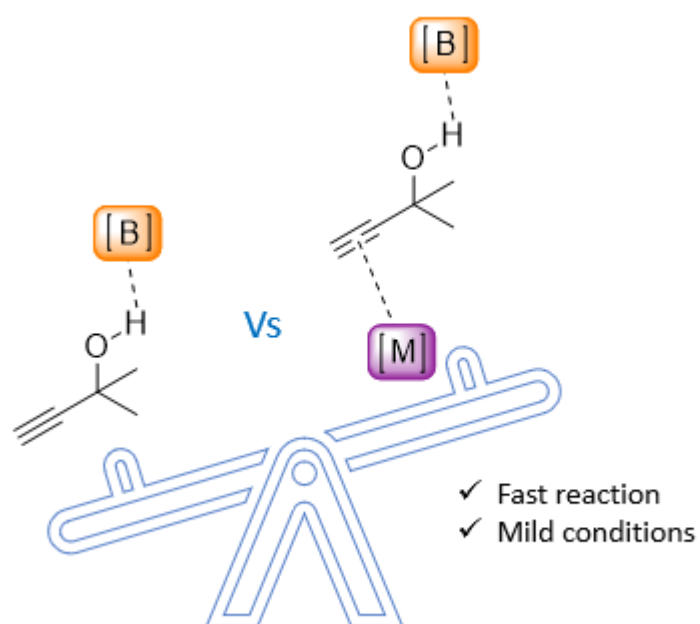


Figure S 8. ¹H and ¹³C NMR characterisations of purified 4-methyl-5-methylene-4-vinyl-1,3-dioxolan-2-one synthesised by [(nBu₄N)₂][Ox] promoted coupling of CO₂ with 2-methyl-3-butyne-2-ol (Conditions: 50 bar, 6 h, 80 °C, 5 mol% of catalyst).

CHAPTER 3

Dual activation catalysts for the selective synthesis of alkylidene cyclic carbonates



Chapter 3

This chapter includes results that are published in;

Charlène Ngassam Tounzoua, Bruno Grignard, Antoine Brège, Christine Jérôme, Thierry Tassaing, Raphaël Méreau and Christophe Detrembleur. ACS Sustainable Chem. Eng. 2020, 8, 9698–9710

The DFT computational studies were conducted by Dr Raphael Mereau of the university of Bordeaux

Table of contents

1. Introduction	85
2. Results.....	87
2.1. Preliminary experiments.....	87
2.2. Screening of metal salts cocatalysts and solvent	88
2.3. Kinetic studies by infrared spectroscopy	89
2.4. Mechanism of the reaction.....	95
3. Conclusions	97
4. Experimental section	98
4.1. Materials.....	98
4.2. Analytical methods	98
4.3. Experimental procedures	98
5. Supplementary Information	100

1. Introduction

In the previous chapter, we developed organic catalysts for the synthesis of alkylidene cyclic carbonates. We isolated two catalysts which gave interesting activities, tetrabutylammonium oxalate ($[\text{Bu}_4\text{N}][\text{Ox}]$) and tetrabutyl ammonium phenolate ($[\text{Bu}_4\text{N}][\text{OPh}]$). $(\text{Bu}_4\text{N})_2[\text{Ox}]$ required 5h to reach full conversion, a 99% selectivity in DMACC was observed, meanwhile, $[\text{Bu}_4\text{N}][\text{OPh}]$ gave full conversion in 1 h, however with a 90% selectivity in DMACC at 80°C and 50 bar in ACN. The side reactions observed were the hydrolysis of αCCs into hydroxyketones and the formation of the linear *oxo*-carbonate by the addition of the propargylic alcohol onto αCCs . In prelude to our following study (**chapter 4**) which focuses on the domino synthesis of polycarbonates by step-growth polymerisation, a catalyst with a high basicity is ideal, hence we selected $[\text{Bu}_4\text{N}][\text{OPh}]$ due to the higher basicity of the phenolate (pKa of conjugate acid = 9.8) in comparison to oxalate (1.27, 4.28). In addition, because we will be implementing a one-pot approach which involves no isolation and purification of the cyclic carbonate intermediate, it is important that the latter be formed with the highest selectivity possible. Therefore, it was necessary to further optimise the $[\text{Bu}_4\text{N}][\text{OPh}]$ catalyst for the synthesis of the αCCs .

From the literature, we know that the addition of a metal cocatalyst such as silver (Ag(I))^[50,72,73,204–206] or copper (Cu(I))^[43,94,207,208] that can pi-activate the triple bond of the propargylic alcohol, helps to accelerate the rate of cyclisation. This should therefore allow to carry out the reaction under milder conditions, which should in turn disfavour the occurrence of secondary reactions, notably the alcoholysis of the αCC by addition of the propargylic alcohol. Using copper as cocatalyst was highly desirable due to its lower cost in comparison to silver.

At the time of this study, very few dual systems involving Cu as cocatalyst had been reported. In 1997, Kim et al. reported the first copper catalytic system which was composed of a copper ferrocene complex ($[\text{Cu}(\text{dppj})(\text{MeCN})_2][\text{PF}_6 \cdot \text{CH}_2\text{Cl}_2]$) used in combination to an amine (bipyridine). A temperature of 100 °C and $\text{PCO}_2 = 38$ bar was employed and a 95% yield in the $\alpha\text{CC 2}$ was obtained.^[94] Besides the high temperatures required by this system, one can also point out the multistep synthesis of the copper complex. Other systems were later proposed such as $\text{CuCl}/[\text{BMIm}][\text{PhSO}_3]$ ^[70] and CuI/DIPEA ^[208] systems which afforded high yields in the $\alpha\text{CC 2}$ at 80-120 °C, 1-10 bar and 50-100 mol% of the II. The main drawbacks here again are the high temperatures required as well as the large amount of the ionic liquid cocatalyst. Recently, CuI used in combination with phosphonium levulinate was reported for the synthesis of $\alpha\text{CC 2}$ under room temperature conditions. However, a high pressure of CO_2 ($\text{PCO}_2 = 100$ bar) was required and the phosphonium salt was used in a large amount (66 mol%).^[75]

Some heterogenous systems had also been reported to prepare $\alpha\text{CC 2}$ in high yields, however either very high pressures were employed such as with the dimethylamino)methyl-

Chapter 3

polystyrene-supported copper(I) iodide (DMAM-PS-CuI) system (120 bar, 40 °C)^[80] or room temperature conditions were used with a 100 mol% of the base cocatalyst (DBU), as it is the case with MOFs/COVs based catalysts.^[207]

If we consider the Ag based dual catalysts, various systems have been reported such as AgOAc/ [nHep₄N][Br]^[72], AgOAc/DavePhos^[209], Ag₂CO₃/PPh₃^[76], Ag₂WO₄/PPh₃^[73], AgI/KOAc^[74]. These catalysts afforded the desired cyclic carbonates in high yields (85-99%), under mild-moderate conditions (25-60 °C, 1-20 bar) and low catalyst loadings (2-10 mol%). They have been reviewed and discussed in **chapter 1**, section 2.2.

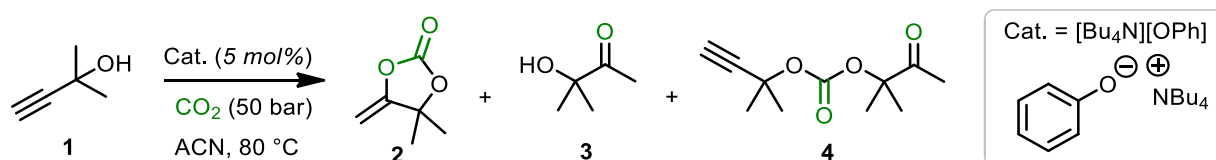
Bearing in mind that we need a catalyst with sufficient basicity to promote our step-growth polymerisation, one of the Ag-based systems which matched this criterion was the AgOAc/DBU. However, the authors used 100 mol% of DBU in order to obtain high yields of the α CC at 25 °C, 10 bar.^[204] Moreover, Ca et al. had shown in their studies that DBU was not selective for the synthesis of α CC and yielded as major product the unsymmetrical linear carbonate from the secondary alcoholysis of α CC by the residual propargylic alcohol.^[48]

Hence in this chapter, we optimised the activity and selectivity of [Bu₄N][OPh] for the synthesis of α CCs and bis α CCs by incorporating a Cu- or Ag-based cocatalyst. FT-IR studies coupled with DFT modelling were performed to understand the action mode of the catalytic system.

2. Results

2.1. Preliminary experiments

Initially we studied the influence of decreasing the reaction temperature from 80 to 60 or 40 °C on the activity of the $[\text{NBu}_4][\text{OPh}]$ catalyst for the carboxylative cyclisation of our model alcohol, 2-methyl-3-butyn-2-ol (**Scheme 1**).



Scheme 1. Coupling of CO_2 to 2-methyl-3-butyn-2-ol.

By decreasing the temperature to 60 °C, the reaction slowed down (6 h was required for full conversion) meanwhile the selectivity in **2** increased to 96%, with 4% of hydroxyketone formed from the hydrolysis of αCC (**Table 1**, entry 3). When we further decreased the temperature to 40 °C, the reaction rate decreased considerably with propargylic alcohol conversion of only 6% after 1 h (**Table 1**, entry 4). Importantly, 2-methyl-3-butyn-2-ol was fully and selectively converted into the desired product **2** with no side product when the reaction time was extended to 24 h (**Table 1**, entry 5).

Table 1. Influence of the temperature on the carboxylative cyclisation of CO_2 with 2-methyl-3-butyn-2-ol catalysed by $[\text{nBu}_4\text{N}][\text{OPh}]$.

Entry	Temp. (°C)	Time (h)	Conv. of 1 (%)	Select. for 2 (%)
1	80	1	100	90
2	60	1	20	99
3	60	6	100	96
4	40	1	6	99
5	40	24	100	99

Conditions: 2-methyl-3-butyn-2-ol (2 mL, 0.02061 mol), $[\text{NBu}_4][\text{OPh}]$ (5 mol%), acetonitrile (2 mL), CO_2 (50 bar). The conversions and selectivities were determined by $^1\text{H-NMR}$ spectroscopy in CDCl_3 .

2.2. Screening of metal salts cocatalysts and solvent

To improve the selectivity in α CC **2** without excessively compromising the reaction rate, we considered the use of a cocatalyst that was expected to activate the alkyne for the carboxylative addition.^[75,209] Various copper and silver salts were tested, and results are summarised in **Table 2**. Note that these screening experiments were carried out at a pressure of 15 bar as we were able to show by kinetic studies (see section **2.3**) that further increasing the pressure had no real impact on the reaction.

Table 2. Screening of cocatalyst and solvents for the coupling of CO₂ to 2-methyl-3-butyn-2-ol catalysed by [NBu₄][OPh].

Entry	Cocatalyst	Solvent	Conv. of 1 (%)	Selectivity for 2 (%)
1	/	ACN	6	100
2	Ag ₂ CO ₃	ACN	70	100
3	AgI	ACN	100	100
4	AgOAc	ACN	38	100
5	CuCl	ACN	50	100
6	CuBr	ACN	47	100
7	CuI	ACN	81	100
8	CuI	CDCl ₃	63	100
9	CuI	THF	70	100
10	CuI	DMSO	58	100
11	CuI	Neat	92	98

Conditions: 2-methyl-3-butyn-2-ol (2 mL, 0.0206 mol), [NBu₄][OPh] (5 mol%), cocatalyst (5 mol%), solvent (2 mL), CO₂ (15 bar), 1 h, 40 °C. The conversions and selectivity were determined by ¹H-NMR in CDCl₃ (see Figure S1 for the procedure).

The addition of a silver (I) or copper (I) salt was found favourable. The best catalytic activity was obtained when [NBu₄][OPh] was combined to CuI or AgI, with an increase in the conversion of **1** from 6 % (without cocatalyst, **Table 2**, entry 1) to 81 % (with CuI, **Table 2**, entry 7) or 100 % (with AgI, **Table 2**, entry 3) in 1 h at 15 bar and 40 °C. Both [NBu₄][OPh]/CuI and [NBu₄][OPh]/AgI binary systems drove the reaction with a 100 % selectivity in the targeted product **2** as confirmed by ¹H-NMR spectroscopy (**Figure S 2**). The difference in activity for the reactions carried out in the presence of the different silver salts (Ag₂CO₃, AgOAc and AgI) is at this stage difficult to rationalize. However, the different solubility of the

silver salts in the reaction medium might be at the origin of this observation. Indeed, when preparing the reaction medium before pressurisation with CO₂, none of these cocatalysts were fully soluble. However, quantifying their solubility in the reaction medium under pressure was not possible.

We then screened some solvents using CuI as cocatalyst, as we know that solvent effects play an important role in this carboxylative cyclisation reactions. The reaction was fastest in acetonitrile and slowest in DMSO (**Table 2**, entries 7 and 11), nonetheless, the same selectivity in product **2** (100 %) was obtained in both cases.

2.3. Kinetic studies by infrared spectroscopy

Model alcohol

To understand the influence of the reaction parameters (pressure and solvent) on the rate of formation of carbonate **2**, we studied the kinetics of the reaction using online high-pressure FT-IR spectroscopy using the CuI/[NBu₄][OPh] catalyst. **Figure 1** shows an overlay of the IR spectra at different times obtained with the [NBu₄][OPh]/CuI system.

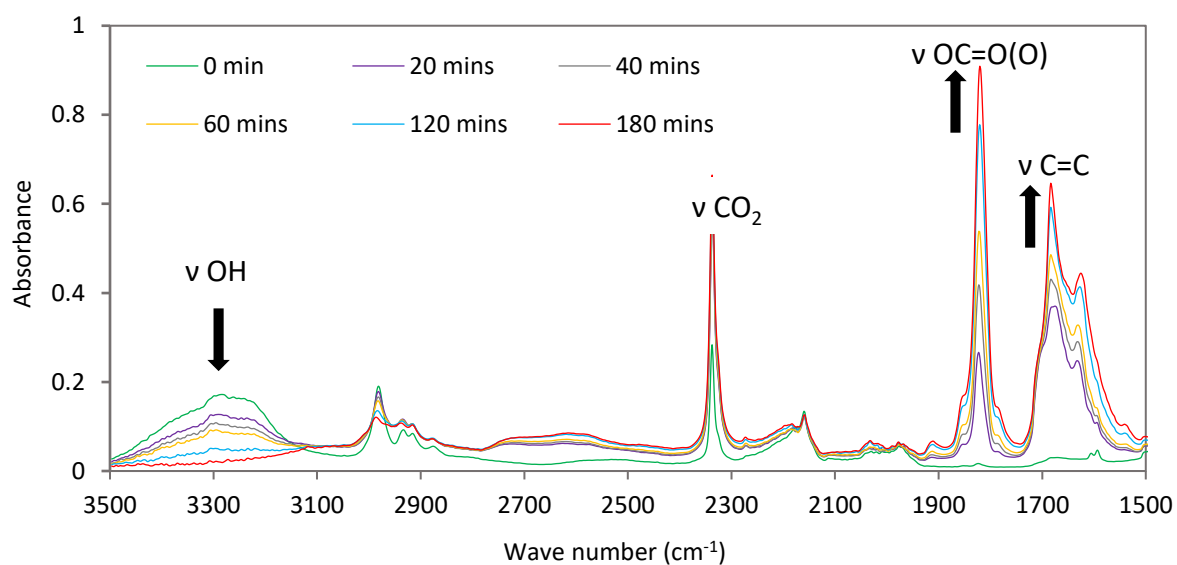


Figure 1. Synthesis of 4,4-dimethyl-5-methylene-1,3-dioxolan-2-one by organocatalysed coupling of CO₂ to 2-methyl-3-butyn-2-ol. FT-IR spectra at different times for the [NBu₄][OPh]/CuI catalysed reaction. Conditions: 2-methyl-3-butyn-2-ol (16 mL, 0.165 mmol), [NBu₄][OPh] (5 mol%), CuI (5 mol%), T = 40 °C, PCO₂ = 15 bar, solvent = DMSO (V = 16 mL).

We observed a signal at 3300 cm⁻¹ corresponding to the OH band of the alkynol which decreased gradually overtime and the concomitant formation of the cyclic carbonate and exovinylene group with characteristic vibrations of ν C=O at 1823 cm⁻¹ and ν C=C at 1680 cm⁻¹. The CO₂ band at 2330 cm⁻¹ was observed and remained constant due to the large excess of CO₂ under the investigated conditions. By following the evolution of the ν C=O band at 1823 cm⁻¹ over time, the yield in exovinylene cyclic carbonate **2** was determined (See **SI- 3**).

In **Figure 2a**, we plotted the yield in carbonate **2** obtained at different pressures under neat conditions at 30 °C. A slower reaction rate is observed at 5 bar, with only 65% yield in the carbonate **2** after 135 min. Increasing the pressure to 15 bar, resulted in >99% yield in the cyclic carbonate. Further increasing the pressure to 20 bar and then 30 bar resulted in a slight increase in the reaction rate, with the maximum yield obtained after 110 and 90 min respectively. The very little difference in the results observed at 15, 20 and 30 bar, justified our choice of 15 bar as the reaction pressure for the next experiments.

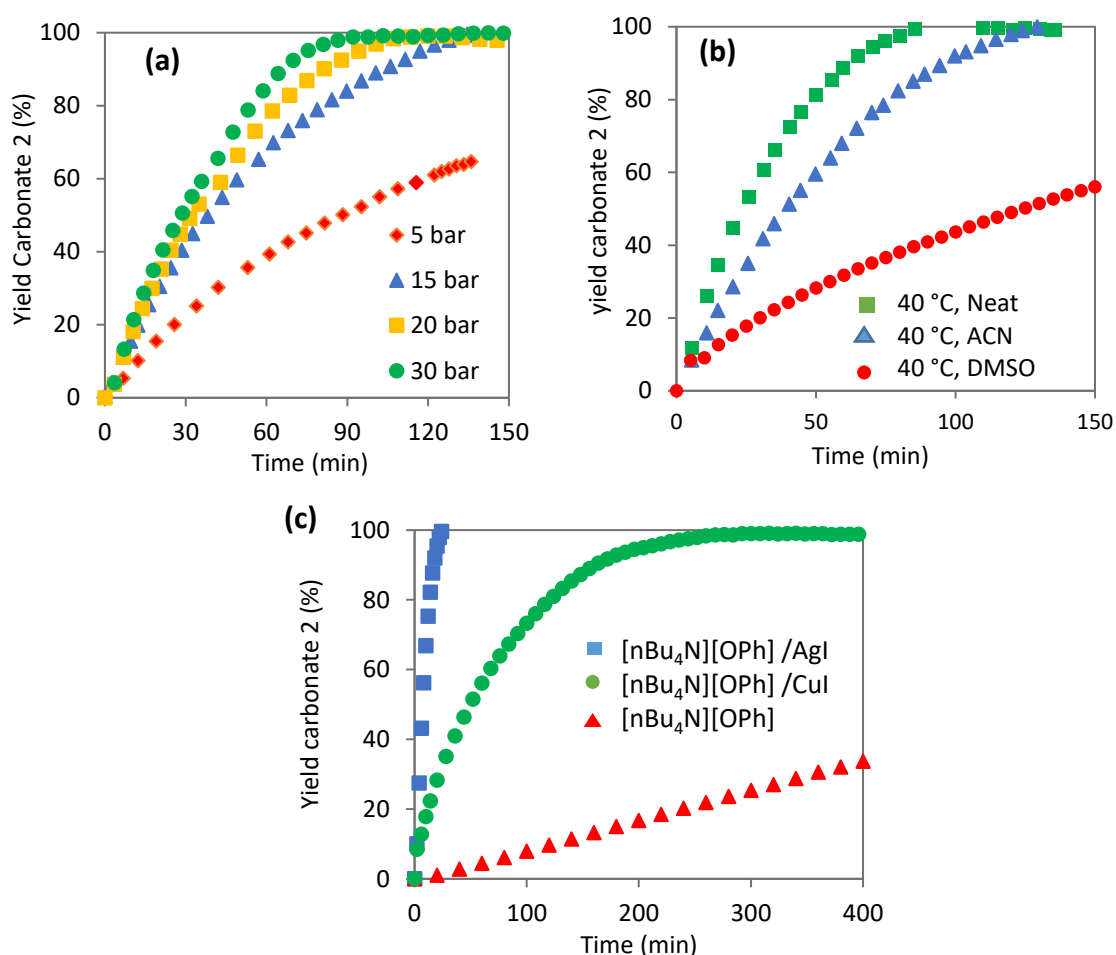


Figure 2. Time evolutions of the yield in **2** (4,4-dimethyl-5-methylene-1,3-dioxolan-2-one) obtained by organocatalysed coupling of CO₂ to 2-methyl-3-butyn-2-ol. (a) Influence of pressure at 30 °C under neat conditions in the presence of [nBu₄N][OPh]/CuI (5 mol%) as catalyst (b) Influence of solvent at 40 °C in the presence of [nBu₄N][OPh]/CuI (5 mol%) as catalyst, PCO₂ = 15 bar and (c) Influence of the different catalytic systems in DMSO, PCO₂ = 15 bar. General conditions: 2-methyl-3-butyn-2-ol (16 mL, 0.165 mol), [nBu₄N][OPh] (5 mol%), AgI or CuI (5 mol%), if solvent (V = 16 mL).

Next, we studied the influence of solvent, at 40 °C and 15 bar (**Figure 2b**). Under neat conditions, a very fast reaction rate was observed with >99% yield in carbonate **2** in 85 minutes, while in ACN, 125 min was required to obtain >99% yield. The slowest reaction rate was obtained in DMSO, with only 55% yield in carbonate **2** after 150 min, thereby confirming the trends reported in **Table 2**.

In prelude of our subsequent study on the preparation of poly(oxo-carbonate)s by the domino reaction, we selected DMSO as the solvent to continue our study. Unlike acetonitrile, its choice was justified by its ability to solubilise the bis-propargylic alcohol and provide homogeneous conditions at the initial stage of the reaction. We then benchmarked the activity of the $[n\text{Bu}_4\text{N}][\text{OPh}]$, $\text{CuI}/[n\text{Bu}_4\text{N}][\text{OPh}]$ and $\text{AgI}/[n\text{Bu}_4\text{N}][\text{OPh}]$ catalysts (**Figure 2c**).

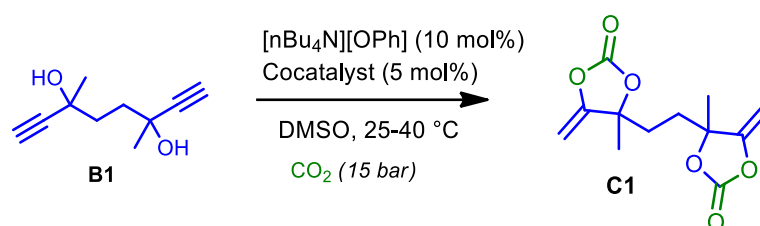
The cycloaddition was complete in 180 min with the $[n\text{Bu}_4\text{N}][\text{OPh}]/\text{CuI}$ binary system, and in less than 50 min with the $[n\text{Bu}_4\text{N}][\text{OPh}]/\text{AgI}$ system, no secondary product was detected as already noted during the batch screening tests. By using $[n\text{Bu}_4\text{N}][\text{OPh}]$ as sole catalyst, the reaction was extremely slow, requiring 24 h for completion, but remained selective. This comparative study highlights the synergistic role of the cocatalyst.

As discussed in the introduction section, only a few dual systems based on copper had been reported for the carboxylative coupling of CO_2 and propargylic alcohols. In general, they required high temperatures (80-120°C) and/or high organic catalyst loading to afford high yields in the αCC .^{[94][75]} Our system involving $[n\text{Bu}_4\text{N}][\text{OPh}]/\text{CuI}$ is thus competitive for the synthesis of αCC **2** under mild reaction conditions, and at a low catalyst loading (5 mol%).

Considering the Silver based catalysts, $[n\text{Bu}_4\text{N}][\text{OPh}]/\text{AgI}$ system is also competitive as it affords the desired αCC **2** under mild conditions and low catalyst loading (5 mol%), similar to those reported.^[73,76,77] However, it has the added advantage of the higher basicity of the phenolate which could be exploited for catalysing polymerisations unlike PPh_3 ^[73] or $[n\text{Hep}_4\text{N}][\text{Br}]$ ^[72].

Bispropargylic alcohol

We then studied the kinetics of cycloaddition of CO_2 to a model bispropargylic alcohol, using both $[n\text{Bu}_4\text{N}][\text{OPh}]/\text{CuI}$ and $[n\text{Bu}_4\text{N}][\text{OPh}]/\text{AgI}$ catalytic system (**Scheme 2**).



Scheme 2. Coupling of CO_2 to 3,6-dimethylocta-1,7-diyne-3,6-diol.

Figure 3a shows the 3D profile of the reaction catalysed by $[n\text{Bu}_4\text{N}][\text{OPh}]/\text{AgI}$ at 40 °C. Upon addition of CO_2 , we observed a small band at 1610 cm^{-1} which corresponds to the carbonated alcohol (RCO_3^-). Then as expected, we observed the rapid growth of the bands at 1820 cm^{-1} and 1686 cm^{-1} typical of the carbonate and alkene bond of the bis αCC . After approximately 170 min of reaction, we observed an abrupt decrease in the intensity of the carbonate and alkene band (0.5 absorbance unit in 10 min), and then an equilibrium was reached (**Figure 3b**).

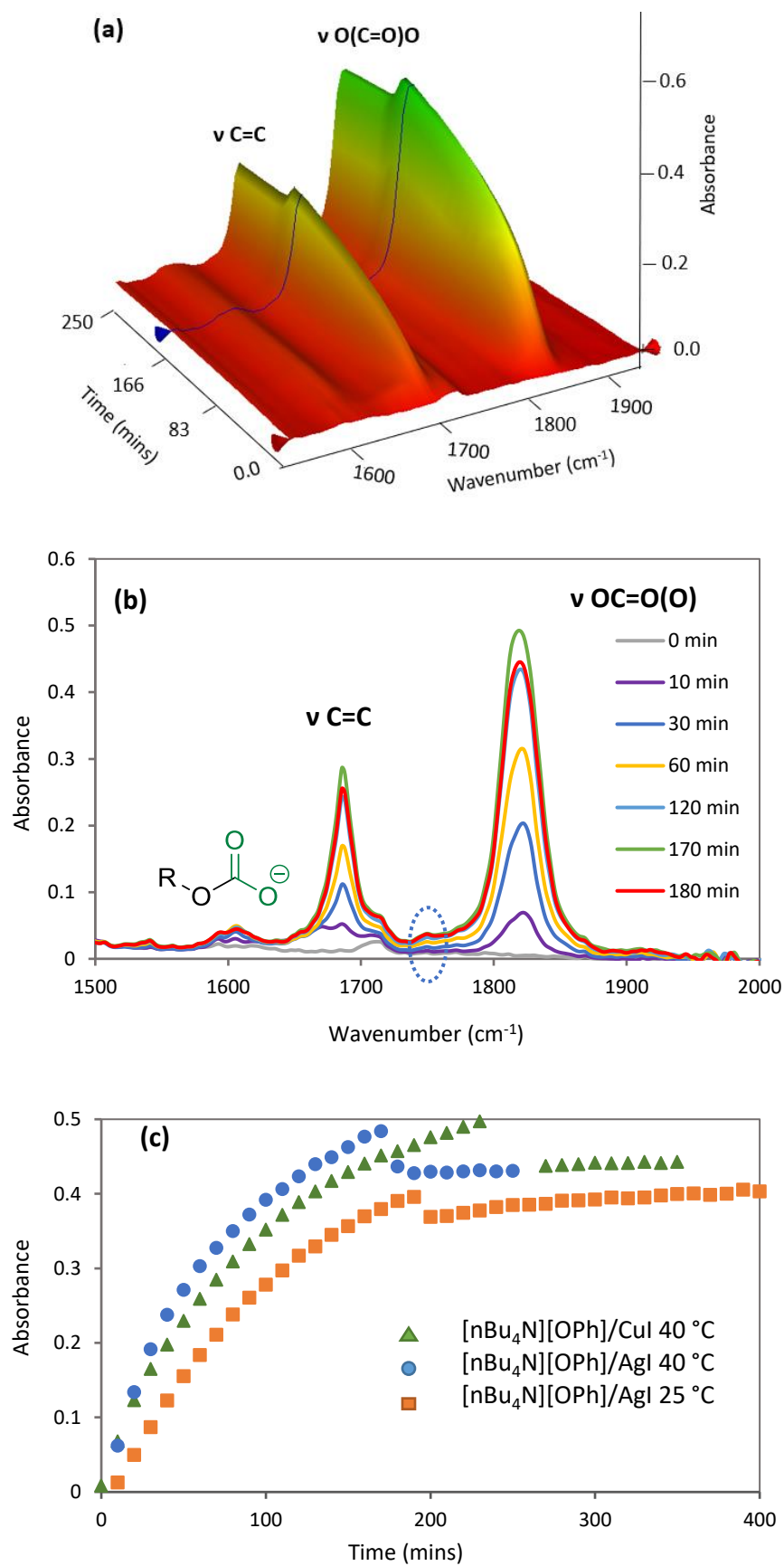


Figure 3. Coupling of CO₂ and 3,6-dimethylocta-1,7-diyne-3,6-diol. (a) 3D profile (b) Superposition of IR spectra obtained at various times at 40 °C with [nBu₄N][OPh]/AgI. (c) Absorbance of the cyclic carbonate band ($\nu = 1820\text{ cm}^{-1}$) for the reaction performed with different catalytic systems at 25 and 40 °C. Conditions: 3,6-dimethylocta-1,7-diyne-3,6-diol (3 g, 18.02 mmol), [nBu₄N][OPh] (10 mol%), AgI/CuI (5 mol%), T = 40 °C, PCO₂ = 15 bar, solvent = DMSO (V = 10 mL).

A similar observation was made when working with the [nBu₄N][OPh]/CuI system after 260 min of reaction. Note that the plateau is reached for the same absorbance with both systems. We then carried out the reaction at 25 °C with the [nBu₄N][OPh]/AgI system and noted the same evolution (**Figure 3c**).

To rationalise the above observations, we initially assumed that some secondary alcoholysis reactions were occurring, i.e. by reaction of unreacted propargylic alcohol with an α CC ring. However, the signal at 1750 cm^{-1} and 1720 cm^{-1} , characteristic of the linear carbonate and ketone did not show any abrupt increase of intensity that remained low, thus not in favour of our hypothesis. Next, we considered the change in the homogeneity of the reaction mixture, as this could impact the measured absorbance. Indeed, for all the experiments, when we opened the reactor, we noticed that a fraction of bis α CC had precipitated. This would have as direct consequence, the decrease in the bis α CC concentration in the liquid phase and hence the measured absorbance, based on the proportionality of the Beer Lambert's law ($A = \epsilon \cdot c \cdot l$).

If we consider **Figure 3c**, we realise that the precipitation occurred at a lower absorbance (0.41) for the reaction at 25 °C in comparison to that carried out at 40 °C (absorbance = 0.48), which is logical considering that solubility generally decreases when lowering the temperature.

The reaction mixtures were also characterised by ¹H-NMR spectroscopy at the end of the FT-IR monitoring, which allowed us to confirm total conversion of the bispropargylic alcohol at both 25 °C and 40 °C. The presence of signals at 4.66-4.88 and 1.60 ppm of the methylene and the methyl protons confirmed the formation of the bis α CC (**Figure 4**). The signals at 1.15 and 1.44 ppm correspond to the methyl groups of the hydroxyketone and a linear carbonate that originates from the hydrolysis and alcoholysis respectively of some alkylidene cyclic carbonate moieties. However, these side reactions remained low (5 and 10 mol %) at 25 °C and 40 °C respectively.

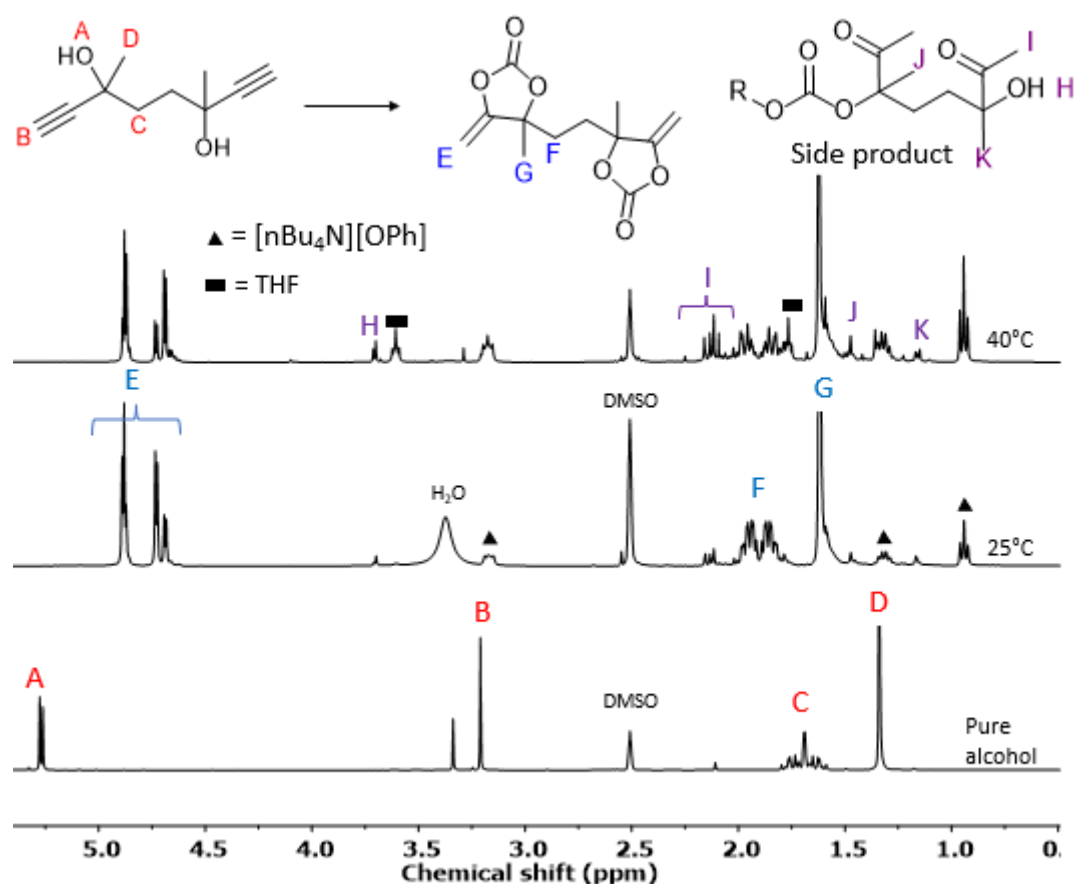


Figure 4. $^1\text{H-NMR}$ in $\text{DMSO-}d_6$ showing the pure propargylic alcohol, the crude reaction mixtures obtained for the coupling of CO_2 and 3,6-dimethylocta-1,7-diyne-3,6-diol at 25 and 40 °C after the FT-ATR monitoring experiments.

In the pioneering study describing the synthesis of bis alkylidene cyclic carbonates from bispropargylic alcohols, the authors employed a ZnI/NEt_3 system, that required 100 mol% of the amine base, 20 mol% of ZnI_2 , 100 bar at 40 °C.^[18] We have shown that these conditions could be softened to 15 bar/25-40 °C using 5 mol% of our catalytic system ($[\text{nBu}_4\text{N}][\text{OPh}] / \text{CuI}$ or AgI) while still affording full conversion in the propargylic alcohol with a 90-95% selectivity in the bis alkylidene cyclic carbonate.

There are only two other studies published by Schaub et al. which described the synthesis of bis alkylidene cyclic carbonates. This was achieved by using either the $\text{DavePhos}/\text{AgOAc}$ ^[209] catalytic system (2/2 mol%) or the expanded ring-NHC- CuCl/CsF (5 mol%)^[43] at 20 bar and 25 °C, affording yields ranging from 85-95% in the bis alkylidene cyclic carbonates. The main advantage of their systems relies on their ability to promote the cyclisation of the more challenging primary propargylic alcohol substrates. Nonetheless, one can point as drawback the cost of the catalyst, in comparison to the cheap synthesis of $[\text{nBu}_4\text{N}][\text{OPh}]$ usually obtained in a >50g scale.

2.4. Mechanism of the reaction

The mechanism of the carboxylative cyclisation of **1** was then investigated by DFT calculations (**Figure 5**) with the help of the M062X functional (see ESI for details) where the Gibbs free energy of each structure is relative to the sum of the individual Gibbs free energy of the reactants for each pathway, i.e. : propargylic alcohol + CO₂ + [nBu₄N][OPh] for the reaction catalysed by the sole [nBu₄N][OPh] ; propargylic alcohol + CO₂ + [nBu₄N][OPh] + CuI (AgI) for the reaction catalysed by [nBu₄N][OPh] / CuI (AgI). For the sake of comparisons between the different systems, the starting point energies for all systems coincide with zero energy.

We initially explored the reaction pathway with [nBu₄N][OPh] as catalyst only, which is composed of two elementary steps. From the van der Waals complex that exhibits hydrogen bonding between the oxygen atom of the phenolate anion and the hydrogen atom of the hydroxyl group of 2-methyl-3-butyn-2-ol, the first step consists of the deprotonation of the propargylic alcohol simultaneously to the nucleophilic attack onto the carbon atom of CO₂ with the formation of a carbonate anion intermediate (-11.2 kcal.mol⁻¹). The activation barrier of this first step is calculated to be 5.9 kcal.mol⁻¹ and, as the transition state associated to it is submerged with respect to the separated reactant limit (fixed at the zero Gibbs free energy), it is supposed to occur very quickly. The second step, which is the rate-determining step with a barrier height of 23.2 kcal.mol⁻¹, involves the intramolecular nucleophilic addition from the carbonate anion to the C≡C bond and the simultaneous protonation of the alkenyl anion by the PhOH leading to the formation of **2** and the regeneration of [nBu₄N][OPh] catalyst.

In the presence of CuI or AgI as cocatalyst, the Gibbs free energy profile encountered an important exothermicity (about tens of kcal.mol⁻¹), which considerably accelerated the reaction kinetics as observed experimentally. While the first step of the whole reaction is identical to the one with the sole [nBu₄N][OPh] catalyst, the 2 remaining steps to form the target product **2** are thus : i) the ring formation from the carbonate anion together with the attack of the CuI (AgI) on the C≡C bond with an associated Gibbs free energy barrier of 24.5 kcal.mol⁻¹ (18.8 kcal.mol⁻¹), ii) from the alkenyl metal intermediate a proto-demetalation takes place and the final product is formed by hydrogen proton transfer from PhOH. The Gibbs free energy activation barrier of this last step is calculated to be 10.1 kcal.mol⁻¹ and 9.4 kcal.mol⁻¹ for the cocatalysis with CuI and AgI, respectively.

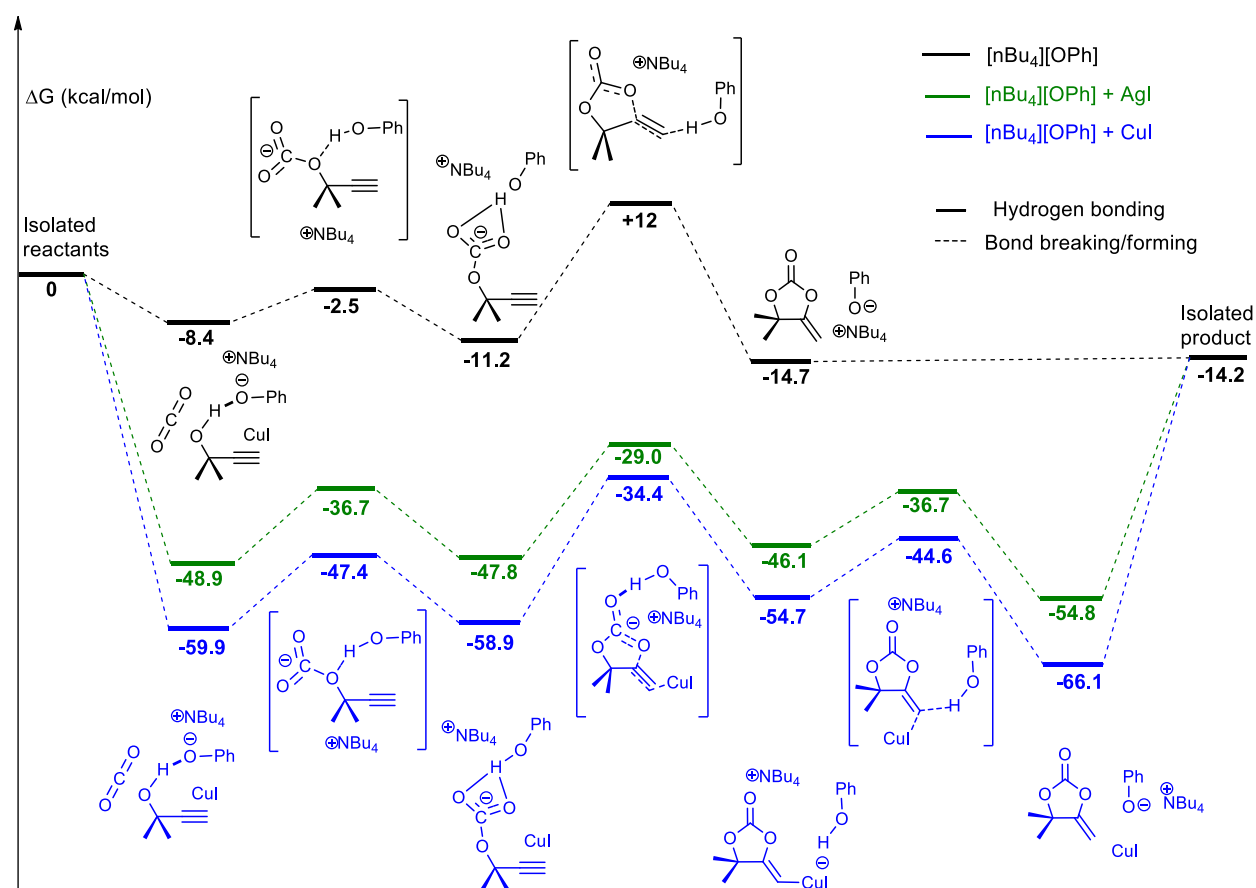


Figure 5. Gibbs free energy profiles for α -methylene carbonate formation with $[n\text{Bu}_4\text{N}][\text{OPh}]$, $[n\text{Bu}_4\text{N}][\text{OPh}]/\text{CuI}$ and $[n\text{Bu}_4\text{N}][\text{OPh}]/\text{AgI}$ as catalytic system. NB: the intermediates drawn for the $[n\text{Bu}_4\text{N}][\text{OPh}]/\text{CuI}$ system applies also for the $[n\text{Bu}_4\text{N}][\text{OPh}]/\text{AgI}$ system.

In summary, after the first step, that is the addition of CO_2 to the propargylic alcohol, the reactants must overcome the highest energy transition state of +12 kcal/mol for the reaction catalysed by $[n\text{Bu}_4\text{N}][\text{OPh}]$ only. In contrast, due to the strong exergonicity observed in the presence of CuI (AgI), the reactants might spontaneously react without any stabilisation and accelerate the reaction kinetic compared to the case of the reaction catalysed by $[n\text{Bu}_4\text{N}][\text{OPh}]$ only. On the other hand, in the presence of CuI (AgI), the remaining part of the species that could be stabilized must undergo activation energies of 18.8 kcal/mol and 23.2 kcal/mol for the reactions co-catalysed by AgI and CuI respectively, indicating that the reaction catalysed by $[n\text{Bu}_4\text{N}][\text{OPh}]/\text{AgI}$ is the fastest which is in good agreement with the kinetics studies by online FT-IR experiments.

3. Conclusions

In this chapter, we optimised the activity of the organic catalyst [nBu₄N][OPh] by incorporating either CuI or AgI as metal cocatalyst. We showed that the reaction temperature could be reduced from 80 °C to 40 °C, while maintaining a good reactivity (conversion of 100% in 50 min and 180 min with CuI and AgI respectively) and improving the selectivity from 90-100% in the α CC **2**. For the bis α CC, further reducing the temperature to 25 °C, allowed to obtain a 95% yield. Operando FT-IR spectroscopy correlated to DFT calculations provided kinetic and mechanistic insights that helped to rationalise the reactivity, the efficiency, and the selectivity of the binary catalytic system.

4. Experimental section

4.1. Materials

Ethynylmagnesium bromide (Acros), silver iodide, silver acetate, silver carbonate, copper chloride, copper bromide, copper iodide, zinc iodide, 2,5-hexandione, 2-methyl-3-butyn-2-ol, 3-methyl-1-pentyn-3-ol, 3,5-dimethyl-1-hexyn-3-ol were purchased from Aldrich. CO₂ (N27) was purchased from Air liquid, dimethyl sulfoxide (DMSO), dimethyl formamide (DMF), acetonitrile (ACN), methanol (MeOH), diethylether. DMSO was dried on a 3 Å molecular sieve conditioned at 100 °C under vacuum for 24 h. All the other reagents were used as received without any further purification. DMSO-*d*₆ was purchased from Eurisotop.

4.2. Analytical methods

¹H NMR analyses were performed on Bruker Advance 400 MHz spectrometer in DMSO at 25 °C in the Fourier transform mode. 16 scans for ¹H spectra and 512 or 2048 scans for ¹³C spectra were recorded.

Fourier transform infrared spectra were recorded using a Nicolet IS5 spectrometer (Thermo Fisher Scientific) equipped with a transmission or with a diamond attenuated transmission reflectance (ATR) device. Spectra were obtained in transmission or ATR mode as a result of 32 spectra accumulation in the range of 4000 – 500 cm⁻¹, with a nominal resolution of 4 cm⁻¹.

In-situ IR spectroscopy experiments were conducted using a stainless-steel reactor suitable for high-pressure measurements (up to 400 bar) and high temperature (up to 100 °C) coupled with a FT-MIR spectrometer from Bruker, equipped with an air-cooled globar source (12 V), a KBr beam splitter, a mechanical rocksolid interferometer, permanently aligned, a diamond ATR fibre probe IN350-T (Ø 6 mm) and a liquid nitrogen cooled mercury cadmium telluride (MCT). Single beam spectra recorded in the spectral range (670-3500 cm⁻¹) with a 4 cm⁻¹ resolution were obtained after the Fourier transformation of 32 accumulated interferograms until the end of reaction time.

4.3. Experimental procedures

Screening of the reaction parameters for the carboxylative coupling of CO₂ to 3-methyl-2-butyn-3-ol.

In a clean dry reactor, equipped with a magnetic rod, a manometer and a gas inlet/outlet, were introduced 3-methyl-2-butyn-3-ol (2 mL, 20.61 mmol), tetrabutylammonium phenolate [nBu₄N][OPh] (0.3459 g, 1.031 mmol), CuI (0.1963g, 1.031 mmol) and acetonitrile (2 mL). The reactor was closed and placed in a silicon oil bath set at the desired temperature. After 30 minutes, CO₂ gas was added at a constant pressure. The reaction ran for 1 h after which the reactor was depressurised and placed in a water bath to cool it down to room temperature.

The crude reaction mixture was characterised by $^1\text{H-NMR}$ spectroscopy. For the screening of the reaction parameters (T, solvent, catalyst), a similar protocol was applied.

Monitoring of the carboxylative coupling of CO_2 to 3-methyl-2-butyn-3-ol by online FT-IR.

In a clean dry reactor of 80 mL equipped with a manometer, a heating mantle, gas inlet/outlets, a mechanical stirrer and a high-pressure FT-IR probe, were introduced 3-methyl-2-butyn-3-ol (16 mL, 164.9 mmol), tetrabutylammonium phenolate [nBu_4N][OPh] (2.7603 g, 8.225 mmol), the metal salt (AgI, 8.225 mmol) and dried DMSO (16 ml). The reactor was closed and heated to the desired temperature, after which the FT-IR acquisition was launched. Then CO_2 gas was added at constant pressure. Spectra were recorded every 2 min. Once the reaction was complete, the reactor was cooled down to room temperature and depressurised. The crude mixture was recovered and characterised by $^1\text{H-NMR}$ spectroscopy.

4,4-dimethyl-5-methylene-1,3-dioxolan-2-one (2) $^1\text{H NMR}$ (400 MHz, $\text{DMSO-}d_6$) δ (in ppm) = 4.79 (d, $J = 3.8$ Hz, 1H), 4.65 (d, $J = 3.8$ Hz, 1H), 1.60 (s, 6H). $^{13}\text{C NMR}$ (100.6 MHz, $\text{DMSO-}d_6$) δ (in ppm) = 158.67, 151.28, 85.92, 85.56, 27.37.

Monitoring of the carboxylative coupling of CO_2 to 3,6-dimethylocta-1,7-diyne-3,6-diol by online FT-IR.

In a clean dry reactor of 40 mL internal volume, equipped with a manometer, a heating mantle, gas inlet/outlets, a mechanical stirrer and a high-pressure FT-IR probe were introduced 3,6-dimethylocta-1,7-diyne-3,6-diol (3g, 18.02 mmol), tetrabutylammonium phenolate [nBu_4N][OPh] (0.6081g, 1.812 mmol), the metal salt, AgI (0.2116g, 0.911 mmol) and dried DMSO (10 ml). The reactor was closed and heated to the desired temperature, after which the FT-IR acquisition was launched. Then CO_2 gas was added at constant pressure. Spectra were recorded every 10 min. Once the reaction was complete, the reactor was cooled down to room temperature and depressurised. The crude mixture which was partially soluble was recovered with CH_2Cl_2 and extracted with a mixture of $\text{CH}_2\text{Cl}_2/\text{H}_2\text{O}$ to remove DMSO. The organic fraction was collected, and the excess organic solvent evaporated. The crude product was then purified by silica gel chromatography, using as eluent ethyl acetate/ petroleum ether. Then the product was recrystallized in acetonitrile at room temperature and then -20°C to afford the pure bis αCC (4'-(ethane-1,2-diyl)bis(4-methyl-5-methylene-1,3-dioxolan-2-one).

4'-(ethane-1,2-diyl)bis(4-methyl-5-methylene-1,3-dioxolan-2-one)

$^1\text{H NMR}$ (400 MHz, $\text{DMSO-}d_6$) δ in ppm 4.89 (d, $J = 3.9$ Hz, 1H), 4.73 (d, $J = 3.9$ Hz, 1H), 1.95 (ddd, $J = 10.2, 7.8, 5.4$ Hz, 1H), 1.86 (ddd, $J = 9.5, 7.8, 5.4$ Hz, 1H), 1.62 (s, 3H). $^{13}\text{C NMR}$ δ 156.71, 151.21, 87.10, 87.06, 33.32, 26.04, 25.92.

5. Supplementary Information

SI- 1. Determination of the propargylic alcohol conversion for the carboxylative cyclisation of 2-methyl-3-butyn-2-ol.

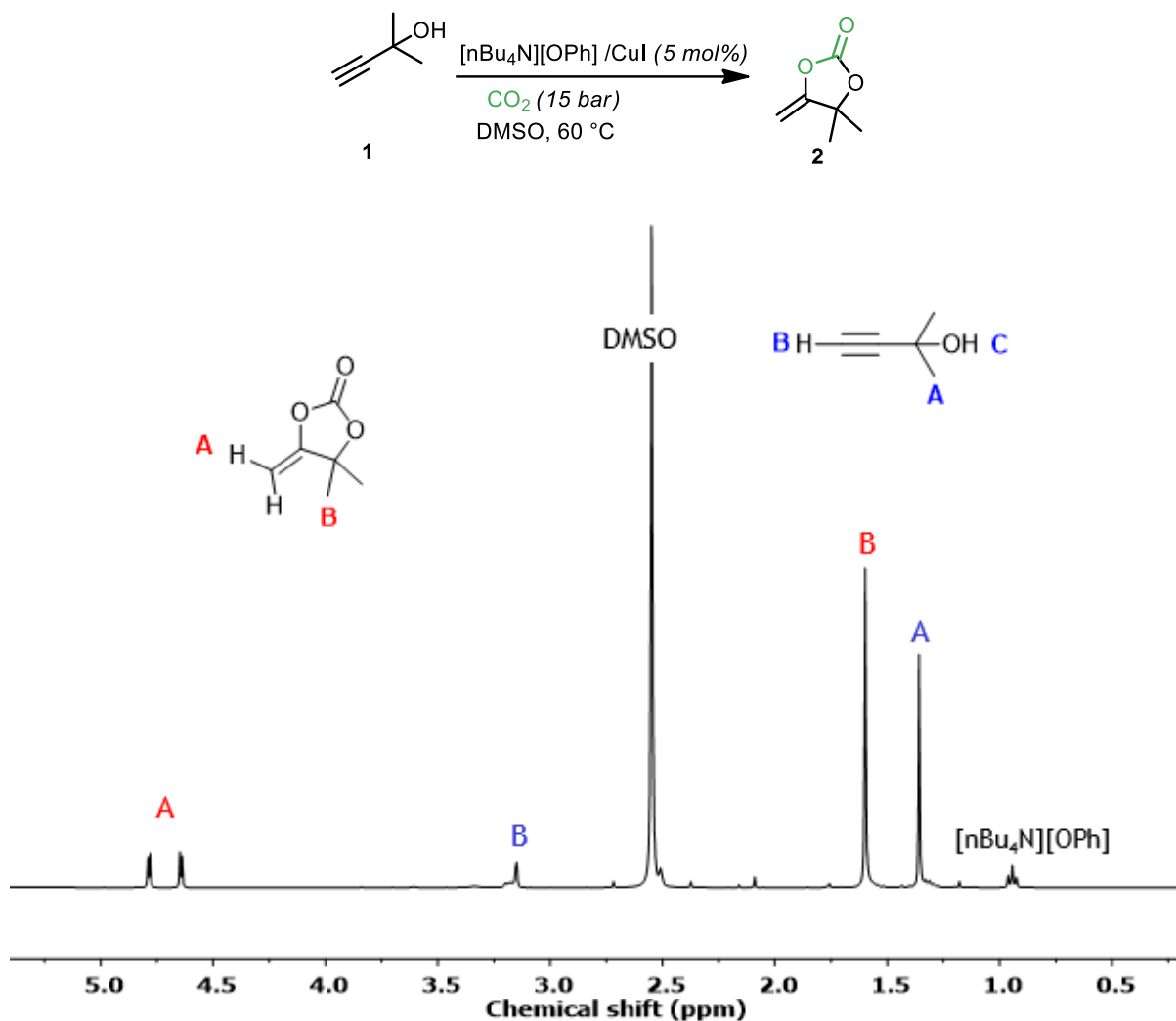


Figure S 1. Representative ¹H-NMR spectrum (in DMSO-*d*₆) for the reaction of 2-methyl-3-butyn-2-ol with CO₂ (15 bar) in the presence of [nBu₄N][OPh] (5 mol%) and CuI (2.8 mol%) in DMSO after 2 h at 60 °C.

The 2-methyl-3-butyn-2-ol conversion was estimated by comparison of the relative intensities of the peaks associated to olefinic protons at 4.64 and 4.79 ppm of the cyclic carbonate, and the peak of the methyl groups of the alkyne at 1.35 ppm according to the equation:

$$\text{Conversion \%} = \left(1 - \left(\frac{\frac{I_{1.36}}{6}}{\left(\frac{I_{4.64} + I_{4.79}}{2} \right) + I_{1.36}/6} \right) \right) \times 100$$

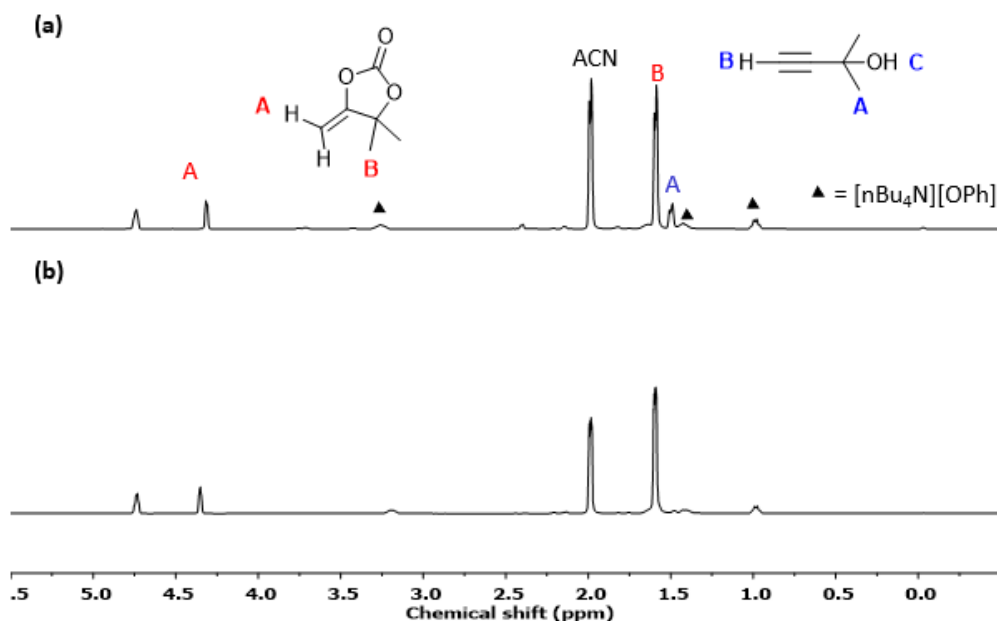
SI- 2. ^1H NMR spectra of the reaction mixture catalysed by $[\text{nBu}_4\text{N}][\text{OPh}]$ and CuI/AgI 

Figure S 2. Synthesis of 4,4-dimethyl-5-methylene-1,3-dioxolan-2-one by organocatalysed coupling of CO_2 to 2-methyl-3-butyn-2-ol. (a) $[\text{nBu}_4\text{N}][\text{OPh}]/\text{CuI}$ and (b) $[\text{nBu}_4\text{N}][\text{OPh}]/\text{AgI}$. Conditions: 2-methyl-3-butyn-2-ol (2 mL, 0.0206 mmol), $[\text{nBu}_4\text{N}][\text{OPh}]$ (5 mol%), CuI/AgI (5 mol%), 40°C , 15 bar, ACN (2 mL).

SI- 3. Determination of the yield in cyclic carbonate by FT-IR spectroscopy

For a reaction wherein complete conversion of 2-methyl-3-butyn-2-ol into 100% αCC is obtained, the concentration of αCC will be given by the following equation:

$$\text{Concentration} \left(\frac{\text{mol}}{\text{l}} \right) = \left(\frac{n_{\text{alkynol}}}{V_{\text{solvent}}} \right) = 10.30 \text{ mol/l}$$

The molar extinction coefficient of the cyclic carbonate was determined based on Beer Lambert's. The absorbance of a solution of known concentration was measured, and the molar extinction coefficient determined based on the following equation:

$$\text{Absorbance} = (\epsilon l C)$$

$$\epsilon l = \left(\frac{\text{Absorbance}}{C_{\alpha\text{CC}}} \right)$$

From the above equation, we could then convert the absorbances measured after various times into a concentration and hence determine the yield in cyclic carbonate.

$$C_{\alpha\text{CC}} = \left(\frac{\text{Absorbance}}{\epsilon l} \right)$$

$$\text{Yield}_{\alpha\text{CC}}(\%) = \left(\frac{C_{\text{DMACC determined}}}{10.30} \times 100 \right)$$

A similar procedure was followed for the determination of the yield in *oxo*-alkylcarbonate

SI- 4. Computational details

Preliminary calculations of equilibrium structures were performed using a semi-empirical model (PM6-D3H4) to determine the most stable conformations. These semi-empirical calculations were performed using the AMPAC software. The CHAIN algorithm was used for locating intermediates and transition states along the reaction path. The lowest energy structures obtained at the PM6-D3H4 level were further investigated using the Density Functional Theory method (DFT) implemented in the Gaussian 16 package. DFT calculations of geometries, energies, and vibrational frequencies reported in this chapter were carried out with the M06-2X functional using the 6-311 G(d,p) basis set except for Ag, Cu and I atoms which have been treated with the help of the LANL2DZ pseudo potential. All frequencies of each structure have also been calculated to verify the presence of a single imaginary frequency for transition states and the absence of imaginary frequency for ground states. The intrinsic reaction coordinate (IRC) method has been used to verify that the obtained transition states were effectively connected to the desired minima. For all activating systems, a wide range of possible configurations and interactions have been modelled and the more stable of them are reported in this work. To consider entropic effects, the energies mentioned in this study correspond to the Gibbs free energy (G).

SI- 5. Supplementary NMR characterisation

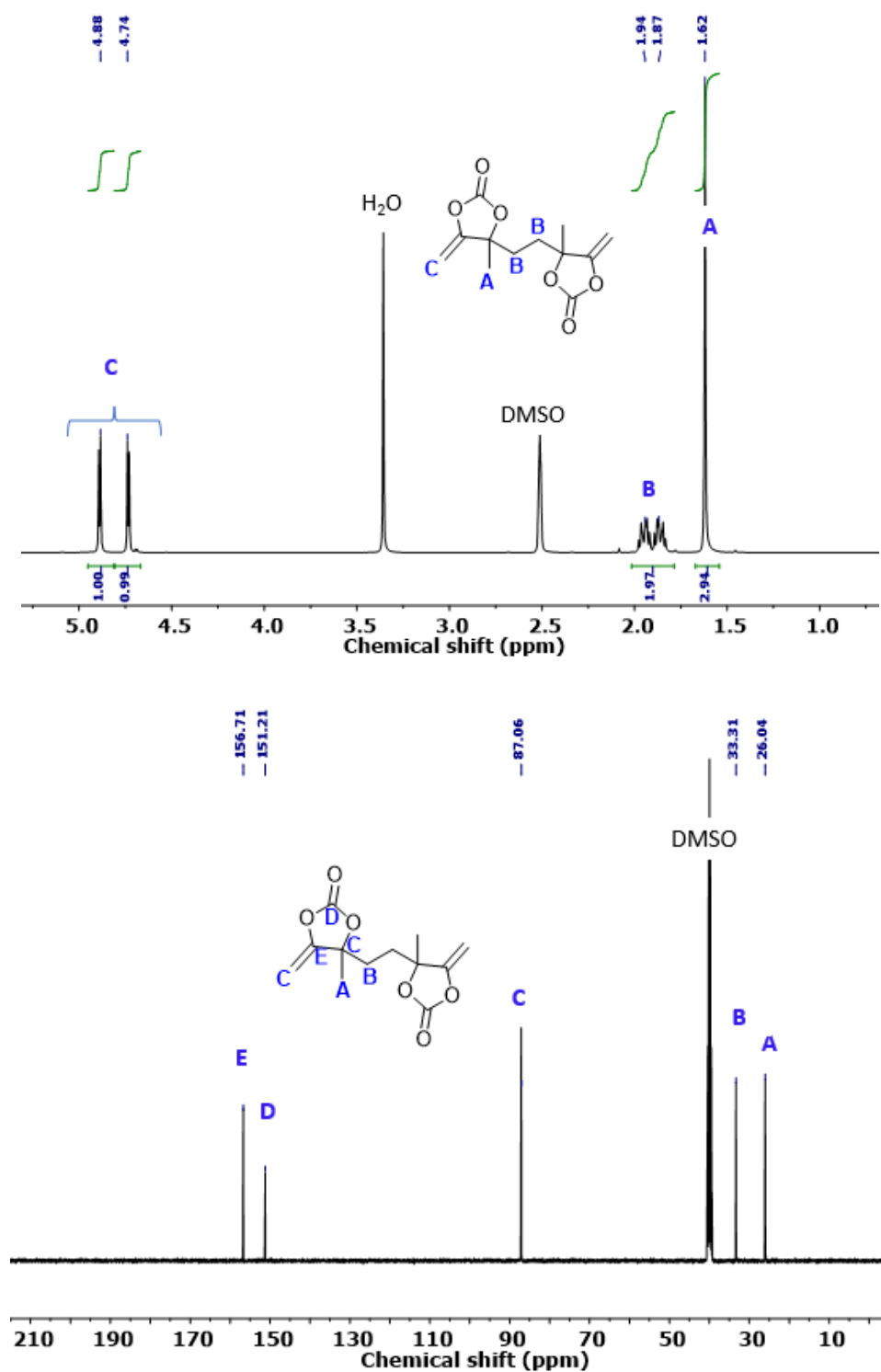
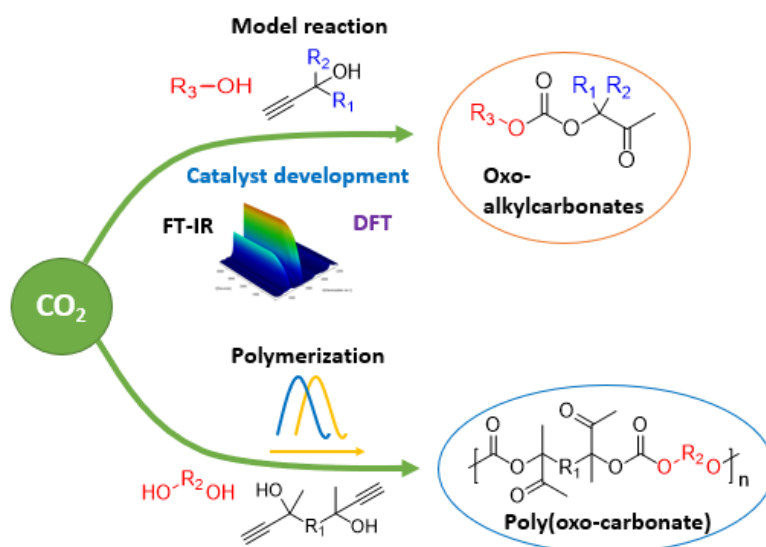


Figure S 3. $^1\text{H-NMR}$ and $^{13}\text{C-NMR}$ spectrum of 4'-(ethane-1,2-diyl)bis(4-methyl-5-methylene-1,3-dioxolan-2-one).

CHAPTER 4

A catalytic domino approach towards *oxo*-alkylcarbonates and poly(*oxo*-carbonate)s from CO₂, propargylic alcohols and (mono- and di-) alcohols



Chapter 4

This chapter includes results that are published in;

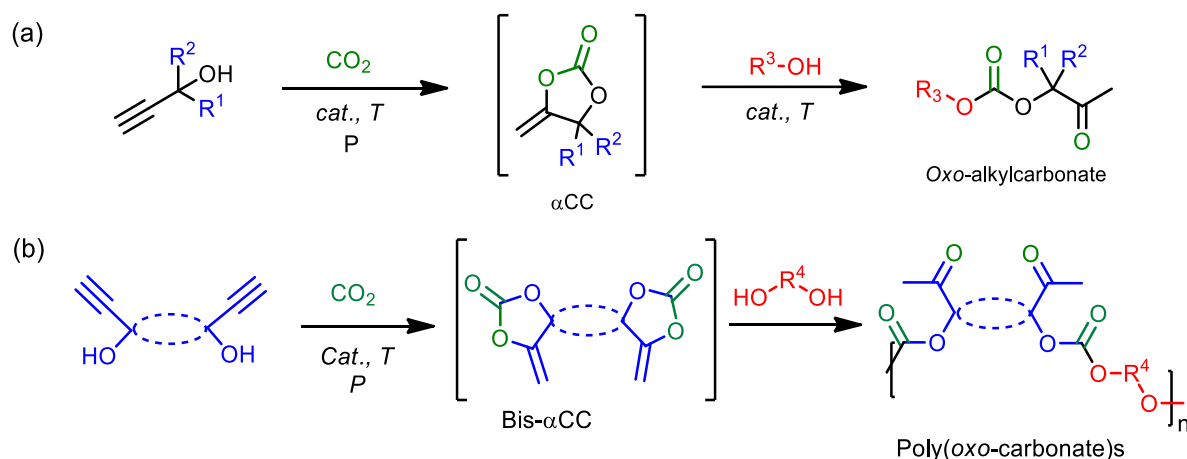
Charlène Ngassam Tounzoua, Bruno Grignard, Antoine Brège, Christine Jérôme, Thierry Tassaing, Raphael Mereau and Christophe Detrembleur. ACS Sustainable Chem. Eng. 2020, 8, 9698–9710

Table of content

1. Introduction	106
2. Results.....	107
2.1. Synthesis of <i>oxo</i> -alkylcarbonates	107
2.2. Synthesis of poly(<i>oxo</i> -carbonate)s	112
3. Conclusions	121
4. Experimental section	122
4.1. Materials.....	122
4.2. Analytical methods	122
4.3. Experimental procedures	123
5. Supplementary informations	126

1. Introduction

In the previous chapter, we developed a dual catalytic system composed of $[\text{nBu}_4\text{N}][\text{OPh}]/\text{AgI}$ that allowed the quantitative and selective synthesis of bis(alkylidene cyclic carbonate) (bis αCC) monomers under mild reaction conditions (25 °C, 15 bar). In this chapter, we explore the one-pot cascade synthesis of *oxo*-alkylcarbonates from propargylic alcohols, CO_2 and alcohols, and for the first time, the one-pot cascade synthesis of poly(*oxo*-carbonate)s from bispropargylic alcohols, CO_2 and diols (**Scheme 1**).



Scheme 1. General scheme showing the cascade synthesis of (a) *oxo*-alkylcarbonates and (b) poly(*oxo*-carbonate)s.

Few catalytic systems have been reported for the synthesis of *oxo*-alkylcarbonates, they include DBU/Zn salts^[108] (40:20 mol%), $\text{AgCl}/[\text{BMIm}][\text{OAc}]$ ^[210], $\text{Ag}_2\text{CO}_3 / \text{PPh}_3$ ^[211]. As discussed in **Chapter 1**, section 3.2, although these systems afforded the *oxo*-alkylcarbonates in low to excellent yields (22-99%), under moderate conditions (1-10 bar, 80 °C, 24 h) the organic cocatalyst was often used in large amounts (40-100 mol%) and the alcohol sometimes used in excess. Zhang's system based on silver sulfadiazine/EtNBr was the only system which afforded high yields in the desired *oxo*-alkylcarbonates while using catalytic amounts of the catalyst (5 mol%). Still, the latter system suffers from the multi-step synthesis of sulfadiazine.^[111,212] In addition, none of these systems have been utilised for both the quantitative synthesis of bis αCC s and their *in-situ* transformation into poly(*oxo*-carbonate)s in a cascade reaction. The development of new simple efficient systems is thus still desirable. To pursue our goal, we further optimised the reaction conditions using our dual system $[\text{NBu}_4][\text{OPh}]/\text{AgI}$ which gave the highest activity for the synthesis of DMACC. Kinetic insights via operando FT-ATR spectroscopy, enabled us to understand the reactivity of the catalyst. Finally, this process was exploited for the cascade synthesis of PCs.

2. Results

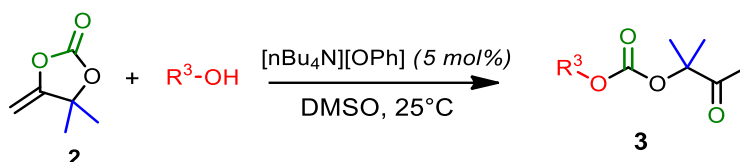
2.1. Synthesis of oxo-alkylcarbonates

Before trying to implement the cascade synthesis of oxo-alkylcarbonates, it was important to verify that our organic catalyst $[n\text{Bu}_4\text{N}][\text{OPh}]$ could indeed catalyse the alcoholysis of αCC **2**.

By the alcoholysis of DMACC

We evaluated the capacity of the $[n\text{Bu}_4\text{N}][\text{OPh}]$, $[n\text{Bu}_4\text{N}][\text{OPh}]/\text{CuI}$, $[n\text{Bu}_4\text{N}][\text{OPh}]/\text{AgI}$ dual systems to catalyse the alcoholysis of αCC **2** into oxo-alkyl carbonates **3** at room temperature ($T = 25\text{ }^\circ\text{C}$) in DMSO. The reaction was tested for different alcohols and the results are summarised in **Table 1**.

Table 1. Alcoholysis of 4,4-dimethyl-5-methylene-1,3-dioxolan-2-one (αCC , **2**) catalysed by $[n\text{Bu}_4\text{N}][\text{OPh}]$.



Entry	Catalyst	Alcohol	Alcohol structure	Conv. of 2 (%)	Yield in 3 (%)
1	-	1-butanol		0	0
2	$[n\text{Bu}_4\text{N}][\text{OPh}]$	1-butanol		100	100
3	$[n\text{Bu}_4\text{N}][\text{OPh}]/\text{AgI}$	1-butanol		100	100
4	$[n\text{Bu}_4\text{N}][\text{OPh}]/\text{CuI}$	1-butanol		0	0
5	$[n\text{Bu}_4\text{N}][\text{OPh}]$	benzyl alcohol		100	100
6	$[n\text{Bu}_4\text{N}][\text{OPh}]$	propan-2-ol		68	100
7	$[n\text{Bu}_4\text{N}][\text{OPh}]$	2-methyl-2-butanol		0	/

Conditions: αCC **2** (0.5 g, 3.904mmol), alcohol (3.904 mmol), $[n\text{Bu}_4\text{N}][\text{OPh}]$ (66 mg, 5 mol%), cocatalyst (AgI or CuI: 5 mol%), DMSO (1 ml), $T = 25\text{ }^\circ\text{C}$, $t = 1\text{ h}$. The conversions and selectivities were determined by $^1\text{H-NMR}$ in DMSO- d_6 . (see **SI-1** for the procedure).

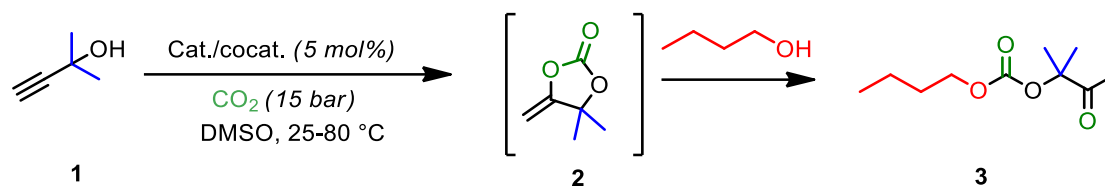
Importantly, [nBu₄N][OPh] (5 mol%) displayed sufficient basicity to enable the complete and selective conversion of α CC **2** into the corresponding oxo-alkylcarbonate **3** when reacted with 1-butanol for 1 h at 25 °C, while no reaction was noted without the catalyst (**Table 1**), entries 1-2). The [nBu₄N][OPh] acted as a hydrogen bond acceptor, thereby activating the alcohol molecule. When AgI was used as cocatalyst in combination to [nBu₄N][OPh] α CC **2** was selectively converted into the oxo-alkylcarbonate (**Table 1**, entry 3), similarly to the reaction performed with [nBu₄N][OPh] only (**Table 1**, entry 2). The addition of AgI did not induce any side reaction, at least during the investigated reaction period. We repeated this experiment for a shorter reaction time (15 min instead of 1 h) and an identical conversion of **2** (100%) and selectivity for **3** (100%) were again noted. Although further experiments would be required, it suggests that the silver salt has no noticeable effect on the alcoholysis of the α -alkylidene cyclic carbonate, in line with reports of Li^[111] and Han^[210]. However, when [nBu₄N][OPh]/CuI was used as catalyst, the alcoholysis reaction did not occur, no conversion of the DMACC was noted (**Table 1**, entry 4), even after 24 h. At this stage, we are unable to explain this observation. However, we believe that the CuI and phenolate might form a complex in the presence of butanol.

When using benzyl alcohol, the reaction carried out with [nBu₄N][OPh] was also fast, quantitative, and selective (**Table 1**, entry 5). In addition, the selectivity was still excellent, the conversion in α CC dropped to 68% when using a less reactive secondary alcohol, 2-propanol, under identical conditions (**Table 1**, entry 6). No reaction was however noted with the tertiary alcohol, 2-methyl-2-butanol (**Table 1**, entry 7). The lower reactivity of the secondary and tertiary alcohol arose from their steric hindrance that decreased their nucleophilic character.

Cascade reaction on model compounds

As [nBu₄N][OPh]/AgI was able to catalyse both the selective formation of DMACC by coupling CO₂ to 2-methyl-3-butyn-2-ol and its alcoholysis by primary and secondary alcohols, we then evaluated its ability to catalyse the one-pot cascade synthesis of the corresponding oxo-alkylcarbonate **3** from CO₂, 2-methyl-3-butyn-2-ol and 1-butanol (**Table 2**). The reactions were carried out at 15 bar for 6 h, using 5 mol% of [nBu₄N][OPh] with and without AgI, and different temperatures were screened.

At 25-60 °C with [nBu₄N][OPh] only, no reaction is observed, whereas 15% conversion is observed at 80 °C after 6 h (**Table 2**, entries 1-4). With the [nBu₄N][OPh]/AgI system, while only a minim conversion is observed at 25 °C, increasing the temperature to 40 °C gave full conversion of **1** after 6 h of reaction (**Table 2**, entry 5 and 6). However, the main product was α CC **2** (93%), with only 7% of the desired oxo-alkylcarbonate **3** formed. By further increasing the reaction temperature to 60 or 80 °C, the yield in **3** was increased to 20 or 74%, respectively (**Table 2**, entries 7 and 8).

Table 2. Cascade synthesis of butyl (2-methyl-3-oxobutan-2-yl) carbonate from 2-methyl-3-butyn-2-ol, CO₂ and the primary alcohol 1-butanol.

Entry	Catalyst	T (°C)	Conv. of 1 (%)	Yield in 2 ^a (%)	Yield in 3 ^b (%)
1	[nBu ₄ N][OPh]	25	0	0	0
2	[nBu ₄ N][OPh]	40	0	0	0
3	[nBu ₄ N][OPh]	60	0	0	0
4	[nBu ₄ N][OPh]	80	15	15	0
5	[nBu ₄ N][OPh]/AgI	25	11	11	0
6	[nBu ₄ N][OPh]/AgI	40	100	93	7
7	[nBu ₄ N][OPh]/AgI	60	100	80	20
8	[nBu ₄ N][OPh]/AgI	80	100	23	74

Conditions: 2-methyl-3-butyn-2-ol (2 ml, 0.02061 mol), 1-butanol (1.89 ml, 0.02065 mol), [nBu₄N][OPh] (5 mol%), AgI (5 mol%), DMSO (2 ml), CO₂ (15 bar), 6 h. ^a Selectivity for **2**. ^b Selectivity for **3**. The conversions and selectivity were determined by ¹H-NMR in DMSO-d₆. (see SI – 2 for the procedure).

The influence of the working pressure on the yield and selectivity of the reaction was then evaluated by on-line ATR-IR spectroscopy at 60 °C. Unfortunately, because the bands corresponding to the CC triple bond (890 and 960 cm⁻¹) and the OH bond (3260 cm⁻¹) of the propargylic alcohol overlapped with other bands, we could not follow the consumption of the propargylic alcohol over time. However, by analysing a sample of the reaction mixture at the end of each experiment by ¹H-NMR spectroscopy, we could confirm the total conversion of the propargylic alcohol for reactions performed at PCO₂ of 1, 5 or 15 bar. We monitored the formation of αCC **2** and its conversion into the oxo-alkylcarbonate **3** by following the evolution of the carbonyl band of the cyclic carbonate **2** at 1820 cm⁻¹ and of the linear carbonate **3** at 1740 cm⁻¹ (Figure 1a). The yields of each product are plotted vs time in Figure 1b. At 60 °C and 15 bar of CO₂, the formation of the oxo-alkyl carbonate **3** was observed after about 2.5 h of reaction and was relatively slow. After 20 h of reaction, a mixture of product **2** (45%) and **3** (40%) was collected. By decreasing the CO₂ pressure to 5 bar, the formation of αCC **2** was faster and its conversion into **3** started after 45 min. After 20 h, the yield in **2** was only 3% while the desired product **3** was formed with 87% yield. Importantly, when the pressure was

further reduced to 1 bar, α CC **2** was rapidly formed and was simultaneously converted into **3**. The domino reaction was complete in less than 10 h at 1 bar and selective towards the formation of **3** (Figure 1a and b). These kinetics studies clearly highlighted that a low CO₂ pressure was required for an efficient domino reaction and for the selective production of **3**. It was assumed that high CO₂ pressure favoured the carbonation of 1-butanol, consequently deactivating it for the alcoholysis of the α CC **2** formed in-situ.

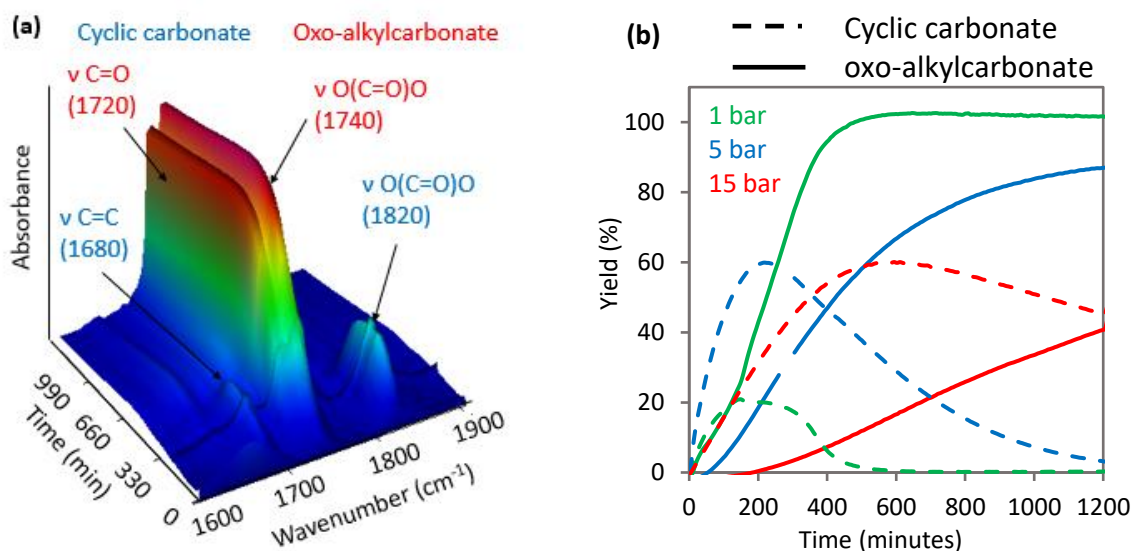


Figure 1. One pot domino synthesis of butyl-(2-methyl-3-oxobutan-2-yl) carbonate from CO₂, 2-methyl-3-butyn-2-ol and 1-butanol catalysed by [nBu₄N][OPh]/AgI at 60 °C. (a) 3D profile for a reaction conducted at PCO₂ of 1 bar; (b) influence of CO₂ pressure on the formation of cyclic carbonate **2** and oxo-alkylcarbonate **3**. Conditions: [nBu₄N][OPh] (5 mol%), AgI (5 mol%), 2-methyl-3-butyn-2-ol (12 mL), 1-butanol (11.3 mL), DMSO (12 mL).

To give additional clue to this hypothesis, we monitored by online FT-ATR spectroscopy the possible formation of a zwitterionic compound from 1-butanol, CO₂ and [nBu₄N][OPh] in the solvent used for the reaction (DMSO) at a pressure of 15 bar. We indeed observed the rapid growth (< 5 min) of a band at 1660 cm⁻¹ which is typical of the ν C=O of a carbonate anion,^[32] thus supporting the *in-situ* carbonation of 1-butanol favoured at high pressure of 15 bar (Figure 2).

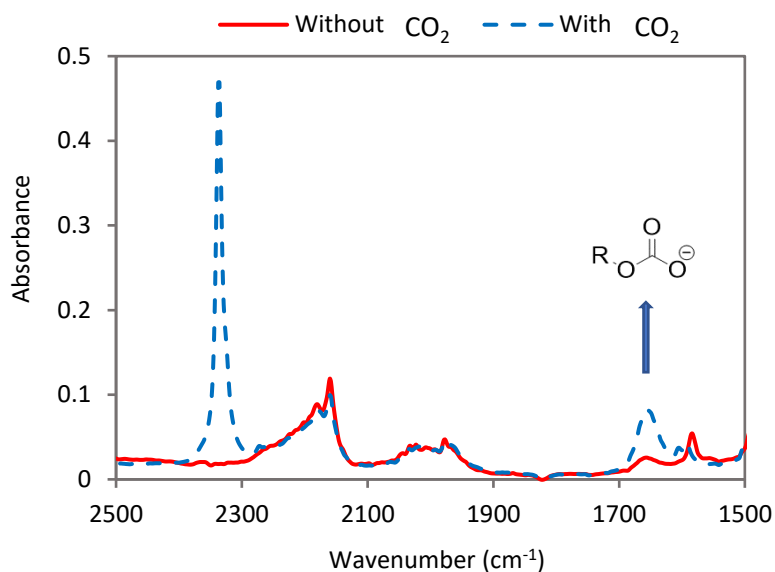
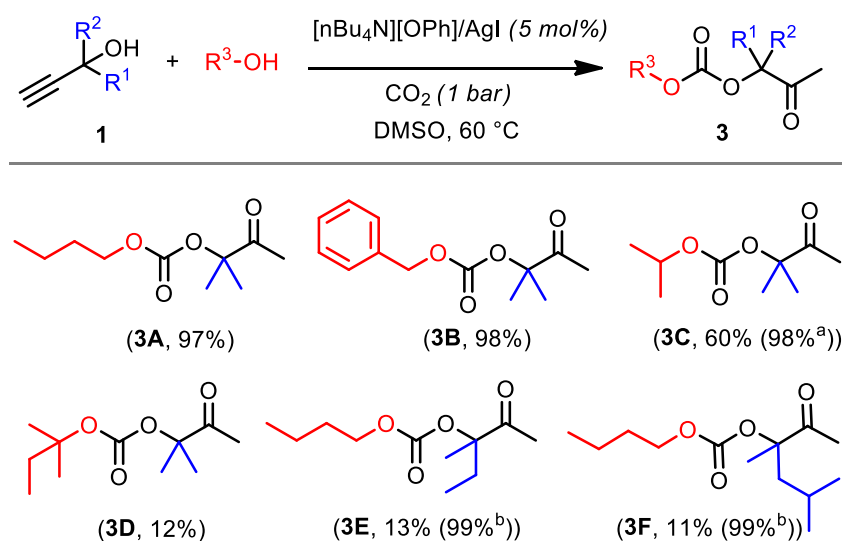


Figure 2. FT-IR spectra of a mixture of [nBu₄N][OPh] (5 mol%), 1-butanol and DMSO exposed (blue) or not (red) to CO₂ (15 bar) for 5 min at 60 °C.

To highlight the versatility of the [nBu₄N][OPh]/AgI catalytic system for the domino reaction under the optimum conditions (60 °C, PCO₂ = 1 bar, 10 h), we enlarged the scope of propargylic alcohols and mono-alcohols to access various *oxo*-alkylcarbonate compounds (**Scheme 2**).



Scheme 2. Product scope for the synthesis of *oxo*-alkylcarbonates. Conditions: propargylic alcohol (20.61 mmol), aliphatic alcohol (20.61 mmol), [nBu₄N][OPh]/AgI (5 mol%), DMSO (2 mL), PCO₂ = 1 bar, t = 10 h. Yields were determined by ¹H NMR spectroscopy in DMSO-d₆ after 24 h (^a) and 72 h (^b) under neat conditions. ¹H and ¹³C NMR as well as FT-IR characterisations are illustrated in **Figure S 3** to **S 7**.

In all cases, all propargylic alcohols were fully consumed. The corresponding *oxo*-alkylcarbonates were formed with a high yield (≥ 97%) when primary alcohols such as 1-butanol or benzyl alcohol were reacted with the less sterically hindered propargylic alcohol,

2-methyl-3-butyn-2-ol. When a secondary 2-propanol or tertiary alcohol 2-methyl-2-butanol was employed together with 2-methyl-3-butyn-2-ol, the yields in *oxo*-alkylcarbonate dropped to 60% (product **3C**) and 12% (product **3D**), respectively. Similarly, when 1-butanol was reacted with more sterically hindered propargylic alcohols such as 3-methyl-1-pentyn-3-ol and 3,5-dimethyl-1-hexyn-3-ol, incredibly low yields (13% for product **3E**, and 11% for product **3F**), respectively, were obtained. The remaining percentage corresponded to the unreacted cyclic carbonate intermediate. Interestingly, by extending the reaction time to 72 h, the selectivity and yield in the target *oxo*-alkylcarbonates increased to 99% for both **3E** and **3F**.

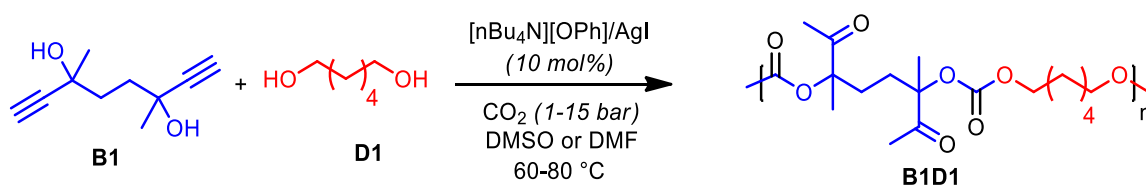
If we consider the systems published in the literature on the synthesis of *oxoalkyl* carbonates, such as DBU/Zn salts^[108] (40:20 mol%), AgCl/[BMIIm][OAc]^[210], Ag₂CO₃ / PPh₃^[211], which functioned at 80°C, 1-10 bar, with large amounts (40-100 mol%) of the organo catalyst and the alcohol sometimes used in excess, our [nBu₄N][OPh]/AgI system is thus very competitive, as it allows us to prepare the *oxoalkyl* carbonates in very high yields, while working at moderate temperature (60°C), atmospheric pressure, with stoichiometric amounts of the propargylic alcohol and monoalcohol, and under low loadings of the catalyst (5 mol%). Moreover [nBu₄N][OPh] has the added advantage of its relative simple synthesis and having sufficient basicity to eventually be used as catalyst for our step-growth polymerisation, in comparison to the silver sulfadiazine system^[111,212] which also functioned under low catalyst loading.

2.2. Synthesis of poly(*oxo*-carbonate)s

In section 2.1., we optimised the reaction parameters to promote the cascade synthesis of *oxoalkylcarbonates* and found the optimum conditions to be 60 °C, 1 bar in DMSO with 5 mol % of [nBu₄N][OPh]/AgI as binary catalytic system. This parameters would now be applied for the cascade synthesis of poly(*oxo*-carbonate)s. In order to account for the bifunctionality of the monomers, the amount of catalyst was increased to 10 mol%.

By the one pot cascade terpolymerisation

The reaction conditions were first optimised for the terpolymerisation of 4,4'-(ethane-1,2-diyl)bis(4-methyl-5-methylene-1,3-dioxolan-2-one) **B1**, 1,6-hexanediol **D1** and CO₂ using [nBu₄N][OPh]/AgI as binary catalytic system (**Scheme 3**), the results are summarised in (**Table 3**).



Scheme 3. One pot synthesis of poly(*oxo*-carbonate)s, model reaction.

When the reaction was carried out in DMSO at 1 bar of CO₂, oligomers with a number average molar mass (M_n) of 1000 g/mol were obtained after 48 h at 60 °C (**Table 3**, entry 1). By

increasing the CO₂ pressure to 15 bar, the M_n increased to 1500 g/mol after 24 h. We extended the reaction time to 72 h to see if this would allow for an increase in the diol conversion and hence the M_n however no significant evolution was observed (**Table 3**, entries 2 and 3). When the reaction was performed under neat conditions, similar results were obtained. In the pioneering study on which this work relies, the authors had pointed out an influence of solvent on the outcome of the polymerisation, they indeed observed an increase in the masses obtained from 13000-17000 g/mol when using DMF in place of CHCl₃.^[18] This thus prompted us to test DMF as solvent, an interestingly the molar mass was almost doubled (**Table 3**, entries 8-9). Increasing the reaction temperature to 80 °C was detrimental to the polymerisation with the formation of oligomers of lower M_n (**Table 3**, entries 4 and 5 in DMSO and entry 10 in DMF). Several factors might be at the origin of this observation. First, we demonstrated in **chapter 3** that increasing the reaction temperature decreased the selectivity in the *in-situ* formed bis α CC, with the resultant being that the stoichiometry between bis α CC and alcohol groups is not respected. Secondly, it has been shown that some thermally induced side reactions (e.g. transcarbonation) were favoured at high temperatures of 80 °C thereby leading to a deviation from the perfect stoichiometry, hence lowering the molar mass of the polymer obtained.

Table 3. Screening of parameters for the one pot domino synthesis of poly(oxo-carbonate)s.

Entry	Solvent	P (bar)	T (°C)	Time (h)	^a Conv. B ₁ (%)	^a Conv. D1 (%)	^b M _n (g/mol)	^b M _w (g/mol)	^b Đ
1	DMSO	1	60	48	100	20	<1000	-	-
2	DMSO	15	60	24	100	61	1500	1900	1.3
3	DMSO	15	60	72	100	55	1700	2300	1.3
4	DMSO	15	80	24	100	44	1500	1900	1.3
5	DMSO	15	80	72	100	50	1500	1800	1.2
6	Neat	15	60	24	100	35	1400	1700	1.2
7	Neat	15	60	72	100	62	2150	3100	1.4
8	DMF	15	60	24	100	73	2700	4300	1.6
9	DMF	15	60	72	100	65	2600	3900	1.5
10	DMF	15	80	72	100	60	1600	1950	1.2

Conditions: bis(propargylic alcohol) **B1** (0.3 g, 1.802 mmol), 1,6-hexanediol (**D1**) (0.213 g, 1.802 mmol), [nBu₄N][OPh]/AgI (10 mol%), [bis(propargylic alcohol)]=1.8 M when a solvent was used. ^a determined by ¹H NMR spectroscopy (**Figure S 8**). ^b determined on crude products by GPC using DMF as eluent with PS standard.

The SEC elugrams obtained on the crude reaction media (to avoid any fractionation of the sample during purification) are presented in **Figure 3**. They show that polymers prepared in DMF were of higher molar mass compared to those produced in DMSO or in the bulk. In the two latter cases, dimers and trimers were clearly observed. Dispersities were rather low for a step-growth polymerisation process but are the result of the low molar mass polymers.

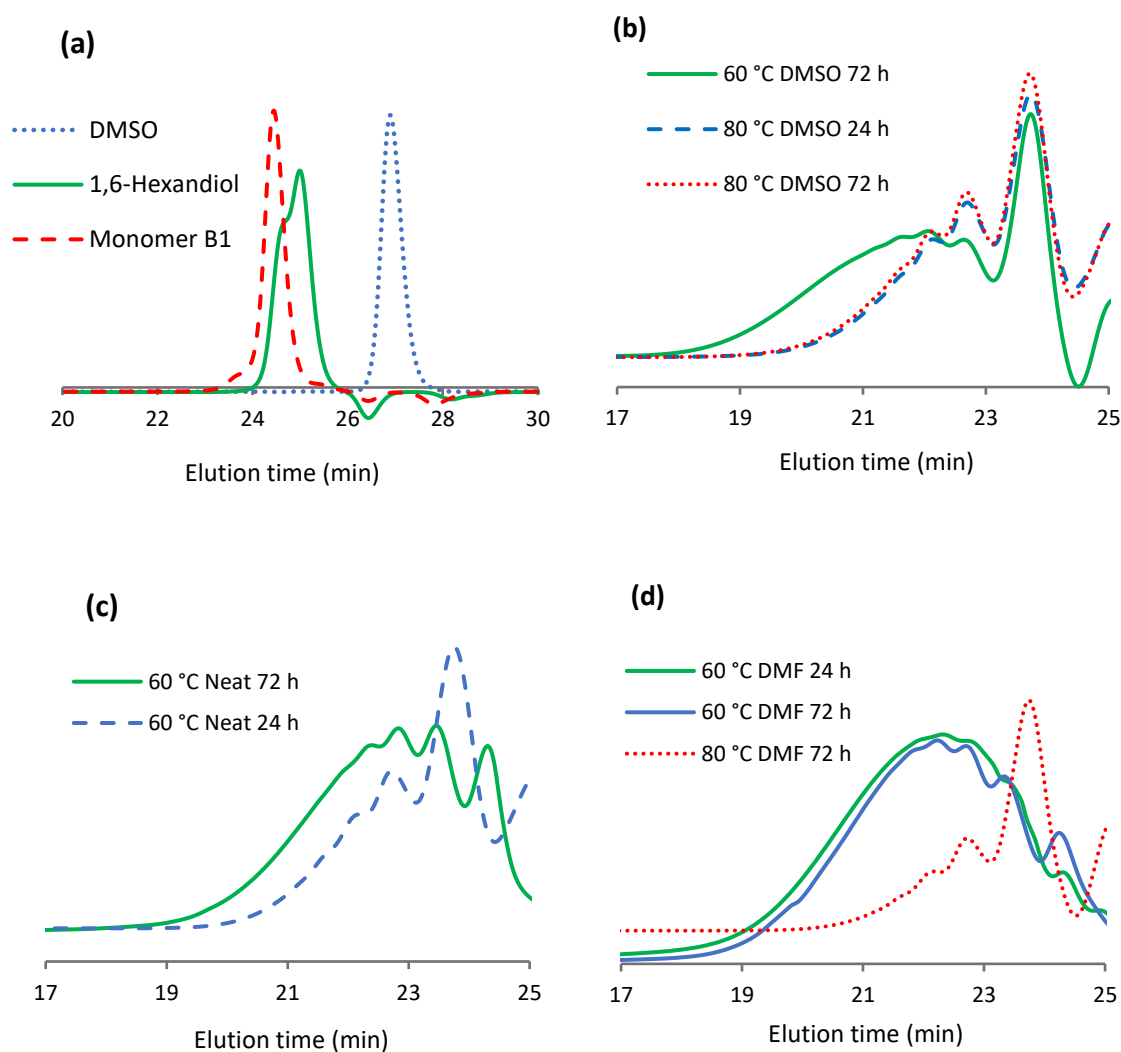


Figure 3. One pot domino synthesis of poly(*oxo-carbonate*)s. Size exclusion chromatography traces of (a) monomers (b) the crude mixtures reported in (**Table 3**, entries 3, 4 and 5), (c) (**Table 3**, entries 6 and 7) and (d) (**Table 3**, entries 8, 9 and 10).

The structure of the poly(*oxo-carbonate*) was evidenced by $^1\text{H-NMR}$ spectroscopy (**Figure 4a**) by the presence of a singlet at $\delta = 2.11$ ppm typical of the methyl group in alpha position of the ketone, at $\delta = 1.44$ ppm characteristic of the methyl group in alpha of the carbonate and at $\delta = 4.06$ ppm characteristic of the methylene linked to the carbonate group. The $^{13}\text{C-NMR}$ (b) analysis of the polymer evidenced the resonance of the ketone at $\delta = 206$ ppm and the

carbonate at $\delta = 153$ ppm. All assignments were further confirmed by HSQC analysis (Figure 4).

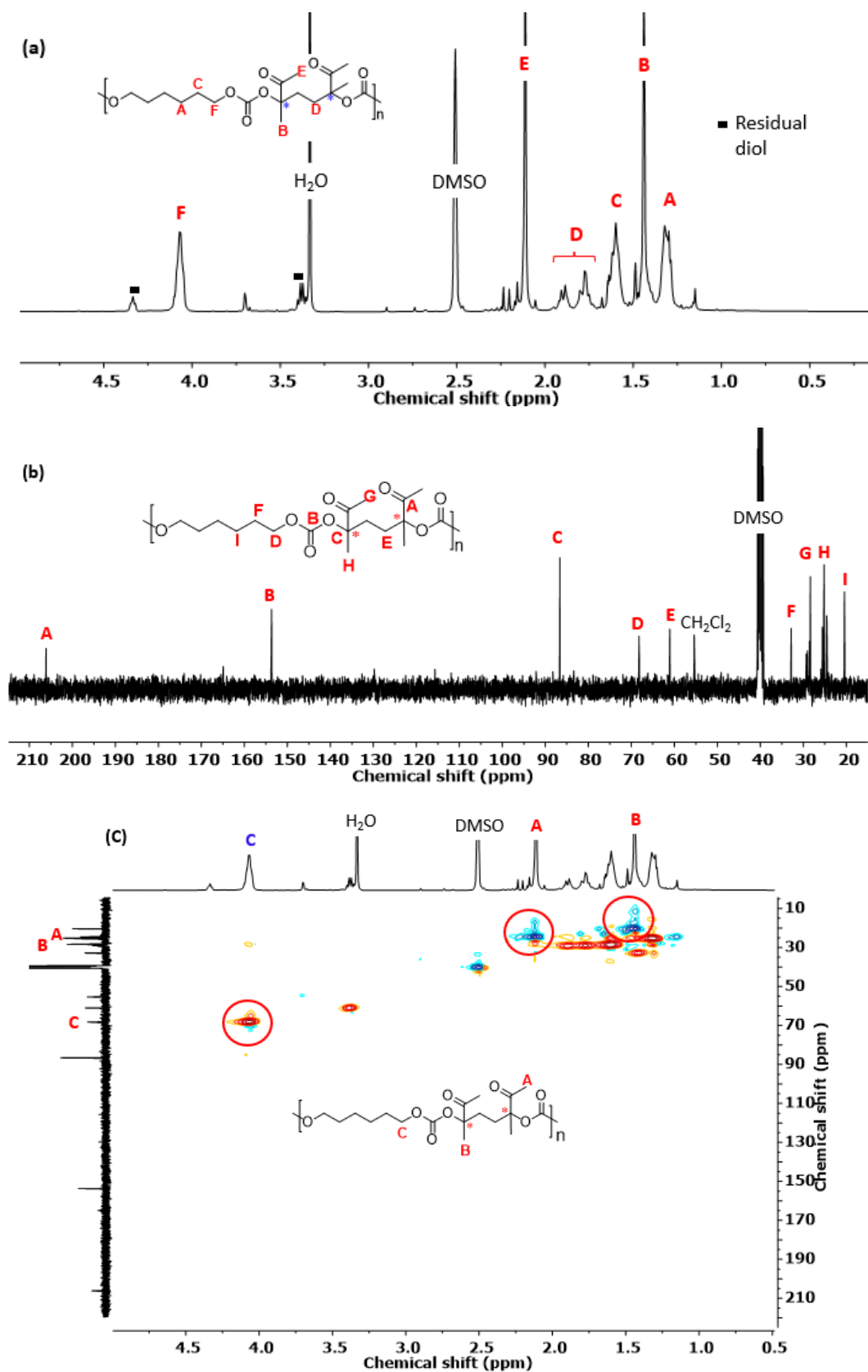
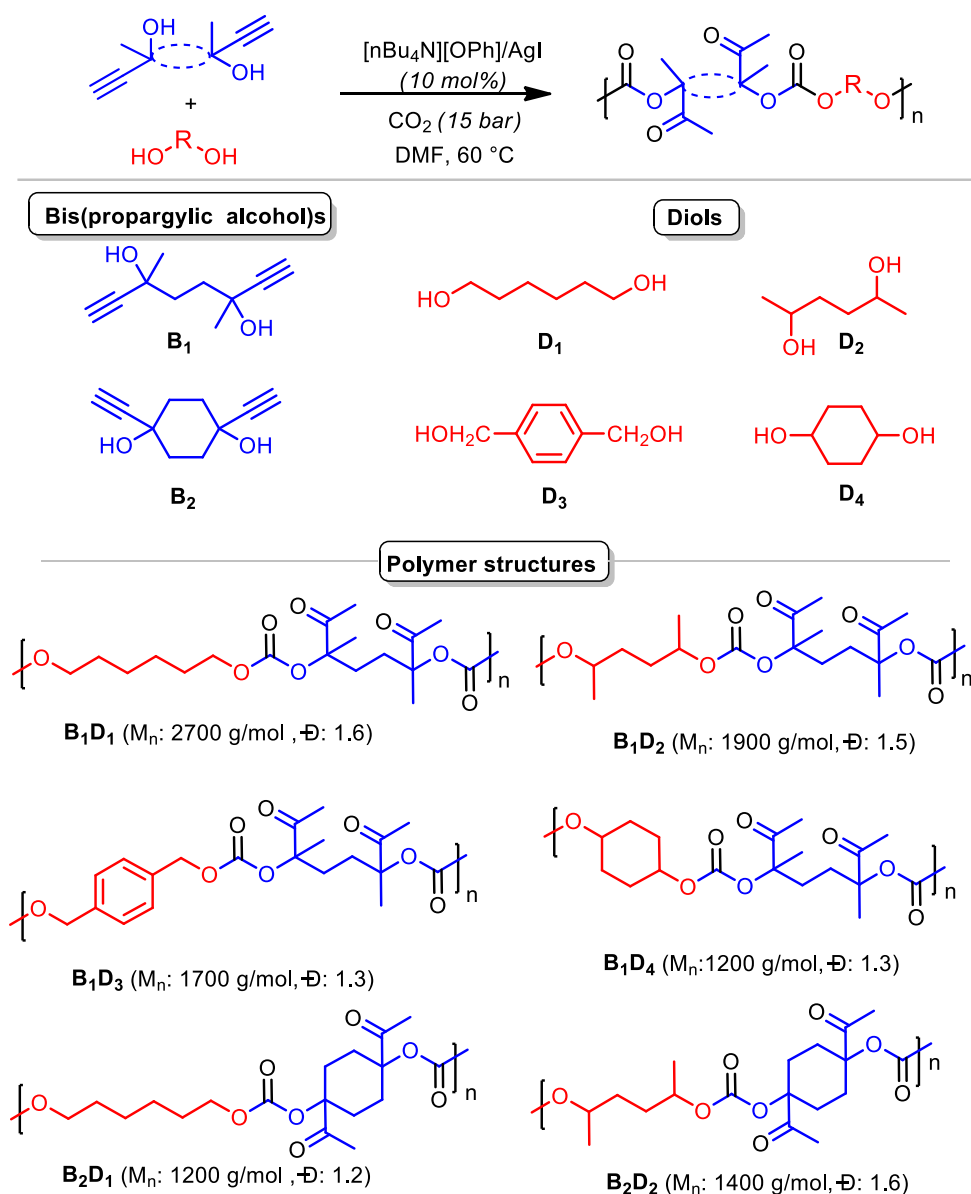


Figure 4(a) $^1\text{H-NMR}$ and **(b)** $^{13}\text{C-NMR}$ spectra and **(c)** HSQC in DMSO-d_6 of purified poly(*oxo*-carbonate) **B1D1**.

The substrate scope was extended by testing other diols (primary **D3** and secondary **D2**, **D4**) and a cycloaliphatic bis(propargylic alcohol) (**B2**) (**Scheme 4**). The corresponding poly(*oxo*-carbonate)s were obtained in all cases, with the structures that were confirmed by $^1\text{H-NMR}$ analyses (**Figure S 9** and **10**).



Scheme 4. One-pot domino synthesis of poly(*oxo*-carbonate)s and reagent scope. M_n and \bar{D} determined by SEC in DMF/LiBr with PS standards on crude products. SEC chromatograms of the crude products are provided in **Figure 5**.

Although the molar masses of the polymers cannot be compared (because they are obtained based on a polystyrene calibration and the polymers are characterised by different hydrodynamic volumes), the highest M_n of 2700 g/mol ($M_w = 4300$ g/mol) was obtained for

B1D1 (Scheme 4). Lower molar masses were collected for polymers prepared from the cycloaliphatic bis(propargylic alcohol) **B2**. As both **B2D1** and **B2D2** copolymers were only partly soluble in DMF at room temperature, and because no common organic solvent could totally dissolve them, fractionation of the samples occurred prior their analyses. Their molar masses determined by size exclusion chromatography were probably underestimated. Due to this lack of solubility, the determination of the degree of polymerisation by $^1\text{H-NMR}$ spectroscopy was not performed.

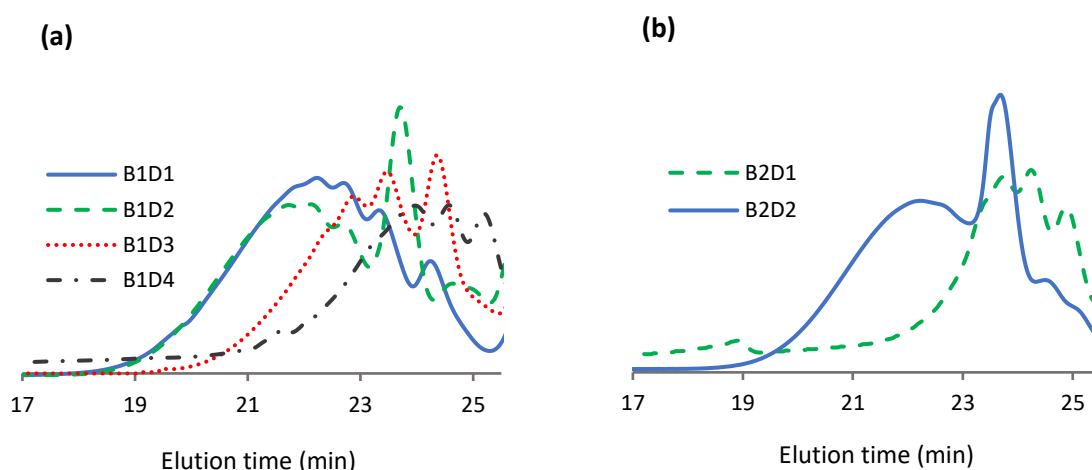
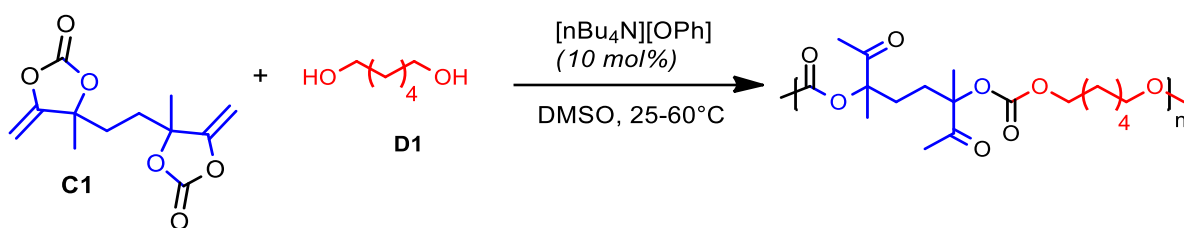


Figure 5. SEC chromatograms (before purification) of poly(oxo-carbonate)s (a) B1D1, B1D2, B1D3 and B1D4, (b) B2D1 and B2D2 synthesised at 60 °C, 15 bar in DMF for 72 h.

Control experiment: synthesis of poly(oxo-carbonate)s by the alcoholysis of bis α CC

To understand the limitations observed with the one-pot cascade process, we studied the alcoholysis of preformed bis α CC (**C1**) by 1,6-hexanediol, under identical conditions to the terpolymerisation reaction ([$n\text{Bu}_4\text{N}$][OPh] as catalyst, 60 °C, DMSO 1.8 M), and for comparison purposes at the ideal temperature of 25 °C.

At 25 °C, after 3 h, we obtained 97% and 86% conversion in the bis α CC and diol respectively (**Table 4**, entry 1) and an $M_n = 5400$ g/mol (**Figure 6**). After 7 h, 100% conversion in the bis α CC is obtained with an $M_n = 4600$ g/mol. It is worth noting that the reaction media was vitrified and no more stirring was possible, which could explain why no further positive evolution of the GPC elugram was observed after 24 h. Slightly diluting the medium should help to reduce the viscosity of the reaction media, thus allowing to attain higher molar masses, however this was not tested. At 60 °C after 3 h, a lower M_n of 1300 g/mol was observed (**Table 4**, entry 4), which is similar to that obtained for the terpolymerisation (**Table 3**, entry 2). Allowing the reaction for a longer period resulted in a further decrease in M_n (**Table 4**, entries 4-6).

Table 4. Synthesis of poly(oxo-carbonate)s by the alcoholysis of bis α CC.

Entry	T (°C)	Time (h)	^a Conv. C1 (%)	^a Conv. D1 (%)	^b M _n (g/mol)	^b M _w (g/mol)	^b Đ
1	25	3	97	86	5400	8600	1.57
2	25	7 ^c	100	85	4600	7600	1.64
3	25	24	100	83	4200	6800	1.60
4	60	3	100	53	1300	1900	1.52
5	60	7	100	52	1200	1700	1.48
6	60	24	100	49	1050	1500	1.40

Conditions: bis α CC **C1** (0.5 g, 1.96 mmol), 1,6-hexanediol (**D1**) (0.23 g, 1.96 mmol), [nBu₄N][OPh] (10 mol%), [bis(propargylic alcohol)]=1.96 M, DMSO as solvent. ^a determined by ¹H NMR spectroscopy. ^b determined on crude products by GPC using DMF as eluent with PS standard. ^c the reaction medium was vitrified.

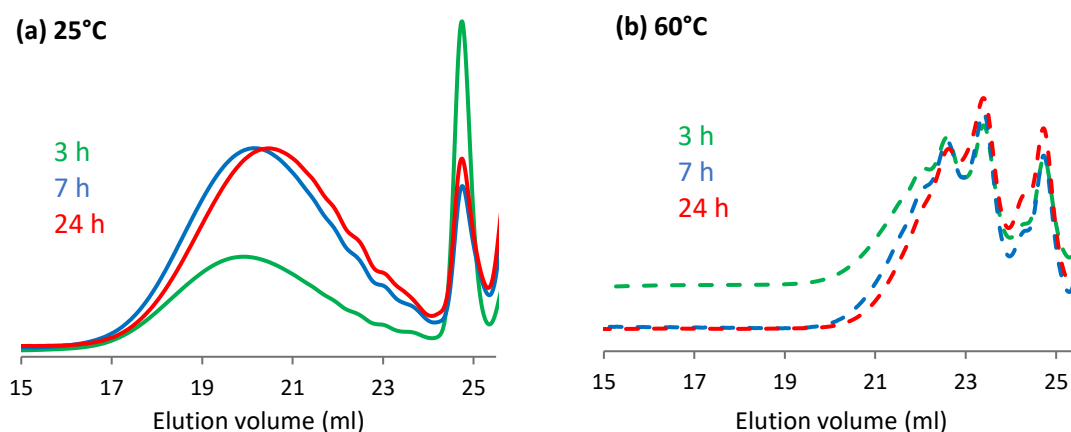
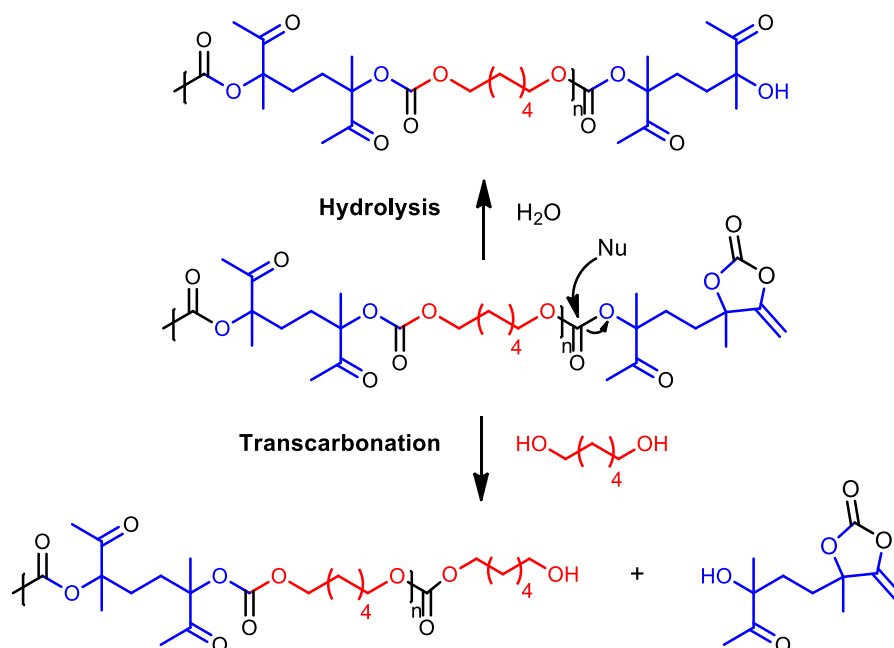


Figure 6. Synthesis of poly(oxo-carbonate)s by the alcoholysis of bis α CC. Size exclusion chromatography traces of the crude mixtures (a) reported in **Table 4** entries 1-3 (b) reported in **Table 4** entries 4-6.

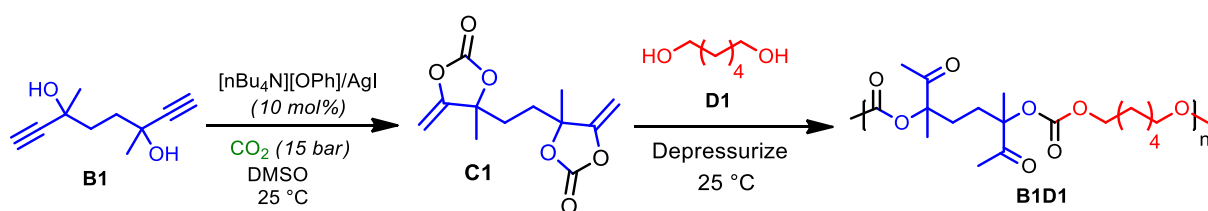
If we look at the conversions, we realise that 100% conversion of the Bis α CC was obtained in contrast to only 53% for the diol at 60 °C, suggesting the occurrence of secondary reactions which consumed Bis α CC. Indeed, ^1H - and ^{13}C -NMR analysis of the crude polymer (**Figure S11**) revealed the characteristic signals of the hydroxy ketone fragment, which has been shown in another study to arise from the hydrolysis of bis α CC and transcarbonation reactions (**Scheme 5**).^[107] These side reactions result in polymer chains with unreactive ends, creating a deviation from the ideal stoichiometry and thus explains the lower masses observed at 60 °C. This study helped to rationalize the lower masses obtained with the cascade approach.



Scheme 5. Secondary reactions observed during the step-growth polymerisation of bis α CC **C1** and 1,6-hexanediol (**D1**) at 60 °C.^[107]

Cascade one-pot two-steps synthesis of poly(oxo-carbonate)s from bispropargylic alcohol and diol

From the above experiments it was clear that the high temperature used for the terpolymerisation was an issue. We also showed that the step-growth polymerisation was slowed down by the carbonation of the primary alcohol. To tentatively solve these issues, we decided to implement the cascade one-pot two-steps process, hence first preparing the Bis α CC and then depressurising the reactor prior to the addition of 1,6-hexanediol. This way, the synthesis of Bis α CC can be carried out under the optimum conditions of 25 °C and 15 bar, while the step-growth polymerisation with the diol can be conducted in the absence of CO_2 , thus avoiding its carbonation **Scheme 6**.



Scheme 6. One-pot two-steps cascade synthesis of poly(oxo-carbonates).

We carried out an initial test, the carboxylative coupling of bispropargylic alcohol **B1** at 25 °C for 7 h, then we depressurised the reactor before adding the diol **D1**. Sampling of the reaction was taken after 24 h and 40 h and analysed by SEC and $^1\text{H-NMR}$, and the results are presented below.

Table 5. Cascade one-pot two-steps synthesis of poly(oxo-carbonate)s from bispropargylic alcohol and diol.

Entry	Time (h)	^a Conv. C1 (%)	^a Conv. D1 (%)	^b M _n (g/mol)	^b M _w (g/mol)	^b Đ
1	24	>99	42	2230	3460	1.54
2	40	100	38	2240	3530	1.57
3 ^c	24	100	61	1500	1900	1.3

Conditions: bis(propargylic alcohol) **B1** (0.3 g, 1.802 mmol), 1,6-hexanediol (**D1**) (0.213 g, 1.802 mmol), $[n\text{Bu}_4\text{N}][\text{OPh}]/\text{AgI}$ (10 mol%), $[\text{bis(propargylic alcohol)}]=1.8$ M, DMSO as solvent. ^a determined by $^1\text{H-NMR}$ spectroscopy. ^b determined on crude products by GPC using DMF as eluent with PS standard. ^c Results of the terpolymerisation under identical conditions presented in **Table 3**, entry 2.

After 24 h of polymerisation, we observed a M_n of 2230 g/mol (**Table 5**, entry 1) which is a slight amelioration from that obtained with the terpolymerisation approach (**Table 5**, entry 3). Allowing the reaction for a longer time did not lead to any further increase in M_n. It is important to note that a sample of the reaction medium analysed before the addition of the diol **D1** revealed a 90% yield for bis α CC and the presence of some hydrolysis products. Moreover, some drops of the reaction medium were lost during the depressurisation process, thus causing a deviation from the stoichiometry. At this stage we did not try to further optimise the reaction.

3. Conclusions

In this work, we have disclosed a domino approach to prepare *oxo*-alkylcarbonate scaffolds and poly(*oxo*-carbonate)s from CO₂, propargylic alcohols, and mono-alcohols under moderate operating conditions (PCO₂ = 1-15 bar, T = 40-80 °C). The keystone lied in the utilisation of a binary catalyst composed of tetrabutylammonium phenolate that operated in synergy with a Ag(I) salt. Remarkably, this dual catalyst (at 5 mol% loading) enabled to drive the fast, selective and quantitative formation of exovinylene cyclic carbonates by carboxylative coupling of CO₂ to various propargylic alcohols, and it also catalysed the alcoholysis of the *in-situ* generated 5-membered cyclic carbonates, providing an efficient platform for the preparation of *oxo*-alkylcarbonates in high yield. Unfortunately, using tetrabutylammonium phenolate/Cu(I) did not allow to obtain the alcoholysis of the alkylidene cyclic carbonate. Operando FT-IR spectroscopy provided kinetic insights that helped us to optimise the one-pot process. When this catalytic system was used on mixtures of CO₂, bis(propargylic alcohol)s and diols, poly(*oxo*-carbonate)s oligomers with M_n ranging from 1200-2700 g/mol were produced by a new domino polymerisation process under moderate conditions (60 °C, 15 bar). By varying the nature of the bis(propargylic alcohol) and the diol, various poly(*oxo*-carbonate)s oligomers were successfully prepared, enlarging the scope of the process. Ongoing work focuses on the optimisation of the one-pot cascade approach to access higher molar masses.

4. Experimental section

4.1. Materials

Ethynylmagnesium bromide (Acros), silver iodide, copper iodide, zinc iodide, 2,5-hexandione, 1,4-cyclohexandione, 2-methyl-3-butyn-2-ol, 3-methyl-1-pentyn-3-ol, 3,5-dimethyl-1-hexyn-3-ol were purchased from Aldrich. CO₂ (N27) was purchased from Air liquid, dimethyl sulfoxide (DMSO), dimethyl formamide (DMF), acetonitrile (ACN), methanol (MeOH), diethylether. DMSO was dried on a 3 Å molecular sieve conditioned at 100 °C under vacuum for 24h. All the other reagents were used as received without any further purification. DMSO-*d*₆ was purchased from Eurisotop.

4,4'-(ethane-1,2-diyl)bis(4-methyl-5-methylene-1,3-dioxolan-2-one) was prepared following the procedure described in chapter 3.

4.2. Analytical methods

¹H NMR analyses were performed on Bruker Avance 400 MHz spectrometers in DMSO at 25 °C in the Fourier transform mode. 16 scans for ¹H spectra and 512 or 2048 scans for ¹³C spectra were recorded.

Fourier transform infrared spectra were recorded using a Nicolet IS5 spectrometer (Thermo Fisher Scientific) equipped with a transmission or with a diamond attenuated transmission reflectance (ATR) device. Spectra were obtained in transmission or ATR mode as a result of 32 spectra accumulation in the range of 4000 – 500 cm⁻¹, with a nominal resolution of 4 cm⁻¹.

Number-average molecular weight (*M*_n) and dispersity (*Đ*) of the different polymers were determined by size exclusion chromatography (SEC) in dimethylformamide (DMF) containing LiBr (0.025 M) at 55 °C (flow rate: 1 mL/min) with a Waters chromatograph equipped with two columns dedicated to the analysis of low molar mass polymers (PSS gram analytical 100 Å, separation range 300-60000 Da) and a pre column (100 Å), a dual λ absorbance detector (Waters 2487) and a refractive index detector (Waters 2414). A previously established PS calibration curve was used.

In-situ IR spectroscopy experiments were conducted using a stainless-steel reactor suitable for high-pressure measurements (up to 400 bar) and high temperature (up to 100 °C) coupled with a FT-MIR spectrometer from Bruker, equipped with an air-cooled globar source (12 V), a KBr beam splitter, a mechanical rocksolid interferometer, permanently aligned, a diamond ATR fibre probe IN350-T (Ø 6 mm) and a liquid nitrogen cooled mercury cadmium telluride (MCT). Single beam spectra recorded in the spectral range (670-3500 cm⁻¹) with a 4 cm⁻¹ resolution were obtained after the Fourier transformation of 32 accumulated interferograms until the end of reaction time.

4.3. Experimental procedures

General procedure for the synthesis of butyl-(2-methyl-3-oxobutan-2-yl) carbonate by alcoholysis of α CC 2.

In a clean dry glass reaction tube, equipped with a magnetic rod and a three-way stopcock were introduced; 4,4-dimethyl-5-methylene-1,3-dioxolan-2-one (0.5 g, 3.904 mmol), butanol (0.357 ml, 3.904 mmol), tetrabutylammonium phenolate [nBu₄N][OPh] (0.0664 g, 0.1952 mmol) and DMSO (1 ml). The reaction tube was placed in a silicon oil bath set at 25 °C. The reaction mixture was sampled after 15 min, 1 h, 2 h and 24 h, and characterised by ¹H NMR spectroscopy in DMSO-d₆.

General procedure for the domino synthesis of butyl-(2-methyl-3-oxobutan-2-yl) carbonate from 2-methyl-3-butyn-2-ol, CO₂ and alcohol.

In a stainless-steel reactor of 12 mL equipped with a magnetic bar, a manometer and a gas inlet/outlet were introduced 3-methyl-2-butyn-3-ol (2 mL, 20.61 mmol), tetrabutylammonium phenolate [nBu₄N][OPh] (0.3459 g, 1.031 mmol), AgI (0.2419 g, 1.031 mmol) and 1-butanol (1.88 mL, 20.55 mmol). The reactor was closed and placed in a silicon oil bath set at 60 °C. After 30 min, CO₂ was added at a constant pressure of 15 bar. The reaction ran for 6 h after which the reactor was slowly depressurised and placed in a water bath to cool it down to room temperature. The crude reaction mixture was characterised by ¹H-NMR spectroscopy in DMSO-d₆. Then the catalyst was removed by silica gel chromatography with CH₂Cl₂, and the product dried under vacuum at room temperature for 24 h.

Monitoring of the synthesis of butyl-(2-methyl-3-oxobutan-2-yl) carbonate by on-line FT-IR.

In a clean dry reactor of 80 mL equipped with a manometer, a heating mantle, gas inlet/outlets, a mechanical stirrer and a high-pressure FT-IR probe were introduced 3-methyl-2-butyn-3-ol (12 mL, 123.6 mmol), 1-butanol (11.3 mL, 123.6 mmol), [nBu₄N][OPh] (2.0749 g, 6.182 mmol), AgI (6.182 mmol) and dried DMSO (12 mL). The reactor was closed and heated to the desired temperature after which the FT-IR acquisition was launched and recorded every 5 min. Then CO₂ gas was added at constant flow. Once the reaction was complete, the reactor was cooled down to room temperature and depressurised. The crude mixture was recovered and characterised by ¹H-NMR spectroscopy in DMSO-d₆.

Butyl-(2-methyl-3-oxobutan-2-yl) carbonate (product 3A). ¹H NMR (400 MHz, DMSO-d₆) δ (in ppm) = 4.08 (t, J = 6.6 Hz, 2H), 2.12 (s, 3H), 1.62 – 1.52 (m, 2H), 1.43 (s, 6H), 1.42 – 1.28 (m, 2H), 0.89 (t, J = 7.4 Hz, 3H). ¹³C NMR (100.6 MHz, DMSO-d₆) δ (in ppm) = 206.50 (C=O), 153.92 (OC=OO), 85.11, 67.90, 40.90, 30.55, 24.13, 23.33, 18.83, 13.92.

These NMR data are in agreement with those reported in the scientific literature.^[210] The FT-IR-spectrum of the molecule is provided in the supporting information section (**Figure S4**)

Benzyl-(2-methyl-3-oxobutan-2-yl) carbonate (Product 3B). ¹H NMR (400 MHz, DMSO-d₆) δ (in ppm) = 7.39 (s, 4H), 7.45 – 7.32 (m, 1H), 5.15 (s, 2H), 2.10 (s, 3H), 1.45 (s, 6H). ¹³C NMR

(100.6 MHz, DMSO- d_6) δ 206.43 (C=O), 153.77 (OC=OO), 135.78, 128.97, 128.89, 128.60, 85.50, 69.55, 24.18, 23.34.

These NMR data are in agreement with those reported in the scientific literature.^[109] The FT-IR-spectrum of the molecule is provided in the supporting information section (**Figure S4**)

Isopropyl-(2-methyl-3-oxobutan-2-yl) carbonate (Product 3C). ^1H NMR (400 MHz, DMSO- d_6) δ (in ppm) = 4.74 (p, J = 6.2 Hz, 1H), 2.11 (s, 3H), 1.43 (s, 6H), 1.23 (d, J = 6.2 Hz, 6H). ^{13}C NMR (100.6 MHz, DMSO- d_6) δ (in ppm) = 206.57 (C=O), 153.32 (OC=OO), 84.95, 72.30, 24.08, 23.34, 21.86

These NMR data are in agreement with those reported in the scientific literature.^[210] The FT-IR spectrum of the molecule is provided in the supporting information section (**Figure S5**)

2-methyl-3-oxobutan-2-yl tert-pentyl carbonate (Product 3D). ^1H NMR (400 MHz, DMSO- d_6) δ (in ppm) = 2.10 (s, 3H), 1.75 (q, J = 7.5 Hz, 2H), 1.40 (s, 6H), 1.37 (s, 6H), 0.84 (dt, J = 9.3, 7.5 Hz, 3H). ^{13}C NMR (100.6 MHz, DMSO- d_6) δ (in ppm) = 206.24 (C=O), 152.19 (OC=OO), 84.91, 84.35, 36.29, 25.38, 23.71, 23.16, 8.21

Butyl-(3-methyl-2-oxopentan-3-yl) carbonate (Product 3E). ^1H NMR (400 MHz, DMSO- d_6) δ (in ppm) = 4.08 (tt, J = 6.9, 3.4 Hz, 2H), 2.10 (s, 3H), 1.87 (dq, J = 15.0, 7.5 Hz, 1H), 1.72 (dq, J = 14.7, 7.5 Hz, 1H), 1.57 (h, J = 6.3, 5.8 Hz, 2H), 1.43 (s, 3H), 1.34 (h, J = 7.3 Hz, 2H), 0.90 (t, J = 7.4 Hz, 3H), 0.81 (t, J = 7.5 Hz, 3H). ^{13}C NMR (100.6 MHz, DMSO- d_6) δ (in ppm) = 206.43 (C=O), 153.77 (OC=OO), 87.94, 68.46, 30.86, 28.89, 24.32, 19.68, 18.70, 14.06, 7.45

IR-spectra of the molecule is provided in the supporting information (**Figure S 6**)

Butyl (3,5-dimethyl-2-oxohexan-3-yl) carbonate (Product 3F). ^1H NMR (400 MHz, DMSO- d_6) δ (in ppm) = 4.08 (td, J = 6.6, 3.1 Hz, 2H), 2.11 (s, 3H), 1.71 (dd, J = 13.2, 6.9 Hz, 2H), 1.58 (dd, J = 8.3, 6.3 Hz, 2H), 1.48 (s, 3H), 1.33 (q, J = 7.5 Hz, 3H), 0.90 (dt, J = 8.0, 4.4 Hz, 9H). ^{13}C NMR (100.6 MHz, DMSO- d_6) δ (in ppm) = 206.24 (C=O), 153.77 (OC=OO), 87.58, 67.83, 44.07, 30.54, 24.60, 23.85, 23.78, 20.79, 18.80, 13.92

IR-spectra of the molecule is provided in the supporting information (**Figure S 7**)

General procedure for the synthesis of poly(b-oxocarbonate)s by the alcoholysis of bis α CC.

In a clean dry reaction tube equipped with a magnetic rod and a threeway stopcock were introduced 4'-(ethane-1,2-diyl)bis(4-methyl-5-methylene-1,3-dioxolan-2-one) **C1** (0.5g, 1.96 mmol), 1,6-hexandiol **D1** (0.2320 g, 1.96 mmol), tetrabutylammonium phenolate (65.8 mg, 0.196 mmol) and DMSO (1 mL). The reaction tube was placed in a silicon oil bath set at 25 °C. Sampling of the reaction was done after 3 h and 24 h, characterised by ^1H - and ^{13}C -NMR in DMSO- d_6 to determine the conversion and by SEC to evaluate the molecular parameters of the polymer.

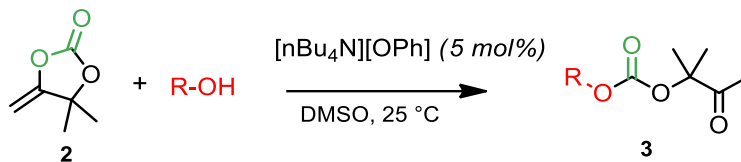
General procedure for the domino synthesis of poly(b-oxocarbonate)s by terpolymerisation.

In a stainless-steel reactor of 12 mL equipped with a magnetic bar, a manometer and a gas inlet/outlet were introduced 3,6-dimethylocta-1,7-diyne-3,6-diol **B1** (0.3 g, 1.802 mmol) prepared following Gennen's protocol^[18], 1,6-hexandiol **D1** (0.2130 g, 1.802 mmol), tetrabutylammonium phenolate (60.5 mg, 0.1802 mmol), AgI (42.3 mg, 0.1802 mmol) and DMF (1 mL). The reactor was closed and placed in a silicon oil bath set at the desired temperature. After 30 min, CO₂ was added at a constant pressure of 15 bar. The reaction ran for 24 h, after which the reactor was depressurised and placed in a water bath to cool it down to room temperature. A sample of the reaction mixture was characterised by ¹H- and ¹³C-NMR in DMSO-d₆ to determine the conversion and by SEC to evaluate the molecular parameters of the polymer. Then the catalyst was removed by silica gel chromatography with CH₂Cl₂. The solvent was evaporated, and the sample washed 4 times with a mixture of water and CH₂Cl₂ (5:1) to eliminate DMF. The organic phase was collected, and CH₂Cl₂ removed under vacuum at room temperature.

For the two-step approach, a similar procedure was followed, however the reactor was depressurised after 7 h, before adding 1,6-hexandiol **D1**.

5. Supplementary informations

SI- 1. Determination of the conversion for the alcoholysis of 4,4-dimethyl-5-methylene-1,3-dioxolan-2-one (α CC)



The α CC conversion was estimated by comparison of the relative intensities of the peaks associated to olefinic protons at 4.64 and 4.79 ppm of α CC and the peak of the methyl group in α -position of the ketone at 2.11 ppm according to the equation:

$$\text{Conversion \%} = \left(\frac{(I_{4.64} + I_{4.79})/2}{((I_{4.64} + I_{4.79})/2) + I_{2.11}/3} \right) \times 100$$

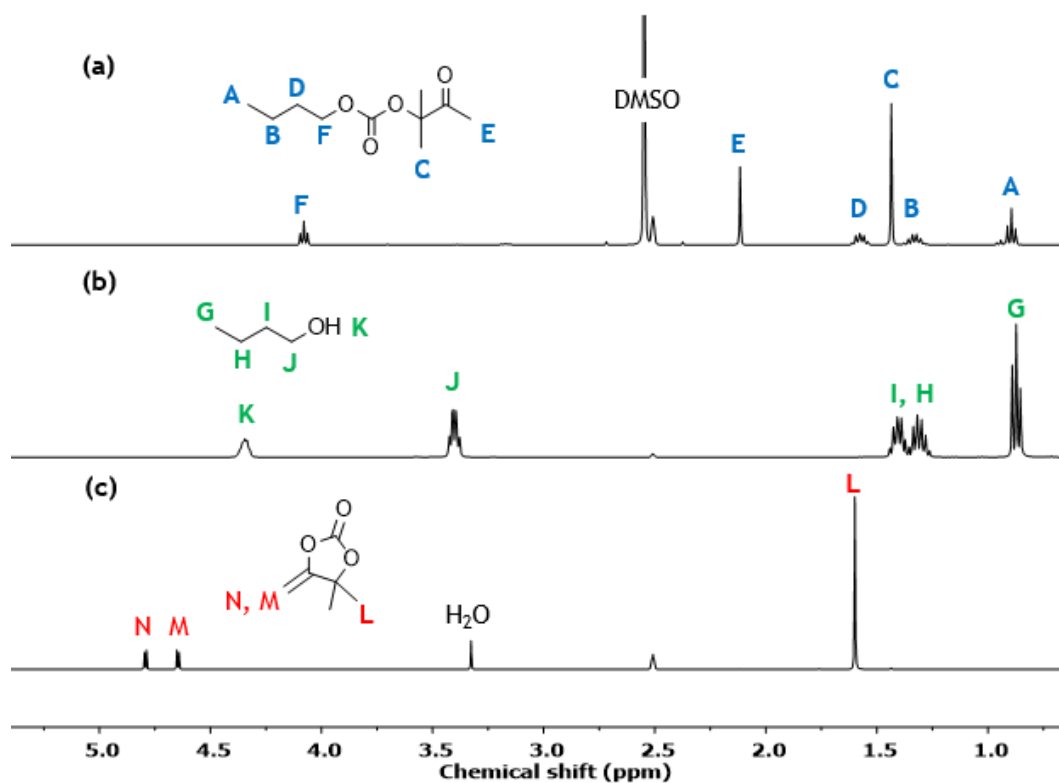
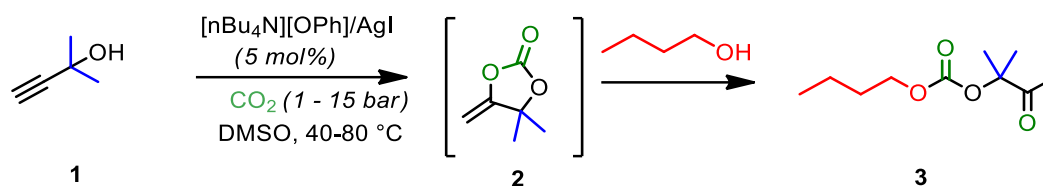


Figure S 1. $^1\text{H-NMR}$ spectra in $\text{DMSO-}d_6$ of (a) the reaction mixture after 1 h at 25 °C, (b) 1-butanol and (c) α CC.

SI- 2. Determination of the conversion for the one-pot cascade reaction of 2-methyl-2-butyn-3-ol, CO₂ and 1-butanol.


The propargylic conversion was estimated by comparison of the relative intensities of the peaks associated to the methyl group in alpha of the ketone at 2.11 ppm of the oxo-alkylcarbonate, and the peak of the methyl groups of the alkynol at 1.35 ppm according to the equation:

$$\text{Conversion \%} = \left(1 - \left(\frac{\frac{I_{1.36}}{6}}{(I_{2.11})/3 + I_{1.36}/6 + I_{1.16}/6} \right) \right) \times 100$$

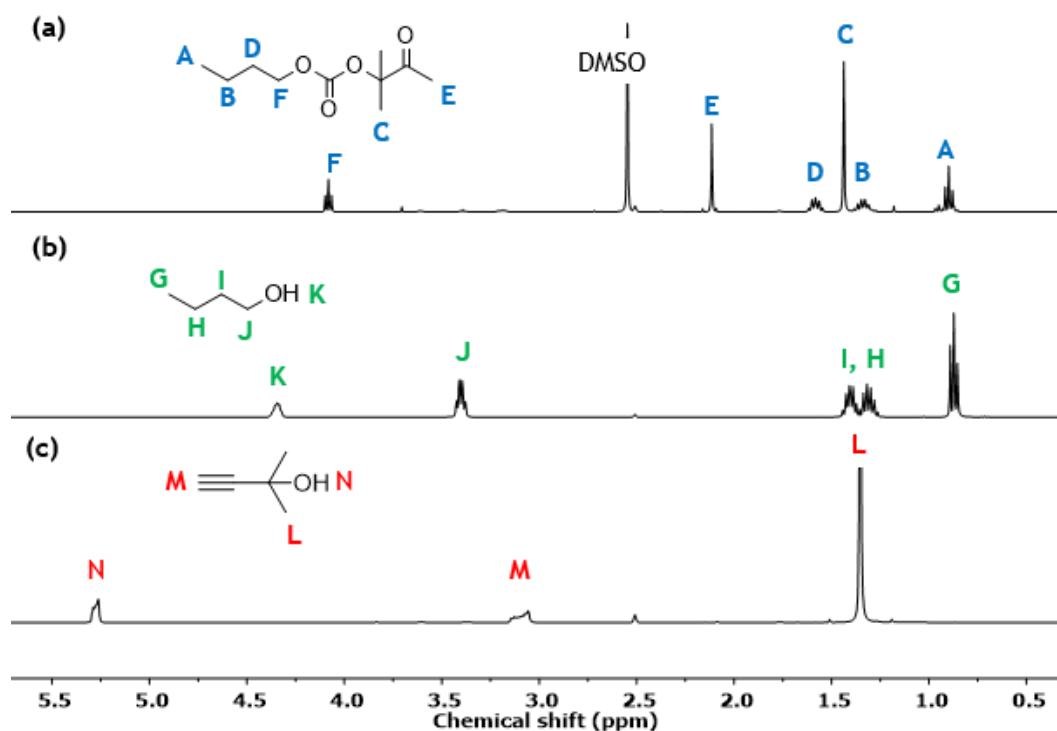


Figure S 2. ¹H-NMR spectra in DMSO-*d*₆ of (a) the reaction mixture at 60 °C after 10 h, (b) 1-butanol and (c) 2-methyl-3-butyn-2-ol.

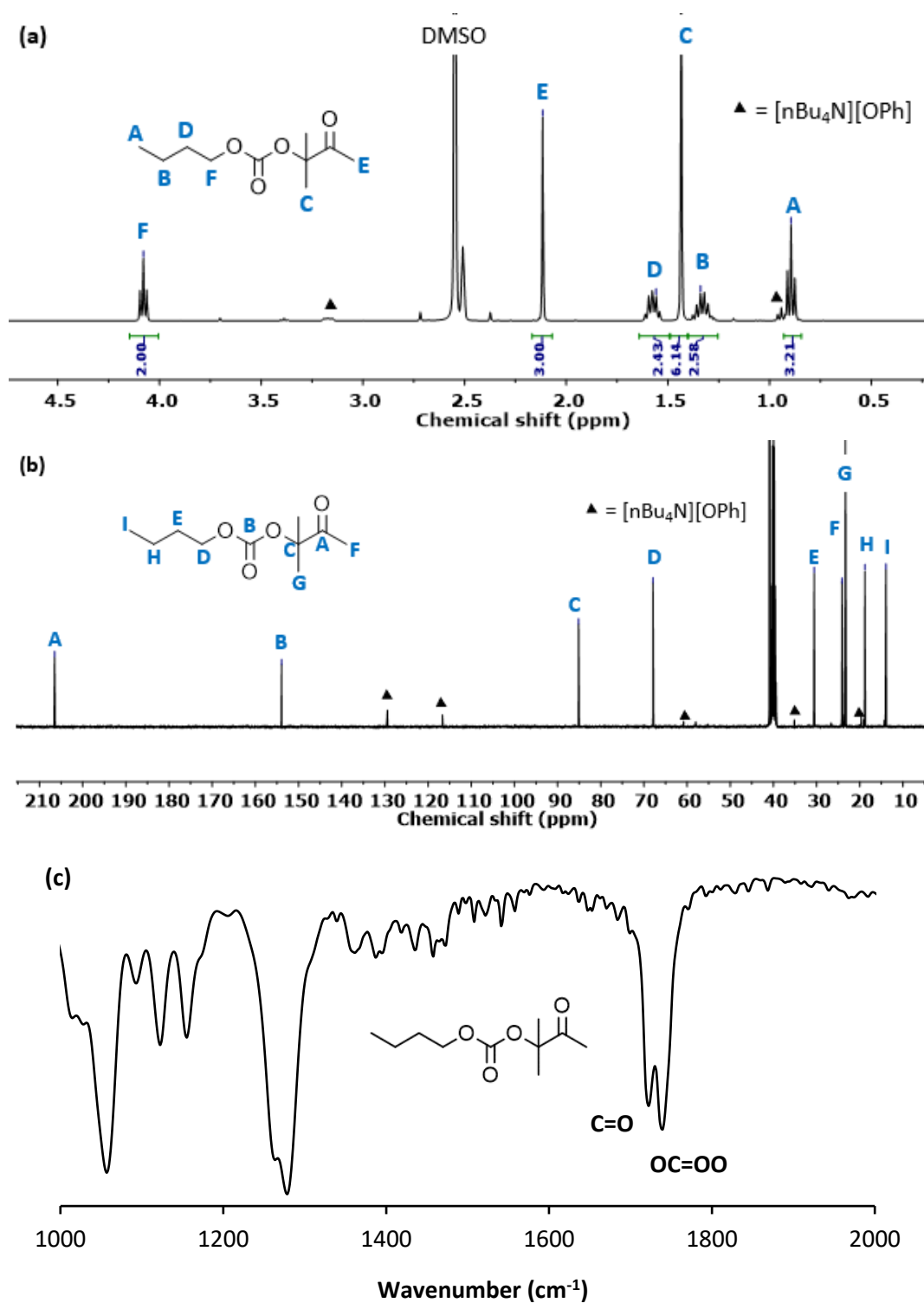
SI- 3. ^1H -, ^{13}C -NMR and IR spectra of oxo-alkylcarbonates

Figure S 3. (a) ^1H -NMR, (b) ^{13}C -NMR spectrum and (c) IR spectrum of butyl (2-methyl-3-oxobutan-2-yl) carbonate in $\text{DMSO}-d_6$. Characterisation in accordance with the literature (J. Hu, J. Ma, Lu Lu, Q. Qian, Z. Zhang, C. Xie, and B. Han, *chemsuschem* 2017, 10, 1292).

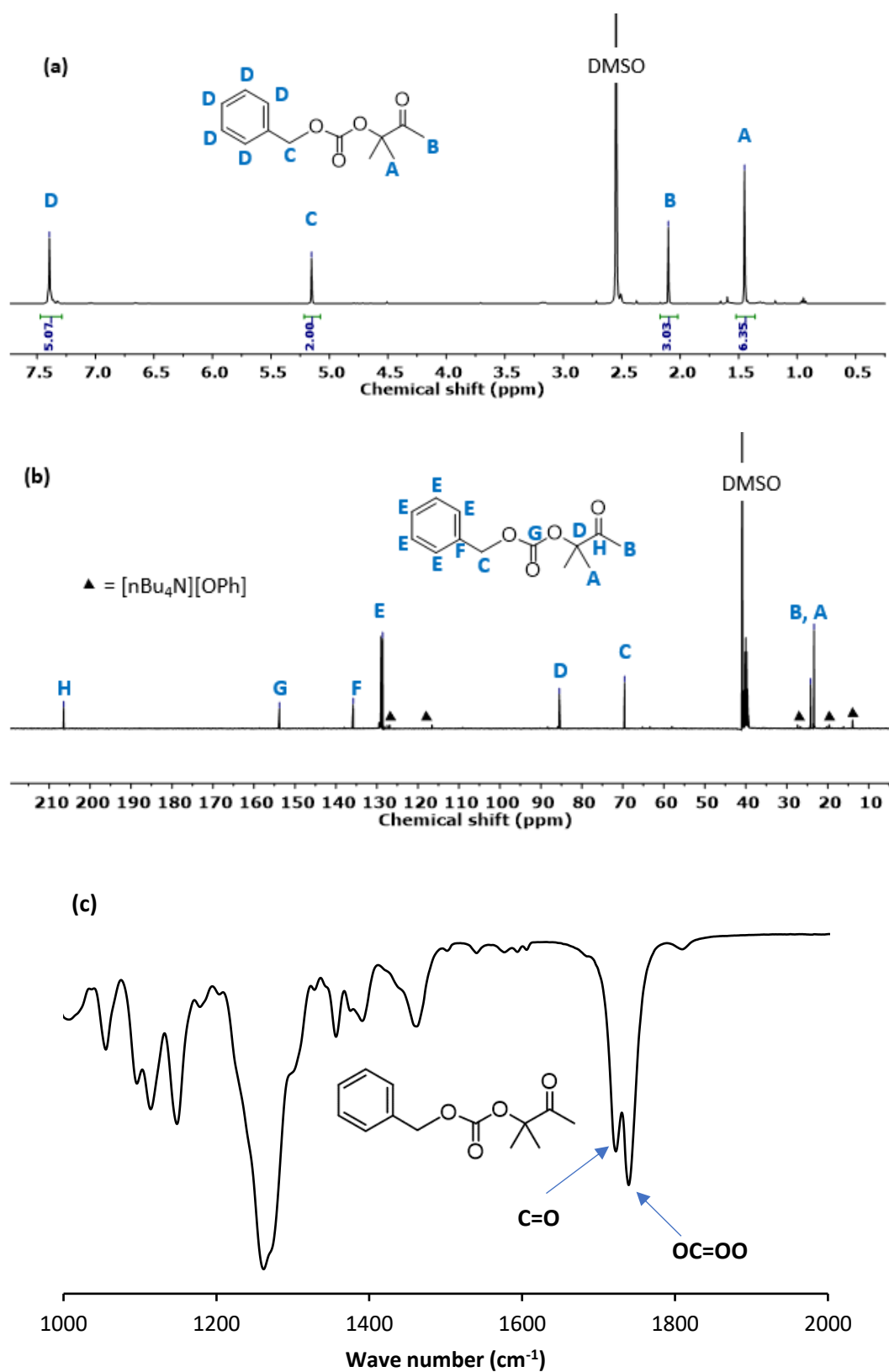


Figure S 4. (a) ¹H-NMR, (b) ¹³C-NMR spectrum in DMSO-d₆ and (c) IR spectrum of benzyl (2-methyl-3-oxobutan-2-yl) carbonate. Characterisation in accordance with the literature (Zhou, Z. H.; Song, Q. W.; Xie, J. N.; Ma, R.; He, L. N. *Chem. Asian J.* 2016, 11, 2065).

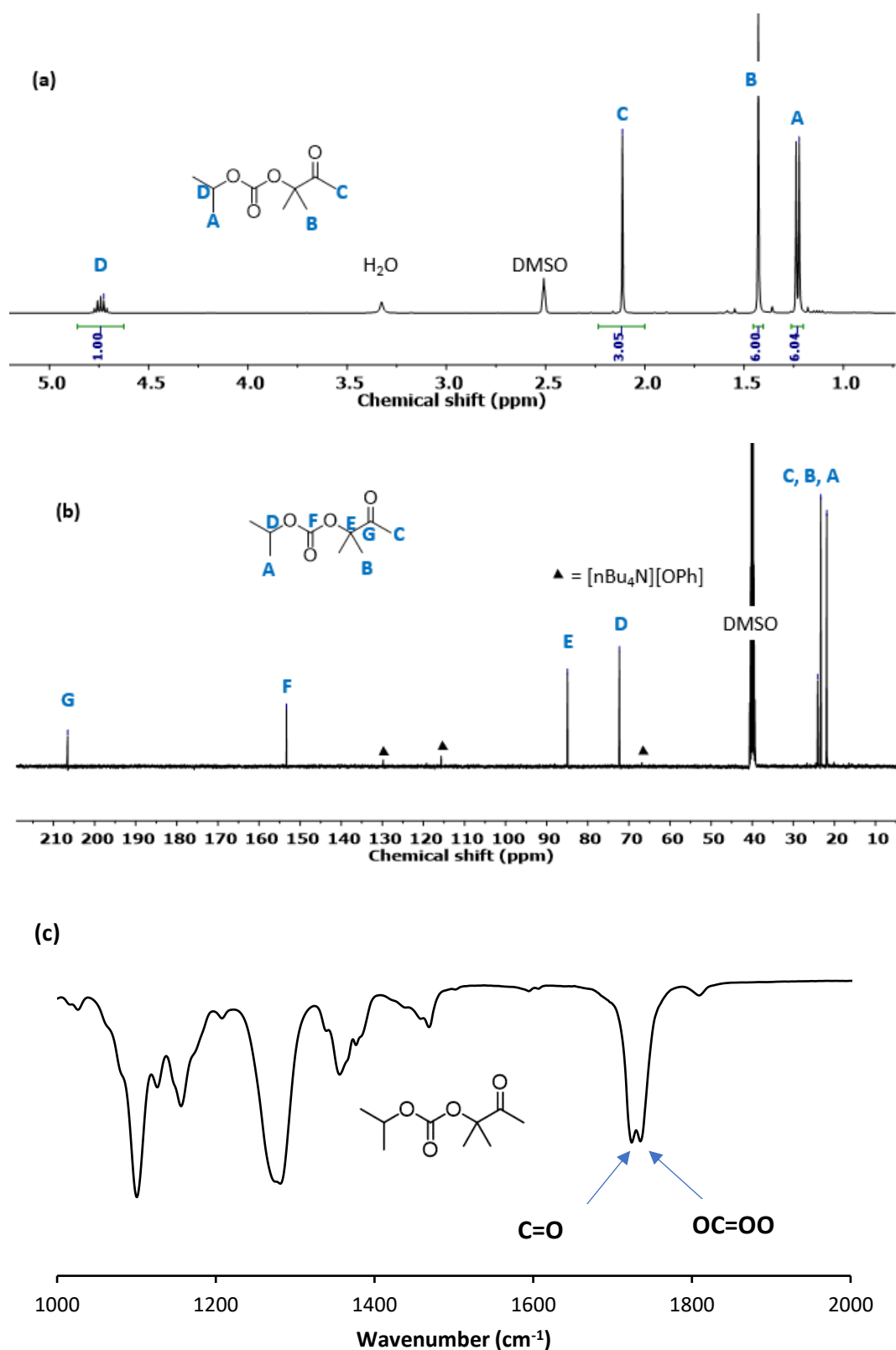


Figure S 5. (a) ¹H-NMR, (b) ¹³C-NMR spectrum in DMSO-d₆ and (c) IR spectrum of isopropyl (2-methyl-3-oxobutan-2-yl) carbonate. Characterisation in accordance with the literature (J. Hu, J. Ma, Lu Lu, Q. Qian, Z. Zhang, C. Xie, and B. Han, *chemsuschem* 2017, 10, 1292).

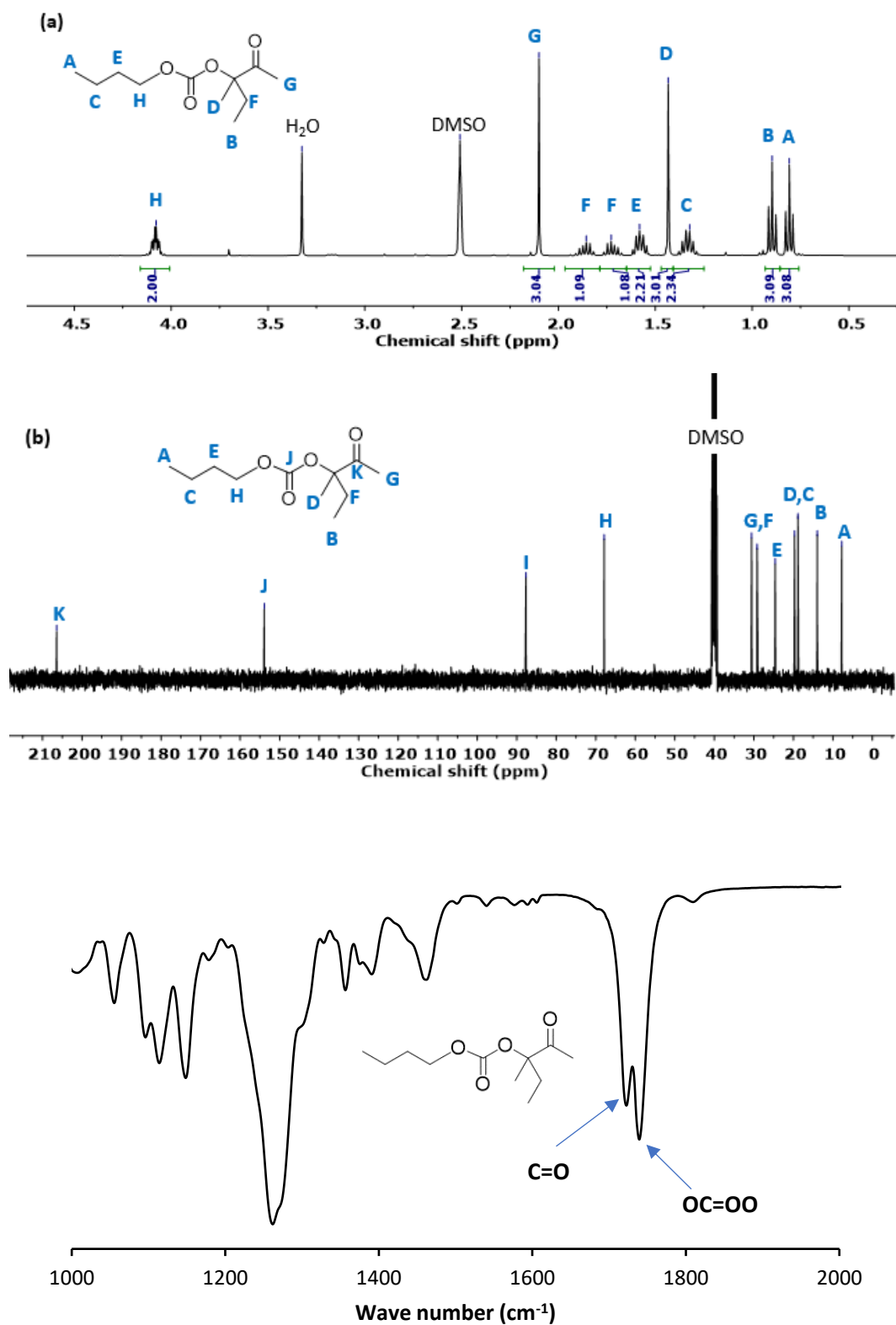


Figure S 6. (a) ^1H -NMR, (b) ^{13}C -NMR spectrum in DMSO-d_6 and (c) IR spectrum of butyl (3-methyl-2-oxopentan-3-yl) carbonate.

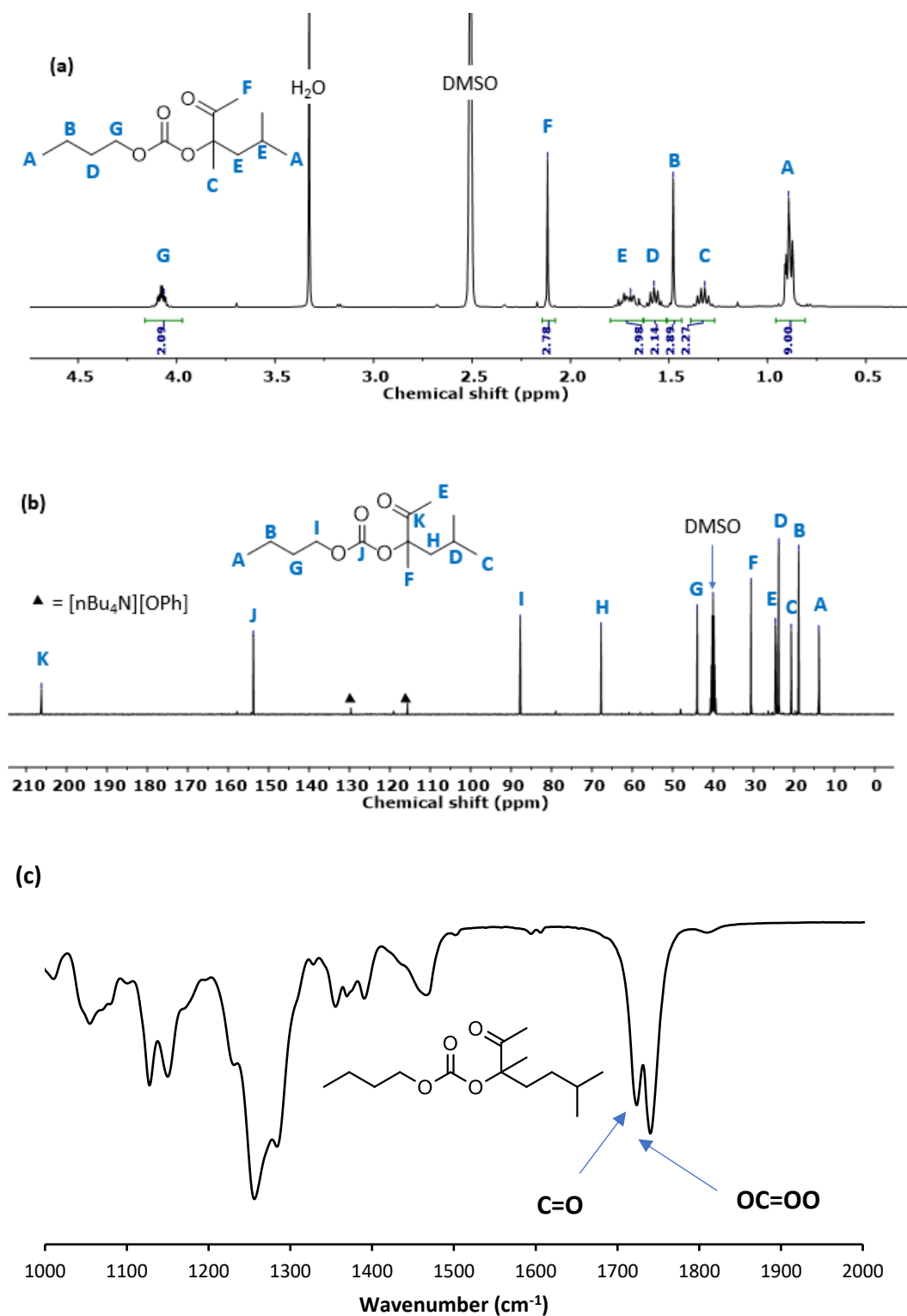


Figure S 7. (a) $^1\text{H-NMR}$, (b) $^{13}\text{C-NMR}$ spectrum in DMSO-d_6 and (c) IR spectrum of butyl (3,5-dimethyl-2-oxohexan-3-yl) carbonate.

SI- 4. Determination of the conversion of diol for the terpolymerisation

The conversion of the 1,6-hexandiol was determined by using the following equation:

$$\text{Conversion D1 \%} = \left(\frac{I_{3.38}}{(I_{4.06} + I_{4.06})} \right) \times 100$$

where $I_{3.38}$ corresponds to the intensity of the peak at 3.38 ppm (C) characteristic of the methylene linked to the OH function in 1,6-Hexandiol and $I_{4.06}$ the intensity of peak at 4.06 ppm (F) characteristic of the methylene linked to the carbonate function of the poly(oxo-carbonate).

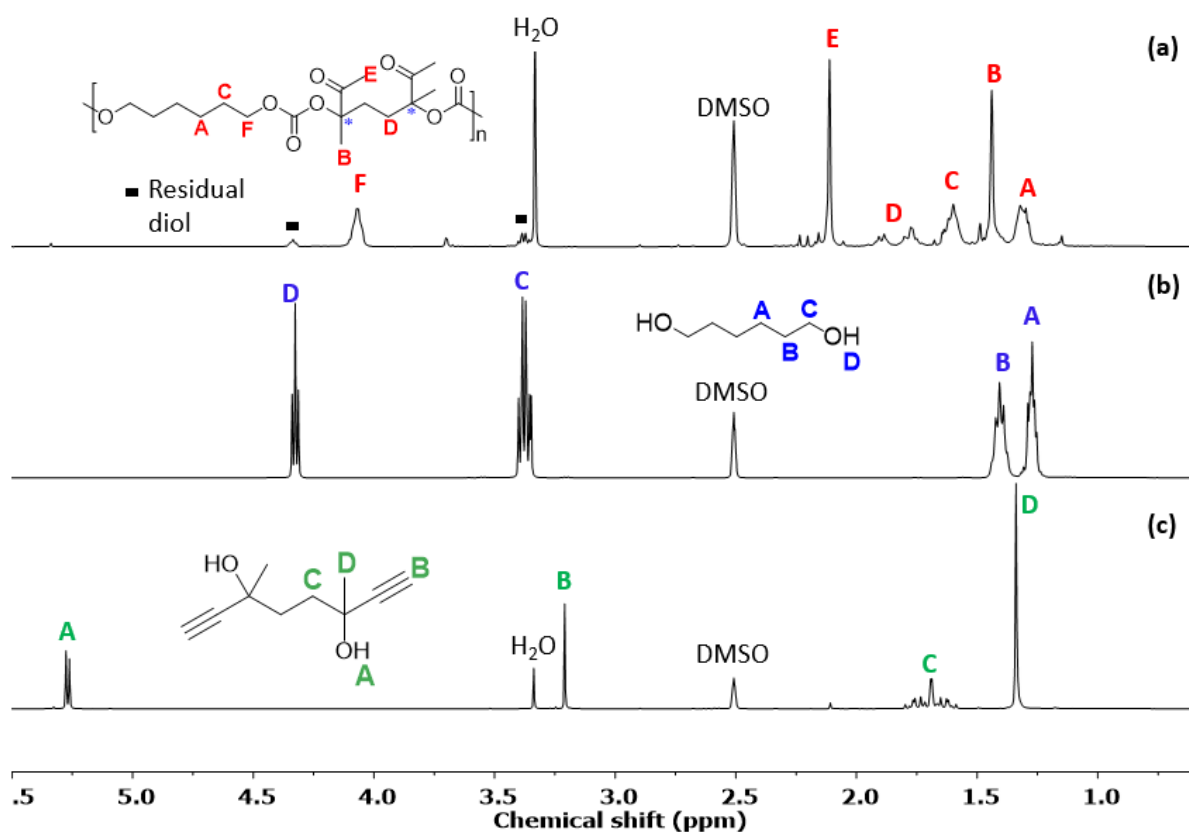
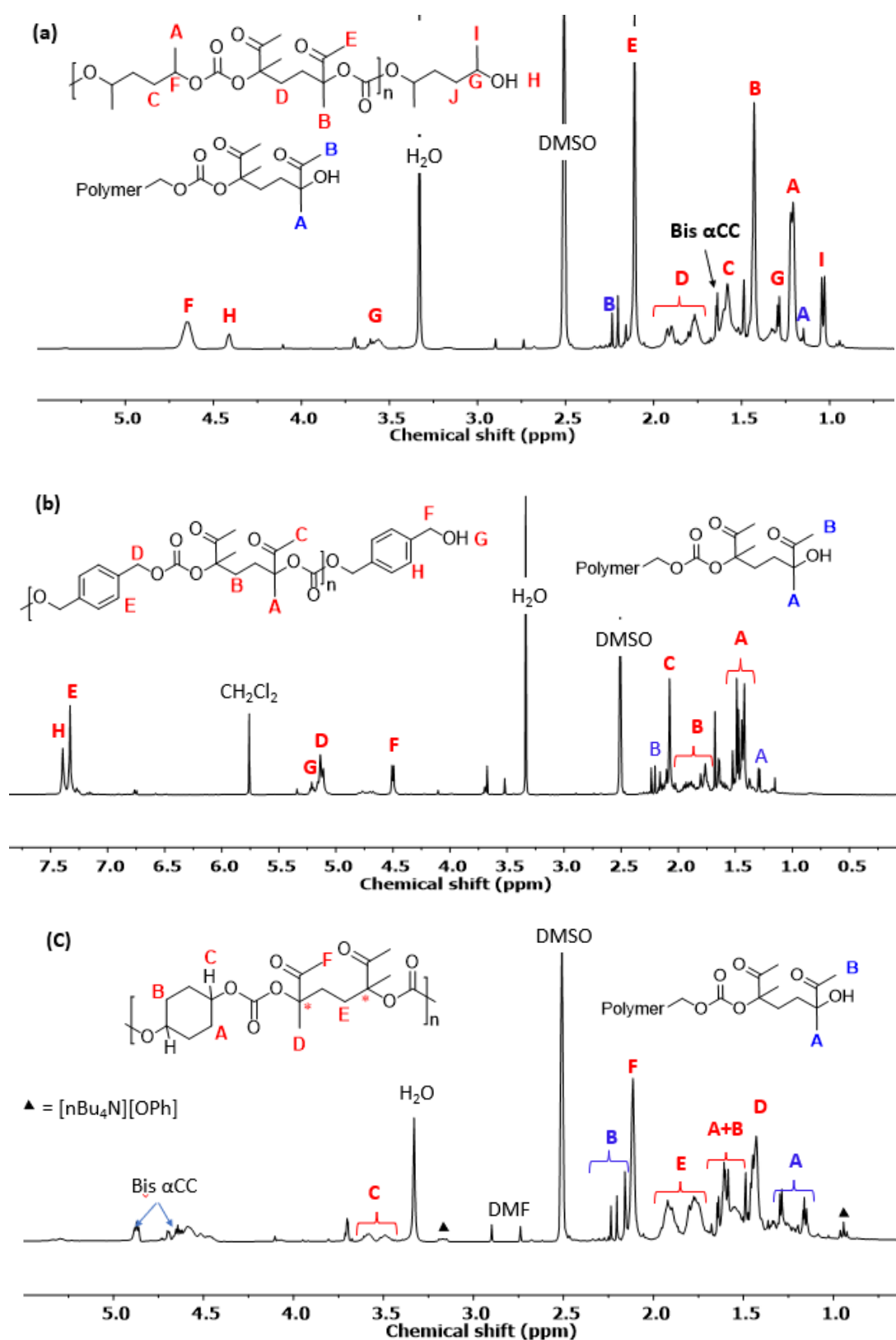


Figure S 8. $^1\text{H-NMR}$ (in DMSO-d_6) of (a) poly(oxo-carbonate)s **B1D1**, (b) 1,6-hexandiol **D1** and bis(propargylic alcohol) **B1** (c).

SI- 5. ^1H NMR characterisations of poly(oxo-carbonate) oligomers.Figure S 9. ^1H -NMR spectra in d_6 -DMSO of poly(oxo-carbonate)s (a) **B1D2**, (b) **B1D3** and (c) **B1D4**.

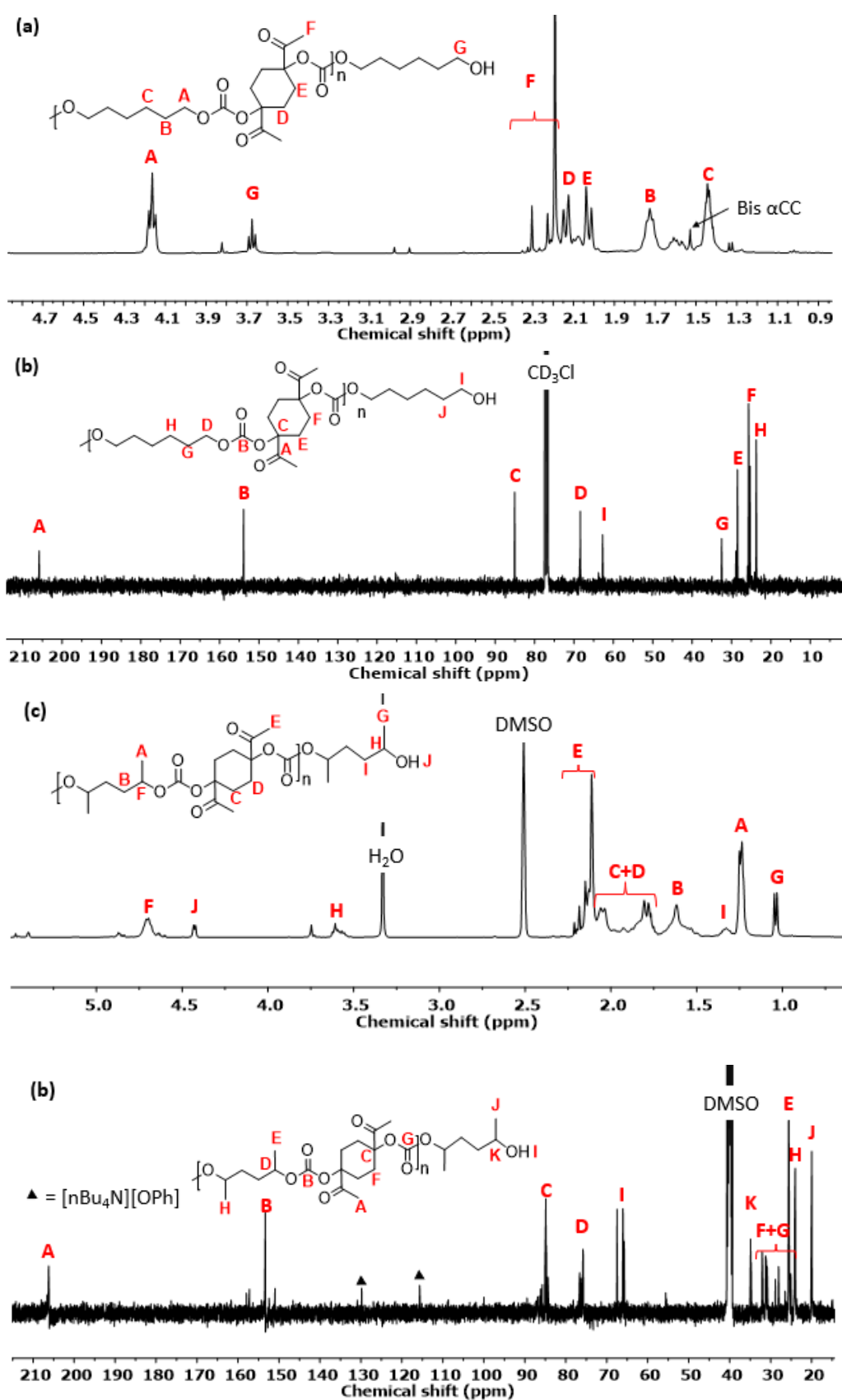


Figure S 10. ^1H - and ^{13}C NMR spectra of poly(oxo-carbonate)s **B2D1** (a) and (b) in DMSO and **B2D2** (c) and (d) in CDCl_3 , after removal of catalyst and DMF.

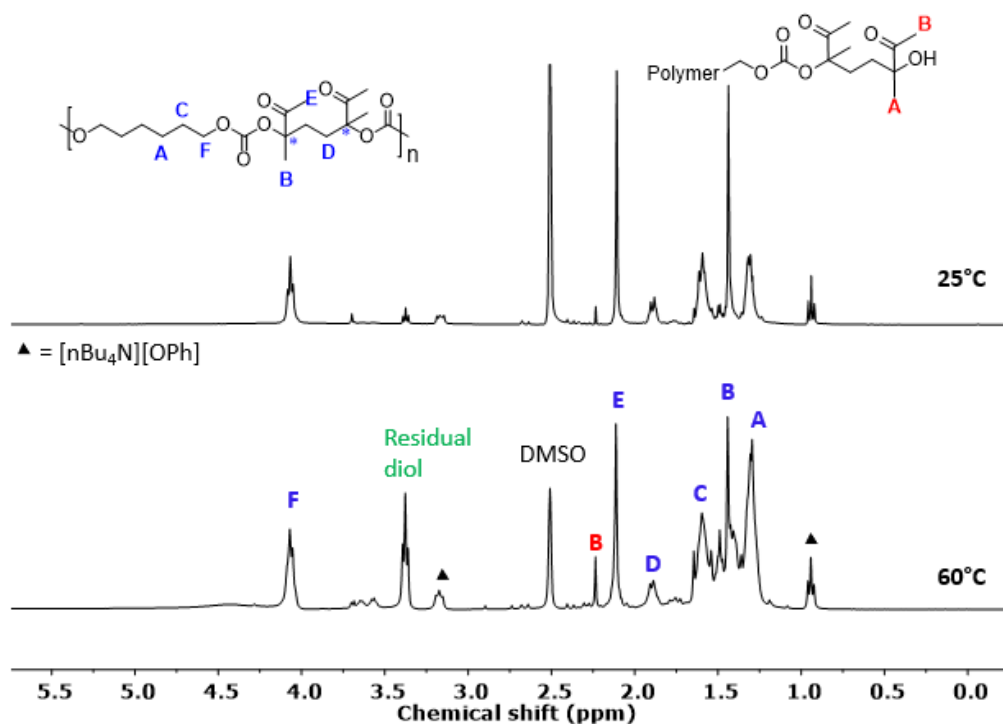


Figure S 11. ¹H-NMR superposition of crude mixture obtained for the synthesis of poly(oxo-carbonate)s B1D1 by the alcoholysis of bis- α -alkylidene cyclic carbonate C1 at 25 °C and 60 °C after 3 h.

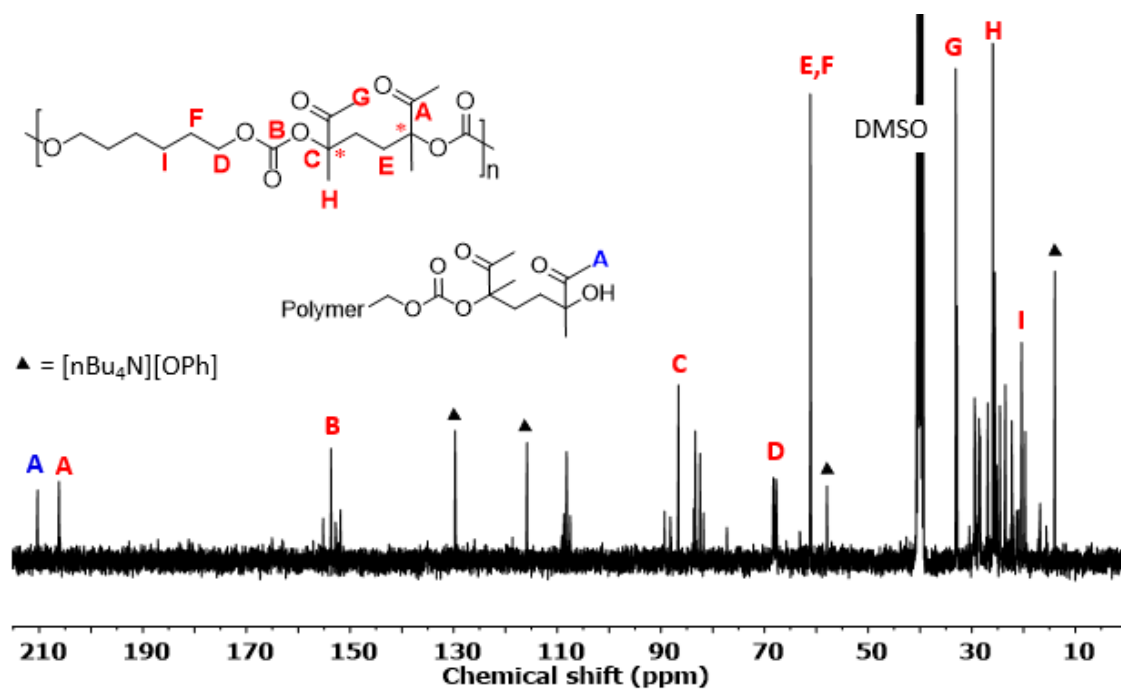
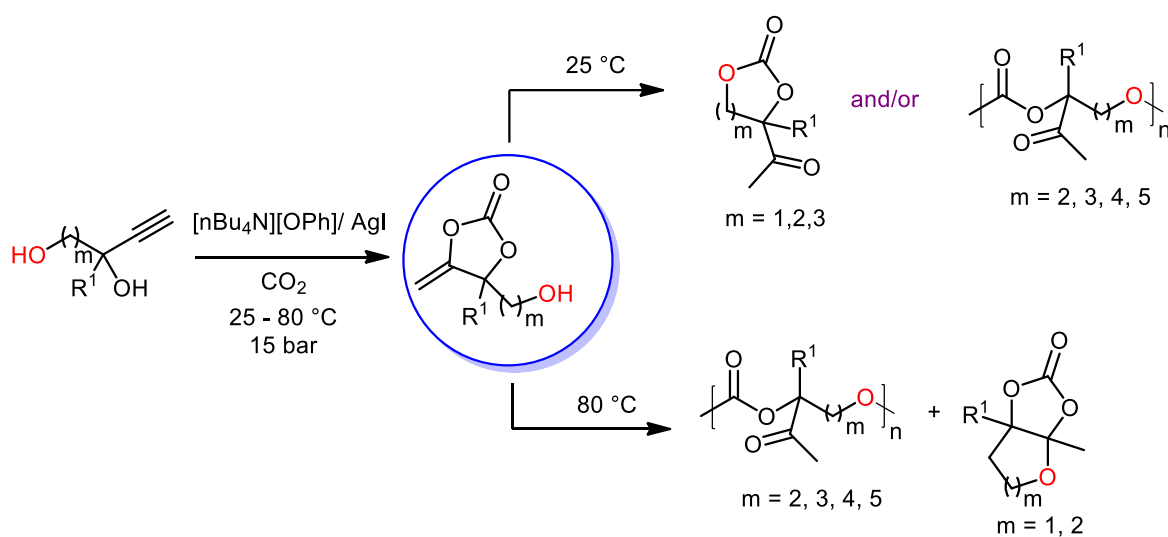


Figure S 12. ¹³C-NMR spectra of the crude mixture obtained for the synthesis of poly(oxo-carbonate)s B1D1 by the alcoholysis of bis- α -alkylidene cyclic carbonate C1 at 60 °C after 24 h.

CHAPTER 5

Cascade transformation of alkyne-1,n-diols into complex cyclic carbonates and poly(oxo-carbonate) oligomers



Chapter 5

Part of the results presented in this chapter are the product of a fruitful collaboration with Prof. Arjan W Kleij's group at ICIQ Tarragona, Spain, and are published in;

Xuetong Li,* Alba Villar-Yanez,* Charlene Ngassam Tounzoua,* Jordi Benet-Buchholz, Bruno Grignard, Carles Bo, Christophe Detrembleur and Arjan W. Kleij. ACS Catalysis, 2022, 12 2854-2860.

* equal co-authors

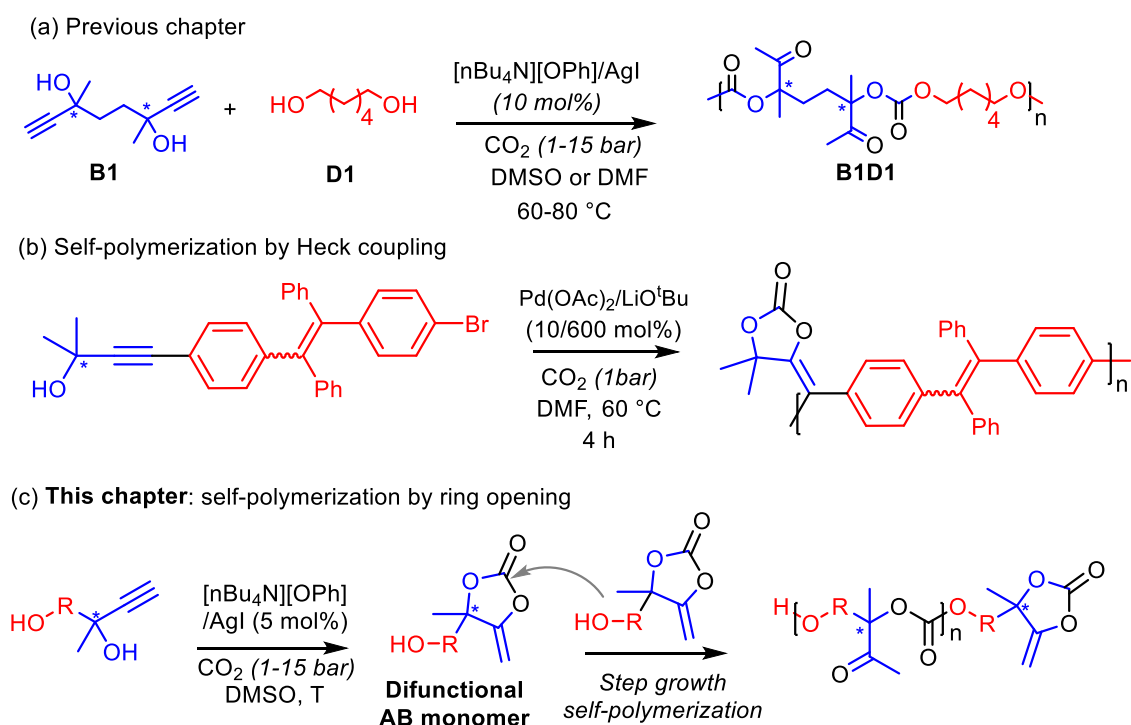
This chapter includes DFT computational studies conducted by Dr Raphaël Méreau of the university of Bordeaux

Table of contents

1. Introduction	139
2. Results	140
2.1. Coupling of CO ₂ with alkyne-1,2-diols	140
2.2. Coupling of CO ₂ with alkyne-1,3-diols	144
2.3. Mechanistic investigation of the formation of the keto-carbonate and tetrasubstituted ethylene carbonate	149
2.4. Coupling of CO ₂ with alkyne-1,4-diols	156
2.5. Coupling of CO ₂ with alkyne-1,5- and 1,6- diols	160
2.6. Coupling of CO ₂ with internal alkyne-1-n-diol	165
3. Conclusions	166
4. Experimental section	167
4.1. Materials	167
4.2. Analytical methods	167
4.3. Experimental procedures	168
5. Supplementary information	174

1. Introduction

In the previous chapter, we implemented the one-pot cascade synthesis of poly(*oxo*-carbonate)s (**Scheme 1a**). One of the problems encountered was having the perfect stoichiometry between the bispropargylic alcohol and the diol, which is a very crucial parameter when considering step-growth polymerisations. To solve this issue, we aimed to prepare new dissymmetric alkyne-1,*n*-diols, which upon reaction with CO₂, will form an AB monomer capable of self-polymerisation. There is only one published study which utilised a similar concept. Tang et al. designed propargylic alcohols bearing an aryl halide, which upon formation of the exovinylene cyclic carbonate polymerised by Heck coupling, providing 5CC based polymers of M_w = 29100 g/mol (Đ 2.83) (**Scheme 1b**).^[177] In this chapter, we sought to merge the presence of an intramolecular alcohol (pro)nucleophile and a reactive exocyclic double bond on the same molecule to promote its self-polymerisation that would result in poly(*oxo*-carbonate)s (**Scheme 1c**).



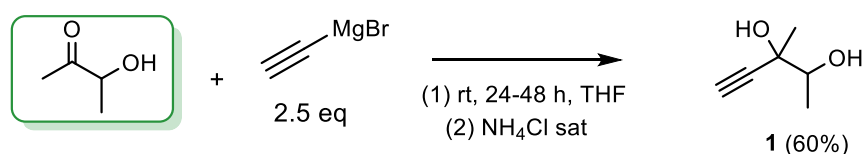
Scheme 1. Cascade step-growth synthesis of (a) poly(*oxo*-carbonate)s from bispropargylic alcohols and diols (b) polycyclic carbonates by Heck coupling and (c) poly(*oxo*-carbonate)s from dissymmetric alkyne-1,*n*-diols.

To understand the influence of the spacer R on the polymerisability of the monomer, various alkyne-1-*n*-diols (*n*=2-6) were prepared and tested for the carboxylative coupling reaction with CO₂ using our dual system [nBu₄N][OPh]/AgI. Kinetics studies via operando FT-IR spectroscopy, as well as DFT computation enabled us to understand the reactivity of these dissymmetric alkyne-1-*n*-diols.

2. Results

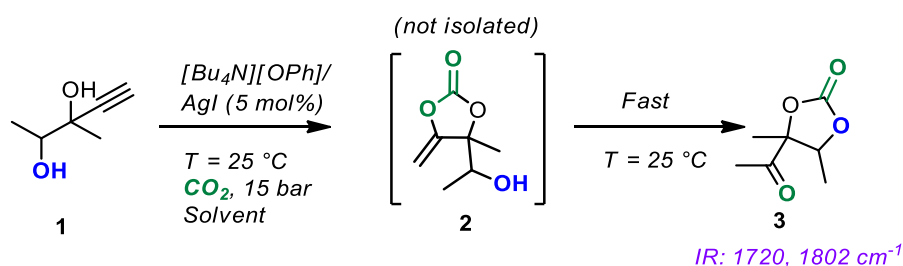
2.1. Coupling of CO₂ with alkyne-1,2-diols

Prior to carrying out any screening experiments, we needed to prepare the alkyne-1,2-diols as they are not commercially available. This was achieved by reacting a commercial hydroxyketone with an excess of ethynylmagnesium bromide (**Scheme 2**). 3-methylpent-4-yne-2,3-diol was obtained as a yellow oil with a 60% yield and characterised by ¹H and ¹³C NMR (**Figure S4**).



Scheme 2. Strategy employed for the synthesis of alkyne-1,2-diols, example of 3-methylpent-4-yne-2,3-diol

Then, the carboxylation of propargylic vicinal diol 3-methylpent-4-yne-2,3-diol (product **1**) was evaluated (**Scheme 3**). The reaction was performed at 25 °C and 15 bar of CO₂ using 5 mol% (with respect to the diol) of our binary catalyst composed of AgI and tetrabutylammonium phenolate ([nBu₄N][OPh]) in DMSO (C = 2.2 M). Under these operating conditions, the elusive trisubstituted ethylene carbonate with a pendant ketone (product **3**) was quantitatively and selectively formed after 24 h instead of the expected hydroxy-functional exovinylene cyclic carbonate (product **2**) or the corresponding poly(oxo-carbonate).



Scheme 3. Carboxylative coupling of 3-methylpent-4-yne-2,3-diol with CO₂.

To further understand the formation of **3**, the reaction was monitored at 25 °C by operando FT-ATR. **Figure 1** illustrates the time evolution of the carbonyl absorption region and highlights the appearance of two signals at 1720 cm⁻¹ and 1802 cm⁻¹ that are typical of a ketone and a 5-membered saturated cyclic carbonate, respectively. The presence of resonances at 206 ppm and 153 ppm in the ¹³C-NMR spectrum is attributed to a ketone and a 5-membered cyclic carbonate (**Figure S 11**). We assumed that the alkyne-1,2-diol reacts with CO₂ to form an α-alkylidene carbonate, which rapidly undergoes a skeletal rearrangement to yield the thermodynamically more stable keto-carbonate.

In order to tentatively push the reaction to polymerisation, we increased the reaction temperature to 80 °C. Product **3** remained however the main product, together with some unidentified products with resonances in the carbonate (157.53, 156.45, 152.45 and 145 ppm) and ketone region (214.26 ppm) (**Figure S 11**). We were not able to isolate these products.

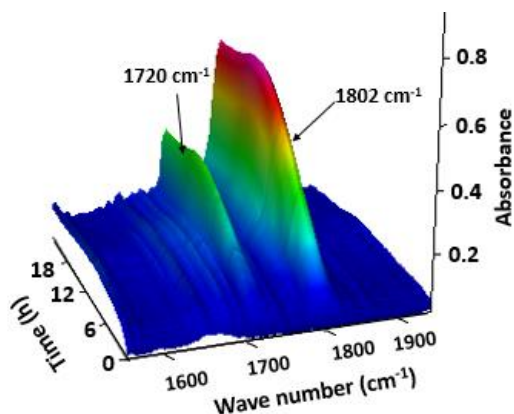
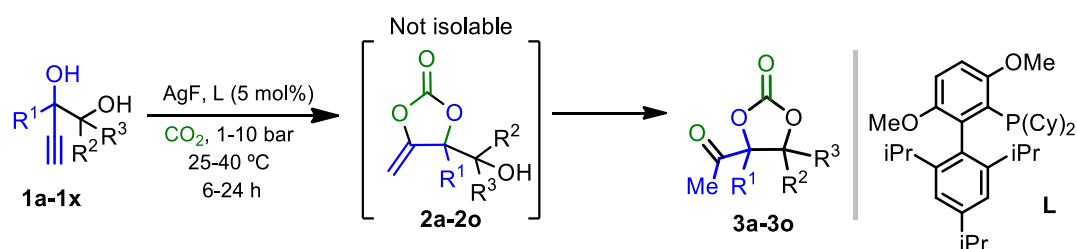


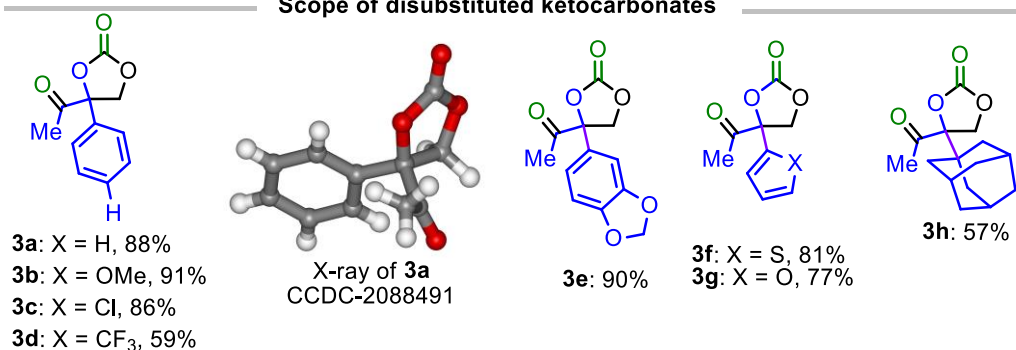
Figure 1. Carboxylative coupling of 3-methylpent-4-yne-2,3-diol with CO₂. 3D profile showing the evolution of the C=O absorption region obtained by operando FT-ATR spectroscopy. Conditions: 3-methylpent-4-yne-2,3-diol (3 g, 26.28 mmol), [Bu₄N][OPh] (5 mol%), AgI (5 mol%), T = 25 °C, PCO₂ = 15 bar, DMSO (12 mL).

Scope of di-, tri- and tetrasubstituted cyclic carbonates derived from substituted alkyne-1,2-diols

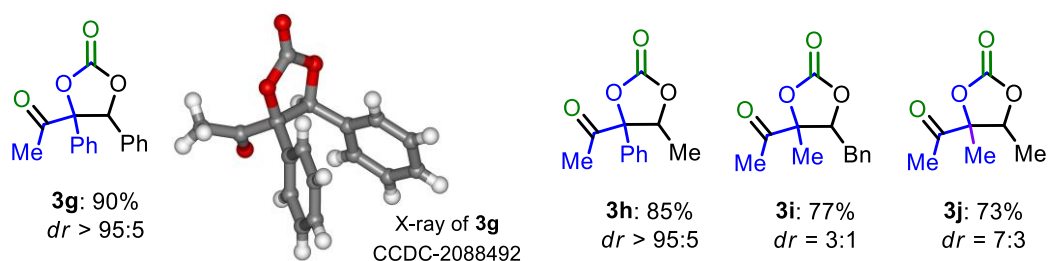
The scope of the alkyne-1,2-diols was evaluated by Xuetong Li of the ICIQ group under the direction of Prof Arjan Kleij. The catalytic system used in this case is the Ag-salt/DavePhos (*rac*).^[77] Using their optimum conditions (40 °C, PCO₂ = 1 bar, DavePhos/AgF (5 mol%), t = 6-24 h) (see manuscript for more details), they explored a large scope of di-, tri- and tetrasubstituted alkyne-1,2-diols, in good to excellent yields (59-91%). **Scheme 4** presents some selected examples of keto-carbonates with structurally diverse functionalities such as aryl (**3a-3e**) and heteroaryl groups (**3f and g**), as well as primary, secondary and tertiary alkyl groups, with the adamantyl-based **3h** (57%) being particularly noteworthy. Trisubstituted, aryl-functionalised keto-carbonates **3g-j** were also obtained in good, isolated yields (76-90%) and under moderate to high diastereocontrol (*dr* 3:1 to >95:5). Furthermore, more challenging tetrasubstituted carbonate heterocycles **3k-3o** could be obtained in isolated yields of up to 91%.



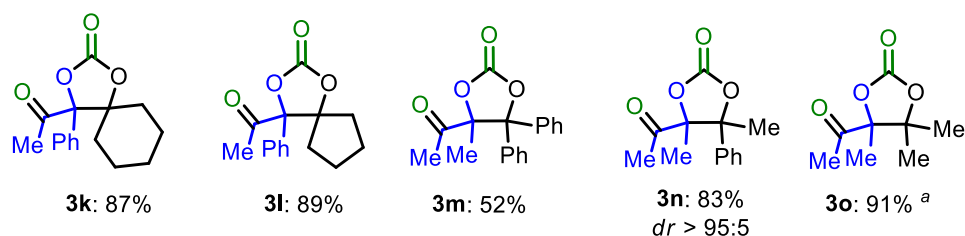
Scope of disubstituted ketocarboxylates



Scope of trisubstituted ketocarboxylates



Scope of tetrasubstituted ketocarboxylates



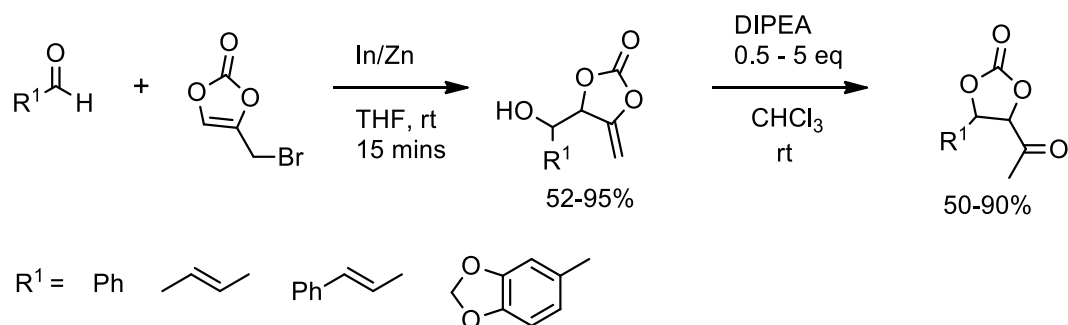
Scheme 4. Carboxylative cyclisation of 1,2-diol using AgOAc /DavePhos catalyst. Selected scope of di-, tri-, and tetra-substituted keto-based cyclic carbonates (**3a-3o**). Yields based on $^1\text{H-NMR}$ (CDCl_3) analysis, using mesitylene as internal standard. Full characterisation of the compounds are available at <https://doi.org/10.1021/acscatal.1c05773>.

By surveying the literature, we found an article by Saicic et al. treating on the synthesis of the family of compounds **2** and **3**. By reacting aldehydes, with 4-(bromomethyl)-1,3-dioxol-2-one in the presence of an Indium or Zinc catalyst, compound **2** with great diversity of substituents were obtained in average to excellent yields (52-95%) (**Scheme 5a**). Surprisingly, the authors did not observe any spontaneous rearrangement of the exovinylene cyclic carbonates into the corresponding 5-membered keto-carbonates for all examples except one. A second

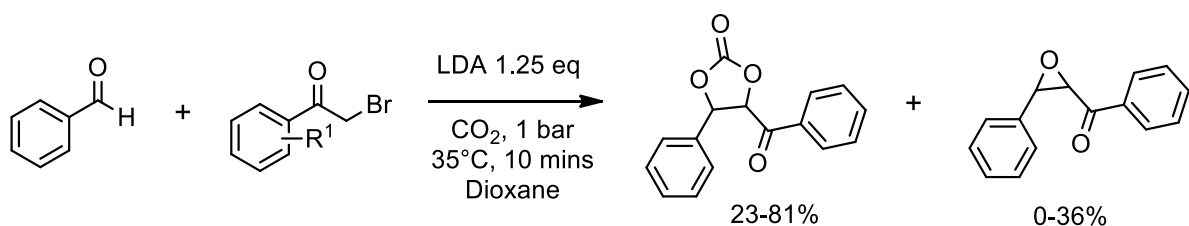
treatment in the presence of 0.5-5 eq of diisopropylethylamine (DIPEA) in chloroform promoted the intramolecular cyclisation into the ketocarbonates.^[213]

Liu et al. prepared 5-membered keto cyclic carbonates by the one-pot cascade reaction of phenacyl bromide and aldehydes in the presence of 1.25 eq of Lithium diisopropylamide (LDA) and CO₂. Although poor to good yields (23-81%) in the keto-compound was obtained, the concomitant formation of an epoxide by-product was also observed **Scheme 5b**.^[214]

(a) Saicic, 2011



(b) Liu, 2011

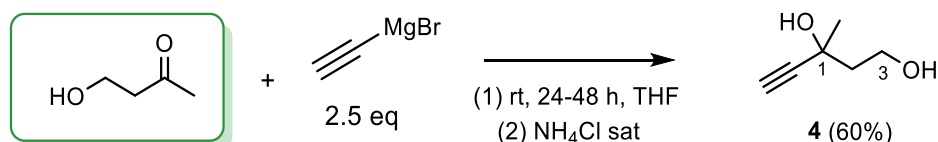


Scheme 5. Previous works on the synthesis of 5-membered keto-cyclic carbonates.^[213,214]

Our approach starting from alkyne-1,2-diols thus represents a direct one pot approach for the synthesis of this highly substituted keto-cyclic carbonates, while using low amounts of additives (5 mol%).

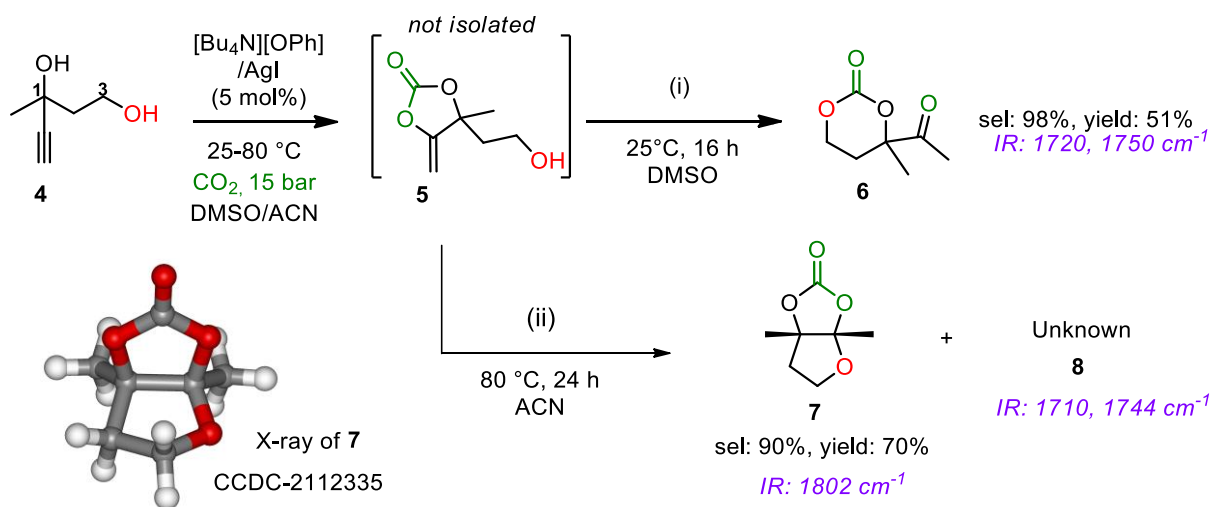
2.2. Coupling of CO₂ with alkyne-1,3-diols

As the alkyne-1,2-diols were not homopolymerising in the presence of CO₂ and the catalyst, we were keen to examine whether the use of higher homologues of alkyne-1,2-diols would serve as suitable reagents towards poly(oxo-carbonate)s or if larger keto-carbonate rings would be formed. Similarly to the alkyne-1,2-diol, the alkyne-1,3-diol was prepared by reacting the adequate hydroxyketone (4-hydroxybutan-2-one) with an excess of ethynylmagnesium bromide. An oil was obtained with a yield of 60% (**Scheme 6**) which was characterised by ¹H and ¹³C NMR (**Figure S5**).



Scheme 6. Strategy employed for the synthesis of alkyne-1,3-diols, example of 3-Methylpent-4-yn-1,3-diol (**4**).

The coupling of alkyne-1,3-diol **4** with CO₂ was monitored by operando FT-ATR at 25 °C, 15 bar in the presence of AgI/[Bu₄N][OPh] in DMSO (2.2 M) as illustrated in **Scheme 7**. It highlights the formation of a species with two carbonyl vibrations at 1720 cm⁻¹ and 1750 cm⁻¹ which are typical of a ketone and a 6-membered cyclic carbonate, respectively. The correlation of the FT-ATR results with ¹H- and ¹³C-NMR structural characterisations of the isolated sample attested to the formation of the elusive product **6** (**Figure S 18**) with a high chemo-selectivity of 98% in 16 h and appreciable isolated yield (51%). Interestingly, **Figure 2a** also revealed the presence of an additional carbonyl elongation of very low intensity at 1820 cm⁻¹ that is characteristic of the carbonyl group of the exovinylene cyclic carbonate. This experimentally suggests that the expected exovinylene cyclic carbonate **5** is formed and certainly follows an intramolecular rearrangement to produce compound **6**.



Scheme 7. Carboxylative coupling of 1,3-diol **4** with CO₂.

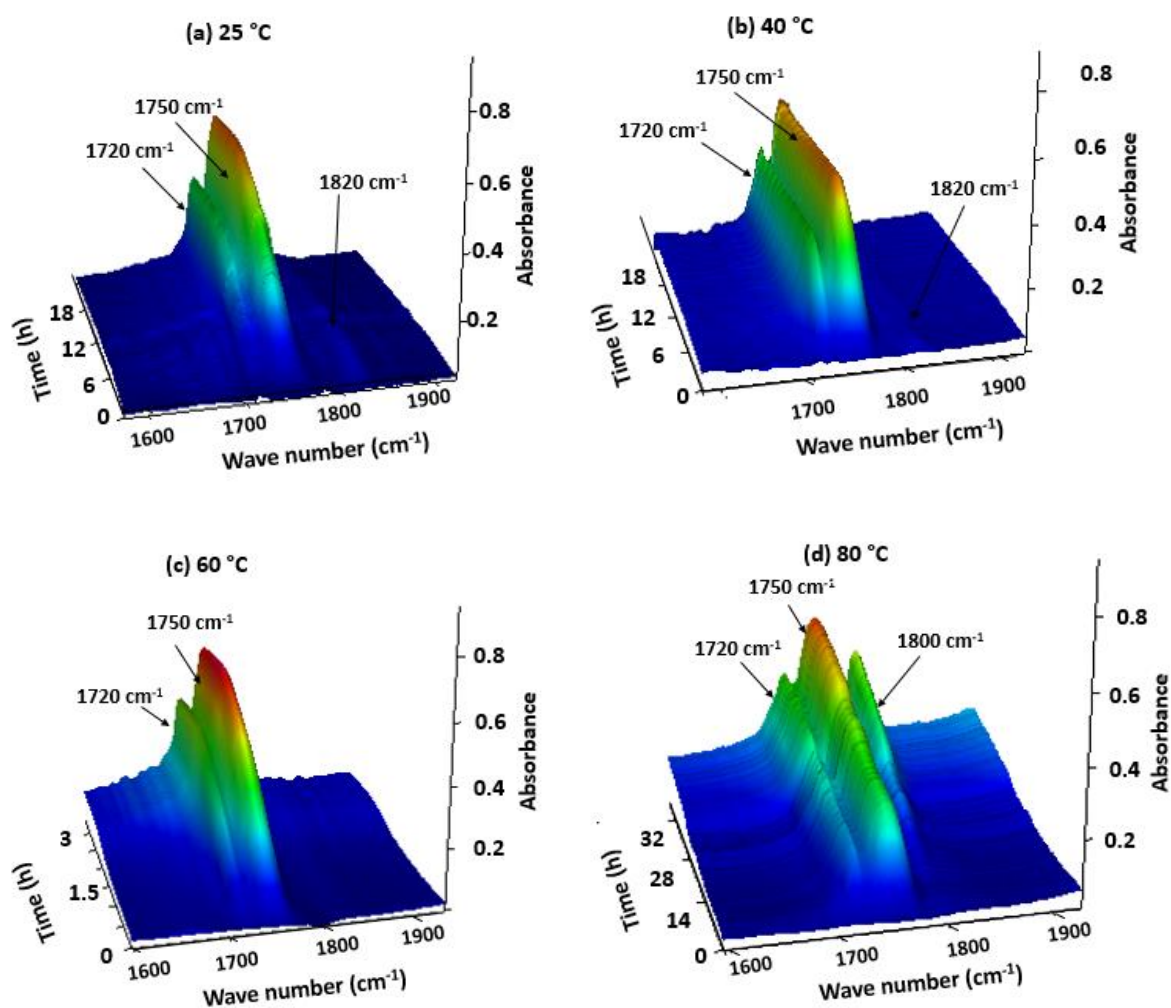


Figure 2. Online monitoring of the carboxylative coupling of 3-methylpent-4-yne-1,3-diol (**5a**) with CO₂ via operando FT-ATR spectroscopy at (a) 25 °C, (b) 40 °C, (c) 60 °C (d) and (e) 80 °C (f) Influence of the temperature on the formation of keto-carbonate **6**. Conditions: 3-methylpent-4-yne-1,3-diol (3 g, 26.28 mmol), [nBu₄N][OPh] (5 mol%), AgI (5 mol%), 15 bar, DMSO (12 mL).

Reproducing the same experiment at higher temperatures (**Figure 2b** and **c**) accelerated the reaction with the quantitative conversion of **4** into **6** in 6 h or 3.5 h at 40 °C or 60 °C, respectively, while keeping an excellent selectivity toward the oxo-substituted trimethylene carbonate **6** above 90-98% (**Table 1**, entry 6). When the temperature was further increased to 80 °C, **6** was also formed during the early stage of the reaction (**Figure 2d**), however only a maximum yield of about 58% was obtained after 14 h (**Figure 3a**). The reaction was also less selective with the formation of the elusive bicyclic tetrasubstituted five-membered cyclic carbonate **7** and an unidentified product **8**. The structure of **7** was confirmed by ¹H- and ¹³C-NMR spectroscopy, HR-MS and X-ray crystallography on the isolated product (**Figure S 19**).

Figure 3a compares the rate of formation of **6** at the different temperatures which varies in the order $60\text{ }^{\circ}\text{C} > 40\text{ }^{\circ}\text{C} > 80\text{ }^{\circ}\text{C} > 25\text{ }^{\circ}\text{C}$. The unexpected behaviour at $80\text{ }^{\circ}\text{C}$ is due to the growth of a new carbonyl elongation, typical of the ethylene carbonate scaffold **7** that is observed at 1800 cm^{-1} after 6 h of reaction, as well as a shouldering at 1744 cm^{-1} and 1710 cm^{-1} (**Figure 3b, Figure S 12**). The concomitant formation of **7** at $80\text{ }^{\circ}\text{C}$ might explain why the formation of **6** was slow compared to the reaction carried out at $60\text{ }^{\circ}\text{C}$ where **7** was not observed.

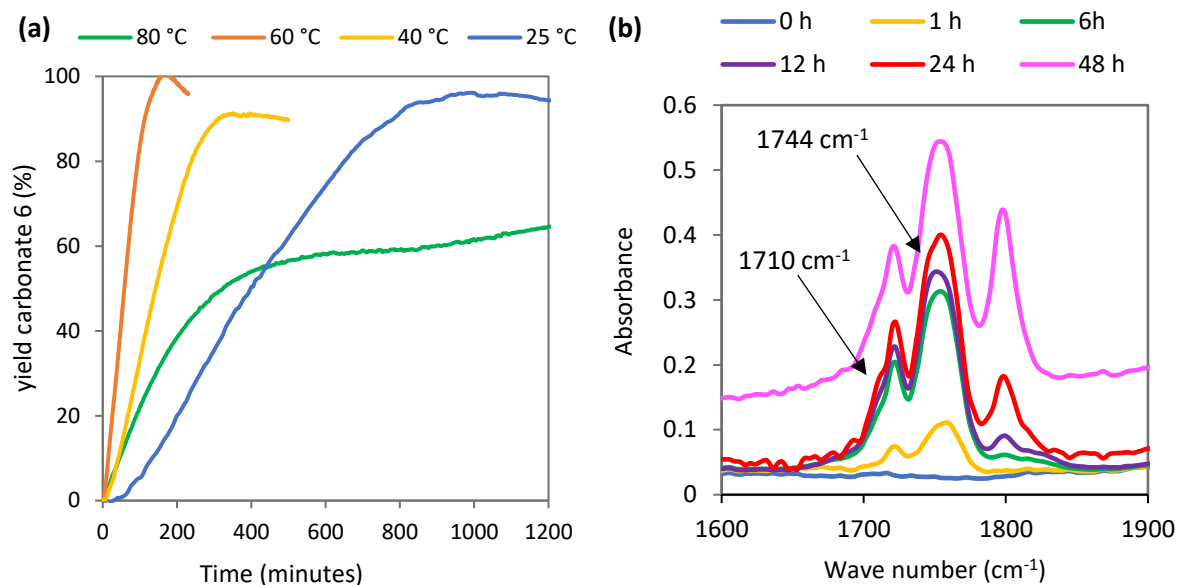


Figure 3. (a) Influence of the temperature on the formation of keto-carbonate **6** for the carboxylative coupling of 3-methylpent-4-yne-1,3-diol (**5a**) with CO_2 , and (b) online monitoring of the formation of **6** via operando FT-ATR spectroscopy at $80\text{ }^{\circ}\text{C}$. Conditions: 3-methylpent-4-yne-1,3-diol (3 g, 26.28 mmol), $[\text{nBu}_4\text{N}][\text{OPh}]$ (5 mol%), AgI (5 mol%), 15 bar, DMSO (12 mL).

To further understand the reactivity of the alkyne-1,3-diol and the formation of the different products, various experimental parameters were screened (temperature, solvent, concentration, and reaction time), and results are summarised in **Table 1**. At $25\text{ }^{\circ}\text{C}$, increasing the concentration to 4.4 M in DMSO, resulted in a decrease in the conversion from 100 to 34% (**Table 1**, entry 3). Working under neat conditions or in acetonitrile gave no conversion (**Table 1**, entries 4-5). When the temperature was increased to $60\text{ }^{\circ}\text{C}$, total conversion of **4** was obtained in ACN 4.4 M, with a selectivity of 57% and 21% for **6** and **7**, respectively (**Table 1**, entry 9). Full conversion of **4** was also achieved under neat conditions, with only 13% of **6**, 42% of **7**, and the remaining 45% for the unidentified product **8** (**Table 1**, 10). To push the formation of **7** to completion, we further increased the reaction temperature to $80\text{ }^{\circ}\text{C}$. In DMSO ($C = 4.4\text{ M}$), **6** and **7** were concomitantly formed with a selectivity of 13 % and 69 %, respectively (**Table 1**, entry 12). Interestingly, we found that, by working in ACN (4.4 M), the chemo-selectivity for **7** was increased to 90%, with an isolated yield of 70% (**Table 1**, entry 14). A similar result was obtained under neat conditions after 72h of reaction (**Table 1**, entry 16).

As noted from **Table 1**, for almost all the experiments conducted, an unidentified product **8** was observed which we believe to be responsible for the shouldering observed at 1744 cm⁻¹ and 1710 cm⁻¹ in FT-IR spectra (**Figure 3b**). The analysis of one of the crude reaction mixtures by SEC revealed an M_n = 440 g/mol with a polydispersity of 1.33 (**Figure 4**), thus suggesting that the unknown molecule is an oligomer. Attempts to isolate and purify these oligomers were unsuccessful, rendering their structural characterisation and identification by NMR rather difficult (**Figure S 20**).

Table 1. Screening of parameters for the carboxylative coupling of 1,3-diol **4** with CO₂.^[a]

Entry	Solvent	Conc. [mol/L]	T [°C]	Conv. of 4 [%] ^[b]	6 [%] ^[b]	7 [%] ^[b]	8 [%] ^[b]
1 ^[c]	DMSO	2.2	25	100	98 (51) ^[d]	–	2
2	DMSO	2.2	25	100	85	–	15
3	DMSO	4.4	25	34	84	–	16
4	ACN	2.2	25	0	–	–	
5	–	–	25	0	–	–	
6 ^[e]	DMSO	2.2	60	100	98	–	2
7	DMSO	4.4	60	100	85	6	9
8 ^[f]	DMSO	4.4	60	100	44	49	7
9	ACN	4.4	60	100	57	21	22
10	–	–	60	100	13	42	45
11	DMSO	2.2	80	100	32	35	33
12	DMSO	4.4	80	100	13	69	16
13	DMF	4.4	80	100	5	86	9
14	ACN	4.4	80	100	0	90 (70) ^[d]	10
15	–	–	80	70	0	67	33
16 ^[f]	–	–	80	100	0	90	10

[a] Conditions: 1,3-diol **4** (1 g, 8.76 mmol), [Bu₄N][OPh] (0.147 g, 0.438 mmol), AgI (0.102 g, 0.438 mmol), p(CO₂) = 15 bar and t = 24 h. [b] Determined by ¹H-NMR spectroscopy with 1,3,5-trimethoxybenzene as internal standard (see **SI-6**). [c] Reaction time was 16 h. [d] Yields in brackets refer to isolated yield after purification by silica gel column chromatography. [e] Reaction time was 3.5 h. [f] Reaction time was 72 h.

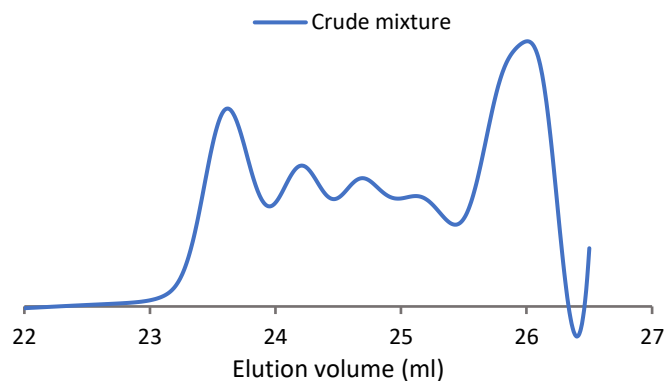
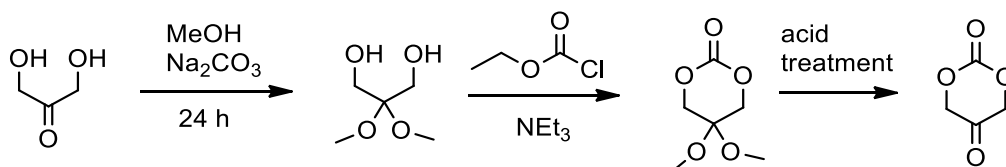


Figure 4. SEC traces of the crude mixture presented in **Table 1**, entry 12.

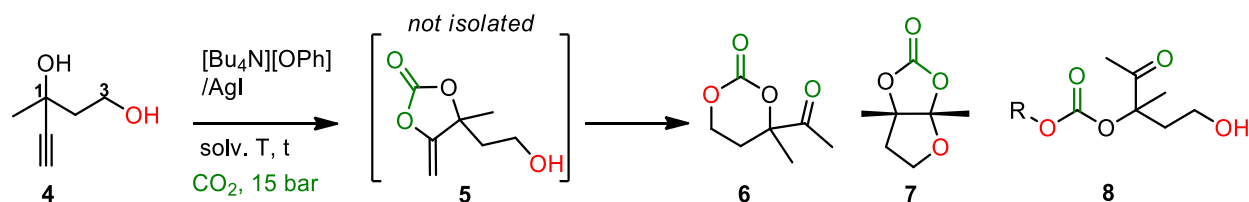
In this section, we described a direct cascade synthesis of 6-membered keto-carbonate **6** and elusive tetrasubstituted ethylene carbonate **7** from an alkyne-1,3-diol. We found only one article in the literature describing the synthesis of a 6-membered cyclic carbonate bearing a ketone function, and it consisted in a multistep approach starting from diols, involving the use phosgene derivatives and protecting groups (**Scheme 8**).^[215] The cascade synthesis described in this chapter, would thus provide an elegant approach towards such 6-membered keto-carbonates, provided we are able to optimise the isolation of the products. Regarding the fused bicyclic compound **7**, there are no works describing the synthesis of this compound.



Scheme 8. Synthesis of 6-membered keto-cyclic carbonate from dihydroxyacetone.^[215]

2.3. Mechanistic investigation of the formation of the keto-carbonate and tetrasubstituted ethylene carbonate

In order to propose a mechanism for the formation of the keto-carbonate **6** and tetrasubstituted ethylene carbonate **7**, DFT computation was carried out using the [nBu₄N][OPh]/AgI system, alkyne-1,3-diol **4**, CO₂, with acetonitrile as solvent (**Scheme 9**).



Scheme 9. Carboxylative coupling of alkyne-1,3-diol **4** with CO₂.

The first part of the mechanism which involves the formation of the exovinylene 5-membered cyclic carbonate (**5**) intermediate is not discussed as we believe that a similar mechanism to that described in **chapter 3** is taking place, albeit with some slight changes in the energy levels/barriers because of the presence of the additional OH function.

For the formation of the keto-carbonate **6** and the tetrasubstituted ethylene carbonate **7**, AgI was not accounted for in the DFT calculations for simplification purposes. These calculations were performed using a Gaussian 16 B.01 program with the implemented functional and basis set PBE0-D3(BJ)/def2tvz being chosen using dispersion correction with Becke-Johnson damping. All calculations were carried out at 298 K using an acetonitrile implicit solvent model SMD.

The Zero energy was set as the sum of the Gibbs free energy of the isolated reactants.

Formation of keto-carbonate **6**

The mechanism begins by the formation of a Van Der Waals complex between **5** and [nBu₄N][OPh], which is stabilized by -4.9 kcal/mol with respect to the isolated reactants (**Figure 5**). Then we have abstraction of the proton of the primary alcohol moieties by the phenolate to form an alkoxide anion. This alkoxide undergoes a nucleophilic attack on the C=O of the carbonate group via a concerted **1-TS1** (-0.5 kcal/mol), to form a bicyclic intermediate **111** (-3.3 kcal/mol). The next step is the ring-opening of the 5-membered cyclic intermediate and ring-closure of the 6-membered one via **1-TS2** (-0.8 kcal/mol) to produce an enolate form of **6** (**1-I2**, -13.3 kcal/mol). Lastly, tautomerization occurs via **1-TS3** (-4.3 kcal/mol) helped by the retrocession of the H atom from PhOH to give **6** (-10.1 kcal/mol) and regenerate the catalyst. The low energy barriers of the transition states (between 2.5 and 9 kcal), coupled with the fact that they are all immersed (under the zero reference) suggests an easy transformation of **5** to **6**. This is in accordance with the FT-IR experimental observations which showed the rapid transformation of **5** into **6** at 25 °C.

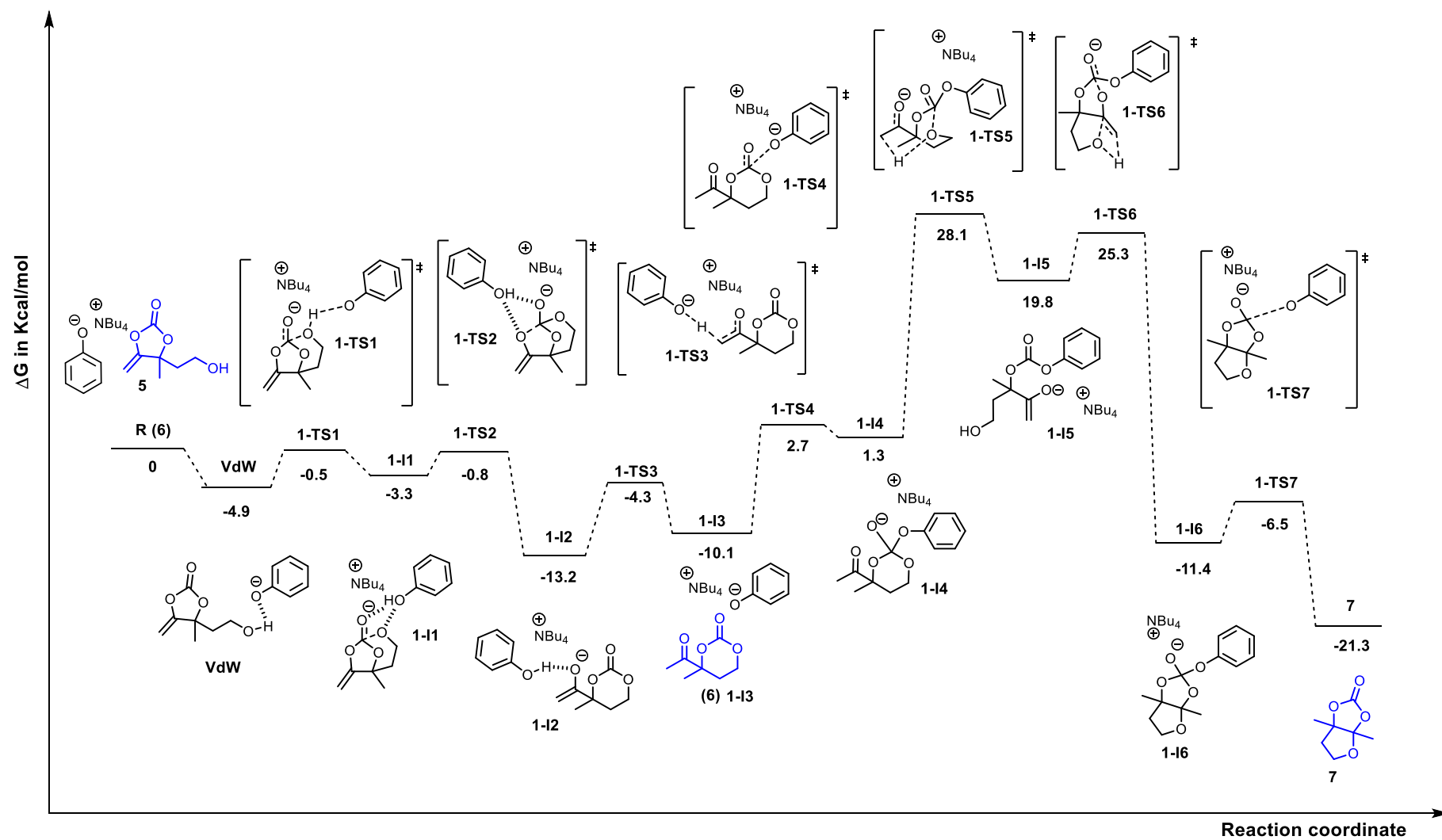
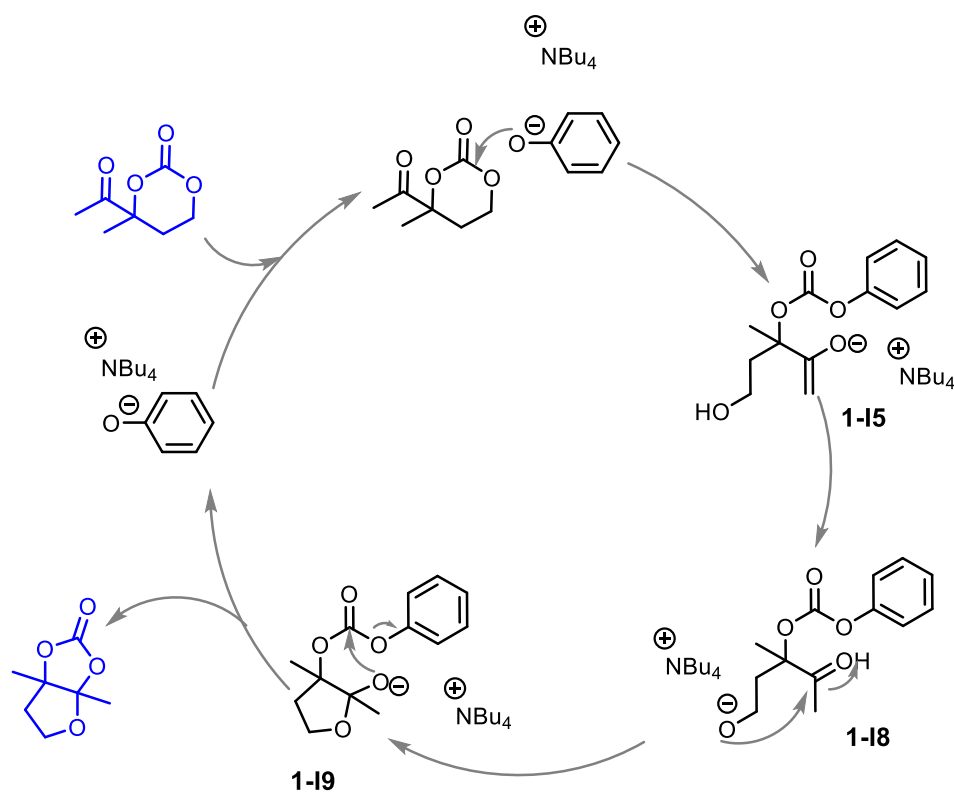


Figure 5. Mechanism for the formation of the keto-carbonate **6** and tetrasubstituted ethylene carbonate **7**.

Formation of tetrasubstituted ethylene carbonate **7** from compound **6**

After the formation of the keto-carbonate **6**, the phenolate anion attacks the C=O of **6**, via **1-TS4** (2.7 kcal/mol) to form the intermediate **1-I4** (1.3 kcal/mol) (**Figure 5**). Next, this intermediate ring-opens into the enolate intermediate **1-I5** (19.8 kcal/mol) via the concerted transition state **1-TS5** (28.5 kcal/mol). This is followed by a complex bicyclisation step which involves the addition of the alcohol unto the carbon of the enolate and the simultaneous attack of the enolate unto the carbon of the carbonate function via **1-TS6** (25.5 kcal/mol) to produce **1-I6** (-11.4 kcal/mol). Finally, the phenolate is eliminated from **1-I6** via **1-TS7** (-6.5 kcal/mol), resulting in the regeneration of the [nBu₄N][OPh] catalyst and the formation of **7** which is stabilised at -21.3 kcal/mol (-11.2 kcal difference with respect to the starting product **6**).

Based on recent studies published by our group on the depolymerisation of poly(oxo-carbonate-co-urea/amide)s^[216] which produced a similar compound to **7** and for which computational studies were performed (in collaboration with Dr. Raphaël Mereau), we believe that another mechanism could be at play (**Scheme 10**). It is suggested that the phenolate ring-opens **6** to provide the corresponding alcoholate derivative (**1-I5**). Then we have the nucleophilic attack of the alcoholate of **1-I8** onto the ketone moiety leading to the corresponding 5-membered cyclic hemiacetal (**1-I9**). The so-formed alcoholate then attacks the carbonate, producing the bicyclic compound **7** and releasing the phenolate leaving group.

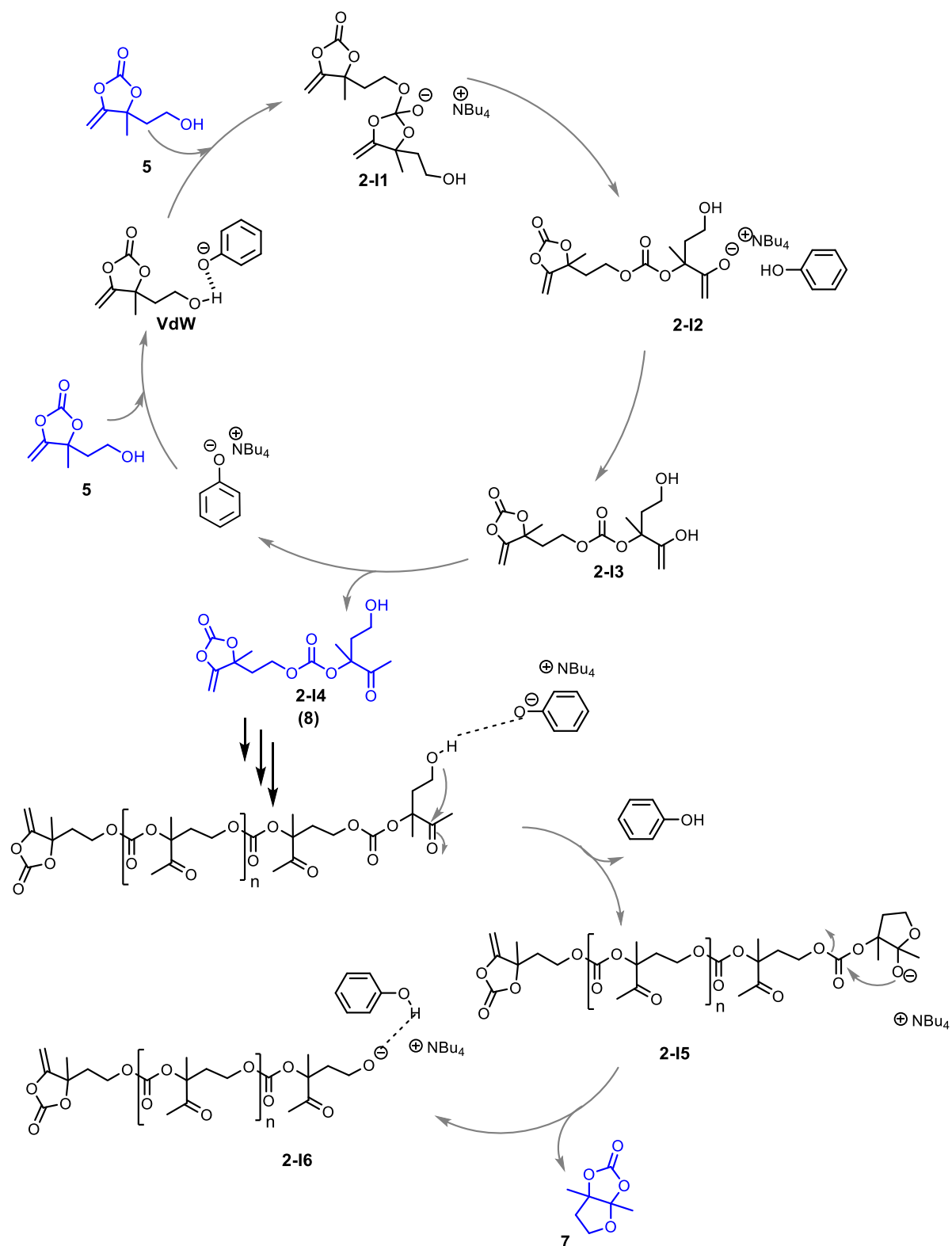


Scheme 10. Alternate mechanism proposed for the formation of tetrasubstituted ethylene carbonate **7** from compound **6**.

Formation of tetrasubstituted ethylene carbonate **7 by depolymerisation of the oligomers **8****

The ring-closure depolymerisation of polycarbonates into cyclic carbonates is known in the literature and has been exploited to synthesise diverse 6-membered cyclic carbonates.^[217–219] We believe that a similar unzipping mechanism might take place during the carboxylative coupling of alkyne-1,3-diol **4** with CO₂ at 80 °C, as oligomers were formed. This hypothesis emerged when observing that the yield in oligomers **8** decreased from 33 to 10% while that of the tetrasubstituted ethylene cyclic carbonate **7** increased from 67 to 90% when the reaction time was extended from 24 h to 72 h (**Table 1**, entries 15-16). The mechanism proposed thereafter (**Scheme 11**) has not been computed by DFT by lack of time, hence the structures of the intermediates might not be totally accurate.

Starting from the isolated reactant **5** and the catalyst [nBu₄N][OPh], we have the formation of the **VdW** complex. Then the phenolate attacks the carbonate of another molecule of **5** to form intermediate **2-I1**. Then the breaking of the carbonate bond of the O atom next to the olefin occurs giving rise to intermediate **2-I2**. Then we have the donation of a proton from PhOH to the alkoxide to form an enol **2-I3** that tautomerises to give the dimer **2-I4**, with the regeneration of the [nBu₄N][OPh] catalyst. If the cycle is repeated starting with **2-I4**, this results in a trimer, tetramer and eventually an oligomer. Alternatively, we can have the depolymerisation of the oligomers to form **7**. We believe that the cyclisation preferably starts from the alcohol group at the polymer chain-end following a cascade back-biting mechanism promoted by the base catalyst. The phenolate activates the alcohol which effects an intramolecular nucleophilic attack on the ketone group, producing a hemiacetal terminated oligomer (**2-I5**). Then **2-I5** undergoes an intramolecular cyclisation by the attack of the alcoholate on the adjacent carbonate group, thus leading to the bicyclic compound **7**, and the one-unit shorter oligomer (**2-I6**) terminated by the alcoholate that can repeat the overall back biting process producing **7**. This mechanism is Based on recent findings describing the depolymerisation of similar poly(oxo-carbonate)s^[107] and poly(oxo-carbonate-co-urea/amide)^[216].

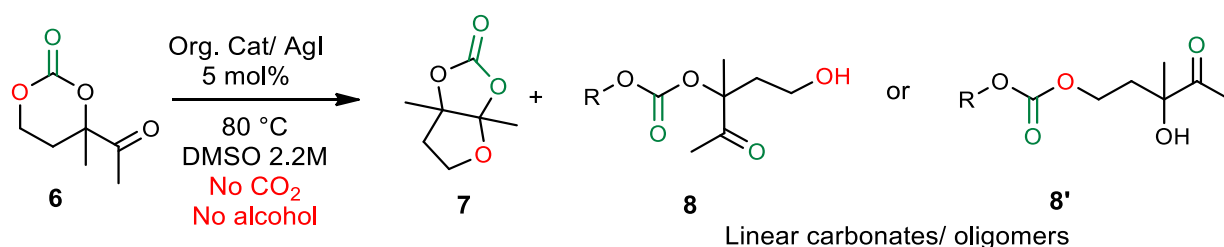


Scheme 11. Proposed mechanism for the formation of tetrasubstituted ethylene carbonate **7** by depolymerisation of oligomers **8**. NB, not computed by DFT.

Model reaction

In order to support or refute our mechanism proposal for the formation of the bicyclic compound **7** from **6** presented in **Figure 5** above, we carried out an additional experiment. We isolated the pure keto-carbonate **6**, dissolved it in DMSO in the presence of [nBu₄N][OPh] as catalyst, and heated the mixture at 80 °C without any co-reactant (**Table 2**). 91% of **6** were converted after 1 h of reaction, with a yield of 74 for **7**. The remaining product was assigned to the oligomer **8** of complex microstructure. Importantly, by allowing the reaction to proceed for 24 h, we achieved a total conversion of **6**, with a yield of 75% for **7** (**Table 2**, entry 2). The model reactions thus support that **6** is converted into **7**, but also that some polycarbonate oligomers are formed.

Table 2. (Organo)Catalysed conversion of the six-membered cyclic carbonate (**6**) 4-acetyl-4-methyl-1,3-dioxan-2-one into the 5-membered one (**7**).



Entry	Catalyst	Time (h)	^b Conv. 6	^b 7	^b 8 or 8'
			%	%	%
1	[nBu ₄ N][OPh]/AgI	1	91	74	17
2	[nBu ₄ N][OPh]/AgI	24	100	75	25

^a Conditions: 4-acetyl-4-methyl-1,3-dioxan-2-one (**6**) (140 mg, 0.88 mmol), [nBu₄N][OPh], silver iodide (AgI) (10.2 mg, 43.8 μmol) and dried DMSO (400 μL) (*C* = 2.2 M). ^b determined by ¹H-NMR spectroscopy with 1,3,5-trimethoxybenzene as internal standard. ¹H-NMR spectra shown in **Figure S 13** for the reaction with [nBu₄N][OPh].

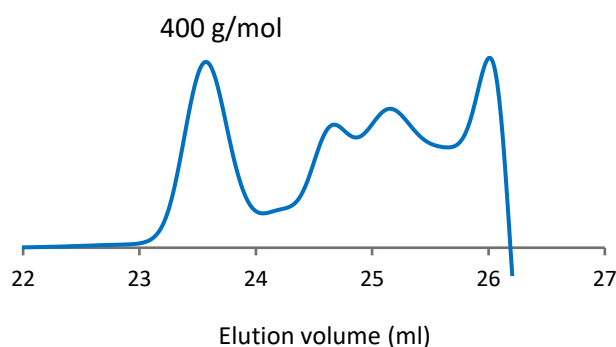
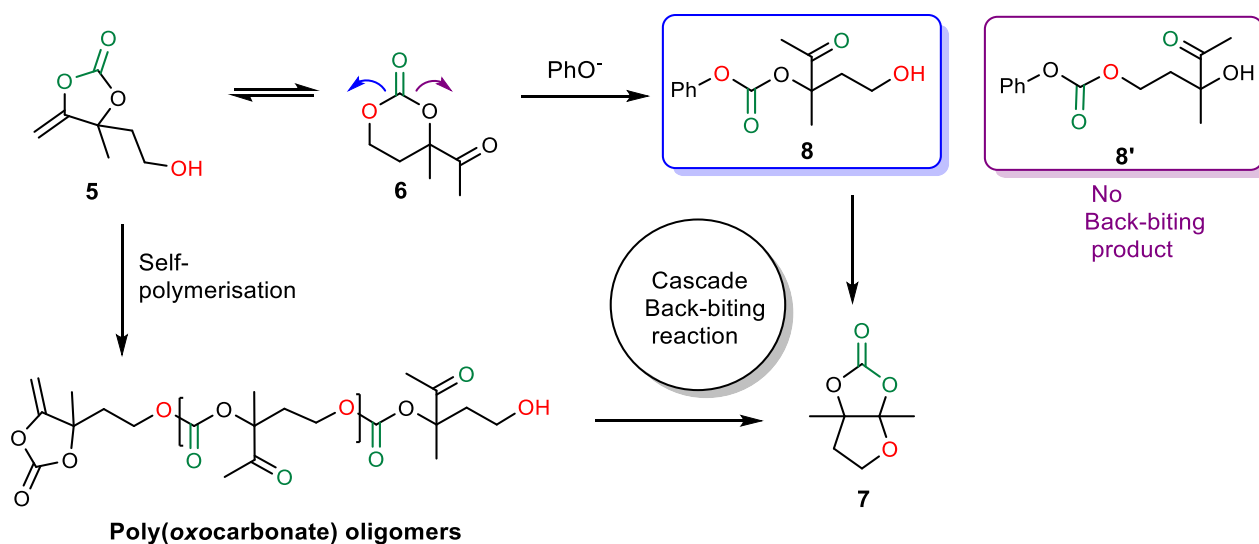


Figure 6. SEC trace of the crude mixture presented in **Table 2**, entry 2.

These oligomers are of very low molar mass as shown by SEC analysis (**Figure 6**) of the crude product. They can originate from the ring-opening oligomerisation of **6** or from the autopolymerisation of the exovinylene cyclic carbonate (AB monomer; product **5**) (**scheme 10 and 11**). Indeed, with the current knowledge of the reaction, one cannot exclude that **6** can revert into the exovinylene cyclic carbonate **5** (AB monomer) in the presence of the organocatalyst. **Scheme 12** summarises the main reactions occurring and illustrates the different products formed when reacting **6** with the phenolate catalyst. The ring-opening of **6** initiated by the addition of the phenolate onto the carbonate group yields two regioisomers, **8** and **8'**. While **8** can undergo a cascade ring-closure process to yield **7**, product **8'** is not prone to this reaction and will remain as a side product. The self-polymerisation of the AB monomer gives the polycarbonate oligomers that can undergo cascade back-biting reactions to produce **7**.

To discriminate which mechanism is predominant, DFT calculations should be conducted.

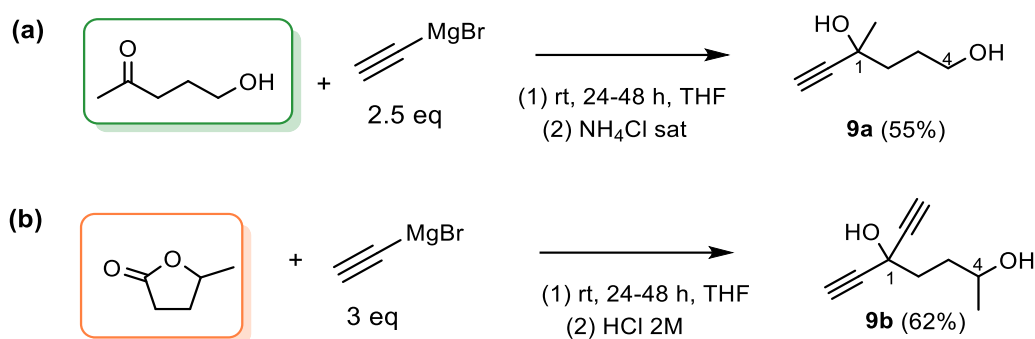


Scheme 12. General scheme showing the reaction of keto-carbonate **6** with the phenolate catalyst and the products formed.

2.4. Coupling of CO₂ with alkyne-1,4-diols

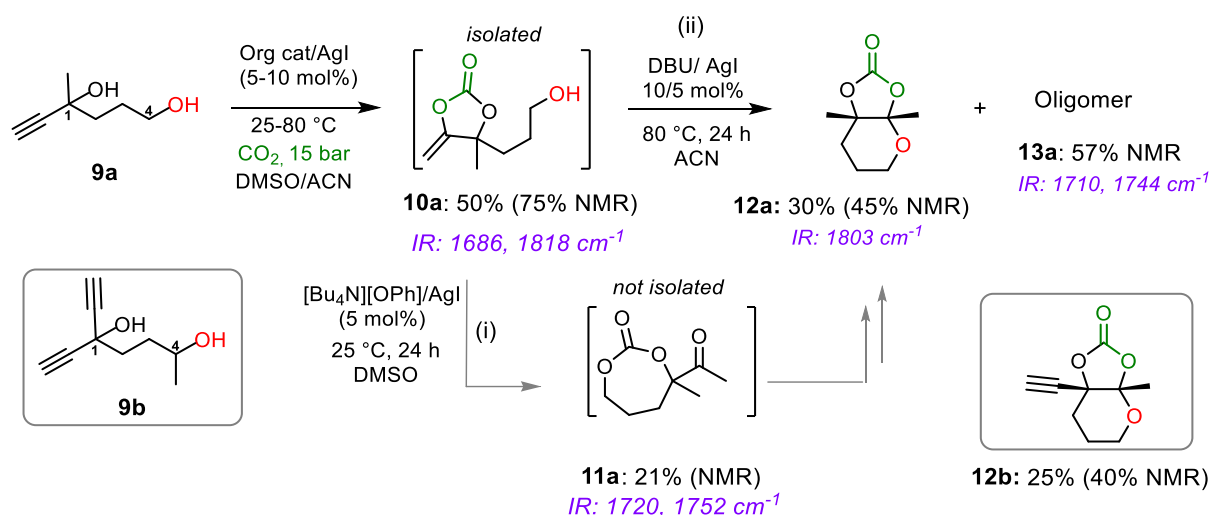
Still interested in preparing an AB monomer that would deliver poly(*oxo*-carbonate)s, we evaluated if increasing the spacer between the propargylic alcohol and the alcohol by using alkyne-1,4-diols, would disfavour the rearrangement into a keto-carbonate and the tetrasubstituted ethylene carbonate.

The alkyne-1,4-diols were prepared by two main approaches, the first involved the reaction of a commercial hydroxyketone with an excess of ethynylmagnesium bromide similar to the alkyne-1,2-diols, and yielding alkyne-1,4-diol **9a** in 55% yield. In the second approach, a 5-membered lactone was used as carbonyl source, providing **9b** which bears an additional alkyne function in 62% yield (**Scheme 13**). ¹H and ¹³C NMR characterisation of pure compounds are given in **Figures S6** and **S7**.



Scheme 13. Strategies employed for the synthesis of alkyne-1,4-diols (a) from a hydroxyketone and (b) from gamma valerolactone, with the respective isolated yields.

We then subjected alkyne-1,4-diol **9a** and **9b** to a similar carboxylation process (**Scheme 14**) and monitored the transformation by operando FT-ATR.



Scheme 14. Carboxylative coupling of 1,4-diols **9a** and **9b** with CO₂.

At 25 °C, 15 bar of CO₂ with [nBu₄N][OPh]/AgI as catalyst, **9a** is converted into a mixture of the exovinylene cyclic carbonate **10a** as attested by the presence of the olefinic and carbonyl vibrations at 1685 cm⁻¹ and 1818 cm⁻¹, respectively, and a seven-membered cyclic carbonate with pendant ketone **11a**, characterised by the carbonyl vibration at 1752 cm⁻¹ (Figure 9). Unlike the 1,2- or 1,3-alkynediols that afforded quantitatively and rapidly the oxo-functional five- and six-membered cyclic carbonate **3** and **6**, the formation of the larger seven-membered cyclic carbonate **11a** is rather slow. This is reflected in Figure 10, that benchmarks the rate of formation of each carbonate ring, obtained by in-situ FT-ATR spectroscopy.

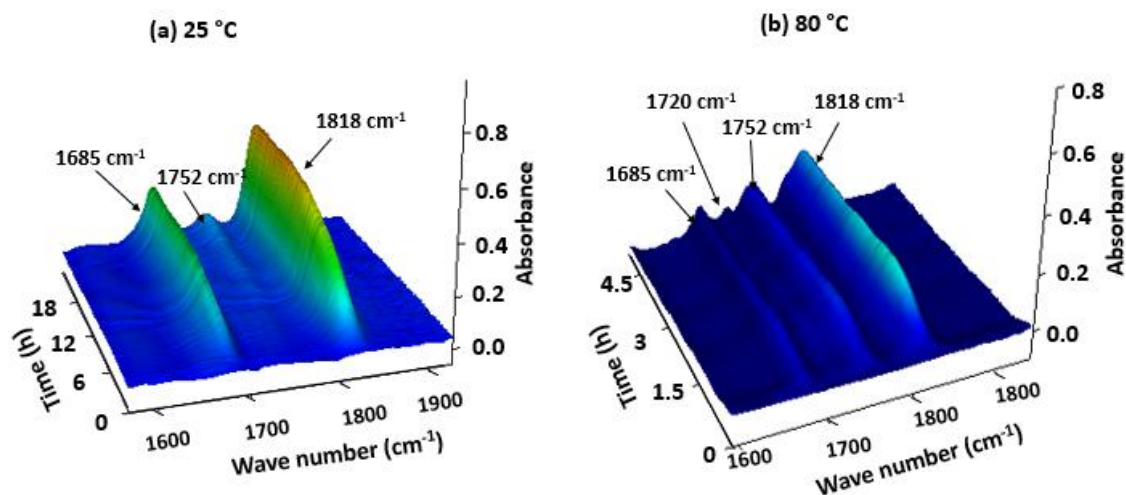


Figure 7. Online monitoring of the carboxylative coupling of 4-methylhex-5-yne-1,4-diol **9a** with CO₂ via operando FT-ATR spectroscopy at (a) 25 °C and (b) 80 °C showing the seven-membered carbonate **10a** with absorptions at 1752 and 1720 cm⁻¹.

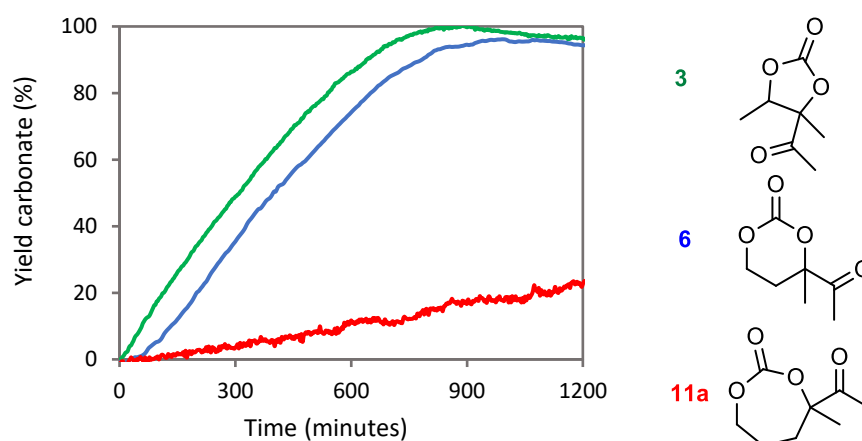


Figure 8. Comparison of the rate of formation of 5CC (**2**), 6CC (**7**) and 7CC (**12**) at 25 °C.

At 80 °C, the formation of the exovinylene cyclic carbonate **10a** is accelerated, as attested by the rapid growth of the bands at 1685 cm⁻¹ and 1818 cm⁻¹ and a plateau attained within 3 h of reaction. We also observed the progressive broadening of the band at 1818 cm⁻¹ with time. This results from the appearance of a band at 1807 cm⁻¹, that is the signature of the tetrasubstituted carbonate **12a**. After optimisation (Table 3), the bicyclic carbonate **12a** could

be produced with a 45% NMR yield (33% isolated) in the presence of AgI/DBU (**Table 3**, entry 6). A similar observation was made when using alkyne-1,4-diol **9b**, and the the bicyclic carbonate **12b** was isolated in 25% yield.

Table 3. Screening of parameters for the carboxylative coupling of alkyne-1,4-diol **9a** with CO₂.

Entry	[AgI] [mol%]	Ligand [mol%]	T (°C)	Conv. 9a [%] ^[a]	10a [%] ^[a]	11a [%] ^[a] 1	12a [%] ^[a]	13a [%] ^[a]
1 ^[b]	5	[Bu ₄ N][OPh], 5	25	>99	75, 50 ^[d]	21	–	–
2 ^[b]	5	[Bu ₄ N][OPh], 5	80	>99	7	1	24	68
3	5	[Bu ₄ N][OPh], 5	80	>99	7	3	16	74
4	5	DBU, 5	80	>99	3	5	25	67
5	–	DBU, 10	80	>99	–	–	24 ^[c]	76
6	5	DBU, 10	80	>99	–	12	45, 33 ^[c]	33

Conditions: 1,4-diol **9** (1 g, 8.76 mmol), AgI (0.102 g, 0.438 mmol), ACN (2 mL), $p_{(\text{CO}_2)} = 15$ bar and $t = 24$ h. [a] Determined by ¹H-NMR spectroscopy with 1,3,5-trimethoxybenzene as internal standard, [b] DMSO as solvent, [c] Isolated yield.

Analogous to the alkyne-1,3-diol/CO₂ coupling, oligomers were also formed, however as the main products at 80 °C. SEC analysis of the crude sample obtained with [nBu₄N][OPh]/AgI as catalyst (**Table 3**, entry 3) revealed oligomers of $M_n = 990$ g/mol ($M_w = 1500$ g/mol)(**Figure 9**).

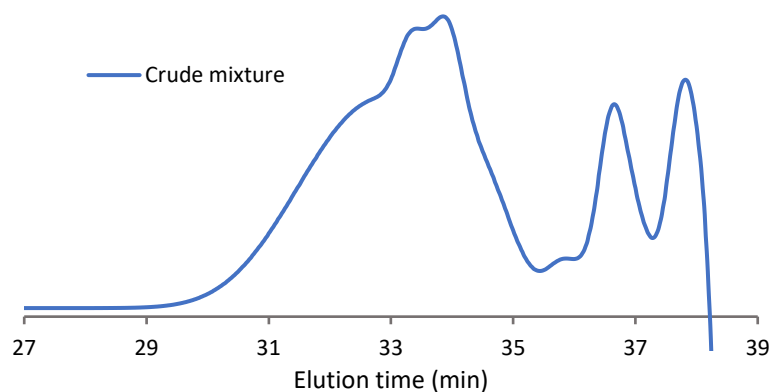
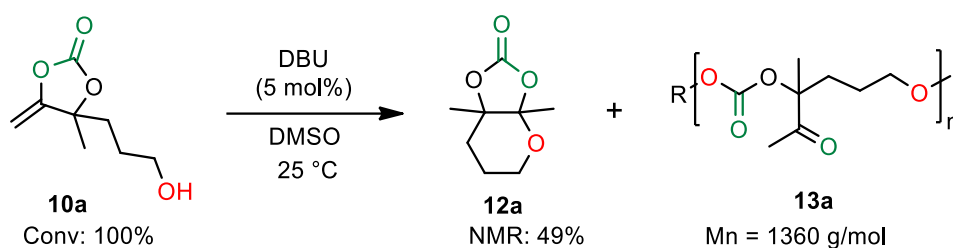


Figure 9. SEC chromatogram of the crude mixture obtained by reaction at 80 °C in ACN after 24 h with [nBu₄N][OPh]/AgI as catalyst (**Table 3**, entry 3).

As the exovinylene carbonate **10a** is a difunctional AB molecule that is expected to self-polymerise in the presence of an appropriate catalyst, we isolated it from the experiment carried out at 25 °C. Then, we studied its homopolymerisation at 25 °C in the presence of DBU (5 mol%), i.e. the organocatalyst commonly used for the step-growth copolymerisation of bis(exovinylene cyclic carbonate)s with diols^[18,107] (**Scheme 15**). After 24 h of reaction, a complete conversion of **10a** was achieved and provided a mixture of **12a** (NMR yield of 49%) and oligomers **13a** ($M_n = 1360$ g/mol, $\mathcal{D} = 1.35$) (**Figure 10**). All attempts to push the polymerisation further to reach higher molar masses were unsuccessful as the formation of product **12a** could not be avoided.



Scheme 15. DBU-catalysed step-growth homopolymerisation of exovinylene cyclic carbonate **10a** at 25 °C.

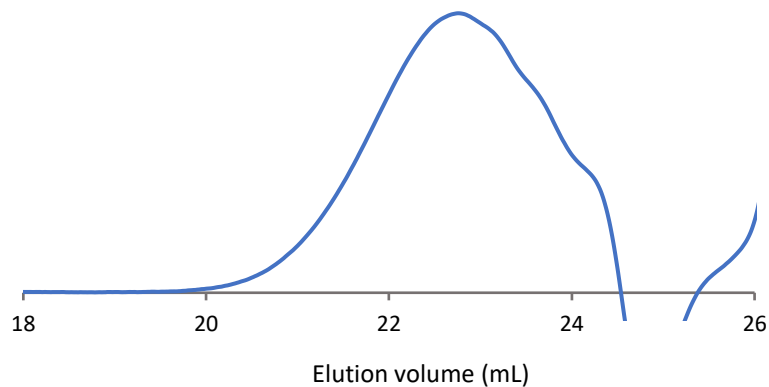
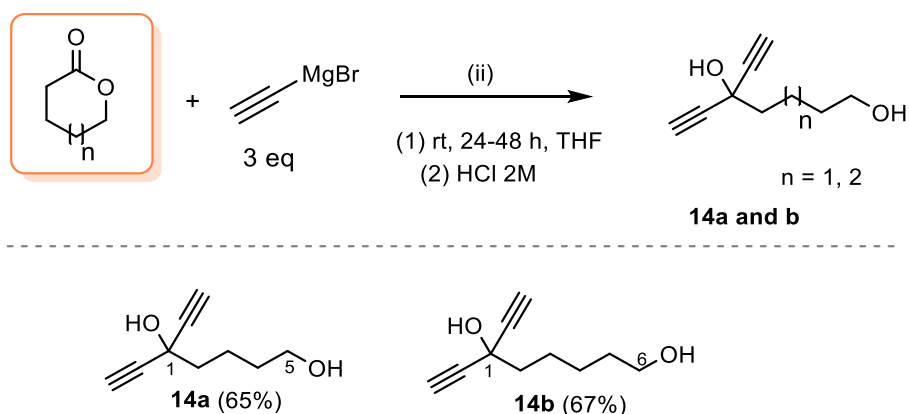


Figure 10. SEC chromatogram of the crude reaction mixture obtained by the DBU-catalysed step-growth homopolymerisation of **10a**.

2.5. Coupling of CO₂ with alkyne-1,5- and 1,6- diols

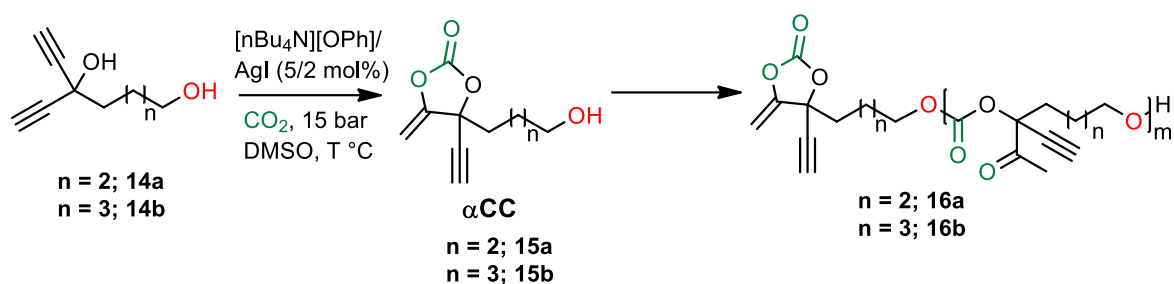
As the alkyne-1,3- and 1,4-diol with ethylene and propylene spacers between the two OH moieties favoured the formation of cyclic products, we postulated that higher alkyne-1,*n*-diols (*n* = 5 or 6) would turn the selectivity of the reaction towards poly(*oxo-carbonate*)s as larger rings are less prone to be formed.

Like previously, the alkyne-1,5 and 1,6-diols had to be synthesised. However, in this case, only the approach involving the reaction of lactones with excess ethynyl magnesium bromide was applied, as there were no commercially available adequate hydroxyketones. By reacting delta δ -valerolactone or ϵ -caprolactone with 3 equivalents of ethynyl magnesium bromide, alkyne-1,5-diol (**14a**) and alkyne-1,6-diol (**14b**) were obtained in 65 and 67% yield respectively (**Scheme 16**) and characterised by ¹H and ¹³C NMR (**Figure S8** and **S9**). Sadly, due to the easy polymerisability of 6- and 7- membered lactones, the corresponding alkyne-diols obtained were contaminated with some polyester oligomers (10-17%) which we could not remove from the crude reaction mixture. Nonetheless, this route afforded monomers with an additional alkyne function, which could be exploited for post polymerisation functionalisation.



Scheme 16. Strategy employed for the synthesis of alkyne-1,5-diol and alkyne-1,6-diol and structure of synthesised alkyne-diols with the respective isolated yields.

We then evaluated the carboxylative cyclisation of the alkyne-1,5-diol (**14a**) and alkyne-1,6-diol (**14b**) with CO₂, using the [nBu₄N][OPh]/AgI catalytic system for 24 h of reaction at 25 °C (**Table 4**).

Table 4. Carboxylative coupling of alkyne-1,5- and 1,6- diols with CO₂.

Entry	Alkyne-1,n-diol	T (°C)	Time (h)	^a Alkyne-1,n-diol Conv.(%)	^a αCC yield (%)	^b M _n (g/mol)	^b M _w (g/mol)	^b Đ
1		25	24	46	16	nd	nd	nd
2	14a	40	24	65	15	1200	1940	1.62
3		80	24	86	2	1100	1900	1.68
4		25	24	65	30	1500	2850	1.86
5	14b	40	24	95	6	1300	2000	1.56
6		40	48	98	3	1600	2880	1.76

Conditions: alkyne-1-n-diol (**14a** or **b**) (0.5 g), [nBu₄N][OPh] (5 mol%), AgI (2 mol%), PCO₂ = 15 bar, DMSO (1 mL, 3 M). ^aDetermined by ¹H NMR spectroscopy with 1,3,5-trimethoxybenzene as internal standard, ^bDetermined by SEC in DMF LiBr with polystyrene calibration.

Under these operating conditions, 46% conversion of alkyne-1,5-diol (**14a**) was observed (Table 4, entry 1). ATR analysis revealed the characteristic vibration of the exocyclic olefin at 1692 cm⁻¹ and the carbonyl elongation at 1828 cm⁻¹ of the exovinylene cyclic carbonate (Figure 11). The quasi absence of other carbonyl signals in 1700-1760 cm⁻¹ region suggested the formation of the exovinylene cyclic carbonate with the supposed structure **15a** as major product. By increasing the temperature to 40 °C, higher **14a** conversion of 65% was attained (Table 4, entry 2). ATR analysis revealed two new bands at 1730 and 1750 cm⁻¹ which corresponds to a ketone and a linear carbonate respectively (Figure 11). The low intensity of the typical elongations of **15a** suggested that this AB monomer was further transformed at 40 °C into linear chains. SEC analysis of the crude product confirmed the formation of oligomers of M_n = 1200 g/mol (Figure 13).

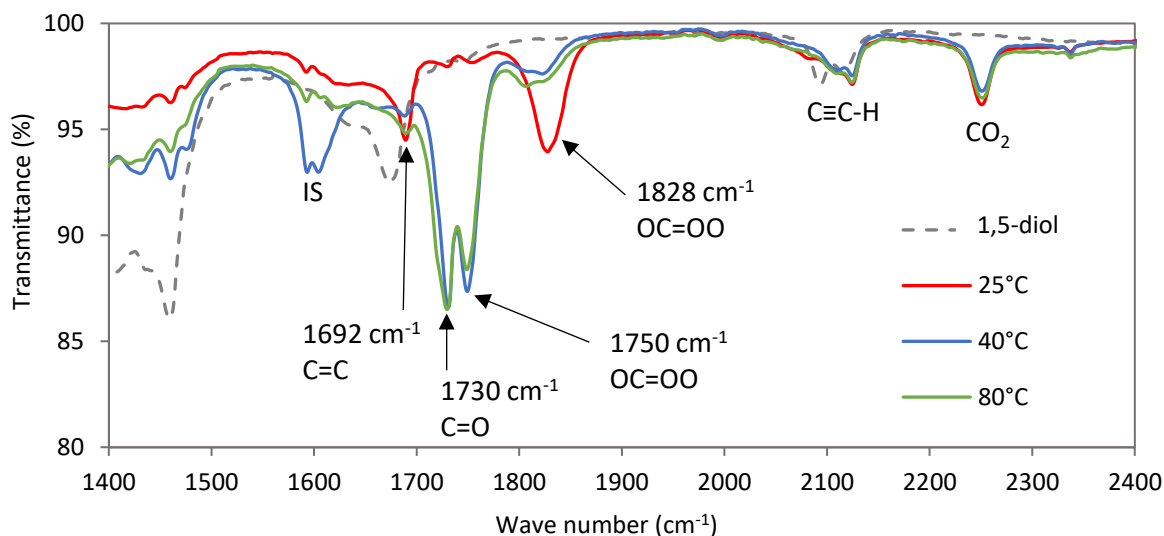


Figure 11. ATR spectra overlay of alkyne-1,5-diol (**14a**) and the crude mixtures obtained after carboxylative coupling with CO₂ at 25, 40 and 80 °C. Conditions: alkyne-1,4-diol **14a** (0.5 g), [nBu₄N][OPh] (5 mol%), AgI (2 mol%), PCO₂ = 15 bar, DMSO (1 mL, 3 M). IS = internal standard.

Further increasing the temperature to 80 °C resulted in a higher **14a** conversion of 86%, however oligomers with a similar M_n were produced (**Table 4**, entry 3).

The crude mixture obtained at 40 °C was further characterised by ¹H- and ¹³C-NMR spectroscopy (**Figure 12**). We observe doublet signals at 4.86 and 5.06 ppm which are characteristics of the alkene protons of the exovinylene cyclic carbonate. In addition, the resonance at 4.11 ppm can be attributed to the methylene protons in α of the carbonate function, as well as two singlets at 2.24 and 2.30 ppm typical of a methyl in α of a ketone function. The presence of resonances at 153.48, 153.60 and 150.54 ppm and at 201 and 206 ppm in ¹³C-NMR can be attributed to carbonates and ketones, respectively. It further corroborates the observations made by ATR analysis which suggested the formation of exovinylene cyclic carbonate **15a** and poly(oxo-carbonate) **16a**. The presence of two ketone signals might suggest the formation of a hydroxyketone, which has been shown to arise from transcarbonatation reactions or hydrolysis of the exovinylene cyclic carbonate.^[107] We did not succeed in isolating the oligomers from the reaction mixture, so cleaner spectra could not be recorded.

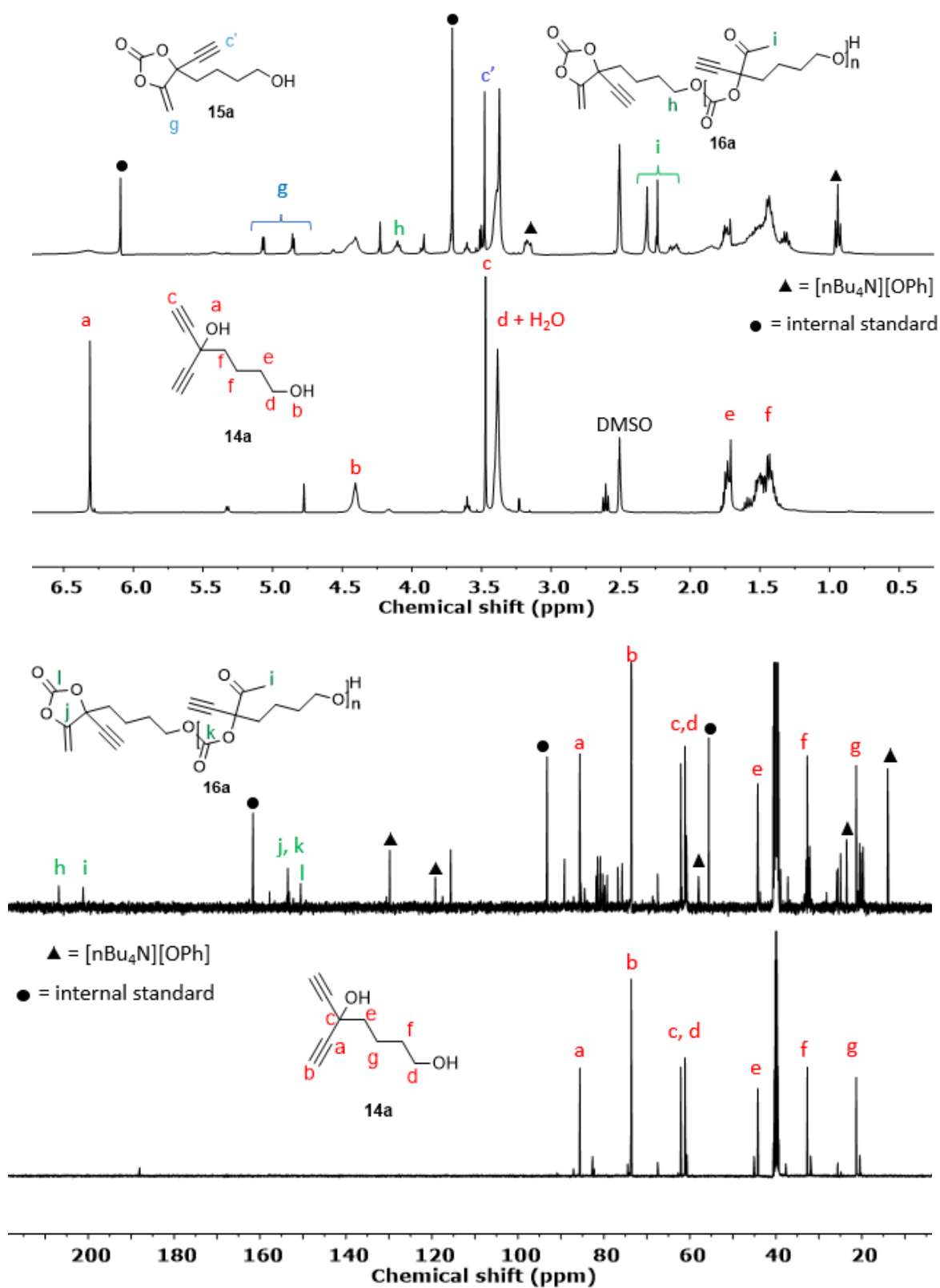


Figure 12. ^1H - and ^{13}C -NMR overlay in $\text{DMSO-}d_6$ of (bottom) alkyne-1,4-diol and (top) the crude mixture obtained after carboxylative coupling with CO_2 at 40°C .

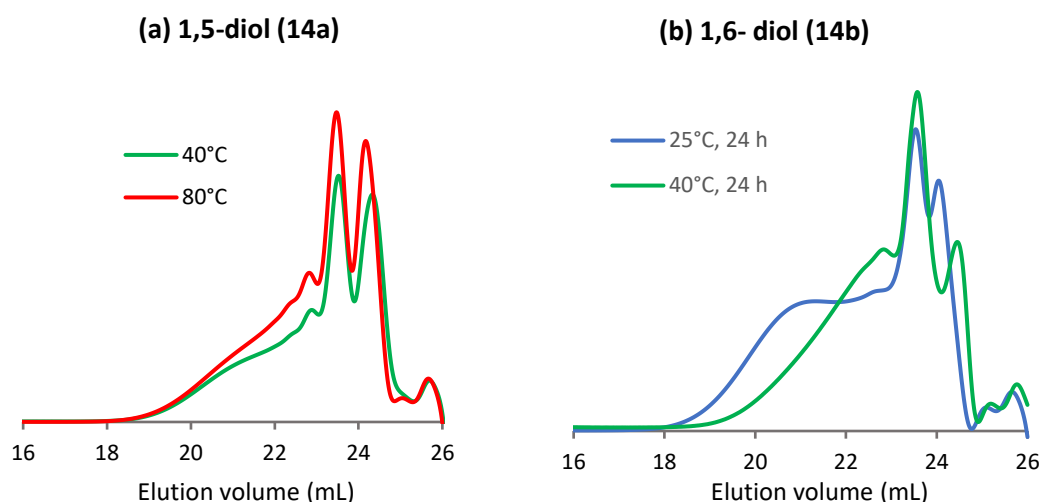


Figure 13. Carboxylative coupling of alkyne-1,5 and 1,6-diols (**14a** & **b**) with CO₂. SEC chromatograms in DMF LiBr obtained on the crude mixtures presented in **Table 4**, entries 2-5.

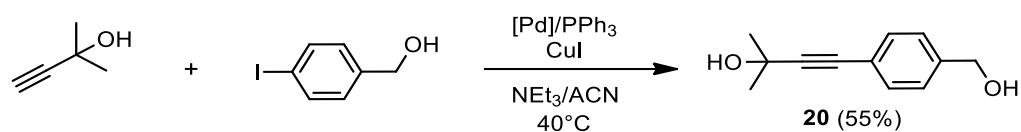
With the alkyne-1,6-diol (**14b**), at 25 °C after 24 h, 65% conversion of the alkyne were obtained, providing a mixture of the exovinylene cyclic carbonate (30%) and oligomers (70%) of $M_n = 1500$ g/mol (**Table 4**, entry 4). Increasing the reaction temperature to 40 °C for 24 h and 48 h resulted in a higher conversion of **14b**, i.e. 95 % and 98% respectively, although no increase in the molar masses of the oligomers was achieved. Nonetheless, the exovinylene cyclic carbonate (**15b**) was only detected as traces (**Table 4**, entries 5-6).

As mentioned in the introductory paragraph, the synthesis of alkyne-1,5 and 1,6-diols **14a** and **14b** by ring-opening of 6- and 7-membered lactones with ethynylmagnesium bromide was rather challenging as these cyclic esters are prone to facile polymerisation. Hence, both products **14a** and **14b** were contaminated by species bearing ester linkages that were difficult to separate (see **Figure S 8** and **Figure S 9**). Unfortunately, the presence of these species may interfere in the preparation of poly(oxo-carbonate)s by our cascade approach as the ester linkages may participate in transesterification reactions. This would result in unreactive chain ends.

Quite unfortunately, our attempts to isolate the oligomers proved to be extremely difficult, thus preventing us from properly characterising the oligomers.

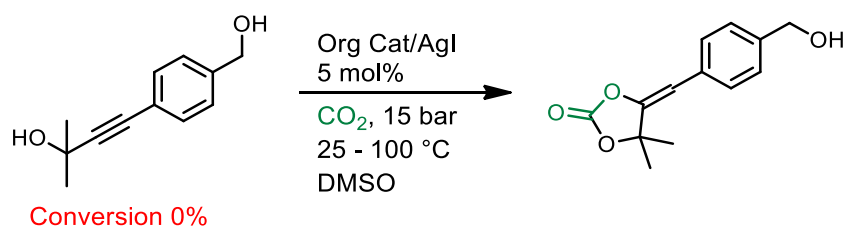
2.6. Coupling of CO₂ with internal alkyne-1-n-diol

In our quest to prepare poly(*oxo*-carbonate)s from alkyne 1,*n*-diols, we synthesised a new monomer with a phenyl group separating the two reactive groups. The rigidity induced by the presence of the phenyl ring is expected to avoid any intramolecular rearrangements, hence making this monomer a suitable candidate for preparing polymers. Moreover, the phenyl ring could bring some interesting mechanical properties, i.e. additional rigidity to the polymer chains. This monomer was synthesised by the Sonogashira coupling between a propargylic alcohol and an iodophenylalcohol compound (**Scheme 17**), which yielded internal alkyne diol **20** in 55% yield (see **Figure S 3 and 10**).^[220]



Scheme 17. Synthesis of internal alkyne-1-n-diol by Sonogashira coupling.

Unfortunately, we were not successful in achieving its carboxylation using our systems based on [nBu₄N][OPh]/AgI or DBU/AgI at 25-100 °C (**Scheme 18**). This is however not surprising as we know from the literature^[73,74] that internal propargylic alcohols are more challenging to carboxylate. The use of another catalytic system such as DavePhos/AgOAc, which has been shown to catalyse the coupling of CO₂ to various propargylic alcohol substrates including internal ones, should allow to solve this reactivity issues.^[77]



Scheme 18. The coupling of CO₂ with 4-(4-(hydroxymethyl)phenyl)-2-methylbut-3-yn-2-ol (**20**).

3. Conclusions

We have reported the synthesis of new alkyne-1-*n*-diols with the objective to utilise them for producing poly(*oxo*-carbonate) by copolymerisation with CO₂. It was indeed hypothesised that the *in-situ* carboxylation of the alkyne-1-*n*-diols would provide an alkylidene cyclic carbonate bearing an alcohol function, thus an AB monomer, that is expected to homopolymerise. Various alkyne-1-*n*-diols were prepared and tested for the reaction. Surprisingly, the use of alkyne-1,2-diols gave a wide range of keto-substituted five-membered carbonates with different and unique degrees of substitutional complexity by using tetrabutyl ammonium phenolate combined to AgI or a DavePhos ligand combined to AgF as catalytic system at 25-40 °C. No polymerisation was achieved under the investigated conditions. With alkyne-1,3 and 1,4-diols, we showed that the corresponding 6- and 7-membered keto-carbonates were also obtained at 25 °C whereas elusive tetrasubstituted carbonate scaffolds were also formed at 80 °C, together with tiny amounts of poly(*oxo*-carbonate) oligomers. By combining operando FT-IR studies, experimental observations and computational studies, we suggested some mechanisms for the formation of the keto-carbonates and the tetrasubstituted ethylene carbonate compounds. We further demonstrated that by using higher alkyne-1,*n*-diols (*n*=5 & 6) the selectivity was tuned towards the formation of poly(*oxo*-carbonate) oligomers, thus expanding the synthetic importance and potential of cascade approaches in the valorisation of carbon dioxide.

4. Experimental section

4.1. Materials

Ethynyl magnesium bromide (Acros), silver iodide, 4-, δ -valerolactone, γ -valerolactone, ϵ -caprolactone, 3-hydroxy-2-butanone, 4-hydroxy-2-butanone, 5-hydroxy-2-pentanone, palladium acetate was purchased from Aldrich/Merch. Iodophenylmethanol was purchased from fluorochem. CO₂ (N27) was purchased from Air liquid, dimethyl sulfoxide (DMSO), dimethyl formamide (DMF), acetonitrile (ACN), methanol (MeOH), diethylether were purchased from Acros. Diazabicyclo(5.4.0)undec-7-ene (DBU) (99%) was purchased from Fluka. DMSO was dried on a 3 Å molecular sieve conditioned at 100 °C under vacuum for 24 h. All the other reagents were used as received without any further purification. DMSO-*d*₆ was purchased from Eurisotop.

Tetrabutylammonium phenolate was prepared following the procedure described in **chapter 2**.

4.2. Analytical methods

¹H NMR analyses were performed on Bruker Advance 400 MHz spectrometers in DMSO at 25 °C in the Fourier transform mode. 16 scans for ¹H spectra and 512 or 2048 scans for ¹³C spectra were recorded.

Fourier transform infrared spectra were recorded using a Nicolet IS5 spectrometer (Thermo Fisher Scientific) equipped with a transmission or with a diamond attenuated transmission reflectance (ATR) device. Spectra were obtained in transmission or ATR mode a32 spectra accumulation in the range of 4000-500 cm⁻¹, with a nominal resolution of 4 cm⁻¹.

Number-average molecular weight (*M*_n) and dispersity (\bar{D}) of the different polymers were determined by size exclusion chromatography (SEC) in dimethylformamide (DMF) containing LiBr (0.025 M) at 55 °C (flow rate: 1 mL/min) with a Waters chromatograph equipped with two columns dedicated to the analysis of low molar mass polymers (PSS gram analytical 100 Å, separation range 300-60000 Da) and a pre column (100 Å), a dual λ absorbance detector (Waters 2487) and a refractive index detector (Waters 2414). A previously established PS calibration curve was used.

In-situ IR spectroscopy experiments were conducted using a stainless-steel reactor suitable for high-pressure measurements (up to 400 bar) and high temperature (up to 100 °C) coupled with a FT-MIR spectrometer from Bruker, equipped with an air-cooled globar source (12 V), a KBr beam splitter, a mechanical rocksolid interferometer, permanently aligned, a diamond ATR fibre probe IN350-T (\varnothing 6 mm) and a liquid nitrogen cooled mercury cadmium telluride (MCT). Single beam spectra recorded in the spectral range (670-3500 cm⁻¹) with a 4 cm⁻¹ resolution were obtained after the Fourier transformation of 32 accumulated interferograms until the end of reaction time.

X-ray analysis. Single crystals of each compound suitable for X-ray diffraction were stable under atmospheric conditions; nevertheless, they were treated under inert conditions immersed in perfluoro-polyether as protecting oil for manipulation. Data Collection: measurements were made on a Bruker-Nonius diffractometer equipped with an APPEX II 4K CCD area detector, a FR591 rotating anode with MoK α radiation, Montel mirrors and a Kryoflex low temperature device ($T = -173$ °C). Full-sphere data collection was used with ω and φ scans. Programs used: Data collection Apex2 V2011.3 (Bruker-Nonius 2008), data reduction Saint+Version 7.60A (Bruker AXS 2008) and absorption correction SADABS V. 2008-1 (2008). Structure Solution: SHELXTL Version 6.10 (Sheldrick, 2000) was used (Sheldrick, G. M. SHELXTL Crystallographic System, version 6.10; Bruker AXS, Inc.: Madison, WI, 2000). Structure Refinement: SHELXTL-97-UNIX VERSION.

DFT Computation. The Gaussian 16 B.01 program was used with the implemented functional and basis set PBE0-D3(BJ)/def2tzv being chosen using dispersion correction with Becke-Johnson damping. All calculations were carried out at 298 K using an acetonitrile implicit solvent model SMD.

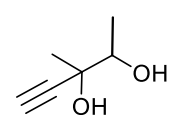
4.3. Experimental procedures

General procedure for the synthesis of alkyne-diols

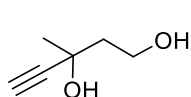
From hydroxy ketones: example of 3-methylpent-4-yne-1,3-diol (4)

In a clean dry double-neck 2L round bottom flask conditioned under an inert atmosphere was introduced EtMgBr (800 mL, 0.5 M in THF, 0.4 mole). Then, 4-hydroxy-2-butanone (13.8 mL, 0.16 mole) was added dropwise using a syringe. The reaction mixture was stirred at room temperature for 48 h, during which the conversion of the ketone was monitored by ATR-IR. Then, a saturated solution of NH₄Cl was added and the mixture was transferred into a separating funnel to recover the organic phase. The aqueous phase was extracted with diethyl ether (200 + 150 mL). The combined organic fractions were dried with anhydrous MgSO₄ and filtered. Then the organic phase was evaporated in vacuo and the residue purified by fractional distillation. A transparent to light yellow oil was recovered in a yield of around 60% at 55 °C with a vacuum of 1 mbar. A similar procedure was applied for the synthesis of **1** and **9** using the appropriate hydroxy ketone precursor giving a similar isolated yield.

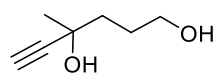
3-methylpent-4-yne-2,3-diol (1)



light pink oil. ¹H NMR (400 MHz, DMSO-*d*₆) δ 5.09 (d, $J = 36.0$ Hz, 1H), 4.57 (s, 1H), 3.41 (s, 1H), 3.11 (s, 1H), 1.27 (d, $J = 13.4$ Hz, 3H), 1.11 (d, $J = 6.4$ Hz, 3H). ¹³C NMR (101 MHz, DMSO-*d*₆) δ (in ppm) 73.10, 65.62, 58.21, 46.12, 39.56, 30.71.

3-Methylpent-4-yne-1,3-diol (4)

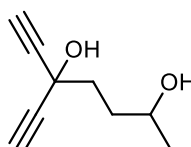
Light yellow oil. ^1H NMR (400 MHz, $\text{DMSO-}d_6$) δ 5.29 (s, 1H), 4.44 (s, 1H), 3.59 (s, 2H), 3.23 (s, 1H), 1.74 (s, 2H), 1.34 (s, 3H); ^{13}C NMR (101 MHz, $\text{DMSO-}d_6$) δ 73.10, 65.62, 58.21, 46.12, 39.56, 30.71.

4-Methylhex-5-yne-1,4-diol (9a)

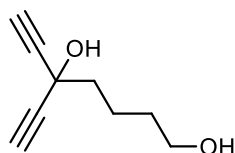
Light orange oil. ^1H NMR (400 MHz, $\text{DMSO-}d_6$) δ 5.23 (s, 1H), 4.42 (t, $J = 5.2$ Hz, 1H), 3.40 (t, $J = 5.7$ Hz, 2H), 3.16 (s, 1H), 1.70 – 1.46 (m, 4H), 1.33 (s, 3H); ^{13}C NMR (101 MHz, $\text{DMSO-}d_6$) δ 89.69, 72.83, 66.44, 61.47, 40.60, 30.33, 28.43.

From lactones: example of 5-ethynylhept-6-yne-2,5-diol (9b).

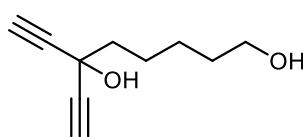
In a clean dry double-neck 2L round bottom flask conditioned under an inert atmosphere was introduced EtMgBr (800 mL, 0.5 M in THF, 0.4 mole). Then, γ -valerolactone (13 mL, 0.16 mole in 20 ml THF) was added dropwise via an addition funnel at rt. The reaction mixture was stirred at room temperature for 48 h, during which the conversion of the ketone was monitored by ATR-IR. Then, HCl 2M solution (200 mL) was added and the mixture was stirred for 2 h, after which the mixture was transferred into a separating funnel to recover the organic phase. The aqueous phase was extracted with diethyl ether (200 + 150 mL). The combined organic fractions were dried with anhydrous MgSO_4 and filtered. Then, the organic phase was evaporated in vacuo and the residue purified by flash silica gel column chromatography with ethyl acetate as eluent. An orange solid was recovered with a yield of around 60%. A similar procedure was applied for the synthesis of **14a** and **b**, using the appropriate lactone precursor giving a similar isolated yield.

5-ethynylhept-6-yne-2,5-diol (9b).

^1H NMR (400 MHz, $\text{DMSO-}d_6$) δ 6.32 (s, 1H), 4.47 (d, $J = 4.7$ Hz, 1H), 3.59 (dq, $J = 11.9, 5.9$ Hz, 1H), 3.54 (s, 2H), 1.78 (dddd, $J = 76.8, 12.7, 9.5, 6.9$ Hz, 2H), 1.52 (tdd, $J = 12.8, 6.3, 4.4$ Hz, 2H), 1.05 (d, $J = 6.2$ Hz, 3H). ^{13}C NMR (101 MHz, $\text{DMSO-}d_6$) δ 85.62, 73.66, 66.04, 62.05, 40.93, 34.41, 24.19.

5-ethynylhept-6-yne-1,5-diol (14a).

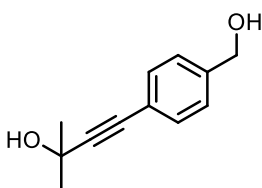
^1H NMR (400 MHz, $\text{DMSO-}d_6$) δ 6.32 (s, 1H), 4.40 (s, 1H), 3.47 (s, 2H), 3.38 (q, 2H), 1.77-1.67 (m, 2H), 1.60-1.33 (m, 4H). ^{13}C NMR (101 MHz, $\text{DMSO-}d_6$) δ 85.59, 73.65, 62.10, 61.12, 44.19, 32.67, 21.31. Note: contaminated with polyesters.

6-ethynyloct-7-yne-1,6-diol (14b).

^1H NMR (400 MHz, Chloroform-*d*) δ 4.09 (t, 1H) 3.66 (s, 2H), 2.64 (s, 2H), 2.59 (s, 1H), 1.94 (s, 2H), 1.64 (s, 4H), 1.44 (s, 2H). ^{13}C NMR (101 MHz, Chloroform-*d*) δ 83.95, 71.79, 62.70, 43.33, 40.73, 32.46, 25.38, 24.10. Note: contaminated with polyesters

By sonogashira coupling: example of 4-(4-(hydroxymethyl)phenyl)-2-methylbut-3-yn-2-ol

In a clean 250 mL round bottom flask equipped with a magnetic bar were added in the following order, iodobenzenemethanol (4g, 17 mmol, 1 eq), acetonitrile (48 mL), triethylamine (38 mL), Pd(OAc)₂ (0.15 g, 0.68 mmol, 0.04 eq), triphenylphosphine (0.36 g, 1.37 mmol, 0.08 eq) and CuI (0.17 g, 0.89 mmol, 0.05 eq). Then, 3-methyl-2-butyn-2-ol (2.878 g, 34.17 mmol, 2 eq) was added dropwise while stirring. The reaction was allowed to run at 40 °C for 24 h. Then a saturated NH₄Cl solution was added, followed by extraction with ethylacetate. The crude organic phase was evaporated to obtain a concentrated oxblood oil. The pure product was purified by silica gel chromatography with eluent ethylacetate/hexane, starting from a 20/80 mixture and gradually increasing to 60/40. A beige solid was recovered upon evaporation of the organic solvents with a 55% yield.

4-(4-(hydroxymethyl)phenyl)-2-methylbut-3-yn-2-ol (20)

Beige solid ^1H NMR (400 MHz, Acetone-*d*₆) δ (in ppm) 7.36 (s, 4H), 4.65 (d, *J* = 5.7 Hz, 2H), 4.46 (s, 1H), 4.33 (t, *J* = 5.8 Hz, 1H), 1.55 (s, 6H). ^{13}C NMR (101 MHz, Acetone-*d*₆) δ (in ppm) 142.68, 131.15, 126.42, 121.67, 94.74, 80.78, 64.22, 63.33, 31.18

Screening of reaction parameters for the carboxylative coupling of CO₂ to 3-methylpent-4-yne-1,3-diol (4)

In a clean dry reactor, equipped with a magnetic rod, a manometer and a gas inlet/outlet were introduced 3-methylpent-4-yne-1,3-diol (1 g, 8.76 mmol), tetrabutylammonium phenolate [nBu₄N][OPh] (0.147 g, 0.438 mmol), silver iodide (AgI) (0.102 g, 0.438 mmol) and dried DMSO (2-4 mL). The reactor was closed and placed in a silicon oil bath set heated at the desired temperature. After 30 min, CO₂ gas was added at a constant pressure. The reaction ran for 24-72 h after which the reactor was depressurised and placed in a water bath to cool it down to room temperature. The crude reaction mixture was characterised by ^1H NMR spectroscopy in DMSO-*d*₆.

Isolation of products was achieved by extraction of the crude mixture with 80 mL of salted water and 80 mL of CH₂Cl₂, followed by a silica gel chromatography (5-50% ethyl acetate/petroleum ether (40/60)).

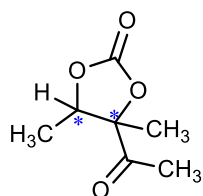
A similar procedure was applied with diol **9**

Monitoring of the carboxylative coupling of CO₂ to alkyne-diols by FT-IR spectroscopy: example of 3-methylpent-4-yne-1,3-diol (4)

In a clean and dry reactor of 40 mL equipped with a manometer, a heating mantle, gas inlet/outlets, a mechanical stirrer and a high-pressure FT-IR probe were introduced 3-methylpent-4-yne-1,3-diol **4** (3 g, 26.28 mmol), tetrabutylammonium phenolate [nBu₄N][OPh] (0.4410 g, 1.3141 mmol), AgI (0.3085 g, 1.3141 mmol) and dry DMSO (12 mL). The reactor was closed and heated to the desired temperature after which the FT-IR acquisition was initiated. Then, CO₂ gas was added and the pressure maintained at 15 bar. Spectra were recorded every 1-5 min. Once the reaction was complete, the reactor was cooled down to room temperature and depressurised. The crude reaction mixture was recovered and analyzed by ¹H NMR spectroscopy.

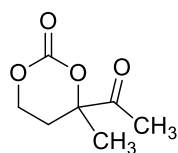
A similar procedure was applied with the diol **1** and **9**

4-acetyl-4,5-dimethyl-1,3-dioxolan-2-one (1)



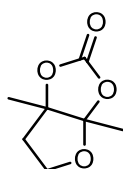
Yellow oil. (70%) Eluent petroleum ether /EtOAc = 3/1 ¹H NMR (400 MHz, DMSO-*d*₆) δ (in ppm) 4.93 (q, *J* = 6.5 Hz, 1H), 2.31 (d, *J* = 4.9 Hz, 4H), 1.61 (s, 1H), 1.46 (s, 3H), 1.37 (d, *J* = 6.6 Hz, 3H), 1.25 (d, *J* = 6.6 Hz, 1H). ¹³C NMR (101 MHz, DMSO-*d*₆) δ 206.51, 206.15, 153.61, 153.13, 88.76, 88.15, 81.20, 77.12, 28.07, 25.55, 21.00, 17.01, 15.38.

4-acetyl-4-methyl-1,3-dioxan-2-one (6)

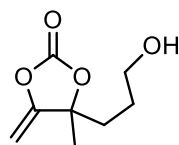


White solid, 51%. Eluent petroleum ether /EtOAc = 1/1 ¹H NMR (400 MHz, DMSO-*d*₆) δ 4.37 (dt, *J* = 11.3, 4.7 Hz, 1H), 4.10 (ddd, *J* = 11.3, 10.2, 4.1 Hz, 1H), 2.41 (dt, *J* = 14.7, 4.1 Hz, 1H), 2.28 (s, 3H), 2.12 (ddd, *J* = 14.7, 10.2, 5.0 Hz, 1H), 1.53 (s, 3H); ¹³C NMR (101 MHz, DMSO-*d*₆) δ 206.91, 147.83, 87.28, 65.52, 39.57, 28.20, 25.15, 23.35; IR (neat) ν = 1750, 1720 cm⁻¹; HRMS (QTOF) *m/z* Calcd for C₇H₁₀NaO₄ [M + Na]⁺ 181.0477; Found 181.0472.

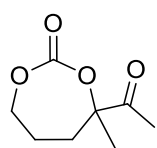
3a,6a-Dimethyltetrahydrofuro[2,3-*d*][1,3]dioxol-2-one (7)



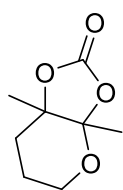
White solid, 70% Eluent hexanes/EtOAc = 5/1. ¹H NMR (400 MHz, DMSO-*d*₆) δ 4.05 (dd, *J* = 9.3, 7.9 Hz, 1H), 3.77 (ddd, *J* = 11.9, 9.4, 4.7 Hz, 1H), 2.29 (dd, *J* = 13.9, 4.6 Hz, 1H), 2.05 (ddd, *J* = 13.9, 11.9, 7.9 Hz, 1H), 1.57 (d, *J* = 4.7 Hz, 6H); ¹³C NMR (101 MHz, DMSO-*d*₆) δ 152.7, 114.8, 91.8, 65.6, 38.2, 20.3, 20.0; IR (neat): ν = 1802 cm⁻¹; HRMS (ESI/TOF) *m/z* Calcd for C₇H₁₀NaO₄ [M + Na]⁺ 181.0471; Found 181.0472. This compound was further characterised by X-ray crystallography

4-(3-Hydroxypropyl)-4-methyl-5-methylene-1,3-dioxolan-2-one (10a)

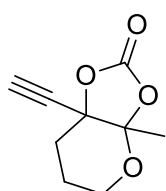
Yellow oil, NMR yield 75%, isolated: 50%. Eluent petroleum ether/ EtOAc 1:1
 ^1H NMR (400 MHz, DMSO- d_6) δ 4.85 (d, J = 3.9 Hz, 1H), 4.63 (d, J = 3.9 Hz, 1H), 4.53 (t, J = 5.2 Hz, 1H), 3.41 (td, J = 6.3, 5.1 Hz, 2H), 1.89 (qdd, J = 14.4, 9.8, 6.0, 2H), 1.60 (s, 3H), 1.43 (m, 2H); ^{13}C NMR (101 MHz, DMSO- d_6) δ 157.43, 151.46, 87.99, 86.46, 60.56, 36.68, 26.72, 25.94; IR (neat) ν = 1686, 1818 cm^{-1} ; HRMS (QTOF) m/z Calcd for $\text{C}_8\text{H}_{12}\text{NaO}_4$ [$\text{M} + \text{Na}$] $^+$ 195.1698; Found 195.0633.

4-Acetyl-4-methyl-1,3-dioxepan-2-one (11a)

Note: This compound was isolated as a mixture with 8. The data are here provided for completion. Selected features: ^1H NMR (400 MHz, DMSO- d_6) δ 4.07 (m, 2H), 2.39 (m, 2H), 2.25 (s, 3H, C(O)Me), 1.80 (m, 2H), 1.49 (s, 3H, Me); ^{13}C NMR (75 MHz, DMSO- d_6) δ 206.51, 153.07, 90.31, 70.04, 36.88; IR (neat) ν = 1720, 1752 cm^{-1} .

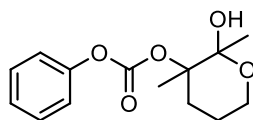
3a,7a-Dimethyltetrahydro-5H-[1,3]dioxolo[4,5-b]pyran-2-one (12a)

White solid, NMR yield 45%, isolated 30%. Eluent hexanes/ EtOAc = 5/1. ^1H NMR (400 MHz, DMSO- d_6) δ 3.72 (td, J = 6.4, 1.9 Hz, 2H), 1.97 (ddd, J = 14.8, 5.5, 4.1 Hz, 1H), 1.85 (ddd, J = 14.7, 10.6, 6.4 Hz, 1H), 1.76 – 1.60 (m, 2H), 1.54 (s, 3H), 1.40 (s, 3H); ^{13}C NMR (101 MHz, DMSO- d_6) δ 153.1, 107.3, 83.6, 60.7, 28.6, 22.9, 19.8, 18.6; IR (neat): ν = 1803 cm^{-1} ; HRMS (ESI/TOF) m/z Calcd for $\text{C}_8\text{H}_{12}\text{NaO}_4$ [$\text{M} + \text{Na}$] $^+$ 195.0628; Found 195.0628.

7a-ethynyl-3a-methyltetrahydro-3aH-dioxolo[4,5-b]pyran-2-one (12b)

White solid, NMR yield 42%, isolated 25%. Eluent hexanes/ EtOAc = 4/1. ^1H NMR (400 MHz, DMSO- d_6) δ 4.19 (s, 1H), 3.83 (dq, J = 12.3, 6.1, 2.2 Hz, 1H), 2.40 (ddd, J = 15.6, 4.1, 2.7 Hz, 1H), 2.22 (ddd, J = 15.5, 13.3, 4.7 Hz, 1H), 1.75 (s, 3H), 1.70 – 1.56 (m, 1H), 1.32 (tdd, J = 13.6, 11.1, 4.1 Hz, 1H), 1.15 (d, J = 6.2 Hz, 3H). ^{13}C NMR (101 MHz, DMSO- d_6) δ 151.61, 107.12, 82.30, 78.34, 78.04, 66.93, 30.07, 25.16, 23.86, 21.87.

IR (neat): ν = 1803 cm^{-1} ;

2-hydroxy-2,3-dimethyltetrahydro-2H-pyran-3-yl phenyl carbonate (13a''). Isolated linear carbonate intermediate

White solid, 3%. Eluent hexanes/ EtOAc = 5/1. ^1H NMR (400 MHz, DMSO- d_6) δ (in ppm) 7.34 – 7.24 (m, 2H), 7.17 – 7.09 (m, 2H), 7.06 – 6.97 (m, 1H), 4.38 (s, 1H), 3.76 – 3.58 (m, 2H), 2.10 (td, J = 13.0, 4.7 Hz, 1H), 1.87 – 1.69 (m, 1H), 1.70 – 1.45 (m, 2H), 1.18 (d, J = 16.7 Hz, 6H). ^{13}C NMR (101 MHz, DMSO- d_6) δ (in ppm) 155.43, 129.62, 125.08, 122.72, 120.98, 105.73, 70.98, 60.70, 34.29, 24.25, 23.29, 17.22.

Step-growth polymerisation of 4-acetyl-4-methyl-1,3-dioxan-2-one (6)

In a 25 mL round bottom flask equipped with a magnetic stirrer were introduced 4-acetyl-4-methyl-1,3-dioxan-2-one (**6**) (140 mg, 0.88 mmol), [nBu₄N][OPh] or diazabicycloundec-7-ene (DBU) (43.8 μmol), the silver iodide (AgI) (10.2 mg, 43.8 μmol) and dried DMSO (400 μL). The flask was closed with a stopcock and immersed in a silicon oil bath set at the desired temperature. A sample of the reaction mixture was taken after 1 h and 24 h of reaction and analysed by ¹H- and ¹³C-NMR spectroscopy in DMSO-*d*₆ and SEC in DMF.

Step-growth polymerisation of 4-methyl-4-(prop-1-en-2-yl)-1,3-dioxan-2-one (10)

In a 25 mL round bottom flask equipped with a magnetic stirrer were introduced 4-(3-Hydroxypropyl)-4-methyl-5-methylene-1,3-dioxolan-2-one (**10**) (0.5 g, 2.90 mmol), diazabicycloundec-7-ene (DBU) (21.65 μL, 5 mol%) and dried DMSO (1 mL). The flask was closed with a stopcock and immersed in a silicon oil bath set at 25 °C. A sample of the reaction mixture was taken after 24 h of reaction and analysed by ¹H- and ¹³C-NMR spectroscopy in DMSO-*d*₆ and SEC in DMF.

5. Supplementary information

SI- 1. Synthesis of alkyne-diols from hydroxy ketones

The total transformation of the hydroxy ketone was confirmed by the total shift of the methyl in α of the ketone at 2 ppm to 1.34 ppm in ^1H NMR, and by the disappearance of the ketone signal at 206 ppm in ^{13}C -NMR.

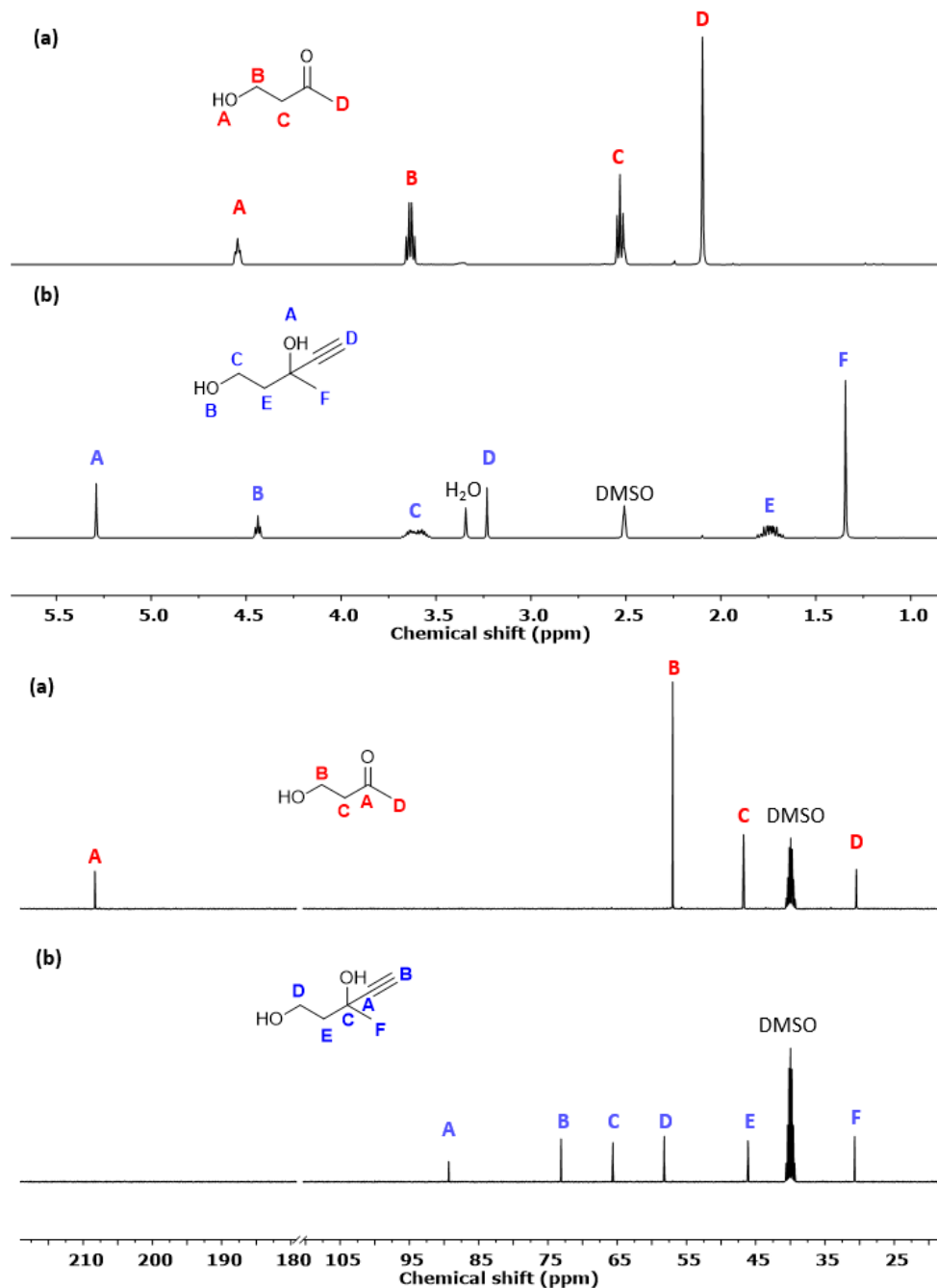


Figure S 1. ^1H -NMR and ^{13}C -NMR spectra in $\text{DMSO-}d_6$ of (a) 4-hydroxy-2-butanone and (b) 3-methylpent-4-yne-1,3-diol (4).

SI- 2. Synthesis of alkyne-diols from lactones

The success of the reaction was attested by the appearance of the alkyne proton D at 3.48 ppm and a shift of the methyne proton from 4.6 to 3.60 ppm. The disappearance of the C=O ester at 177 ppm was a further confirmation. Note that for the δ -valerolactone and ϵ -caprolactone, the diol obtain was contaminated by esters oligomers which we were unable to remove.

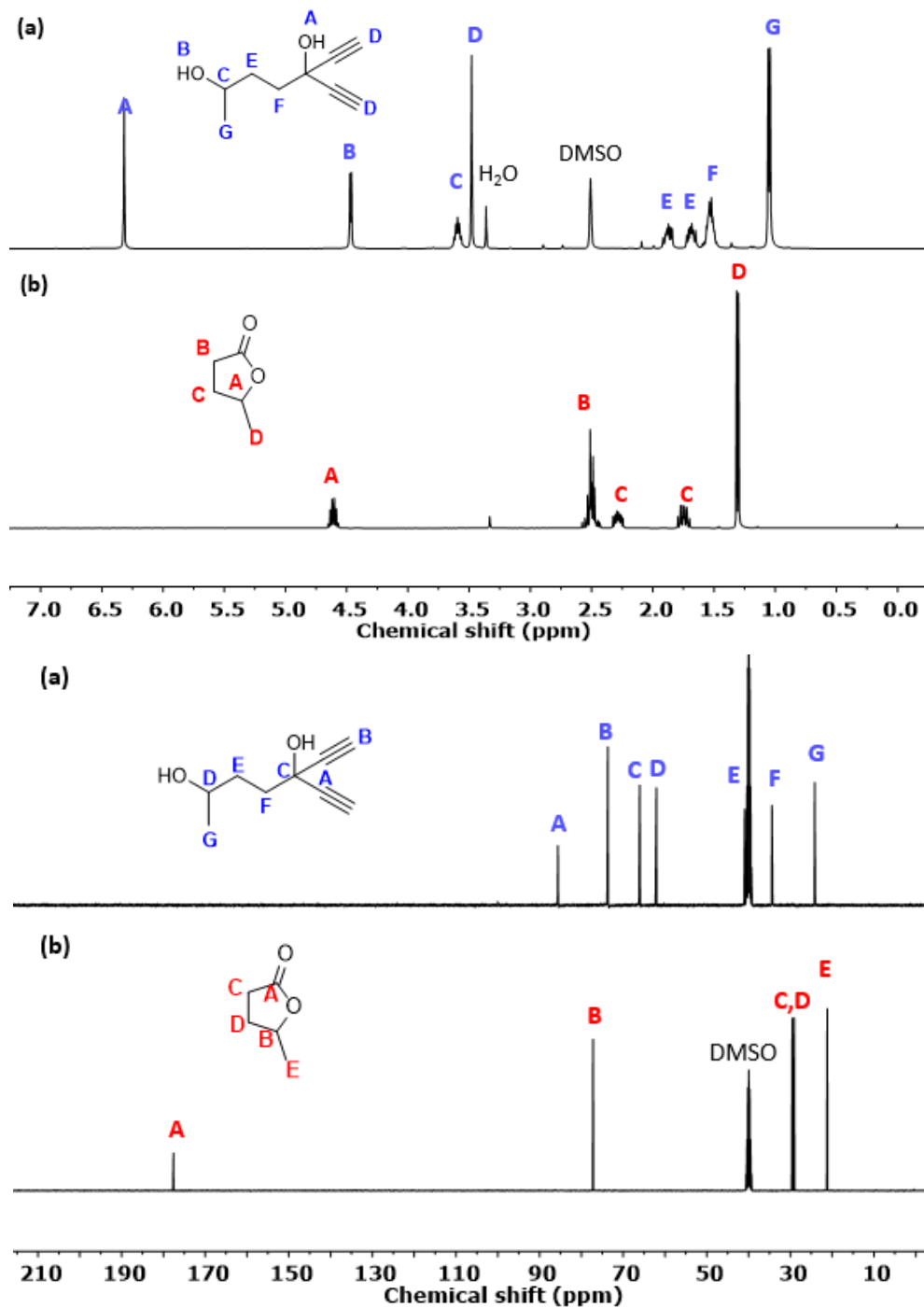


Figure S 2. $^1\text{H-NMR}$ and $^{13}\text{C-NMR}$ spectrum in $\text{DMSO-}d_6$ of (a) 3-ethynyl-6-methylhept-1-yn-3-ol and (b) γ -valerolactone.

SI- 3. Synthesis of alkyne diols by Sonogashira coupling

The success of the reaction was attested by the total disappearance of the alkyne proton at 2.65 ppm and a slight shift of the other signals.

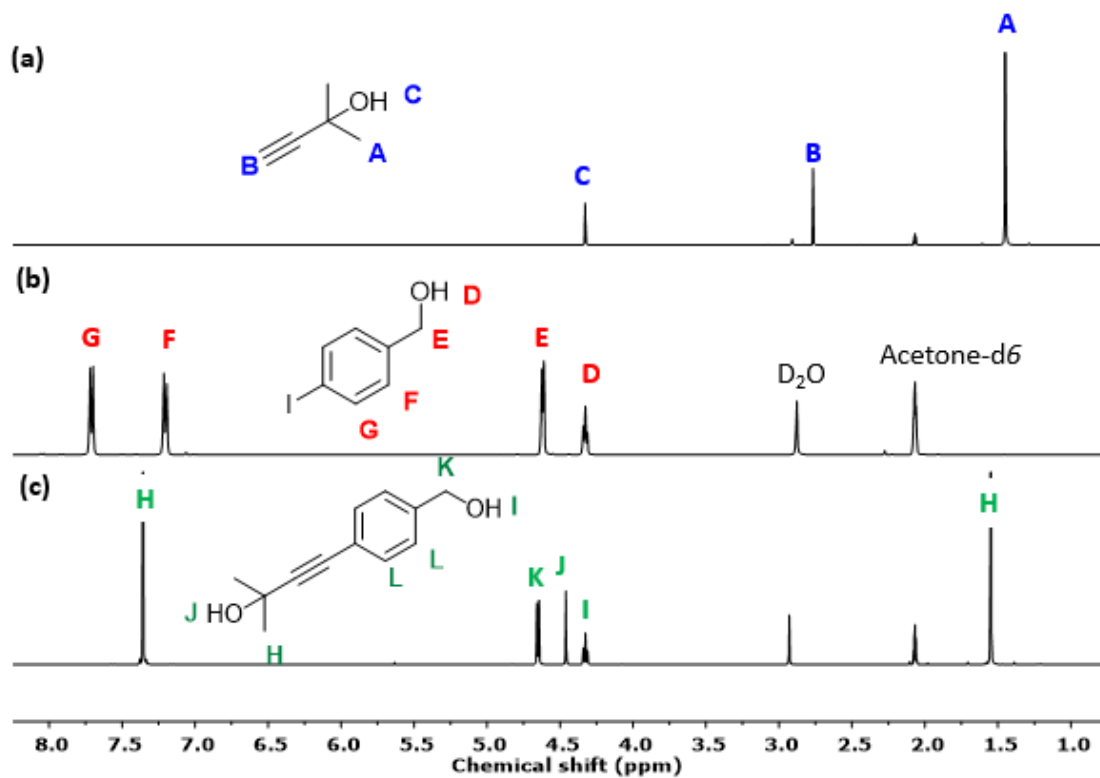
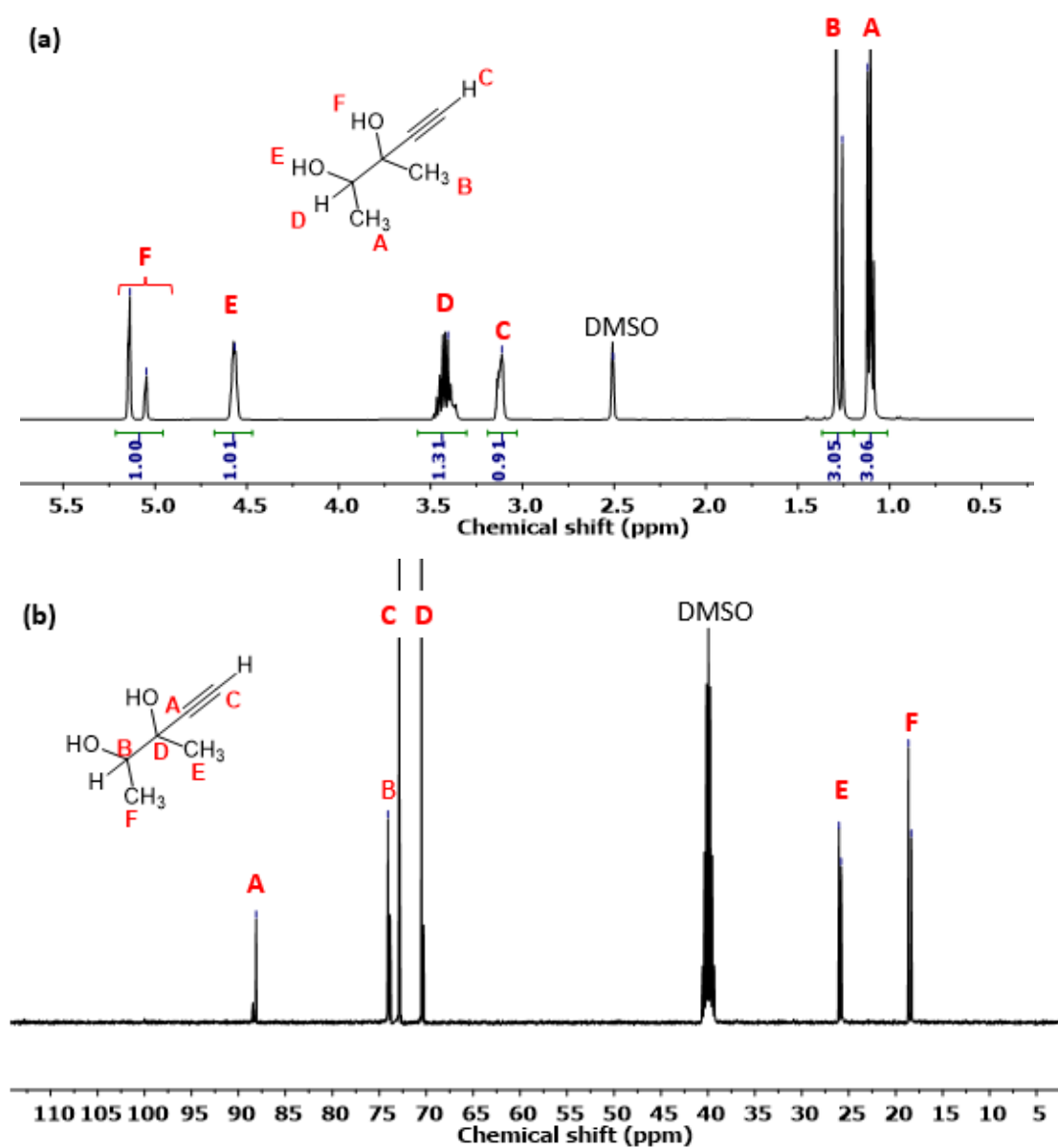


Figure S 3. $^1\text{H-NMR}$ spectra in acetone- d_6 of (a) 3-methyl-2-butyn-2-ol, (b) iodobenzenemethanol and (c) 4-(4-(hydroxymethyl)phenyl)-2-methylbut-3-yn-2-ol.

SI- 4. ^1H -, ^{13}C -NMR and IR spectra of alkyne-diols

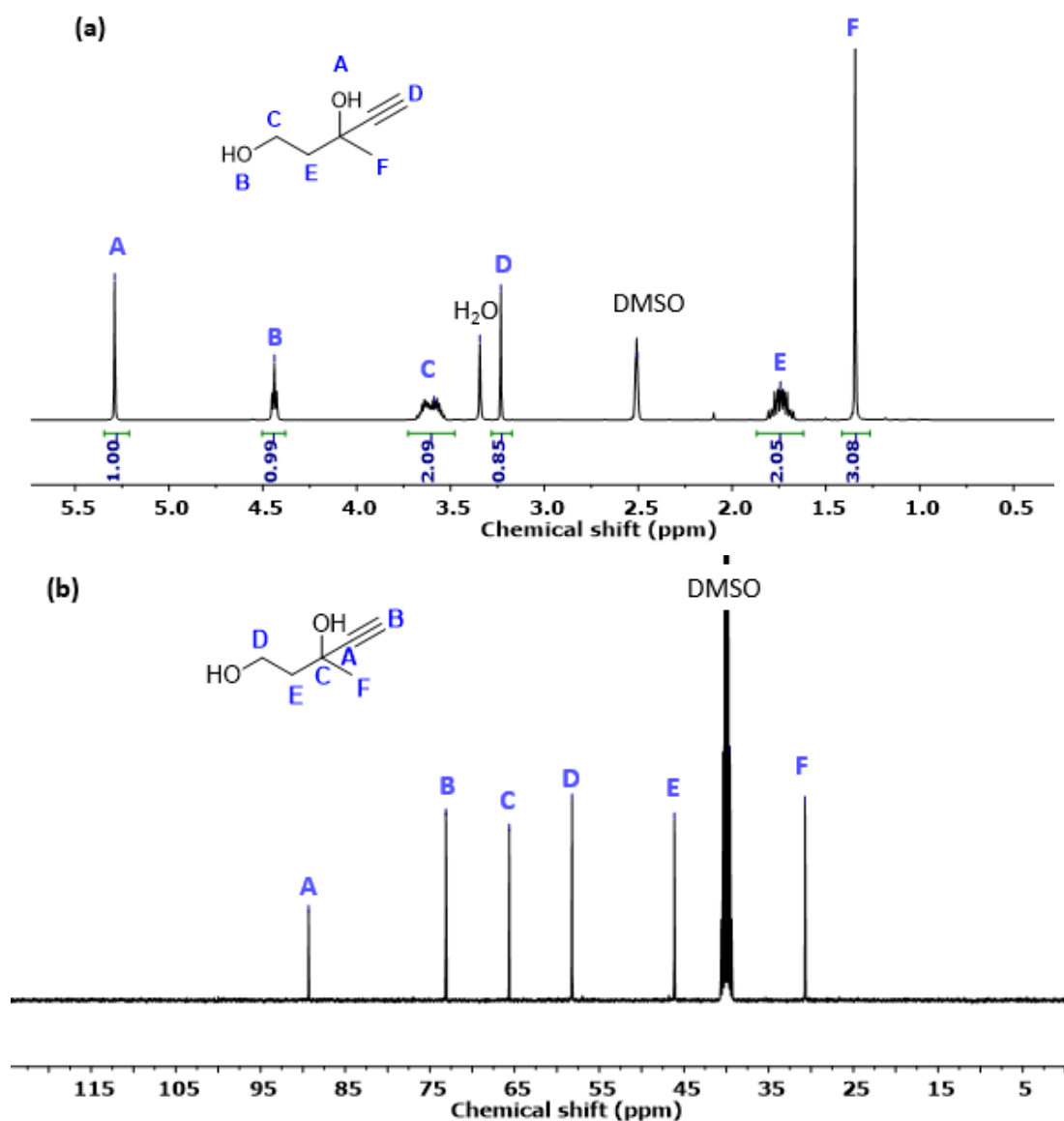
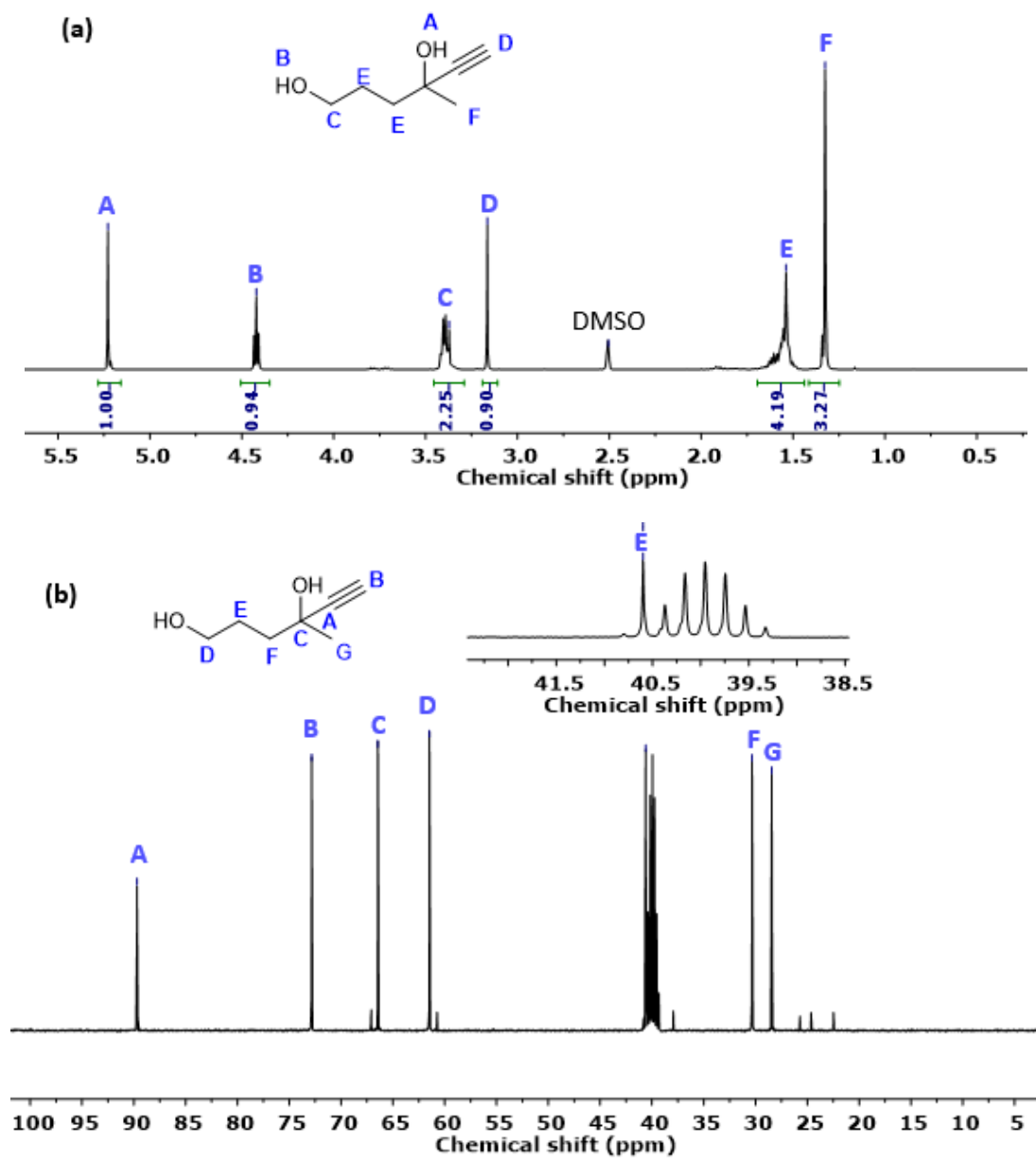
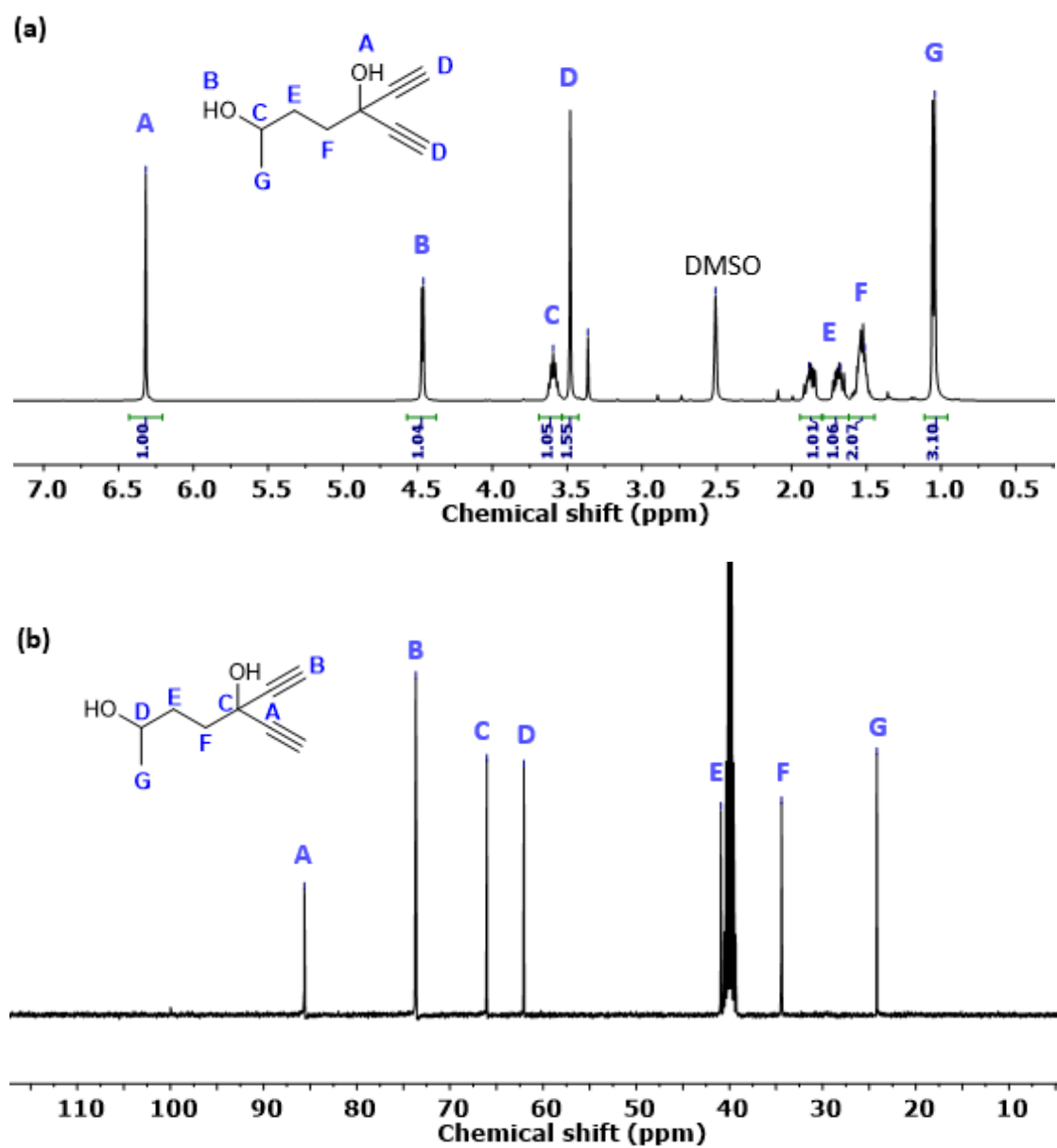
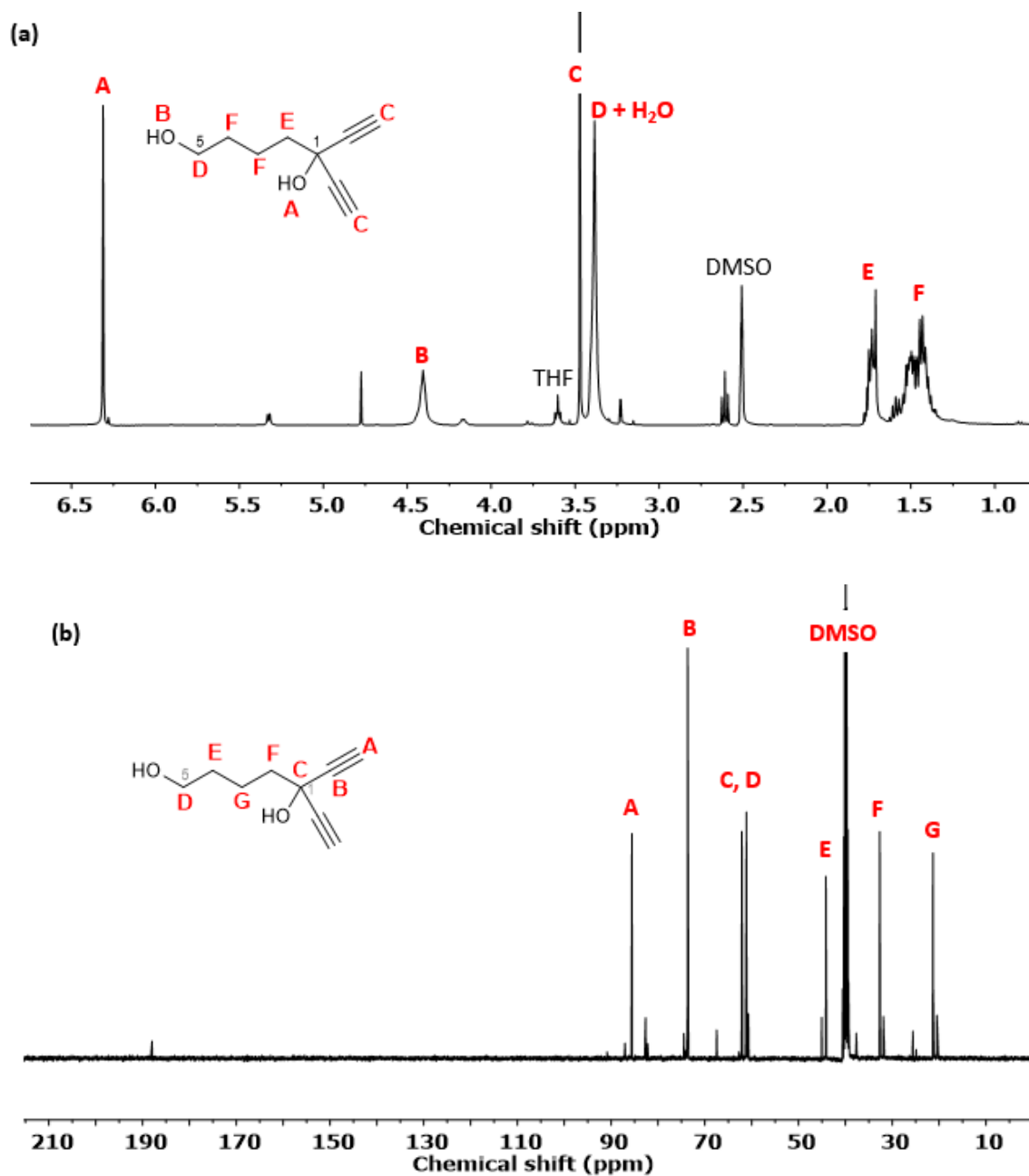


Figure S 5. (a) $^1\text{H-NMR}$, (b) $^{13}\text{C-NMR}$ spectra in $\text{DMSO-}d_6$ of 3-methylpent-4-yne-1,3-diol (4).







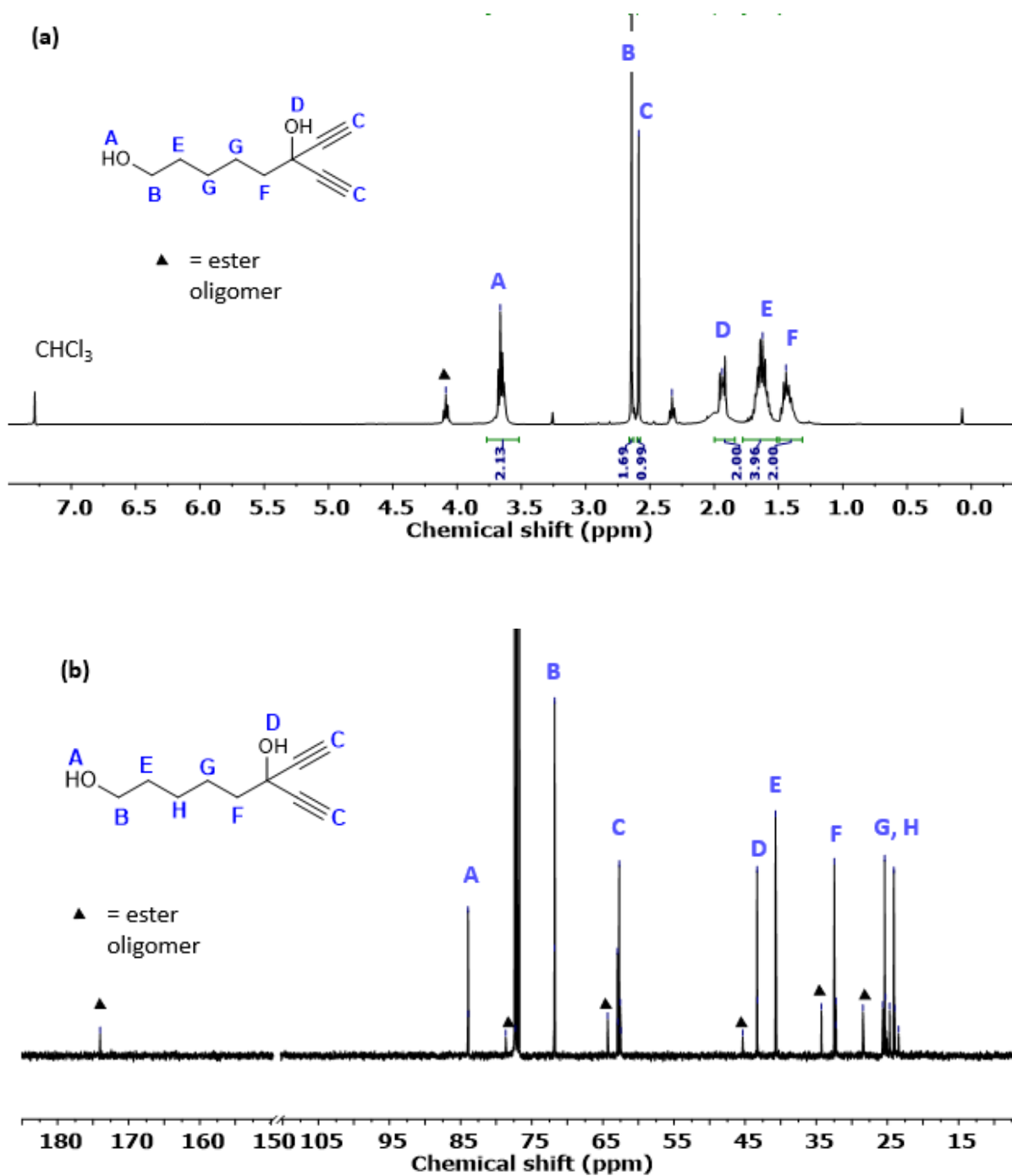
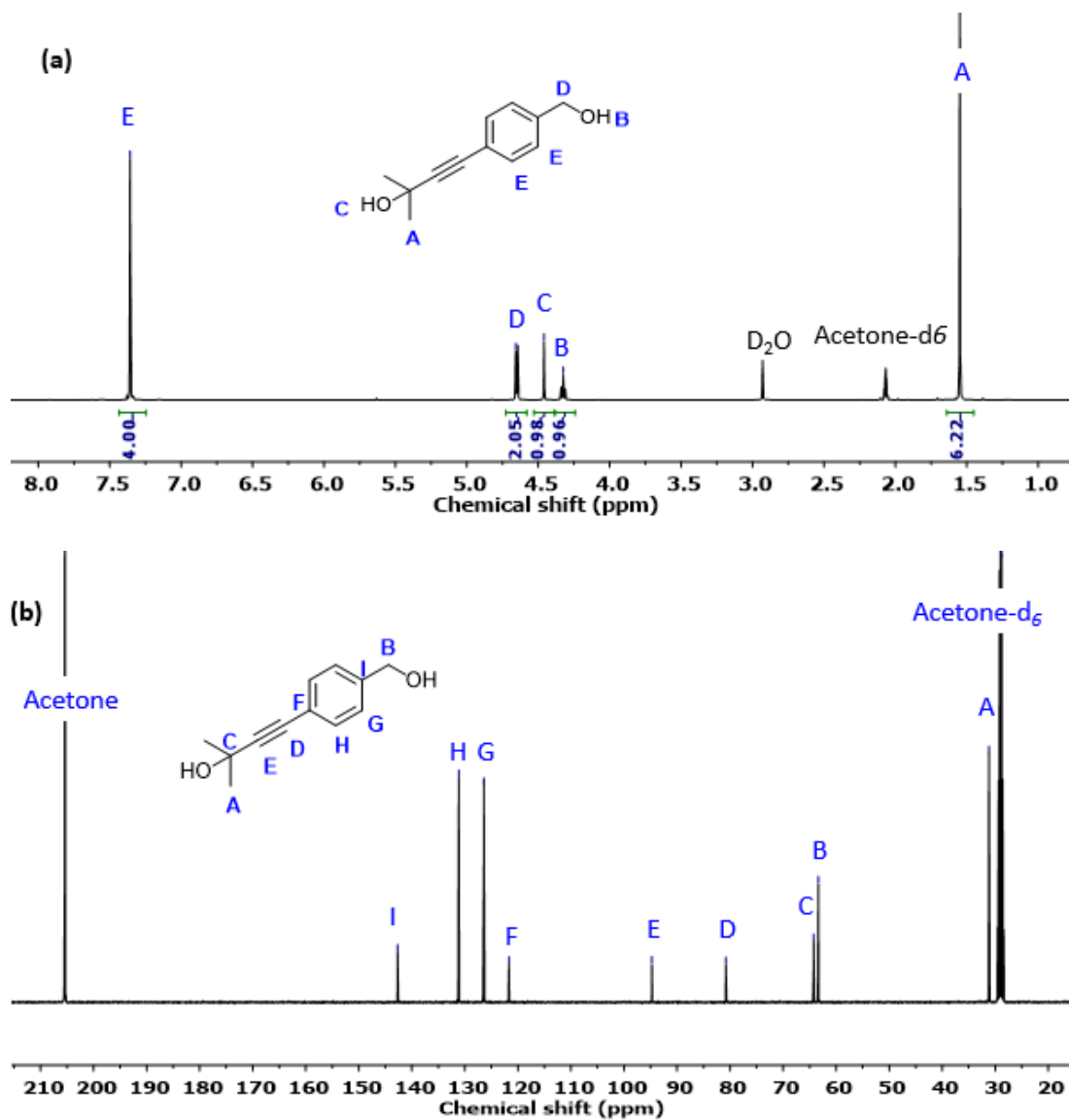


Figure S 9. (a) ¹H-NMR and (b) ¹³C-NMR spectra in CDCl₃ of 6-ethynyloct-7-yne-1,6-diol (**14b**). Alkyne diol contaminated by polyester oligomers.



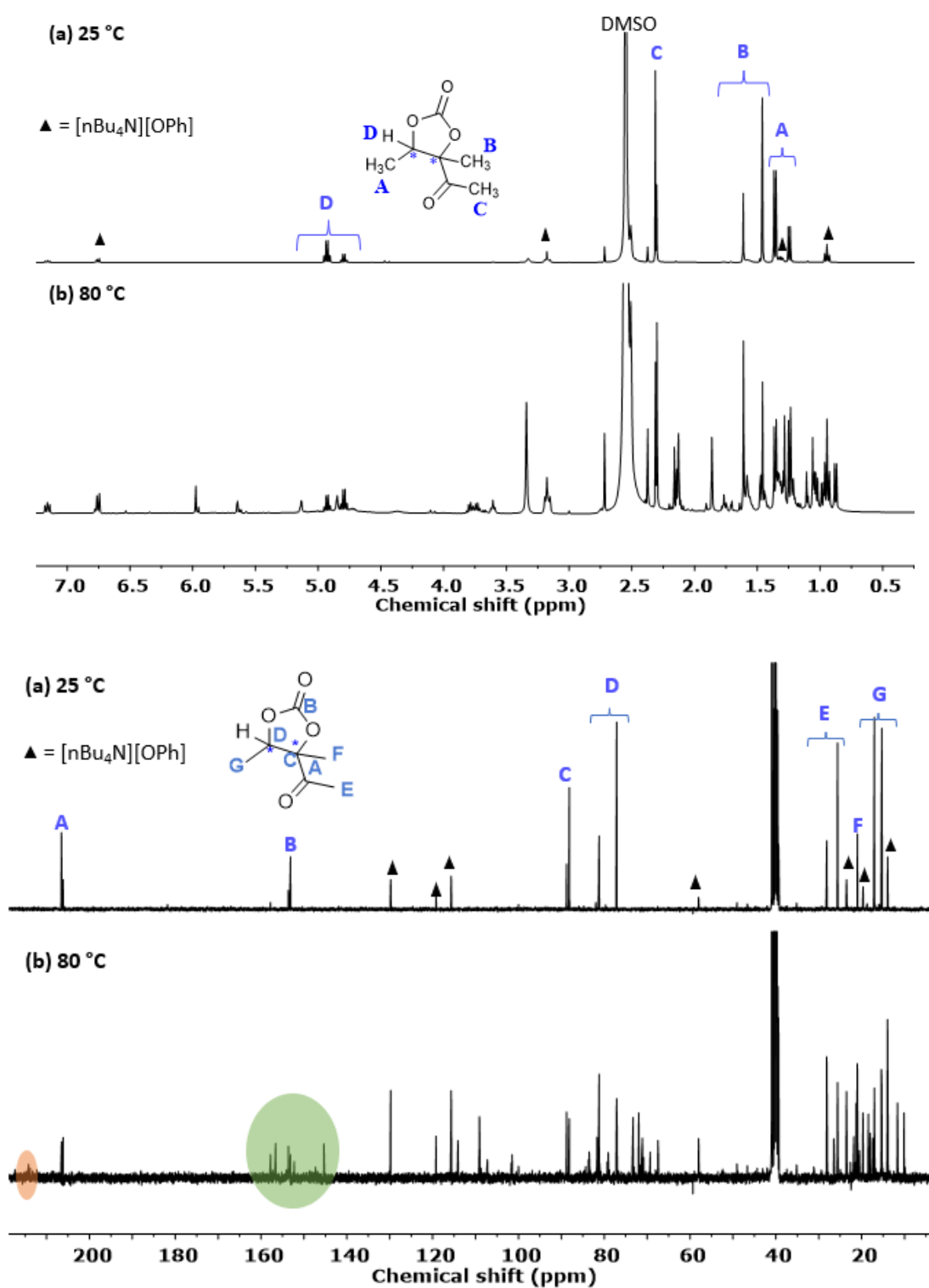
SI- 5. Carboxylative coupling of alkyne-1,2-diol **1** with CO₂

Figure S 11. ¹H- and ¹³C-NMR overlay of the crude reaction mixtures obtained at (a) 25 °C and (b) 80 °C for the carboxylative coupling of CO₂ to 3-methylpent-4-yne-2,3-diol (**1**).

SI- 6. Carboxylative coupling of alkyne-1,3-diol **4** with CO₂.

The % of product **6** was determined by comparing the integration of the methyl signal in alpha position of the ketone at 2.27 ppm, to that of the internal standard at 3.71 ppm according to **Equation S 1** and **Equation S 2**. A similar procedure was applied for diol **4** and product **7**. The remaining percentage was attributed by default to the unidentified oligomer **8**.

$$\text{Equation S 1.} \quad \text{moles carbonate } \mathbf{6} = \frac{I_{6(2.27 \text{ ppm})}}{I_{IS(3.71 \text{ ppm})}} \times \frac{N_{IS}}{N_6} \times \text{moles of internal standard}$$

Where N= number of protons, I= internal standard

$$\text{Equation S 2.} \quad \text{Yield } \mathbf{6} = \frac{\text{moles } \mathbf{6}}{\text{max theoretical moles of } \mathbf{6} \text{ (moles of alkynediol)}} \times 100$$

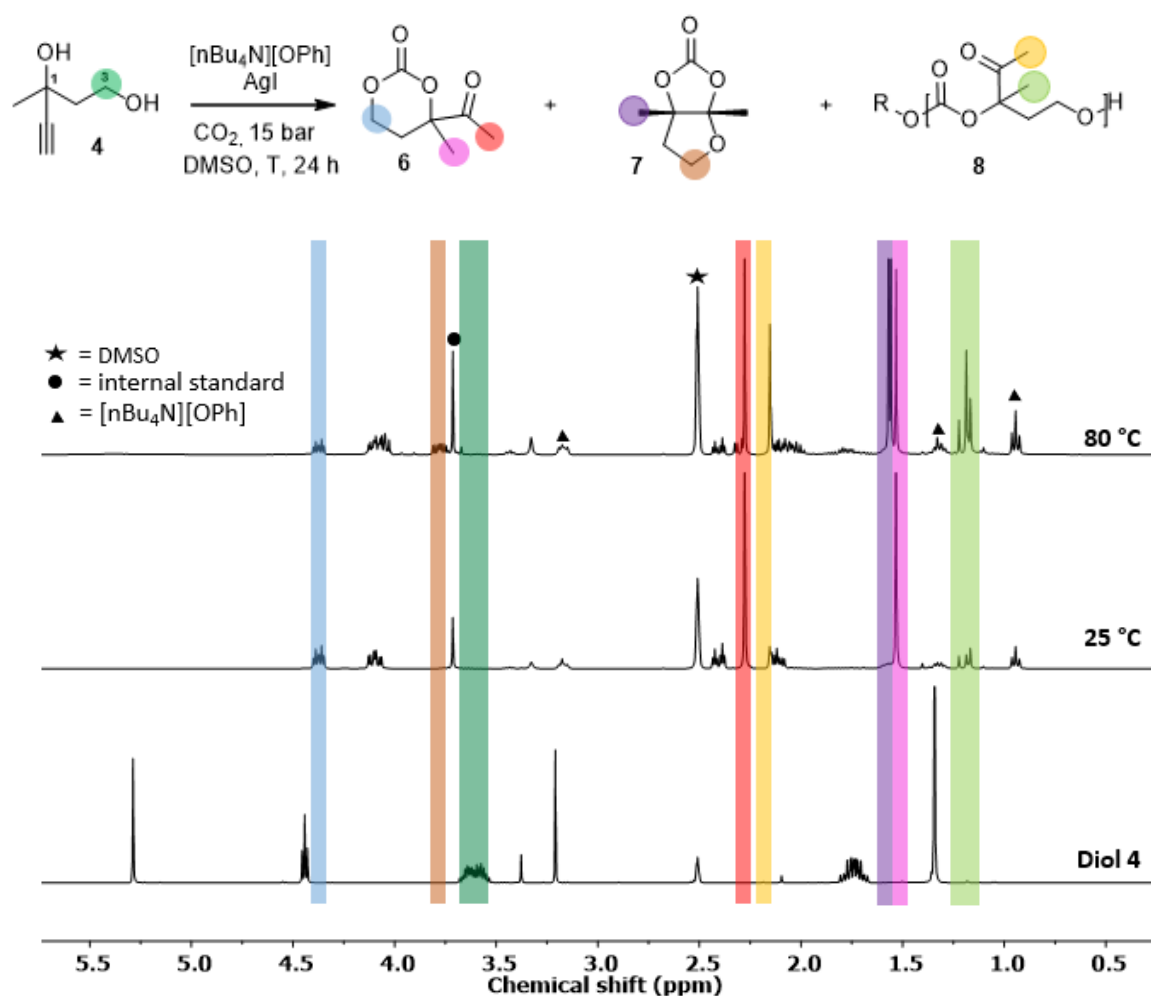


Figure S 12. ¹H-NMR overlay of pure alcohol **4** (bottom), the crude reaction mixtures obtained at 25 °C (middle) and 80 °C (top) for the carboxylative coupling of CO₂ to 3-methylpent-4-yne-1,3-diol **4**.

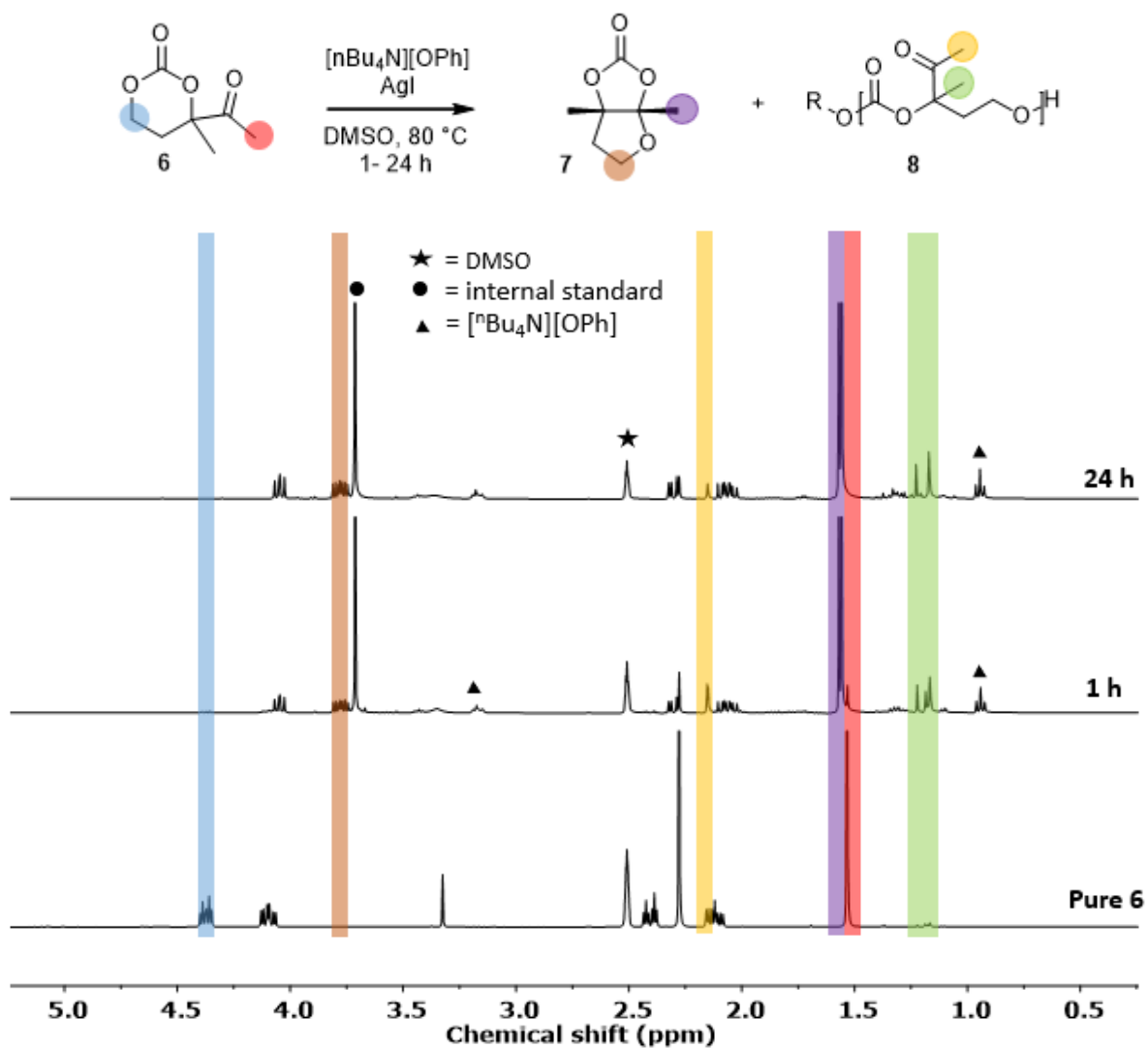
SI- 7. (Organo)Catalysed conversion of the six-membered cyclic carbonate (6) 4-acetyl-4-methyl-1,3-dioxan-2-one into the 5-membered one (7)

Figure S 13. $^1\text{H-NMR}$ spectra in DMSO-d_6 of carbonate **6** and the crude mixtures obtained after 1 h and 24 h of reaction at 80°C in the presence of $[n\text{Bu}_4\text{N}][\text{OPh}]/\text{AgI}$ as catalyst. Data are summarised in Table 2, entries 1 and 2.

SI- 8. Step-growth polymerisation of exovinylene carbonate 10a

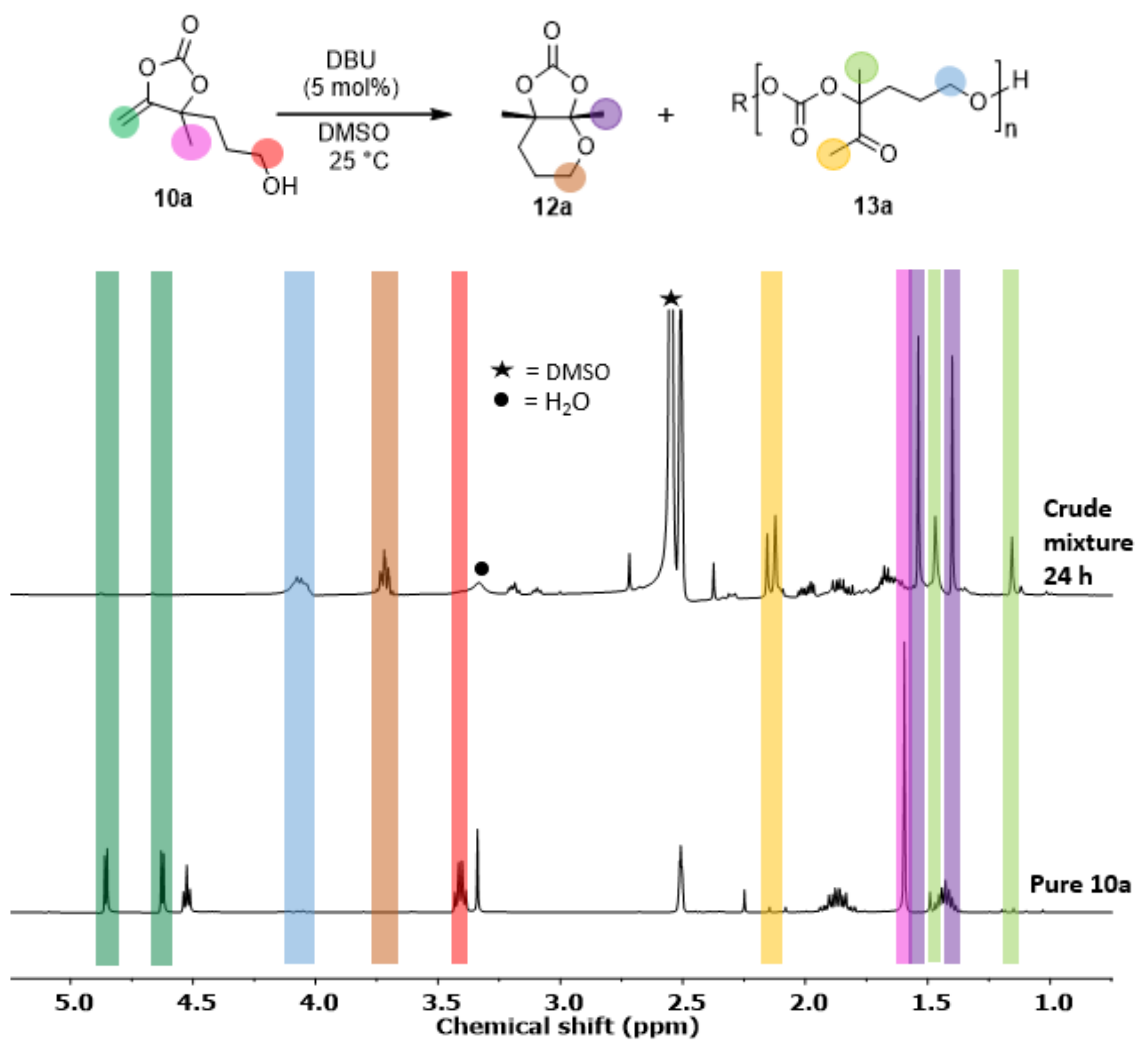


Figure S 14. ¹H-NMR spectra superposition in DMSO-d₆ of carbonate 10a and the crude mixture obtained after 24 h of reaction at 25 °C in the presence of DBU.

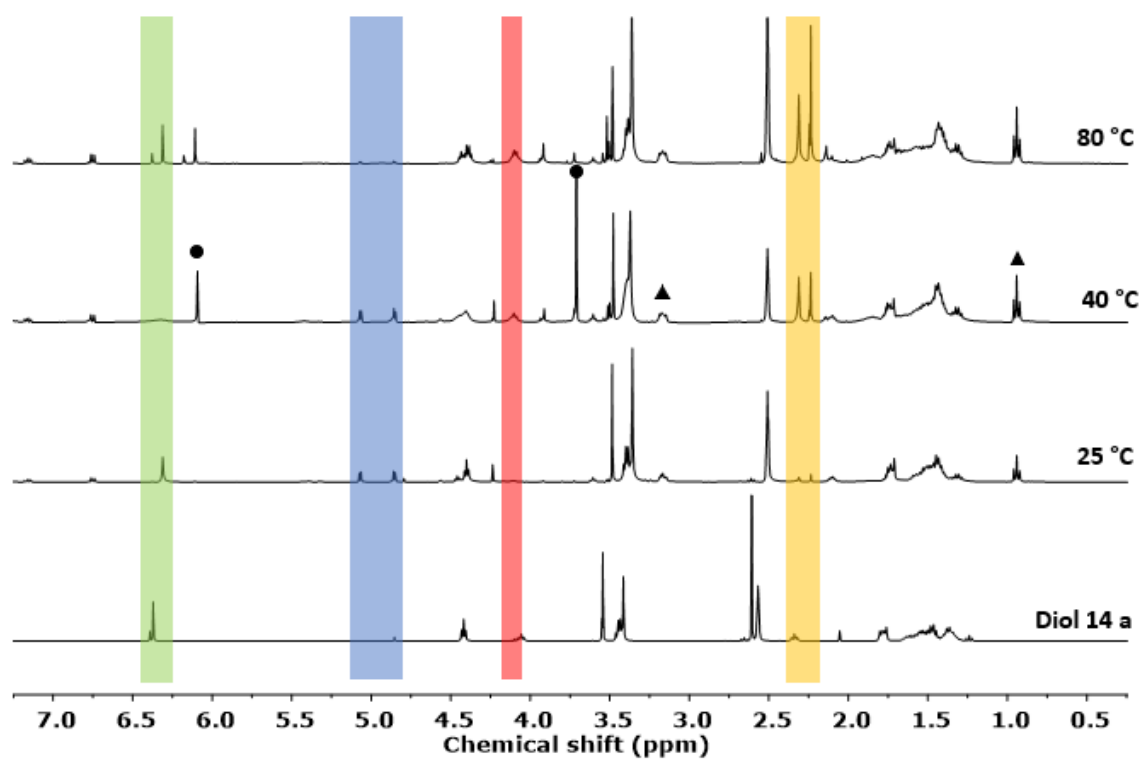
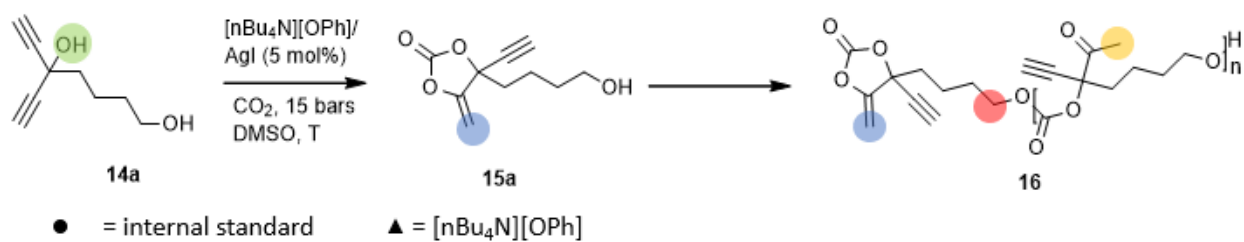
SI- 9. Carboxylative coupling of 1,5-diol **14a** with CO₂

Figure S 15. ¹H-NMR overlay in DMSO-*d*₆ of pure diol **14a** and the crude reaction mixtures obtained for the carboxylative coupling with CO₂ at 25 °C, 40 °C and 80 °C.

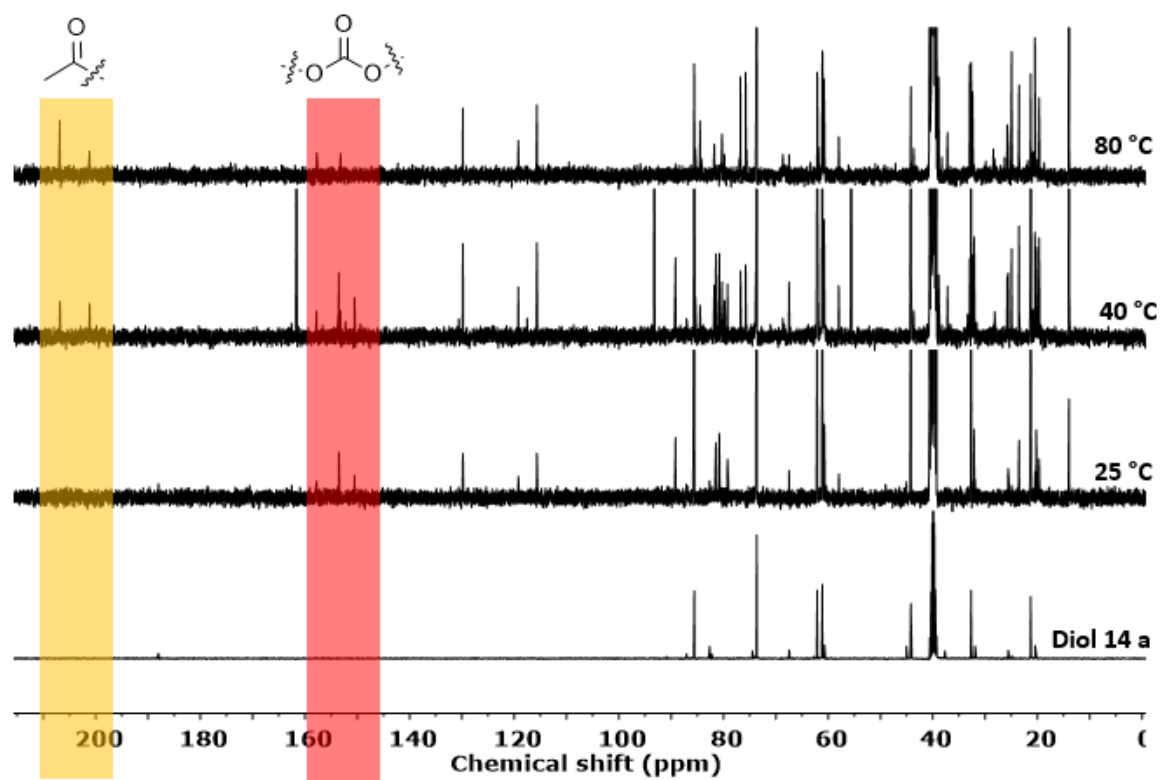
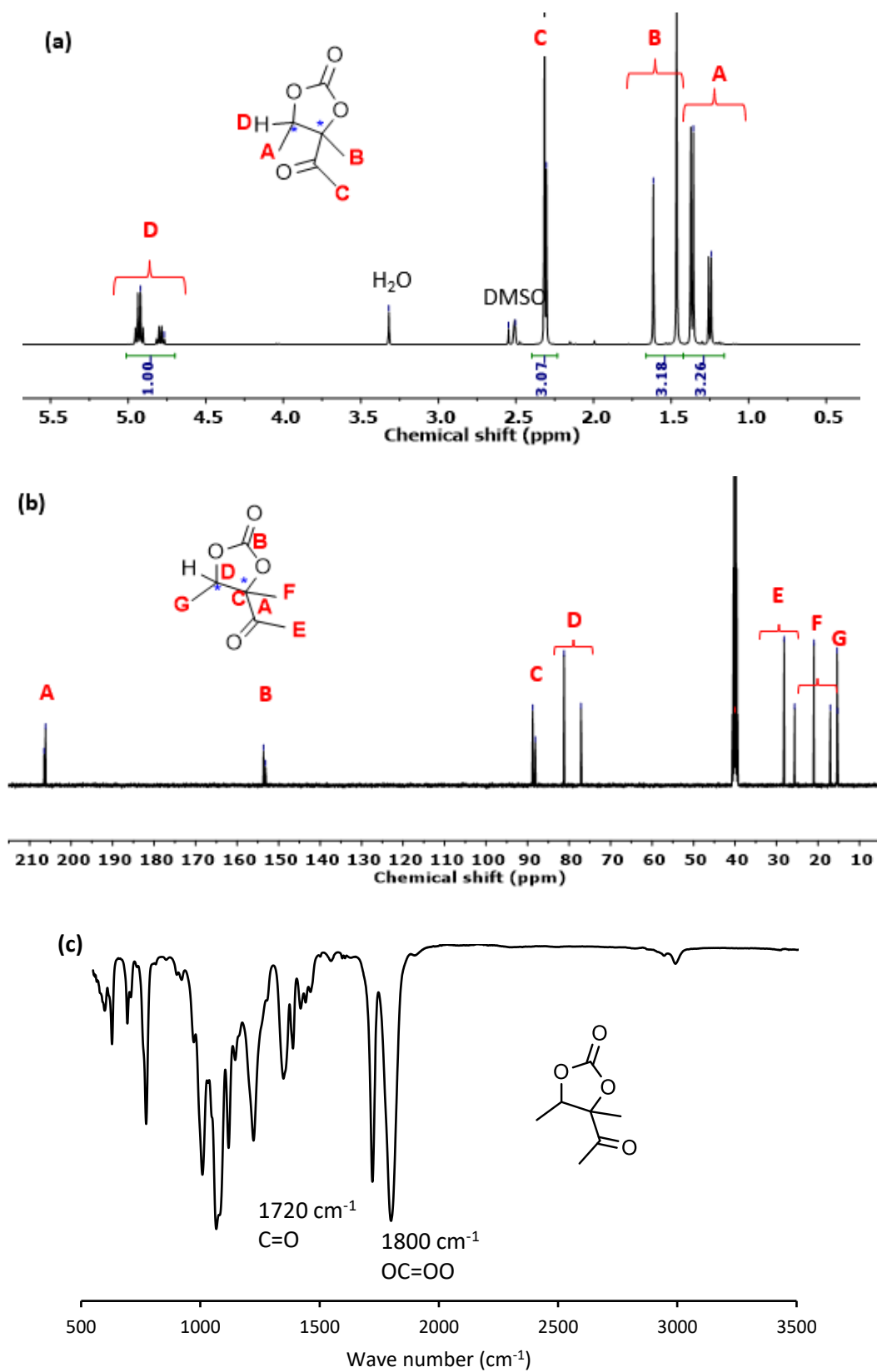


Figure S 16. ^{13}C -NMR overlay in $\text{DMSO-}d_6$ of pure diol **14a**, and the crude reaction mixtures obtained for the carboxylative coupling with CO_2 at 25 °C, 40 °C and 80 °C.

SI- 10. ^1H - and ^{13}C -NMR characterisation and IR spectrum of carbonate compounds

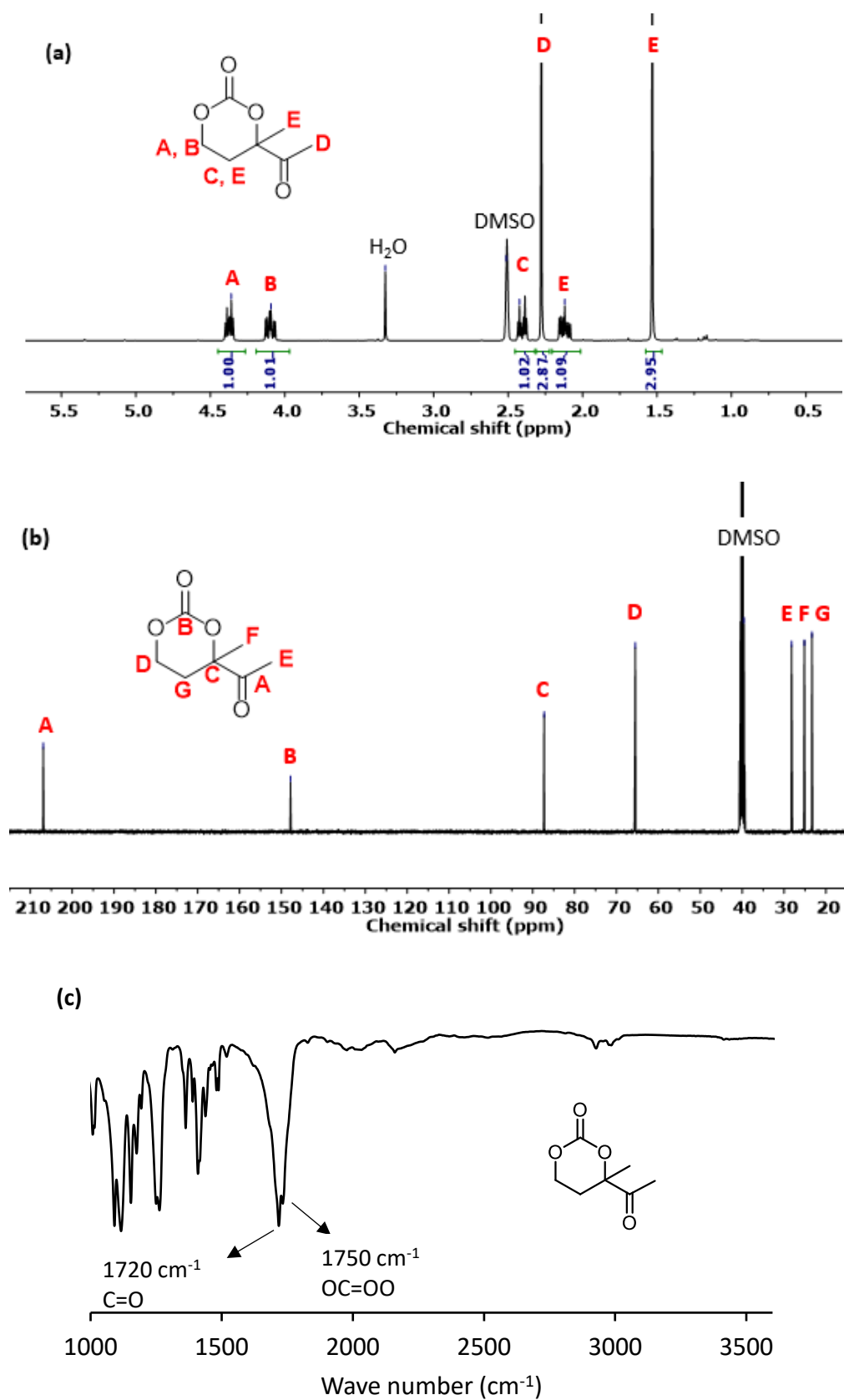
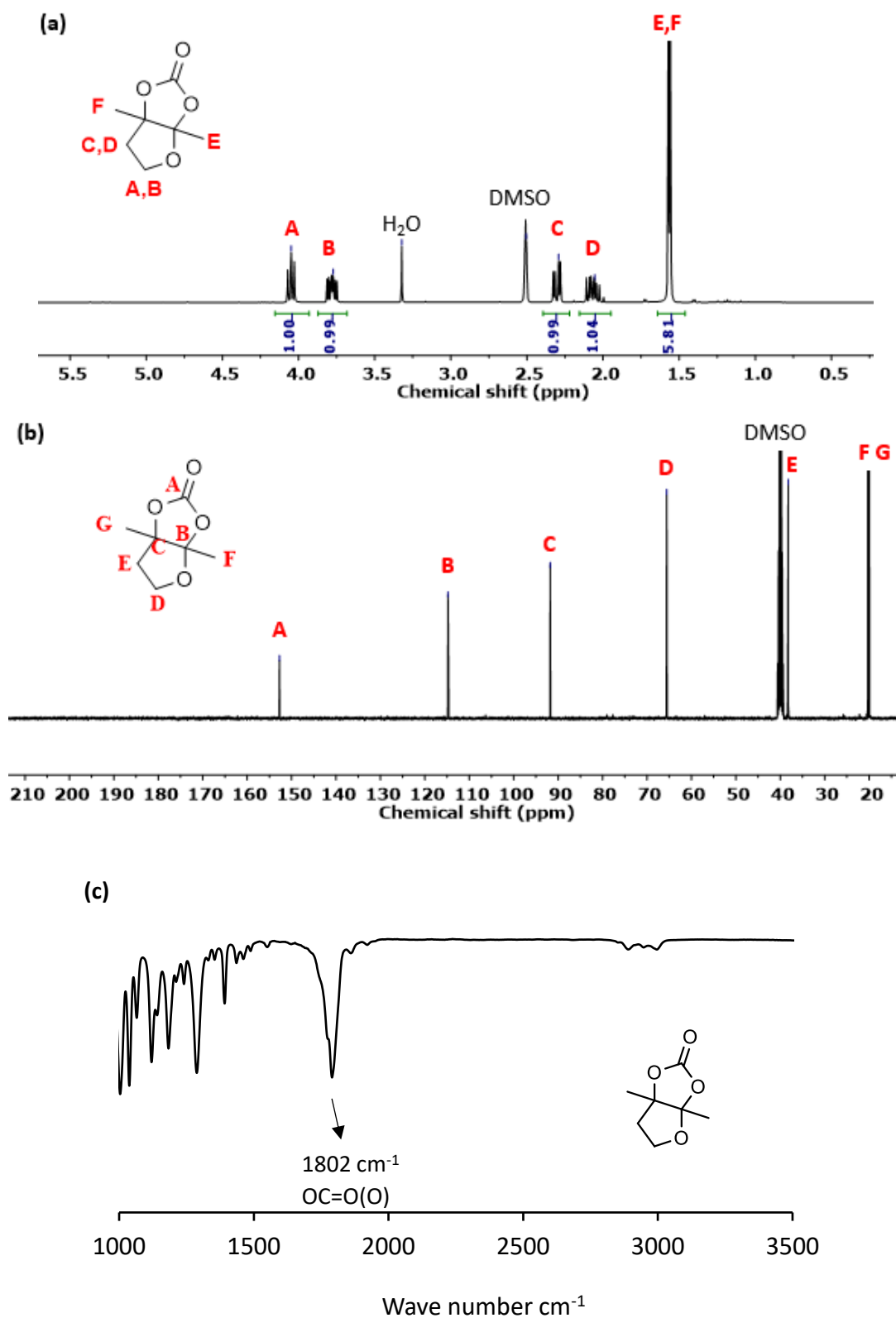


Figure S 18. (a) ^1H -NMR, (b) ^{13}C -NMR spectrum in $\text{DMSO-}d_6$ and (c) IR (Neat) spectrum of **6**.



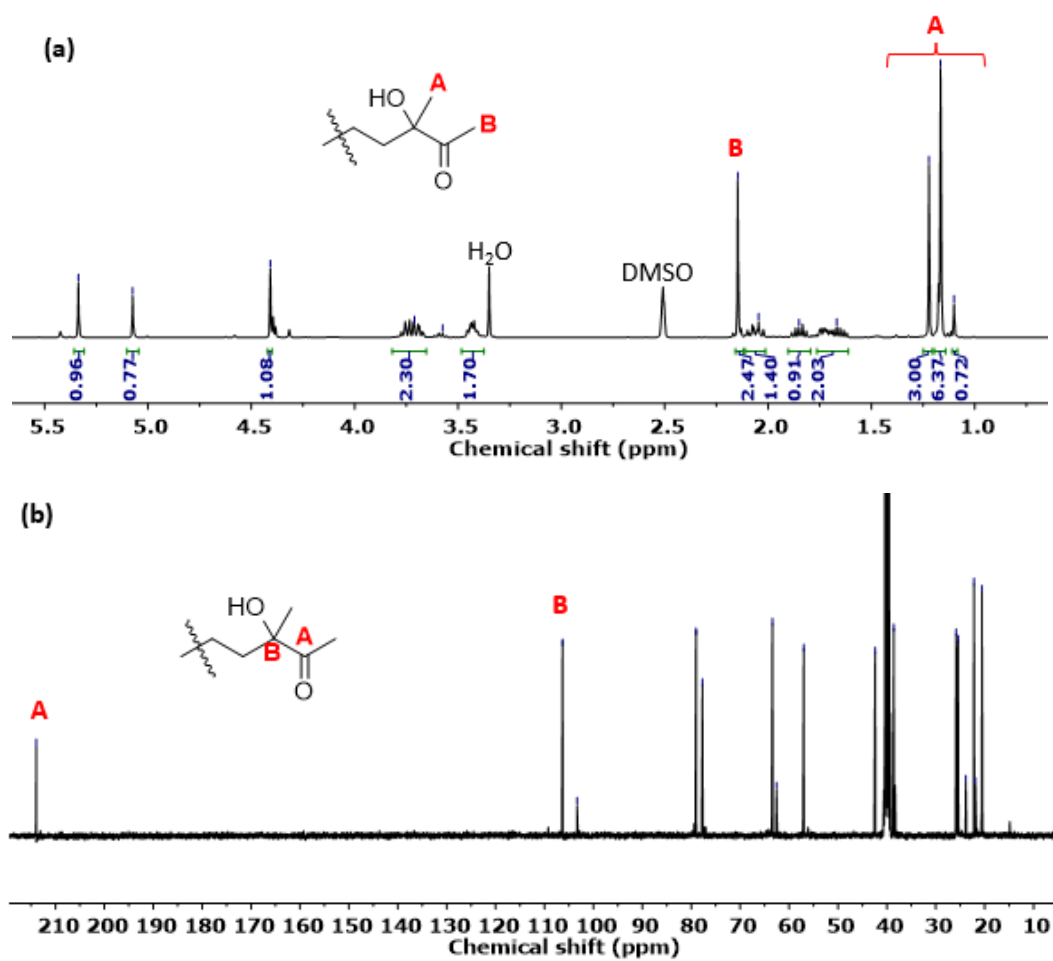


Figure S 20. ^1H -NMR and ^{13}C -NMR spectrum in $\text{DMSO-}d_6$ of decomposed intermediate **8**.

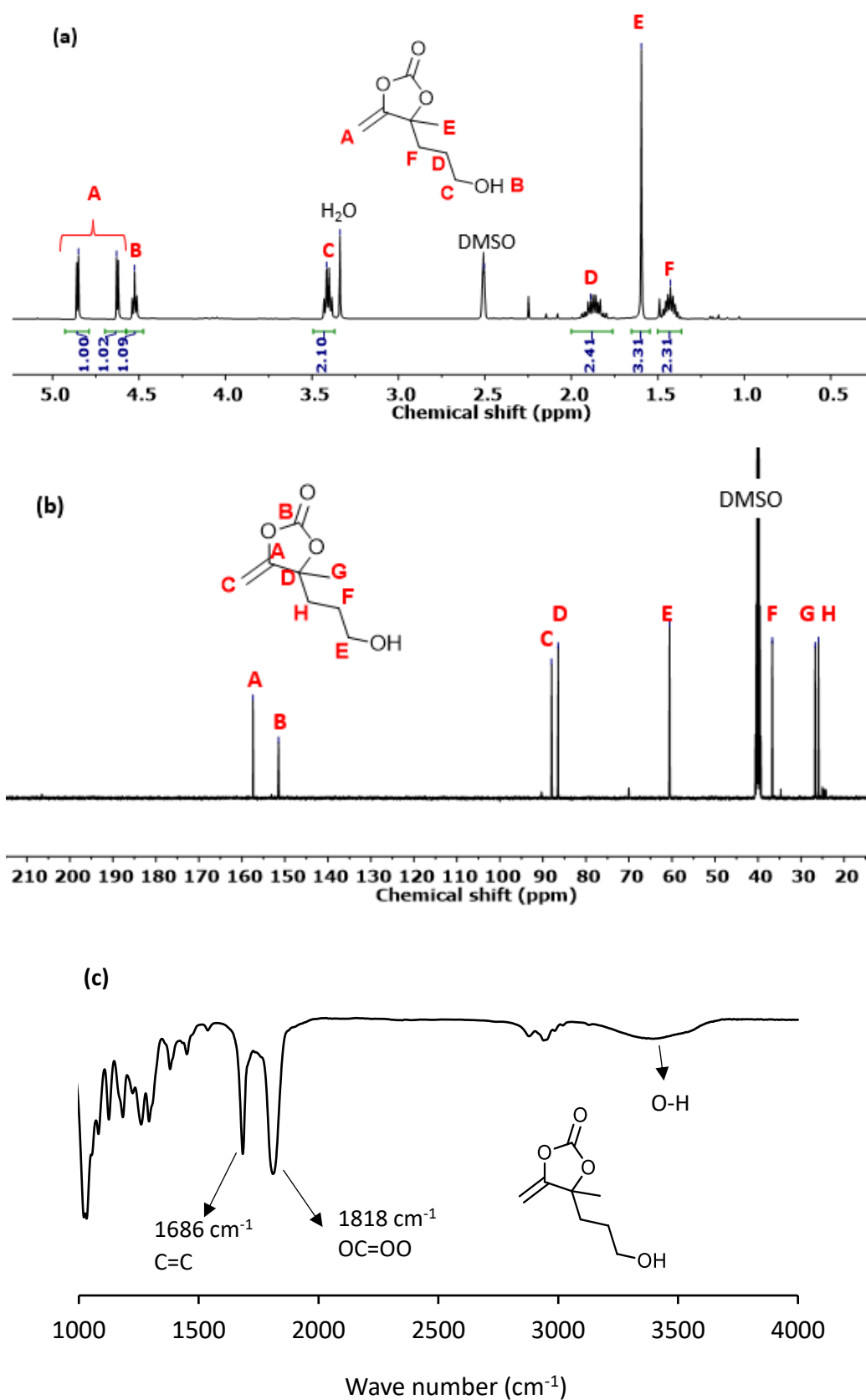
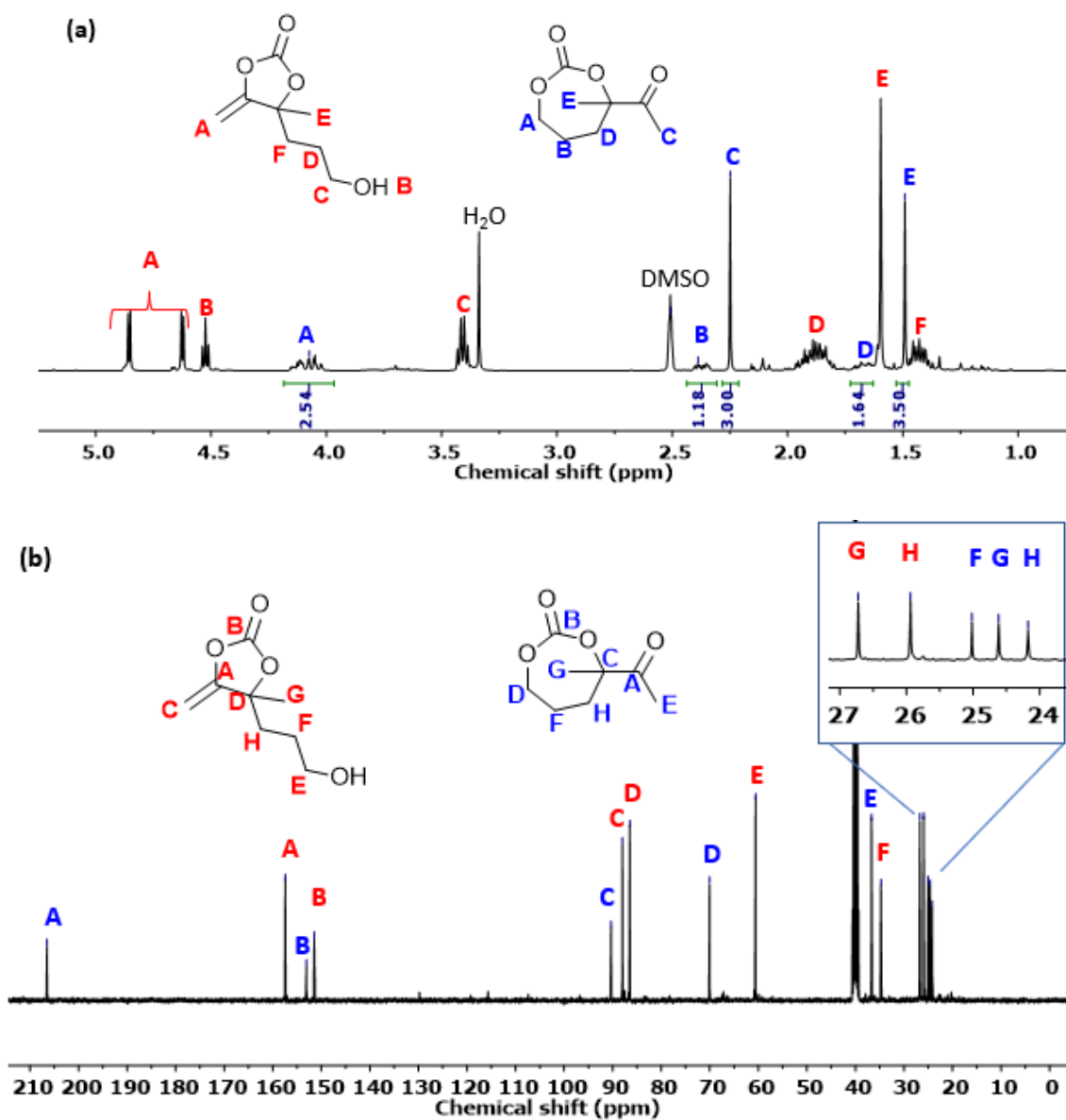


Figure S 21. (a) ^1H -NMR, (b) ^{13}C -NMR spectrum in $\text{DMSO-}d_6$ and (c) IR (neat) spectrum of **10**.

Note: A mixture of both α -alkylidene carbonate **10** and seven-membered carbonate **11**:



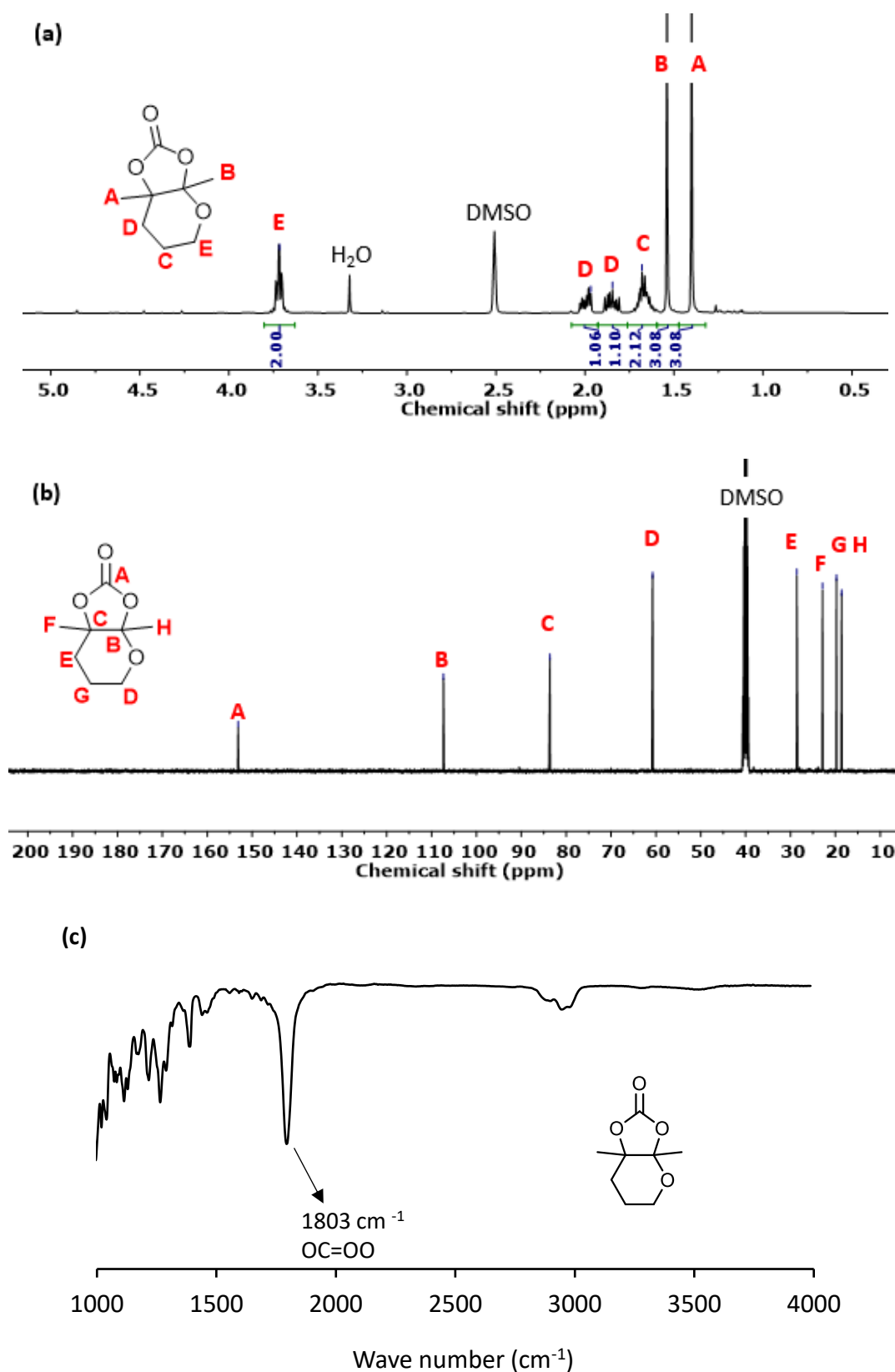


Figure S 23. (a) ^1H -NMR, (b) ^{13}C -NMR spectrum in $\text{DMSO-}d_6$ and (c) IR (neat) spectrum of **12a**.

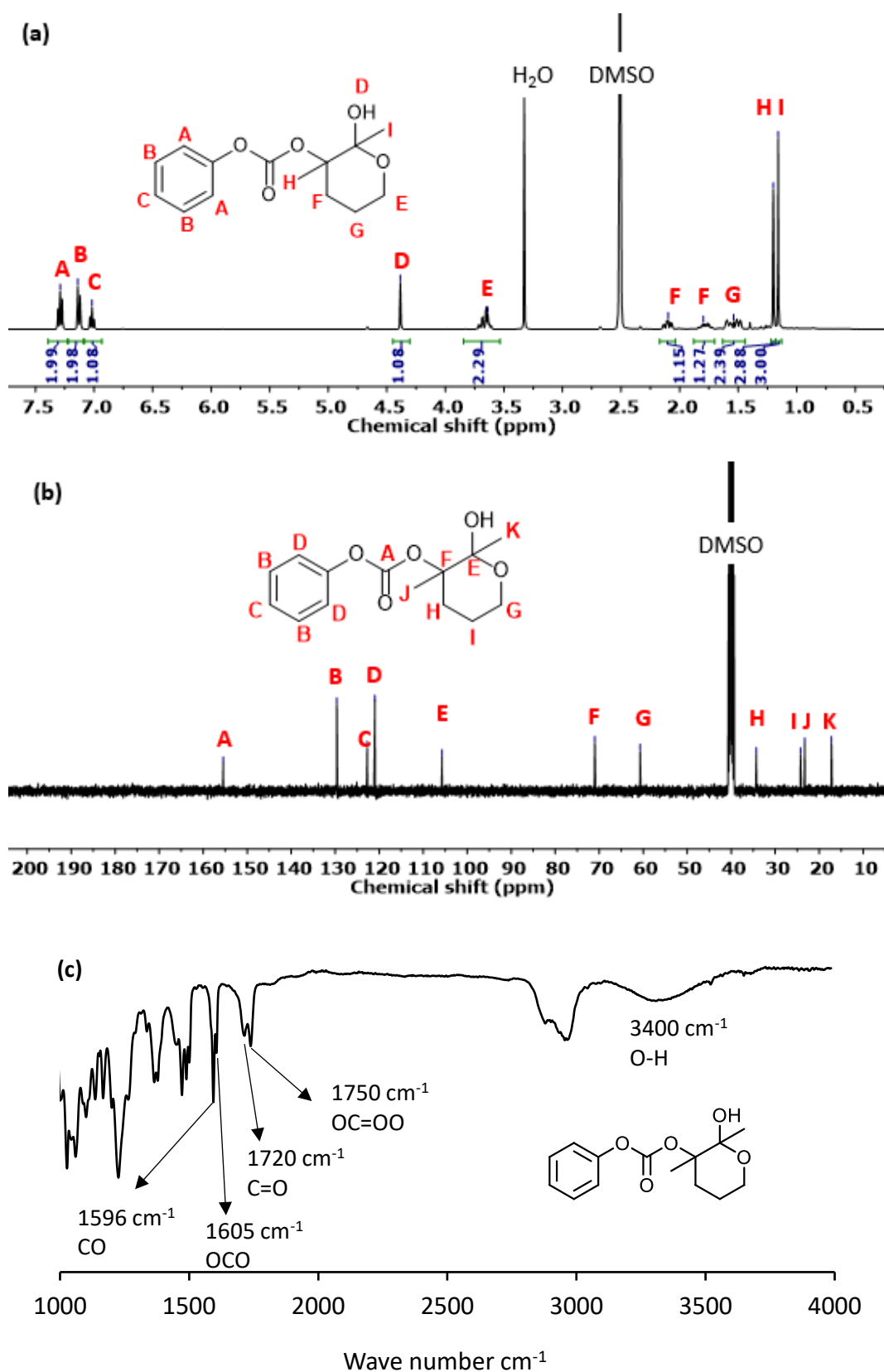


Figure S 24. (a) $^1\text{H-NMR}$, (b) $^{13}\text{C-NMR}$ spectrum in DMSO- d_6 and (c) IR (neat) spectrum of one of the isolated intermediates **13'**

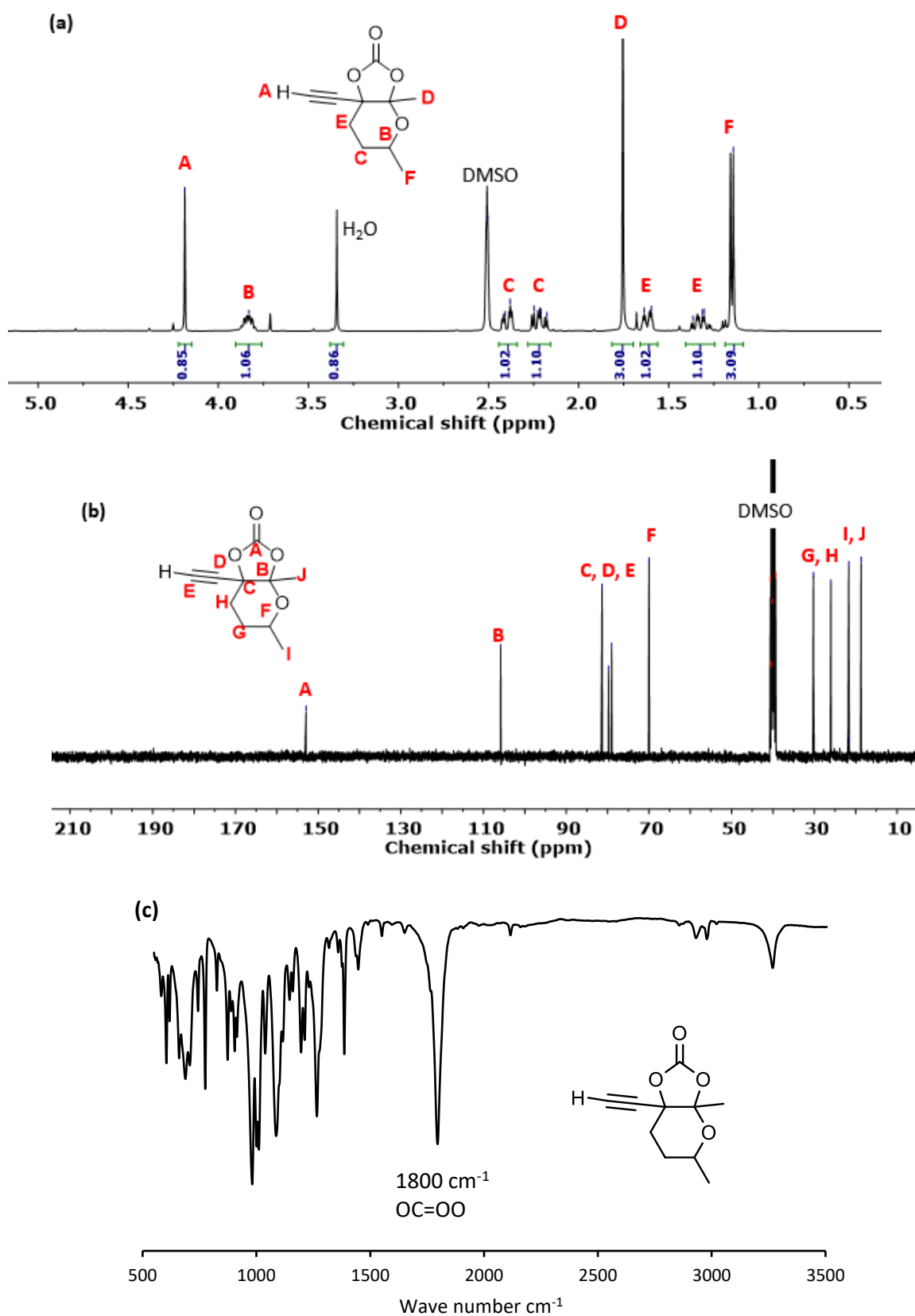


Figure S 25. a) ^1H -NMR and (b) ^{13}C -NMR spectra in $\text{DMSO}-d_6$ and (c) IR (neat) spectrum of 12b.

CHAPTER 6

General conclusions

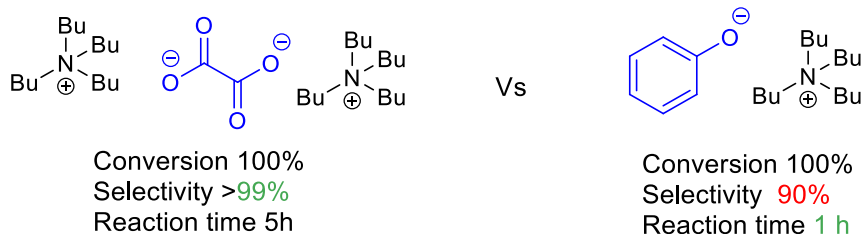
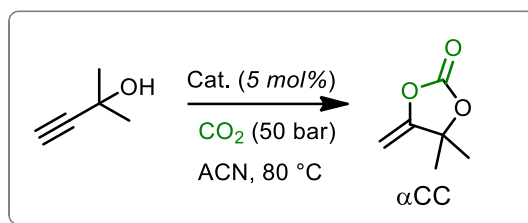
Conclusions

Valorising CO₂ as a cheap, inexhaustible and renewable feedstock imposes itself as a strategic driver for developing low carbon footprint compounds. The synthesis of exovinylene cyclic carbonates is extremely interesting due to the structurally diversified organic compounds and polymers which can be obtained from the latter. In a pioneering study, poly(*oxo*-carbonates with regioregular structures) were prepared by the organocatalysed polyaddition of diols to CO₂-based bis(exovinylene cyclic carbonate)s (bis α CC) under room temperature conditions. However, the synthesis and isolation of bis α CC was an issue with only 30% yield obtained at that time. The aim of my PhD thesis was to investigate the fundamentals that would allow the synthesis of these new poly(*oxo*-carbonate)s in a one-pot cascade process, wherein bis α CC is formed *insitu*, and reacts with a diol by step-growth polymerisation. In order to do that, we aimed to identify highly active organocatalysts and the optimum conditions that would promote both the efficient and selective synthesis of bis α CC by carboxylative coupling of CO₂ to bis-alkynols, and the polyaddition of bis α CCs to diols.

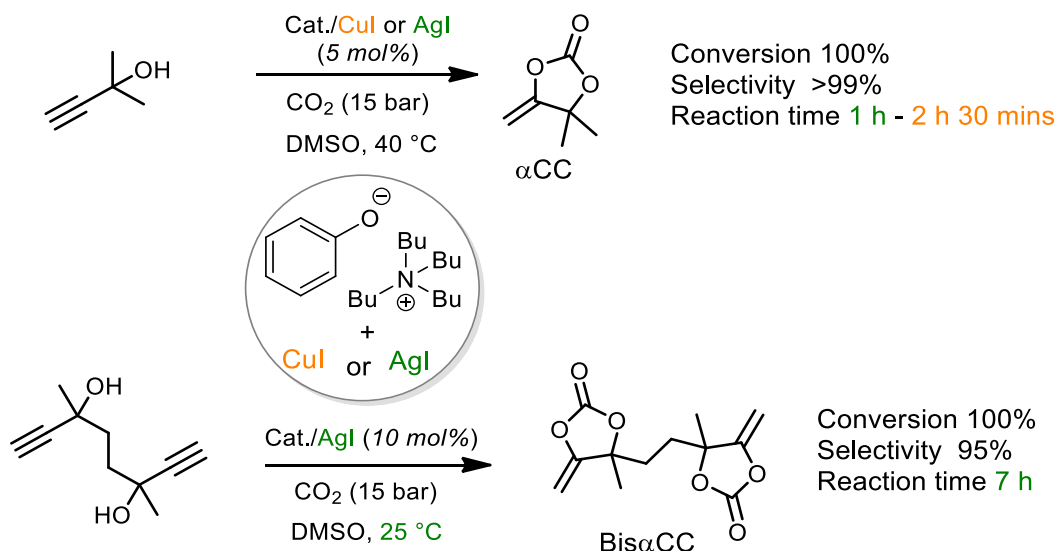
In chapter 1, we reviewed the advances made in the synthesis of α -alkylidene cyclic carbonates (α CCs) from CO₂, their multiple transformation options into structurally divergent organic scaffolds and their brilliant potential for the construction of a broad diversity of novel polymers.

In chapter 2, we prepared various ammonium-based organocatalysts for the carboxylative coupling of CO₂ to alkynols. We used simple procedures for their preparation and benchmarked their activity via batch screening tests and online Raman spectroscopy at 80 °C, 50 bar under neat conditions or with acetonitrile as solvent. Amongst the various candidates that were evaluated, two of them presented high activity at a low catalyst loading (2.5 –5 mol%), i.e. tetrabutylammonium oxalate ([nBu₄N]₂[Ox]) - which gave full conversion of the model propargylic alcohol in 5 h with >99% selectivity for the desired α CC - , and tetrabutyl ammonium phenolate ([nBu₄N][OPh]) - which gave total conversion in 1 h and a selectivity of 90% in α CC both. We were able to correlate the activity of the catalysts to the structural features of the organic catalyst (basicity of the anion and the structure of the cation). The [nBu₄N]₂[Ox] system was used to synthesise various α CCs, thus demonstrating the versatility of the system. This chapter has opened new avenues for the facile and selective synthesis of libraries of α CCs from CO₂ and tertiary propargylic alcohol by using simple organocatalysts.

Conclusions



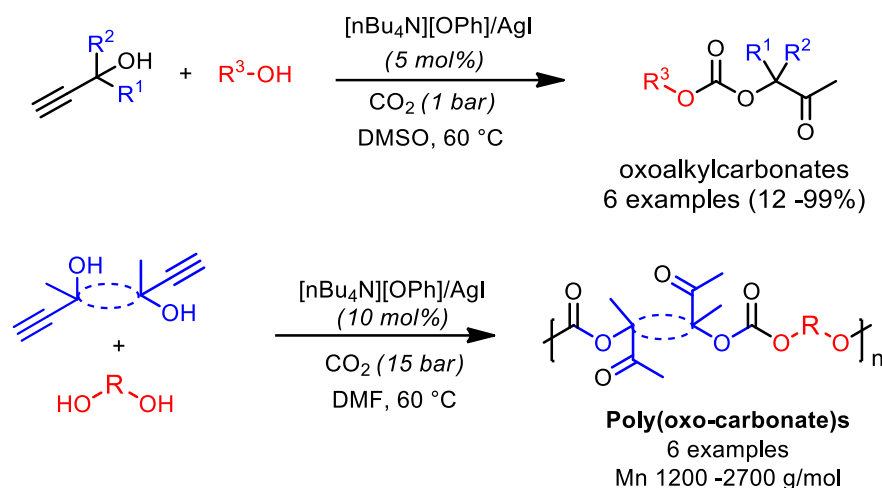
Our desire for a highly basic catalyst, yet selective let us to develop dual catalytic systems composed of an organic catalyst and a metal catalyst. Hence, in chapter 3, we optimised the tetrabutyl ammonium phenolate catalyst by adding a metal cocatalyst, CuI or AgI. This allowed to reduce the reaction temperature to 40 °C and the pressure to 15 bar, while maintaining a fast reaction rate (< 2 h) and a high selectivity (> 99%) for αCC . DFT calculations combined to FT-ATR operando experiments allowed us to rationalize the improved reactivity observed. We then applied the $[\text{nBu}_4\text{N}][\text{O}^-\text{Ph}]/\text{AgI}$ dual system for the carboxylation of a model bis(propargylic alcohol) and obtained the corresponding bis αCC in 90% yield at 40 °C after 4 h of reaction and 95% yield at 25 °C after 7 h.



Then in chapter 4, we implemented the cascade synthesis of oxoalkyl carbonates. Various parameters were screened (solvent, temperature and pressure) to find the optimum conditions for the cascade approach. The CO_2 pressure was identified as one of the crucial parameters, i.e. a too high pressure induced a partial carboxylation of the monoalcohol that consequently limited its reactivity towards the in-situ generated αCC . For the first time, the one-pot terpolymerisation synthesis of poly(oxo-carbonates) was realized. We were however

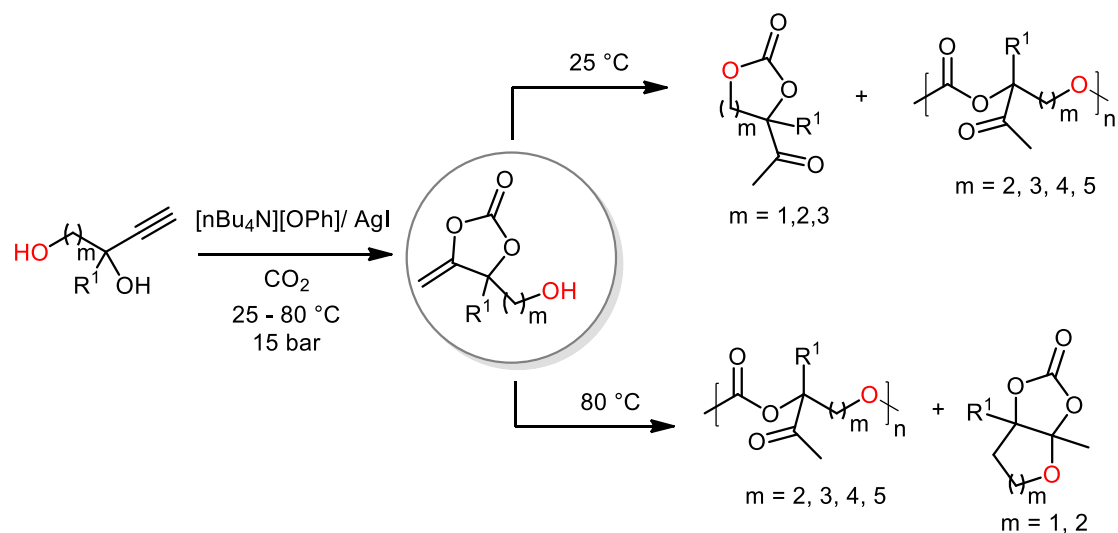
Conclusions

limited on the molar masses obtained, notably due to the higher temperature (> 60 °C) required for the terpolymerisation approach which favored secondary reactions, i.e. transcarbonatation and hydrolysis of bis α CC. Nonetheless, we were able to prepare 6 examples of poly(*oxo*-carbonate)s via this approach. Although the system should be optimised to produce longer polymer chains, this process offers a new phosgene-free alternative to the synthesis of functional polycarbonates under mild conditions.



In the last chapter, we sought to merge the presence of a propargylic alcohol function with another alcohol on the same molecule, which upon carboxylation will result in an exovinylene cyclic carbonate monomer with a pendant alcohol group, capable of self-polymerisation. Thus we prepared various alkyne-1,*n*-diols (*n* = 2 to 6) and tested their ability to self-polymerise. Surprisingly, with alkyne-1,2-diols, elusive di-, tri- or tetra-substituted 5-membered keto cyclic carbonates were obtained as the main products, instead of poly(*oxo*-carbonate)s. With the alkyne-1,3 and 1,4-diols, we obtained 6- and 7-membered keto-carbonates, respectively, at 25 °C. When the reaction temperature was increased to 80 °C, unprecedented fused bicyclic tetrasubstituted ethylene carbonates were obtained, as well as some poly(*oxo*-carbonate) oligomers. DFT computations combined with operando FT-ATR studies as well as model experiments allowed to explain the formation of the different products. By using alkyne-1,5 and 1,6-diols, the selectivity of the reaction was turned towards poly(*oxo*-carbonate)s oligomers (M_n 1200 -1500 g/mol). Here once more, we were limited in the molar masses, which we explained by the purity of the alkyne-1,5 and 1,6-diols.

Conclusions



In conclusion, our aim was to develop a one-pot cascade approach for the synthesis of poly(oxo-carbonate)s. By developing an efficient catalytic system, carrying out detailed experiments, which involved the use of innovative techniques such as high pressure in-situ spectroscopic experiments (Raman and IR) and DFT studies, we achieved our goal. We identified key parameters as well as some of the limitations of our cascade approach, which prevented us from obtaining poly(oxo-carbonate)s of high molar masses. This thus leaves us with some perspectives and preliminary experiments as will be discussed hereafter.

CHAPTER 7. Perspectives

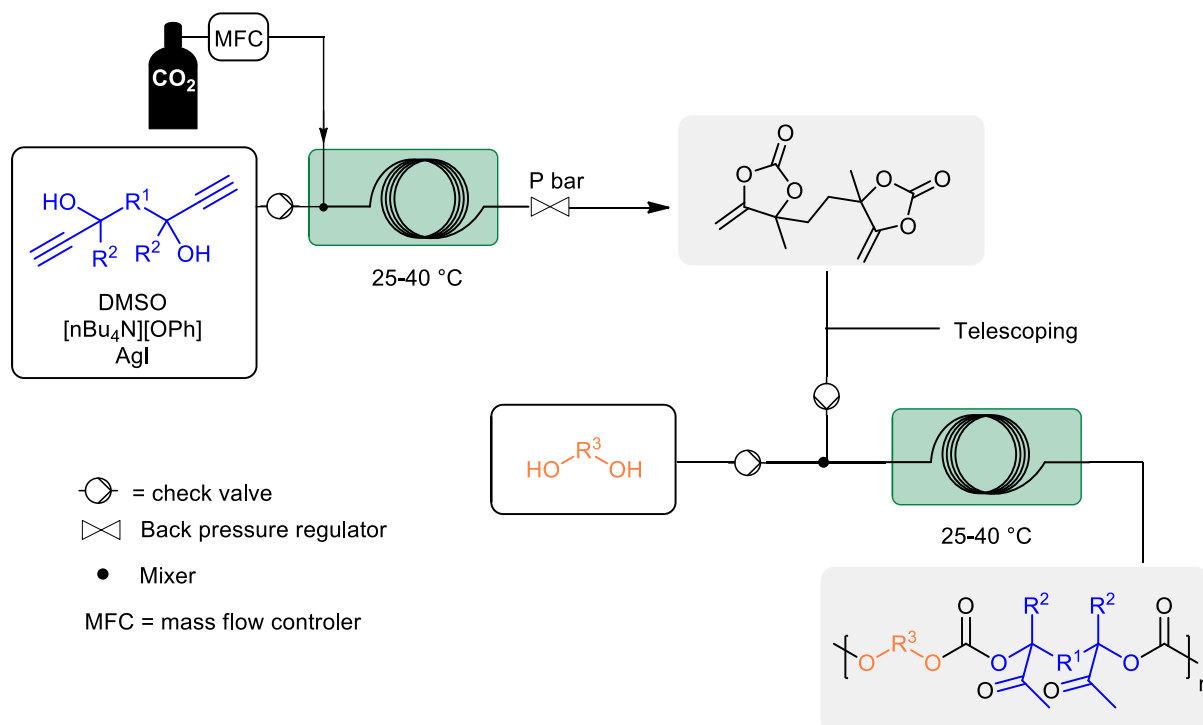
**Preliminary investigation of the synthesis
of poly(*oxo*-carbonate)s in a continuous
flow reactor**

1. Introduction

In chapter 4, we attempted the one-pot cascade synthesis of poly(oxo-carbonates) by terpolymerisation of a bispropargylic alcohol, CO₂ and a diol. This revealed to be challenging due to the occurrence of secondary reactions induced by the temperature (>60 °C) needed for the one-pot cascade approach. Indeed, we know from chapter 3 that the synthesis of the bis(alkylidene cyclic carbonate) is quantitative and the most selective at 25 °C and 15 bar, meanwhile other studies^[18,107] have shown that the step-growth polymerisation works best at 25 °C too. At higher temperature, some side reactions such as transcarbonation reactions were observed, consequently limiting the polymer molar mass.^[71,107] Furthermore, carbonation of the diol during the one-pot cascade reaction also affected the polymerisation process.^[71] Attempts to solve these issues were done by realizing a one-pot two-steps process, thus first by *in-situ* forming Bis α CC by carboxylative coupling of CO₂ to the bis(propargylic alcohol) at 25 °C, followed by depressurization and addition of the diol at 25 °C. However, this depressurization step led to the loss of some of the reaction mixture, thereby causing a deviation from the ideal stoichiometry. An inadequate stirring, caused by using a stainless-steel reactor and a magnetic stirrer, coupled to the increasing viscosity of the medium might also account for an inefficient polymerisation process.

In order to tentatively solve these issues, we envisioned the use of a concatenated continuous microfluidics reactor. In contrast to polymerisations performed in conventional reactors, the two steps of the process could be decoupled in microfluidics with a first zone dedicated to the *in-situ* formation of Bis α CCs and the second one for the step-growth polymerisation after addition of the diol as illustrated in **Scheme 1**. Each step could therefore be separately controlled by the experimental conditions (flow, temperature) and the nature/content of the catalyst.

Perspectives



Scheme 1. Synthesis of poly(oxo-carbonate)s in a continuous flow reactor.

Whilst a lot of progress has been made for chain-growth polymerisations, the implementation of step-growth polymerisations in flow remains relatively unexplored.^[221]

The work described in this chapter is very preliminary and deals with studying the first step of the *in-situ* formation of alkylidene cyclic carbonate, thus the carboxylative cyclisation of CO₂ to a model propargylic alcohol in flow. Herein, we try to understand the influence of the various parameters on the conversion of the propargylic alcohol and selectivity in the desired α CC.

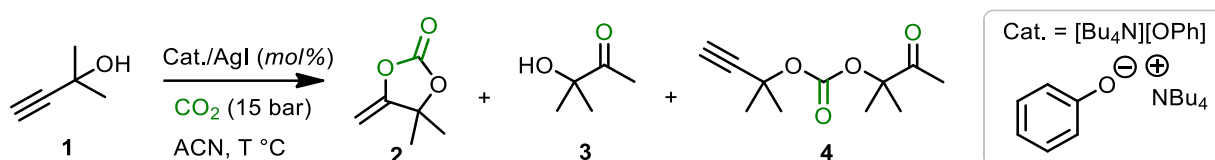
2. Results

2.1. Determining the optimum parameters for the synthesis of α CC in flow

Preliminary tests

The carboxylative coupling of 2-methyl-3-butyn-2-ol was used as the model reaction. Initially, we screened parameters to determine the conditions that would allow total conversion in <15 min in batch (Table 1), as this is a requirement for transfer to microfluidic systems. This was achieved by using our [nBu₄N][OPh]/AgI system at 60 °C and 15 bar, however with a 95% selectivity for DMACC (Table 1, entry 4).

Table 1. Screening of parameters for the coupling of CO₂ to 2-methyl-3-butyn-2-ol.



Entry	Org cat	AgI (mol%)	Temp (°C)	Pressure (bar)	Conversion (%)	Selectivity 2 (%)
1	[nBu ₄ N][OPh]	5	50	15	100	95
2	[nBu ₄ N][OPh]	5	60	15	100	94
3	[nBu ₄ N][OPh]	1	50	15	64	93
4	[nBu ₄ N][OPh]	1	60	15	100	94
5	DBU	1	50	15	76	97
6	DBU	1	60	15	79	97

Conditions: 2-methyl-3-butyn-2-ol (2 mL, 0.0206mol), Organic catalyst (5 mol%), solvent (2 mL), CO₂ (15 bar), 15 minutes. The conversions and selectivity were determined by ¹H-NMR in DMSO-d₆.

We know that increasing the reaction temperature seems contradictory as we have shown in **chapters 2** and **3** that it results in secondary reactions. However, this was the only simple way to increase the kinetics without having to increase the amount of organo-catalyst and was necessary to begin the implementation of the flow process. Once we will have found suitable conditions in flow that allow for the total conversion of the propargylic alcohol, we would then proceed to the optimization of the process to improve the selectivity.

Implementing the synthesis of DMACC in flow

Haven met our requirement by batch, it was time to implement the synthesis of DMACC in flow. The experimental setup is shown in the experimental section 3 and the results are presented in **Table 2**. The initial test conducted at 60 °C/7 bar, 0.2 mL/min flowrate of the reactants, 40 mL/min of CO₂, gave a conversion of 75% in the propargylic alcohol with a 92% selectivity for DMACC after 10 min of stabilization time (entry 1). An attempt to reproduce these results were unsuccessful as we observed clogging of our system at the level of the y-mixer. We believed that it resulted from the low solubility of AgI in DMSO, hence we filtered our reactant solution on a 0.45 µm filter.

We also decreased the pressure to 5.2 bar and increased the CO₂ flow rate to 100 mL/min, a 23% conversion was observed with a 67% selectivity for DMACC and the remainder for the linear carbonate from the alcoholysis of DMACC by the propargylic alcohol (entry 2). When we increased the pressure to 7 bar, we observed again a clogging of our system (entry 3). Next, we decided to carry out the reaction without AgI, surprisingly, we still observed clogging of our system or problems with the CO₂ flowrate (entries 4 and 5). Then we thought that the highly concentrated reactive solution in DMSO and the low temperature in the laboratory might result in the crystallization of DMSO in the syringe, thus we decreased the concentration to 1 M. Still, no conversion of the propargylic alcohol was obtained, increasing the temperature to 80 °C, or the CO₂ flowrate did not seem to influence the outcome of the reaction (entries 6,7 and 8). Then we changed the solvent for ACN, at both 60 and 80 °C, however no conversion was achieved despite we did not experience clogging issues (entries 9 and 10). We decided to reintroduce some AgI, however this time we filtered on a 0.2 µm, about 13-18% conversion was obtained; sadly, we observed some clogging after about 5 minutes of experiment (entries 11 and 12). From the above experiments, it was clear that we needed AgI in our system if we wanted to accelerate the reaction, however we had to deal with clogging issues.

This prompted us to test another mixer, a T-mixer, which does not have any frit in it, with the hope that it would tolerate larger amounts of AgI without clogging. As shown in entries 13-16 we were able to obtain a conversion of 33-39%. Although this is still far from the 100% desired, it was an improvement from the previous results. In addition, we did not observe any clogging after filtrating on 0.2 µm. Another important observation was that we could keep the CO₂ flow rate at lower values (62 mL/min). It is important to note that filtrating on 0.2 µm was expected to remove part of AgI, which might explain the low conversion obtained.

Table 2. Initial screening of parameters for the coupling of CO₂ and 3-methyl-2-butyn-2-ol in a microfluidic reactor.

Entry	Agl (mol%)	T (°C)	BPR (bar)	Solvent/ Conc (M)	Flowrate (mL/min)		τ (min)	Conv. (%)	Select. α_{cc} (%)	Note
					solution	CO ₂				
1	1	60	7	DMSO/ 5.15	0.2	40	10	75	92	/
2	1	60	5.2	DMSO/ 5.15	0.2	100	10	23	67	Filtered on 0.45 μ m
3	1	60	7	DMSO/ 5.15	0.2	100	/	/	/	Filtered on 0.45 μ m, clogging
4	/	60	5.2	DMSO/ 5.15	0.2	100	10	0	/	/
5	/	60	7	DMSO/ 5.15	0.2	100	<10	0	/	Clogging
6	/	60	7	DMSO/ 1	0.2	250	10	0	/	/
7	/	60	7	DMSO/ 1	0.4	250	10	0	/	CO ₂ flow inconsistent
8	/	80	7	DMSO/ 1	0.2	250	1	0	/	CO ₂ flow inconsistent, aborted
9	/	80	7	ACN/1	0.2	250	10	0	/	/
10	/	60	7	ACN/1	0.2	250	10	0	/	/
11	1	60	7	ACN/1	0.2	250	12	18		Filtered on 0.2 μ m
12	1	60	7	ACN/1	0.2	125	10	13		Filtered on 0.2 μ m, clogging at end
13	1	60	7	ACN/1	0.2	125	10	33		T-mixer
14	1	60	7	ACN/1	0.2	62.5	10	39		T-mixer
15	1	60	7	ACN/1	0.05	62.5	30	37		T-mixer
16	1	80	7	ACN/1	0.05	62.5	20	37		T-mixer

Conditions: reactive solution composed of 3-methyl-2-butyn-2-ol in a solvent and [nBu₄N][OPh] (5 mol%), AgI (0-1 mol%). Conversion and selectivity determined by ¹H-NMR in DMSO-d₆. τ = residence time.

Long term perspective

As discussed above, we had issues using our catalytic system [nBu₄N][OPh]/AgI for the synthesis of αCC in a continuous micro fluidic reactor. The difficulty arose from the poor solubility of AgI. In order to solve this issue, various steps could be undertaken; the first would be to use a packed column containing supported AgI. This system seems like something which could be easily implemented, as there are several commercially available resins which could be used for the deposition of AgI. However, we would be switching to a hybrid system (homogenous + heterogenous), which could impact reactivity. Moreover, some leaching of the metal might occur thus deactivating the catalyst on the long run. The second possibility would be to develop a completely different catalytic system in which the Ag (I) would be coordinated to a ligand that would render it soluble. This would allow us to remain with a completely homogenous system. Hence the next stage of this work would be first to optimise our catalytic system to render it suitable for application in the continuous flow synthesis of αCCs. Once we have efficiently implemented the synthesis of the αCCs, we would then move to the synthesis of the bisαCC. Then, we would study the step-growth synthesis of poly(oxocarbonate)s in flow and optimise the reaction parameters. Lastly, we would combine both steps to have a continuous process, i.e. from the synthesis of the bisαCCs to the poly(oxocarbonate)s.

3. Experimental section

3.1. Reagents

3-methyl-2-butyn-2-ol and AgI were purchased from Aldrich/Merck. [nBu₄N][OPh] was synthesised as described in **chapter 2**. CO₂ was purchased from Air Liquid. DMSO-d₆ was purchased from Eurisotop.

3.2. Apparatus

Nuclear magnetic resonance spectroscopy (NMR). The samples were prepared by dissolving 15-20 mg of product in 0.7 mL of DMSO-d₆. ¹H- and ¹³C-NMR spectra were recorded at 298 K with a Bruker advance DRX 400 spectrometer operating at 400.13 MHz, on the Fourier transform mode.

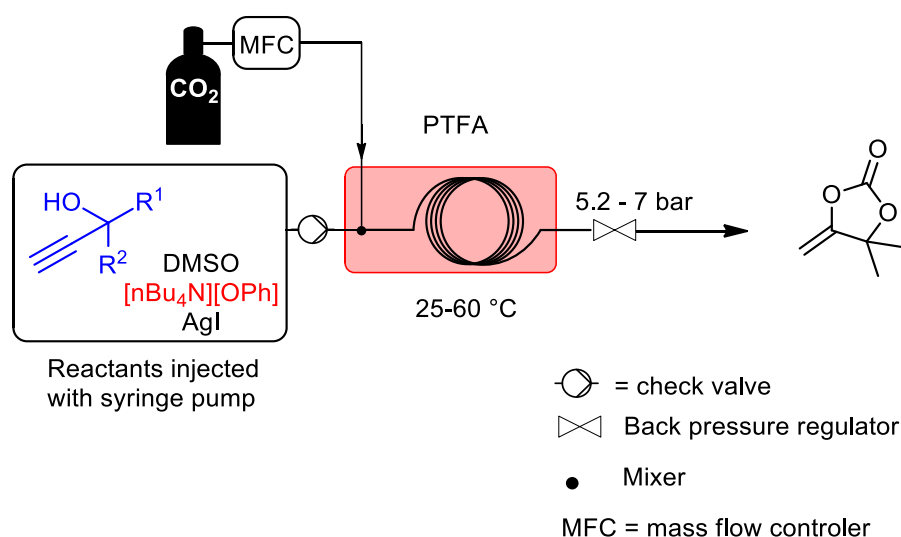
3.3. Experimental procedures

Batch optimization tests

In a representative experiment, a stainless-steel autoclave with a nominal volume of 12 mL, equipped with a magnetic rod, a manometer and a gas inlet/outlet was charged with 2-methyl-3-butyn-2-ol (2 mL, 0.0206 mol) and $[n\text{Bu}_4\text{N}][\text{OPh}]$ (0.3456 g, 1.03 mmol; 5 mol%), and AgI (0.04836 g, 0.206 mmol; 1 mol%). The autoclave was equilibrated at 60 °C for 30 min. Then, the reaction was allowed to run during 15 min at constant CO_2 pressure of 15 bar. The crude reaction mixture was analysed by $^1\text{H-NMR}$ to determine the conversion, identify the products, and determine the selectivity of the reaction.

Flow tests

For the flow experiments, a PTFE reactor of internal diameter of 750 nm and internal volume of 7 mL was used which was heated using a thermostated water bath. A CO_2 cylinder equipped with a pressure regulator and connected to a massflow controller was used. The reactant solution of 1 M was prepared by mixing 2-methyl-3-butyn-2-ol (3 mL) with DMSO (30 mL) and was then added by $[n\text{Bu}_4\text{N}][\text{OPh}]$ (0.5072 g, 1.51 mmol; 5 mol%) and AgI (0.07096 g, 0.3027 mmol; 1 mol%). The solution was injected using a syringe pump. Samples were collected after different residence times (**Scheme 2**).



Scheme 2. Experimental setup used for the continuous flow synthesis of DMACC.

Bibliography

- [1] D. J. Darensbourg, P. Ganguly, D. Billodeaux, *Macromolecules* **2005**, *38*, 5406–5410.
- [2] M. Helou, O. Miserque, J. M. Brusson, J. F. Carpentier, S. M. Guillaume, *Chem. - A Eur. J.* **2010**, *16*, 13805–13813.
- [3] S. Tempelaar, L. Mespouille, O. Coulembier, P. Dubois, A. P. Dove, *Chem. Soc. Rev.* **2013**, *42*, 1312–1336.
- [4] F. Nederberg, B. G. G. Lohmeijer, F. Leibfarth, R. C. Pratt, J. Choi, A. P. Dove, R. M. Waymouth, J. L. Hedrick, *Biomacromolecules* **2007**, *8*, 153–160.
- [5] J. Xu, E. Feng, J. Song, *J. Appl. Polym. Sci.* **2014**, *131*, 39822.
- [6] J. Sun, D. Kuckling, *Polym. Chem.* **2016**, *7*, 1642–1649.
- [7] M. Alves, B. Grignard, R. Mereau, C. Jérôme, T. Tassaing, C. Detrembleur, *Catal. Sci. Technol.* **2017**, *7*, 2651–2684.
- [8] A. W. Kleij, in *Green Synth. Approaches Biol. Relev. Heterocycles*, Elsevier Inc., **2015**, pp. 141–162.
- [9] J. C. Lee, M. H. Litt, *Macromolecules* **2000**, *33*, 1618–1627.
- [10] W. Guerin, A. K. Diallo, E. Kirilov, M. Helou, M. Slawinski, J. M. Brusson, J. F. Carpentier, S. M. Guillaume, *Macromolecules* **2014**, *47*, 4230–4235.
- [11] G. W. Coates, D. R. Moore, *Angew. Chem. Int. Ed.* **2004**, *43*, 6618–6639.
- [12] X. B. Lu, D. J. Darensbourg, *Chem. Soc. Rev.* **2012**, *41*, 1462–1484.
- [13] M. R. Kember, C. K. Williams, *J. Am. Chem. Soc.* **2012**, *134*, 15676–15679.
- [14] J. A. Garden, P. K. Saini, C. K. Williams, *J. Am. Chem. Soc.* **2015**, *137*, 15078–15081.
- [15] M. J. Sanford, L. Peña Carrodegua, N. J. Van Zee, A. W. Kleij, G. W. Coates, *Macromolecules* **2016**, *49*, 6394–6400.
- [16] S. Bian, C. Pagan, A. A. Andrianovaartemyeva, G. Du, *ACS Omega* **2016**, *1*, 1049–1057.
- [17] M. Tamura, K. Ito, M. Honda, Y. Nakagawa, H. Sugimoto, K. Tomishige, *Sci. Rep.* **2016**, *6*, 24038 (1–9).
- [18] S. Gennen, B. Grignard, T. Tassaing, C. Jérôme, C. Detrembleur, *Angew. Chem. Int. Ed.* **2017**, *56*, 10394–10398.
- [19] Q. Song, L. He, in *Adv. CO2 Capture, Sequestration, Convers.*, **2015**, pp. 48–70.
- [20] B. Grignard, S. Gennen, C. Jérôme, A. W. Kleij, C. Detrembleur, *Chem. Soc. Rev.* **2019**, *48*, 4466–4514.
- [21] R. Calmanti, M. Selva, A. Perosa, *Green Chem.* **2021**, *23*, 1921–1941.
- [22] B. Limburg, À. Cristòfol, F. Della Monica, A. W. Kleij, *ChemSusChem* **2020**, *13*, 6056–6065.

- [23] C. Maquilón, B. Limburg, V. Laserna, D. Garay-Ruiz, J. González-Fabra, C. Bo, M. Martínez Belmonte, E. C. Escudero-Adán, A. W. Kleij, *Organometallics* **2020**, *39*, 1642–1651.
- [24] J. W. Comerford, I. D. V. Ingram, M. North, X. Wu, *Green Chem.* **2015**, *17*, 1966–1987.
- [25] L. Guo, K. J. Lamb, M. North, *Green Chem.* **2021**, *23*, 77–118.
- [26] J. Huang, C. Jehanno, J. C. Worch, F. Ruipérez, H. Sardon, A. P. Dove, O. Coulembier, *ACS Catal.* **2020**, *10*, 5399–5404.
- [27] G. A. Bhat, M. Luo, D. J. Darensbourg, *Green Chem.* **2020**, *22*, 7707–7724.
- [28] S. Sopeña, G. Fiorani, C. Martín, A. W. Kleij, *ChemSusChem* **2015**, *8*, 3248–3254.
- [29] M. Alves, B. Grignard, A. Boyaval, R. Méreau, J. De Winter, P. Gerbaux, C. Detrembleur, T. Tassaing, C. Jérôme, *ChemSusChem* **2017**, *10*, 1128–1138.
- [30] G. Fiorani, M. Stuck, C. Martín, M. M. Belmonte, E. Martin, E. C. Escudero-Adán, A. W. Kleij, *ChemSusChem* **2016**, *9*, 1304–1311.
- [31] M. Tamura, K. Ito, M. Honda, Y. Nakagawa, H. Sugimoto, K. Tomishige, *Sci. Rep.* **2016**, *6*, 24038 (1–9).
- [32] A. Brege, R. Méreau, K. McGehee, B. Grignard, C. Detrembleur, C. Jérôme, T. Tassaing, *J. CO2 Util.* **2020**, *38*, 88–98.
- [33] F. D. Bobbink, W. Gruszka, M. Hulla, S. Das, P. J. Dyson, *Chem. Commun.* **2016**, *52*, 10787–10790.
- [34] T. M. McGuire, E. M. López-Vidal, G. L. Gregory, A. Buchard, *J. CO2 Util.* **2018**, *27*, 283–288.
- [35] G. L. Gregory, M. Ulmann, A. Buchard, *RSC Adv.* **2015**, *5*, 39404–39408.
- [36] K. Tomishige, H. Yasuda, Y. Yoshida, M. Nurunnabi, B. Li, K. Kunimori, *Green Chem.* **2004**, *6*, 206–214.
- [37] M. Honda, M. Tamura, K. Nakao, K. Suzuki, Y. Nakagawa, K. Tomishige, *ACS Catal.* **2014**, *4*, 1893–1896.
- [38] Y. N. Lim, C. Lee, H. Y. Jang, *European J. Org. Chem.* **2014**, *2014*, 1823–1826.
- [39] W. Li, D. Huang, Y. Lyu, *Org. Biomol. Chem.* **2016**, *14*, 10875–10885.
- [40] R. Méreau, B. Grignard, A. Boyaval, C. Detrembleur, C. Jerome, T. Tassaing, *ChemCatChem* **2018**, *10*, 956–960.
- [41] Y. Yuan, Y. Xie, C. Zeng, D. Song, S. Chaemchuen, C. Chen, F. Verpoort, *Green Chem.* **2017**, *19*, 2936–2940.
- [42] M. E. Jung, G. Piizzi, *Chem. Rev.* **2005**, *105*, 1735–1766.
- [43] A. Cervantes-Reyes, K. Farshadfar, M. Rudolph, F. Rominger, T. Schaub, A. Ariafard, A. S. K. Hashmi, *Green Chem.* **2021**, *23*, 889–897.

- [44] Y. Kayaki, M. Yamamoto, T. Ikariya, *J. Org. Chem.* **2007**, *72*, 647–649.
- [45] J. Fournier, C. Bruneau, P. H. Dixneuf, *Tetrahedron Lett.* **1989**, *30*, 3981–3982.
- [46] C. Bruneau, P. H. Dixneuf, *J. Mol. Catal.* **1992**, *74*, 97–107.
- [47] J. Hu, J. Ma, Q. Zhu, Q. Qian, H. Han, Q. Mei, B. Han, *Green Chem.* **2016**, *18*, 382–385.
- [48] N. Della Ca', B. Gabriele, G. Ruffolo, L. Veltri, T. Zanetta, M. Costa, *Adv. Synth. Catal.* **2011**, *353*, 133–146.
- [49] A. Boyaval, R. Méreau, B. Grignard, C. Detrembleur, C. Jérôme, T. Tassaing, *ChemSusChem* **2017**, *10*, 1241–1248.
- [50] Y. Kayaki, M. Yamamoto, T. Ikariya, *Angew. Chemie - Int. Ed.* **2009**, *48*, 4194–4197.
- [51] A. H. Liu, Y. L. Dang, H. Zhou, J. J. Zhang, X. B. Lu, *ChemCatChem* **2018**, *10*, 2686–2692.
- [52] H. Zhou, G. X. Wang, X. B. Lu, *Asian J. Org. Chem.* **2017**, *6*, 1264–1269.
- [53] Y. B. Wang, D. S. Sun, H. Zhou, W. Z. Zhang, X. B. Lu, *Green Chem.* **2014**, *16*, 2266–2272.
- [54] H. Zhou, R. Zhang, X. B. Lu, *Adv. Synth. Catal.* **2019**, *361*, 326–334.
- [55] Y.-B. Wang, Y.-M. Wang, W.-Z. Zhang, X.-B. Lu, *J. Am. Chem. Soc.* **2013**, *135*, 11996–12003.
- [56] S. Zhang, Y. Huang, H. Jing, W. Yao, P. Yan, *Green Chem.* **2009**, *11*, 935–938.
- [57] H. Zhou, G. X. Wang, W. Z. Zhang, X. B. Lu, *ACS Catal.* **2015**, *5*, 6773–6779.
- [58] Y. Zhao, Y. Wu, G. Yuan, L. Hao, X. Gao, Z. Yang, B. Yu, H. Zhang, Z. Liu, *Chem. - An Asian J.* **2016**, *11*, 2735–2740.
- [59] B. Grignard, C. Ngassamtounzoua, S. Gennen, B. Gilbert, R. Méreau, C. Jerome, T. Tassaing, C. Detrembleur, *ChemCatChem* **2018**, *10*, 2584–2592.
- [60] J. Qiu, Y. Zhao, Z. Li, H. Wang, M. Fan, J. Wang, *ChemSusChem* **2017**, *10*, 1120–1127.
- [61] Y. Wu, Y. Zhao, R. Li, B. Yu, Y. Chen, X. Liu, C. Wu, X. Luo, Z. Liu, *ACS Catal.* **2017**, *7*, 6251–6255.
- [62] K. Chen, G. Shi, R. Dao, K. Mei, X. Zhou, H. Li, C. Wang, *Chem. Commun.* **2016**, *52*, 7830–7833.
- [63] K. Ueno, H. Tokuda, M. Watanabe, *Phys. Chem. Chem. Phys.* **2010**, *12*, 1649–1658.
- [64] O. Nordness, J. F. Brennecke, *Chem. Rev.* **2020**, *120*, 12873–12902.
- [65] Y. Sasaki, *Tetrahedron Lett.* **1986**, *27*, 1573–1574.
- [66] Y. Inoue, J. Ishikawa, M. Taniguchi, H. Hashimoto, *Bull. Chem. Soc. Jpn.* **1987**, *60*, 1204–1206.
- [67] S. Sun, B. Wang, N. Gu, J. T. Yu, J. Cheng, *Org. Lett.* **2017**, *19*, 1088–1091.
- [68] M. Li, S. Abdolmohammadi, M. S. Hoseininezhad-Namin, F. Behmagham, E. Vessally, *J.*

- CO2 Util.* **2020**, *38*, 220–231.
- [69] Y. Hu, J. Song, C. Xie, H. Wu, T. Jiang, G. Yang, B. Han, *ACS Sustain. Chem. Eng.* **2019**, *7*, 5614–5619.
- [70] Y. Gu, F. Shi, Y. Deng, *J. Org. Chem.* **2004**, *69*, 391–394.
- [71] C. Ngassam Tounzoua, B. Grignard, A. Brege, C. Jerome, T. Tassaing, R. Mereau, C. Detrembleur, *ACS Sustain. Chem. Eng.* **2020**, *8*, 9698–9710.
- [72] Q. W. Song, L. N. He, *Adv. Synth. Catal.* **2016**, *358*, 1251–1258.
- [73] Q. W. Song, B. Yu, X. D. Li, R. Ma, Z. F. Diao, R. G. Li, W. Li, L. N. He, *Green Chem.* **2014**, *16*, 1633–1638.
- [74] Y. Yuan, Y. Xie, C. Zeng, D. Song, S. Chaemchuen, C. Chen, F. Verpoort, *Catal. Sci. Technol.* **2017**, *7*, 2935–2939.
- [75] Y. Hu, J. Song, C. Xie, H. Wu, T. Jiang, G. Yang, B. Han, J. Song, C. Xie, H. Wu, T. Jiang, G. Yang, B. Han, *ACS Sustain. Chem. Eng.* **2019**, *7*, 5614–5619.
- [76] Q. W. Song, W. Q. Chen, R. Ma, A. Yu, Q. Y. Li, Y. Chang, L. N. He, *ChemSusChem* **2015**, *8*, 821–827.
- [77] S. Dabral, B. Bayarmagnai, M. Hermsen, J. Schießl, V. Mormul, A. S. K. Hashmi, T. Schaub, *Org. Lett.* **2019**, *21*, 1422–1425.
- [78] C. Johnson, S. Dabral, P. Rudolf, U. Licht, A. S. K. Hashmi, T. Schaub, *ChemCatChem* **2021**, *13*, 353–361.
- [79] X. YU, Z. Yang, F. Zhang, Z. Liu, P. Yang, H. Zhang, B. Yu, Y. Zhao, Z. Liu, *Chem. Commun.* **2019**, *55*, 12475–12478.
- [80] H. F. Jiang, A. Z. Wang, H. L. Liu, C. R. Qi, *European J. Org. Chem.* **2008**, 2309–2312.
- [81] X. Tang, C. Qi, H. He, H. Jiang, Y. Ren, G. Yuan, *Adv. Synth. Catal.* **2013**, *355*, 2019–2028.
- [82] J. Qiu, Y. Zhao, H. Wang, G. Cui, J. Wang, *RSC Adv.* **2016**, *6*, 54020–54026.
- [83] X. Zhang, K. Chen, Z. Zhou, L.-N. He, *ChemCatChem* **2020**, *12*, 4825–4830.
- [84] D. Chakraborty, P. Shekhar, H. D. Singh, R. Kushwaha, C. P. Vinod, R. Vaidhyanathan, *Chem. - An Asian J.* **2019**, *14*, 4767–4773.
- [85] S. S. Islam, S. Biswas, R. Ali Molla, N. Yasmin, S. M. Islam, *ChemNanoMat* **2020**, *6*, 1386–1397.
- [86] A. K. Ghosh, M. Brindisi, *J. Med. Chem.* **2015**, *58*, 2895–2940.
- [87] H. Babad, G. Zeiler, Andrew, *Chem. Rev.* **1973**, *73*, 75–91.
- [88] S. Yoganathan, S. J. Miller, *Org. Lett.* **2013**, *15*, 602–605.
- [89] Y. Ren, S. A. L. Rousseaux, *J. Org. Chem.* **2018**, *83*, 913–920.
- [90] J. Fournier, C. Bruneau, P. H. Dixneuf, *Tetrahedron Lett.* **1990**, *31*, 1721–1722.

- [91] T. Habets, F. Siragusa, B. Grignard, C. Detrembleur, *Macromolecules* **2020**, *53*, 6396–6408.
- [92] S. Gennen, B. Grignard, C. Jérôme, C. Detrembleur, *Adv. Synth. Catal.* **2019**, *361*, 355–365.
- [93] C. Bruneau, P. H. Dixneuf, *Tetrahedron Lett.* **1987**, *28*, 2005–2008.
- [94] H. S. Kim, J. W. Kim, S. C. Kwon, S. C. Shim, T. J. Kim, *J. Organomet. Chem.* **1997**, *545–546*, 337–344.
- [95] Q. W. Song, P. Liu, L. H. Han, K. Zhang, L. N. He, *Chinese J. Chem.* **2018**, *36*, 147–152.
- [96] Q.-N. Zhao, Q.-W. Song, P. Liu, K. Zhang, J. Hao, *ChemistrySelect* **2018**, *3*, 6897–6901.
- [97] Z. Zhang, H. Gao, H. Wu, Y. Qian, L. Chen, J. Chen, *ACS Appl. Nano Mater.* **2018**, *1*, 6463–6476.
- [98] L. Fan, J. Wang, X. Zhang, S. M. Sadeghzadeh, R. Zhiani, M. Shahroudi, F. Amarloo, *Catal. Letters* **2019**, *149*, 3465–3475.
- [99] H. Liu, R. Hua, *Tetrahedron* **2016**, *72*, 1200–1204.
- [100] Q. Zhang, F. Shi, Y. Gu, J. Yang, Y. Deng, *Tetrahedron Lett.* **2005**, *46*, 5907–5911.
- [101] Y. Gu, Q. Zhang, Z. Duan, J. Zhang, S. Zhang, Y. Deng, *J. Org. Chem.* **2005**, *70*, 7376–7380.
- [102] H. Jiang, J. Zhao, A. Wang, *Synthesis (Stuttg.)* **2008**, 763–769.
- [103] H. F. Jiang, J. W. Zhao, *Tetrahedron Lett.* **2009**, *50*, 60–62.
- [104] J. X. Xu, J. W. Zhao, Z. Bin Jia, *Chinese Chem. Lett.* **2011**, *22*, 1063–1066.
- [105] J. M. Joumier, J. Fournier, C. Bruneau, P. H. Dixneuf, *J. Chem. Soc. Perkin Trans. 1* **1991**, *12*, 3271–3274.
- [106] J. M. Joumier, C. Bruneau, P. H. Dixneuf, *J. Chem. Soc., Perkin Trans. 1* **1993**, *50*, 1749–1751.
- [107] F. Siragusa, E. Van Den Broeck, C. Ocando, A. J. Müller, G. De Smet, B. U. W. Maes, J. De Winter, V. Van Speybroeck, B. Grignard, C. Detrembleur, *ACS Sustain. Chem. Eng.* **2021**, *9*, 1714–1728.
- [108] Q.-W. Song, Q.-N. Zhao, J.-Y. Li, K. Zhang, P. Liu, *Synthesis (Stuttg.)* **2019**, *51*, 739–746.
- [109] Z.-H. Zhou, Q.-W. Song, J.-N. Xie, R. Ma, L.-N. He, *Chem. - An Asian J. J.* **2016**, *11*, 2065–2071.
- [110] J. Hu, J. Ma, L. Lu, Q. Qian, Z. Zhang, C. Xie, B. Han, *ChemSusChem* **2017**, *10*, 1292–1297.
- [111] J. Li, Q. Song, H. Zhang, P. Liu, K. Zhang, J. Wang, D. Zhang, *Tetrahedron* **2019**, *75*, 2343–2349.
- [112] Z. H. Zhou, Q. W. Song, L. N. He, *ACS Omega* **2017**, *2*, 337–345.
- [113] J. Y. Li, L. H. Han, Q. C. Xu, Q. W. Song, P. Liu, K. Zhang, *ACS Sustain. Chem. Eng.* **2019**,

- 7, 3378–3388.
- [114] H. Zhou, H. Zhang, S. Mu, W. Z. Zhang, W. M. Ren, X. B. Lu, *Green Chem.* **2019**, *21*, 6335–6341.
- [115] P. Hoyos, J.-V. Sinisterra, F. Molinari, A. R. Alcántara, P. Domínguez de María, *Acc. Chem. Res.* **2010**, *43*, 288–299.
- [116] M. Kutscheroff, *Berichte der Dtsch. Chem. Gesellschaft* **1881**, *14*, 1540–1542.
- [117] R. J. Thomas, K. N. Campbell, G. F. Hennion, *J. Am. Chem. Soc.* **1938**, *60*, 718–720.
- [118] Y. Zhao, Z. Yang, B. Yu, H. Zhang, H. Xu, L. Hao, B. Han, Z. Liu, *Chem. Sci.* **2015**, *6*, 2297–2301.
- [119] H. He, C. Qi, X. Hu, Y. Guan, H. Jiang, *Green Chem.* **2014**, *16*, 3729–3733.
- [120] D. Li, Y. Gong, M. Du, C. Bu, C. Chen, S. Chaemcheun, J. Hu, Y. Zhang, Y. Yuan, F. Verpoort, *ACS Sustain. Chem. Eng.* **n.d.**
- [121] Z. Zhou, X. Zhang, Y. Huang, K. Chen, L. He, *Chinese J. Catal.* **2019**, *40*, 1345–1351.
- [122] Q.-W. Song, Z.-H. Zhou, M. Wang, K. Zhang, P. Liu, J.-Y. Xun, L.-N. He, *ChemSusChem* **2016**, *9*, 2054–2058.
- [123] F. D. Bobbink, A. P. Van Muyden, P. J. Dyson, *Chem. Commun.* **2018**, *55*, 1360–1373.
- [124] C. Bu, Y. Gong, M. Du, C. Chen, S. Chaemchuen, J. Hu, Y. Zhang, H. D. Velázquez, Y. Yuan, F. Verpoort, *Catalysts* **2021**, *11*, 1–15.
- [125] M. Du, Y. Gong, C. Bu, J. Hu, Y. Zhang, C. Chen, S. Chaemchuen, Y. Yuan, F. Verpoort, *J. Catal.* **2021**, *393*, 70–82.
- [126] P. Chauhan, S. Mahajan, D. Enders, *Chem. Rev.* **2014**, *114*, 8807–8864.
- [127] J. Clayden, P. MacLellan, *Beilstein J. Org. Chem.* **2011**, *7*, 582–595.
- [128] L. A. (Lyaquatali A. Damani, *Sulphur-Containing Drugs and Related Organic Compounds : Chemistry, Biochemistry and Toxicology / Editor: L.A. Damani. Vol.3, Pt.A, Metabolism and Pharmokinetics of Sulphur-Containing Drugs.*, Ellis Horwood, Chichester, **1989**.
- [129] B. Liu, X. Zhang, *Gen. Chem.* **2018**, *4*, 1–6.
- [130] F. Ouhib, B. Grignard, E. Van Den Broeck, A. Luxen, K. Robeyns, V. Van Speybroeck, C. Jerome, C. Detrembleur, *Angew. Chemie - Int. Ed.* **2019**, *58*, 11768–11773.
- [131] Y. Inoue, Y. Itoh, I. F. Yen, S. Imaizumi, *J. Mol. Catal.* **1990**, *60*, L1–L3.
- [132] P. Toullec, A. Carbayo Martin, M. Gio-Batta, C. Bruneau, P. H. Dixneuf, *Tetrahedron Lett.* **2000**, *41*, 5527–5531.
- [133] S. Dabral, U. Licht, P. Rudolf, G. Bollmann, A. Stephen, K. Hashmi, T. Schaub, *Green Chem.* **2020**, *22*, 1553–1558.
- [134] F. E. Golling, R. Pires, A. Hecking, J. Weikard, F. Richter, K. Danielmeier, D. Dijkstra,

- Polym. Int.* **2019**, *68*, 848–855.
- [135] D. M. Segura, A. D. Nurse, A. McCourt, R. Phelps, A. Segura, *Handb. Adhes. Sealants* **2005**, *1*, 101–162.
- [136] F. Monie, T. Vidil, B. Grignard, H. Cramail, C. Detrembleur, *Mater. Sci. Eng. R* **2021**, *145*, 100628 (1–28).
- [137] J. Peyrton, L. Avérous, *Mater. Sci. Eng. R Reports* **2021**, *145*, 100608 (1–31).
- [138] S. Wendels, L. Averous, *Bioact. Mater.* **2021**, *6*, 1083–1106.
- [139] S. Sartori, V. Chiono, C. Tonda-Turo, C. Mattu, G. Ciardelli, *J. Mater. Chem. B* **2014**, *2*, 5128–5144.
- [140] R. J. Zdrahal, I. J. Zdrahala, *J. Biomed. Appl.* **1999**, *14*, 67–90.
- [141] M. Sáenz-Pérez, E. Lizundia, J. M. Laza, J. García-Barrasa, J. L. Vilas, L. M. León, *RSC Adv.* **2016**, *6*, 69094–69102.
- [142] S. A. Cucinell, E. Arsenal, S. A. Cucinell, *Arch. Environ. Health* **1974**, *28*, 272–275.
- [143] A. Cornille, R. Auvergne, O. Figovsky, B. Boutevin, S. Caillol, *Eur. Polym. J.* **2017**, *87*, 535–552.
- [144] D. Zhang, Y. Zhang, Y. Fan, M. N. Rager, V. Guérineau, L. Bouteiller, M. H. Li, C. M. Thomas, *Macromolecules* **2019**, *52*, 2719–2724.
- [145] D. Tian, B. Liu, Q. Gan, H. Li, D. J. Darensbourg, *ACS Catal.* **2012**, *2*, 2029–2035.
- [146] A. Decortes, A. M. Castilla, A. W. Kleij, *Angew. Chemie - Int. Ed.* **2010**, *49*, 9822–9837.
- [147] M. Alves, B. Grignard, S. Gennen, C. Detrembleur, C. Jerome, T. Tassaing, *RSC Adv.* **2015**, 53629–53636.
- [148] S. E. Dechent, A. W. Kleij, G. A. Luinstra, *Green Chem.* **2020**, *22*, 969–978.
- [149] L. Poussard, J. Mariage, B. Grignard, C. Detrembleur, C. Jérôme, C. Calberg, B. Heinrichs, J. De Winter, P. Gerbaux, J. M. Raquez, L. Bonnaud, P. Dubois, *Macromolecules* **2016**, *49*, 2162–2171.
- [150] B. Grignard, J. Thomassin, S. Gennen, L. Poussard, L. Bonnaud, J. Raquez, P. Dubois, M. Tran, C. B. Park, C. Jérôme, C. Detrembleur, *Green Chem.* **2016**, *18*, 2206–2215.
- [151] S. Gennen, B. Grignard, J. M. Thomassin, B. Gilbert, B. Vertruyen, C. Jérôme, C. Detrembleur, *Eur. Polym. J.* **2016**, *84*, 849–862.
- [152] R. H. Lambeth, T. J. Henderson, *Polymer (Guildf)*. **2013**, *54*, 5568–5573.
- [153] A. Cornille, M. Blain, R. Auvergne, B. Andrioletti, B. Boutevin, S. Caillol, *Polym. Chem.* **2017**, *8*, 592–604.
- [154] E. Rix, E. Grau, G. Chollet, H. Cramail, *Eur. Polym. J.* **2016**, *84*, 863–872.
- [155] J. H. Park, J. Y. Jeon, J. J. Lee, Y. Jang, J. K. Varghese, B. Y. Lee, *Macromolecules* **2013**, *46*, 3301–3308.

- [156] A. Y. Yuen, E. Lopez-Martinez, E. Gomez-Bengoia, A. L. Cortajarena, R. H. Aguirresarobe, A. Bossion, D. Mecerreyes, J. L. Hedrick, Y. Y. Yang, H. Sardon, *ACS Biomater. Sci. Eng.* **2017**, *3*, 1567–1575.
- [157] P. Brignou, M. Priebe Gil, O. Casagrande, J. F. Carpentier, S. M. Guillaume, *Macromolecules* **2010**, *43*, 8007–8017.
- [158] F. Suriano, O. Coulembier, J. L. Hedrick, P. Dubois, *Polym. Chem.* **2011**, *2*, 528–533.
- [159] S. M. Guillaume, J.-F. Carpentier, *Catal. Sci. Technol.* **2012**, *1*, 898–906.
- [160] G. L. Gregory, L. M. Jenisch, B. Charles, G. Kociok-ko, A. Buchard, *Macromolecules* **2016**, *49*, 7165–7169.
- [161] S. Venkataraman, J. P. K. Tan, V. W. L. Ng, E. W. P. Tan, J. L. Hedrick, Y. Y. Yang, *Biomacromolecules* **2017**, *18*, 178–188.
- [162] J. Huang, J. De Winter, A. P. Dove, O. Coulembier, *Green Chem.* **2019**, *21*, 472–477.
- [163] M. R. Kember, A. Buchard, C. K. Williams, *Chem. Commun.* **2011**, *47*, 141–163.
- [164] S. Inoue, H. Koinuma, T. Tsuruta, *Polym. Lett.* **1969**, *7*, 287–292.
- [165] D. J. Darensbourg, M. W. Holtcamp, G. E. Struck, M. S. Zimmer, S. A. Niezgoda, P. Rainey, J. B. Robertson, J. D. Draper, J. H. Reibenspies, *J. Am. Chem. Soc.* **1999**, *121*, 107–116.
- [166] M. Cheng, D. R. Moore, J. J. Reczek, B. M. Chamberlain, E. B. Lobkovsky, G. W. Coates, C. U. V, N. York, V. Recci, V. No, V. Re, M. Recci, V. June, *J. Am. CHEM. SOC* **2001**, *123*, 8738–8749.
- [167] S. D. Allen, D. R. Moore, E. B. Lobkovsky, G. W. Coates, *J. Am. CHEM. SOC* **2002**, *124*, 14284–14285.
- [168] X.-B. Lu, Y. Wang, *Angew. Chem. Int. Ed.* **2004**, *43*, 3574–3577.
- [169] C. M. Byrne, S. D. Allen, E. B. Lobkovsky, G. W. Coates, *J. Am. CHEM. SOC* **2004**, *126*, 11404–11405.
- [170] H. Sugimoto, S. Inoue, *J. Polym. Sci. Part A Polym. Chem.* **2004**, *42*, 5561–5573.
- [171] D. J. Darensbourg, R. M. Mackiewicz, A. L. Phelps, D. R. Billodeaux, *Acc. Chem. Res.* **2004**, *37*, 836–844.
- [172] W. Yu, E. Maynard, V. Chiaradia, M. C. Arno, A. P. Dove, *Chem. Rev.* **2021**, *121*, 10865–10907.
- [173] J. H. Jang, J. H. Ha, I. Kim, J. H. Baik, S. C. Hong, *ACS Omega* **2019**, *4*, 7944–7952.
- [174] J. Langanke, A. Wolf, J. Hofmann, K. Böhm, M. A. Subhani, T. E. Müller, W. Leitner, C. Gürtler, *Green Chem.* **2014**, *16*, 1865–1870.
- [175] J. Zhang, J. Yang, T. Dong, M. Zhang, J. Chai, S. Dong, T. Wu, X. Zhou, G. Cui, *Small* **2018**, *14*, 1800821.
- [176] F. Ouhib, L. Meabe, A. Mahmoud, N. Eshraghi, B. Grignard, J. Thomassin, A. Aqil, F.

- Boschini, C. Jérôme, D. Mecerreyes, C. Detrembleur, *Mater. Chem. A* **2019**, *7*, 9844–9853.
- [177] B. Song, T. Bai, X. Xu, X. Chen, D. Liu, J. Guo, A. Qin, J. Ling, B. Z. Tang, *Macromolecules* **2019**, *52*, 5546–5554.
- [178] F. Ouhib, L. Meabe, A. Mahmoud, B. Grignard, J.-M. Thomassin, F. Boschini, H. Zhu, M. Forsyth, D. Mecerreyes, C. Detrembleur, *ACS Appl. Polym. Mater.* **2020**, *2*, 922–931.
- [179] I. C. Lee, Tae-woong, *Makromol. Chem., Rapid Commun.* **1989**, *10*, 453–456.
- [180] P. B. V. Scholten, J. Demarteau, S. Gennen, J. De Winter, B. Grignard, A. Debuigne, M. A. R. Meier, C. Detrembleur, *Macromolecules* **2018**, *51*, 3379–3393.
- [181] P. B. V. Scholten, G. Cartigny, B. Grignard, A. Debuigne, H. Cramail, M. A. R. Meier, C. Detrembleur, *ACS Macro Lett.* **2021**, 313–320.
- [182] J. Demarteau, A. Debuigne, C. Detrembleur, *Chem. Rev.* **2019**, *119*, 6906–6955.
- [183] https://chemicals.basf.com/global/en/Intermediates/Product_groups/acetylenic-alcohols.html **n.d.**
- [184] J. M. McEnaney, B. A. Rohr, A. C. Nielander, A. R. Singh, L. A. King, J. K. Nørskov, T. F. Jaramillo, *Sustain. Energy Fuels* **2020**, *4*, 2752–2759.
- [185] M. N. Kopylovich, A. P. C. Ribeiro, E. C. B. A. Alegria, N. M. R. Martins, L. M. D. R. S. Martins, A. J. L. Pombeiro, in (Ed.: P.J.B.T.-A. in O.C. Pérez), Academic Press, **2015**, pp. 91–174.
- [186] K. Rajabimoghadam, Y. Darwish, U. Bashir, D. Pitman, S. Eichelberger, M. A. Siegler, M. Swart, I. Garcia-Bosch, *J. Am. Chem. Soc.* **2018**, *140*, 16625–16634.
- [187] C. Parmeggiani, C. Matassini, F. Cardona, *Green Chem.* **2017**, *19*, 2030–2050.
- [188] Q. Mei, H. Liu, Y. Yang, H. Liu, S. Li, P. Zhang, B. Han, *ACS Sustain. Chem. Eng.* **2018**, *6*, 2362–2369.
- [189] K.-H. el, Roberto; Kinzelmann, Hans-Georg; Garcia-Miralles, Jose; Kamm, Thomas; Seggewiss, Patrick; Hartmann, Olaf; Licht, Ulrike; Leonhardt, Viktoria; Mormul, Verena; Schumacher, *One Component Moisture Curable Composition Containing Exo-Vinylene Cyclic Carbonate Compounds for Coatings, Sealants or Adhesives*, **2018**, WO 2018162205 A1 20180913.
- [190] G. Hartmann, Olaf; Garcia-Miralles, Jose; Kinzelmann, Hans-Georg; Struempf, Svenja; Kutter, Juliane; Licht, Ulrike; Leonhardt, Viktoria; Mormul, Verena; Schumacher, Karl-Heinz; Boerzsoenyi, *Two-Component Composition Based on Compounds with at Least Two Exo-Vinylene Cyclic Carbonate Units*, **2018**, WO 2018054609 A1 20180329.
- [191] D. Licht, Ulrike; Schumacher, Karl-Heinz; Klopsch, Rainer; Ghislieri, *Copolymer Made from Cyclic Exo-Vinyl Carbonate Acrylates*, **2016**, WO 2016202652 A1 20161222.
- [192] S. Schaub, Thomas; Rudolf, Peter; Licht, Ulrike; Mormul, Verena; Dabral, *Monomers Comprising at Least One 4-(2-Oxyethylidene)-1,3-Dioxolan-2-One Unit and Use Thereof*, **2019**, WO 2019219469 A1 20191121.

- [193] C. Schaub, Thomas; Rudolf, Peter; Licht, Ulrike; Hashmi, A. Stephen K.; Dabral, Saumya; Johnson, *Process for Preparing Cyclic Carbonates with an Exocyclic Vinylidene Group*, **2021**, WO 2021144162 A1 20210722.
- [194] Y. Kayaki, M. Yamamoto, T. Ikariya, *J. Org. Chem.* **2007**, *72*, 647–649.
- [195] M. Yoshida, M. Fujita, T. Ishii, M. Ihara, *J. Am. Chem. Soc.* **2003**, *125*, 4874–4881.
- [196] I. Tommasi, F. Sorrentino, *Tetrahedron Lett.* **2009**, *50*, 104–107.
- [197] K. Fukumoto, M. Yoshizawa, H. Ohno, *J. Am. Chem. Soc.* **2005**, *127*, 2398–2399.
- [198] Z. Song, Y. Liang, M. Fan, F. Zhou, W. Liu, *RSC Adv.* **2014**, *4*, 19396–19402.
- [199] Y. Zhao, D. G. Truhlar, *Theor. Chem. Acc.* **2008**, *120*, 215–241.
- [200] K. Chen, G. Shi, R. Dao, K. Mei, X. Zhou, H. Li, C. Wang, *Chem. Commun.* **2016**, *52*, 7830–7833.
- [201] M. Zaky, A. Boyaval, B. Grignard, R. Méreau, C. Detrembleur, C. Jérôme, T. Tassaing, *J. Supercrit. Fluids* **2017**, *128*, 308–313.
- [202] S. P. F. Costa, A. M. O. Azevedo, P. C. A. G. Pinto, M. L. M. F. S. Saraiva, *ChemSusChem* **2017**, *10*, 2321–2347.
- [203] G. E. S. M. J. Frisch, G. W. Trucks, H. B. Schlegel, **2009**.
- [204] W. Yamada, Y. Sugawara,] Hau, M. Cheng, T. Ikeno, T. Yamada, *Eur. J. Inorg. Chem.* **2007**, 2604–2607.
- [205] S. Yoshida, K. Fukui, S. Kikuchi, T. Yamada, *J. Am. Chem. Soc.* **2010**, *132*, 4072–4073.
- [206] M. Cui, Q. Qian, Z. He, J. Ma, X. Kang, J. Hu, Z. Liu, B. Han, *Chem. - A Eur. J.* **2015**, *21*, 15924–15928.
- [207] Z. Wu, X. Lan, Y. Zhang, M. Li, G. Bai, *Dalt. Trans.* **2019**, *48*, 11063–11069.
- [208] L. Ouyang, X. Tang, H. He, C. Qi, W. Xiong, Y. Ren, H. Jiang, *Adv. Synth. Catal.* **2015**, *357*, 2556–2565.
- [209] S. Dabral, B. Bayarmagnai, M. Hermsen, J. Schießl, V. Mormul, A. S. K. Hashmi, T. Schaub, *Org. Lett.* **2019**, *21*, 1422–1425.
- [210] J. Hu, J. Ma, L. Lu, Q. Qian, Z. Zhang, C. Xie, B. Han, *ChemSusChem* **2016**, *10*, 1292–1297.
- [211] Z.-H. Zhou, Q.-W. Song, J.-N. Xie, R. Ma, L. He, *Chem. - An Asian J.* **2016**, *11*, 2065–2071.
- [212] J.-Y. Li, L.-H. Han, Q.-C. Xu, Q.-W. Song, P. Liu, K. Zhang, *ACS Sustain. Chem. Eng.* **2019**, *7*, 3378–3388.
- [213] M. Bigovic, V. Maslak, Z. Tokic-Vujosevic, V. Divjakovic, R. N. Saicic, *Org. Lett.* **2011**, *13*, 4720–4723.
- [214] P. Yan, X. Tan, H. Jing, S. Duan, X. Wang, Z. Liu, *J. Org. Chem.* **2011**, *76*, 2459–2464.
- [215] A. N. Zelikin, P. N. Zawaneh, D. Putnam, *Biomacromolecules* **2006**, *7*, 3239–3244.

- [216] F. Siragusa, J. Demarteau, T. Habets, I. Olazabal, K. Robeyns, G. Evano, R. Mereau, T. Tassaing, B. Grignard, H. Sardon, C. Detrembleur, *Macromolecules* **2022**, 10.1021/acs.macromol.2c00696.
- [217] T. Endo, K. Kakimoto, B. Ochiai, D. Nagai, *Macromolecules* **2005**, *38*, 8177–8182.
- [218] P. Olsén, K. Odelius, A. C. Albertsson, *Macromolecules* **2014**, *47*, 6189–6195.
- [219] C. Jehanno, J. Demarteau, D. Mantione, M. C. Arno, F. Ruipérez, J. L. Hedrick, A. P. Dove, H. Sardon, *ACS Macro Lett.* **2020**, *9*, 443–447.
- [220] R. Vestberg, R. Westlund, A. Eriksson, C. Lopes, M. Carlsson, B. Eliasson, E. Glimsdal, M. Lindgren, E. Malmström, *Macromolecules* **2006**, *39*, 2238–2246.
- [221] W. Li, H. H. Pham, Z. Nie, B. MacDonald, A. Güenther, E. Kumacheva, *J. Am. Chem. Soc.* **2008**, *130*, 9935–9941.